

THE USE OF THERMOPLASTIC STARCH FOR THE MODIFICATION OF HYDROPHILIC BREATHABLE MEMBRANES

SUVEN PECKU

A dissertation submitted in partial fulfilment of the requirements for the degree
of

MASTER OF ENGINEERING (CHEMICAL ENGINEERING)

In the
**FACULTY OF ENGINEERING
UNIVERSITY OF PRETORIA**

June 2006

SYNOPSIS

Title: The use of thermoplastic starch for modification of hydrophilic breathable membranes

Author: Suven Pecku

Supervisor: Professor W.W. Focke

Department: Chemical Engineering

University: University of Pretoria

Degree: Master of Engineering

The demand for waterproof breathable clothing has steadily been increasing over the past two decades. The technology for developing waterproof breathable textiles is focussed around two key aspects: The polymer membrane that is laminated onto the fabric to render it waterproof and breathable and the lamination technology which allows the proper adhesion of the membrane and fabric. Numerous breakthroughs have been made over the past two decades with regard to the development of new polymer membranes for clothing lamination. These membranes are however patent protected and expensive. This dissertation examines the use of starch as a modifying agent for the development of cheaper membranes that can act as an import replacement for the South African clothing lamination industry.

Table of Contents

<i>1. Introduction</i>	<i>11</i>
<i>2. Literature review</i>	<i>12</i>
2.1 The waterproof breathable fabric market.....	12
2.2. Requirements of waterproof breathable fabrics.....	13
2.3. Applications of waterproof breathable fabrics	14
2.4. Types of waterproof breathable films	14
2.4.1. Hydrophilic films	15
2.4.2. Microporous films	16
2.4.3. Bi-component films.....	16
2.5. Breathable membranes and resins currently commercially available	19
2.5.1. Gore	19
2.5.2. Porvair.....	19
2.5.3. Elf Atochem.....	21
2.5.4. Dow Plastics.....	22
2.6. Mass transfer and permeability models	23
2.6.1 Mass transfer models	23
2.6.2. Permeability models for filled membranes.....	26
2.7. Measurement of breathability	31
2.7.1. Comparison between methods to determine breathability.....	31
2.8. Standards available to test for breathability.....	35
2.8.1. British standards.....	35
2.8.2. Canadian standards.....	35
2.8.3. US standards	36
2.8.4. Italian standards	36
2.8.5. Spanish standards	36
2.8.6. Japanese standards.....	37
2.8.7. Sweating Guarded Hot Plate Tests	37
2.9. Blending	38
2.9.1. Addition of a copolymer.....	41
2.9.2. Reactive compatibilization	42
2.9.3. Methods of blending.....	42
2.10. Starch blends	44
2.11. Recommendations	46
<i>3. Raw Materials</i>	<i>48</i>
<i>4. Experimental</i>	<i>51</i>
4.1. Sample preparation	51



4.2. Testing of permeability.....	52
4.2.1. Apparatus used.....	52
4.2.2. Description of the test method and apparatus.....	52
4.2.3. Calculation of the WVTR.....	53
4.3. Blocking Tests.....	54
4.4. Scanning Electron Microscope.....	54
4.5. Software.....	54
4.6. Tensile Tests.....	55
5. Discussion.....	56
5.1. Commercial membranes.....	56
5.2. Permeability.....	61
5.2.1. TPS filled membranes.....	61
5.2.2. Other fillers.....	77
5.2.3. TPS blends with other fillers.....	83
5.3. Blocking Results.....	88
5.3.1. TPS Blocking and Morphology Results.....	88
5.3.2. Other Fillers Blocking and Morphology Results.....	91
5.3.3. Filled TPS Blocking and Morphology Results.....	91
5.4. Tensile Testing.....	94
5.4.1 Filled Membranes.....	94
5.4.2 Filled Starch-Pellethane Membranes.....	101
5.5. Cost Benefit.....	105
6. Conclusion.....	109
7. Acknowledgments.....	113
8. References.....	114
9. Appendices.....	118

List of Figures

Figure 2.1 European sales figures for coated and laminated fabrics.....	12
Figure 2.2 SEM photograph of Gore-Tex membrane magnified 10 000 times.....	19
Figure 2.3 Porvair film magnified 500 times	20
Figure 2.4 Porvair film magnified 500 times	21
Figure 2.5 SEM photo of Pebax film magnified 20 000 times	22
Figure 2.6 SEM photo of Pellethane film.....	23
Figure 2.7 The types of molecular diffusion that can occur.....	24
Figure 2.8.Schematic representation of the matrix with micro-void model.....	25
Figure 2.9 Mass flux through a matrix filled with a spherical particle of higher permeability than the matrix.....	28
Figure 2.10 Mass flux through a matrix filled with an impermeable particle	28
Figure 2.11 Comparison between ASTM E96 E and BW methods.....	32
Figure 2.12 Resistances in series model for mass transfer	34
Figure 2.13 Sweating hot plate apparatus	38
Figure 2.14 SEM photograph of granular starch incorporated into a polyester polyurethane [Santayanon & Wootthikanokkhan, 2003].....	44
Figure 2.15 SEM photograph of granular starch incorporated into a polyester polyurethane [Santayanon & Wootthikanokkhan, 2003].....	45
Figure 2.16 SEM photograph of treated granular starch incorporated into a polyester polyurethane [Santayanon & Wootthikanokkhan, 2003].....	45
Figure 5.1 WVTR of commercial membranes tested	58
Figure 5.2. Porvair P412 membrane magnified 2000 times (Side not exposed to DMF)	59
Figure 5.3.Pebax Mv 3000 Sa01 membrane magnified 10 000 times.....	60
Figure 5.4 WVTR of Pellethane membranes as a function of thickness	61
Figure 5.5 WVTR of 20% TPS (High Amylose)-Pellethane membranes as a function of thickness. TPS made with 40% glycerol on a starch mass basis	62
Figure 5.6 WVTR comparison of different TPS blends.....	63
Figure 5.7 The change in permeability as a function of filler volume fraction.....	66
Figure 5.8 Comparison between the experimental change in permeability as a function of filler volume fraction and the change in permeability predicted by the Maxwell model for impermeable spheres.....	67
Figure 5.9 The change in permeability as a function of α and filler volume as predicted by the Bruggeman equation.....	68
Figure 5.10.Alignment possibilities for the filled membranes.....	69
Figure 5.11 The change in permeability as a function of shape factor and filler volume as predicted by the Maxwell-Wagner-Sillar model for $\alpha=0.2$	70
Figure 5.12 The change in permeability as a function of shape factor and filler volume as predicted by the Maxwell-Wagner-Sillar model for $\alpha=5$	71
Figure 5.13. 20%TPS containing 30% glycerol and high amylose starch / 80%Pellethane membrane magnified 1000 times	72
Figure 5.14 Comparison between the experimental change in permeability as a function of filler volume fraction and fitted Maxwell and Bruggeman models.....	73
Figure 5.15 Effect of amylose content on permeability of 20% TPS filled made with 40% glycerol	

<i>and starches of different amylose content</i>	75
<i>Figure 5.17 SEM picture of granular starch in TPU membrane</i>	76
<i>Figure 5.18 Comparison between the time to reach equilibrium between membranes containing 20% granular starch and 20% thermoplastic starch</i>	77
<i>Figure 5.19 Comparison between the experimental change in permeability as a function of filler volume fraction and the change in permeability predicted by the Maxwell model for impermeable spheres</i>	78
<i>Figure 5.20 The change in permeability as a function of shape factor and filler volume as predicted by the Maxwell-Wagner-Sillar model for impermeable fillers</i>	79
<i>Figure 5.21 SEM picture of Dicalite filled membrane</i>	80
<i>Figure 5.22 SEM picture of Dicalite filled membrane</i>	80
<i>Figure 5.23 SEM picture of Diatomite filled membrane</i>	81
<i>Figure 5.24 SEM picture of Diatomite filled membrane</i>	81
<i>Figure 5.25 Comparison between the experimental change in permeability as a function of filler volume fraction and the change in permeability predicted by the Maxwell model for impermeable spheres</i>	83
<i>Figure 5.26 Comparison between the experimental change in permeability as a function of filler volume fraction for TPS and filled TPS filled membranes</i>	84
<i>Figure 5.27 Comparison between the experimental change in permeability as a function of filler volume fraction and the change in permeability predicted by the Maxwell model for impermeable spheres</i>	86
<i>Figure 5.28 Comparison between the experimental change in permeability as a function of filler volume fraction and the change in permeability predicted by the Maxwell model for impermeable spheres</i>	87
<i>Figure 5.29 Pellethane membrane magnified 30000 times</i>	89
<i>Figure 5.30 20%TPS (containing 40% glycerol and low amylose starch) / 80%Pellethane membrane magnified 200 times</i>	90
<i>Figure 5.31 20%TPS (containing 40% glycerol and low amylose starch) / 80%Pellethane membrane magnified 1000 times</i>	90
<i>Figure 5.32 20%TPS containing alumina silicate (Plasfill 5) 80%Pellethane membrane magnified 3000 times</i>	92
<i>Figure 5.33 20%TPS containing diatomite 80%Pellethane membrane magnified 3000 times</i>	93
<i>Figure 5.34 20%TPS containing hydrotalcite 80%Pellethane membrane magnified 3000 times</i>	93
<i>Figure 5.35 20%TPS containing calcium carbonate (Kulucote 2) 80%Pellethane membrane magnified 3000 times</i>	94
<i>Figure 5.36.Ultimate tensile strength of membranes</i>	95
<i>Figure 5.37.Yeild stress of membranes</i>	95
<i>Figure 5.38.Elongation to break of membranes</i>	96
<i>Figure 5.39.Tensile modulus of membranes</i>	96
<i>Figure 5.40.Film blowing process</i>	97
<i>Figure 5.41.Film windup process</i>	98
<i>Figure 5.42.Film bubble</i>	98
<i>Figure 5.43.Ultimate tensile strength of membranes containing filled starch</i>	102
<i>Figure 5.44.Yeild strength of membranes containing filled starch</i>	102
<i>Figure 5.45.Elongation to break of membranes containing filled starch</i>	103
<i>Figure 5.46.Tensile modulus of membranes containing filled starch</i>	103



Figure 5.47 Sensitivity analyses performed on the IRR for a proposed plant examining the effect of operating costs, capital and sales fluctuations.....108

List of Tables

Table 2.1. The companies that control the branded breathable membrane market.....	13
Table 2.2. Properties of current films.....	18
Table 2.3. Units obtained for different breathability tests.....	31
Table 2.4 WVTR obtained for Pebax and various other membranes using the ASTM E96 E and BW methods.....	33
Table 2.5 Table of Modifying polymers applications.....	39
Table 2.6 Advantages and Disadvantages of Certain Polymers.....	40
Table 2.7 Copolymers formed from various reactions.....	42
Table 2.8 Advantages and disadvantages of some mixers.....	43
Table 3.1 Polymers tested and the class of polymer.....	49
Table 3.2 Starch details.....	50
Table 5.2 The effect of TPS (Hi Maize) and glycerol in TPS on the WVTR of a polyurethane membrane.....	63
Table 5.5 Predictions of starch permeability based on various models.....	74
Figure 5.16 Comparison between the time to reach equilibrium between membranes containing 20% granular starch and 20% thermoplastic starch.....	76
Table 5.8 The effect of fillers in TPS on the WVTR of a polyurethane membrane.....	84
Table 5.9 The effect of fillers in TPS on the WVTR of a polyurethane membrane.....	88
Table 5.10 The effect of TPS on blocking characteristics of membranes.....	89
Table 5.10 The effect of TPS on blocking characteristics of membranes.....	91
Table 5.11 The effect of Filled-TPS on blocking characteristics of membranes.....	92
Table 5.12. Student t-test results for the tensile property differences in the cross and machine direction.....	99
Table 5.13. Student t-test results for the tensile property differences between Pellethane and filled Pellethane (MD).....	100
Table 5.14. Student t-test results for the tensile property differences between Pellethane and filled Pellethane (CD).....	101
Table 5.15. Student t-test results for the tensile property differences granular starch filled membranes and thermoplastic starch filled membranes (CD).....	101
Table 5.16. Student t-test results for the tensile property differences in the cross and machine direction.....	104
Table 5.17. Student t-test results (P-Values) for the tensile property differences between Starch-Pellethane membranes and filled Starch-Pellethane (CD).....	105
Table 5.18. Student t-test results (P-Values) for the tensile property differences between Diatomite-Starch-Pellethane membranes and unfilled Pellethane (CD).....	105
Table 6.1 Summary of WVTR results.....	110

Nomenclature

Symbol	Definition	Unit
A	Area	m^2
b	Langmuir affinity constant	Pa^{-1}
c	Concentration	$mol.m^{-3}$
C	Sorption	$m^3.m^{-3}$ polymer
C_D	Henry sorption	$m^3.m^{-3}$ polymer
C_H	Langmuir sorption	$m^3.m^{-3}$ polymer
C'_H	Langmuir Saturation Constant	$m^3.m^{-3}$ polymer
CD	Cross Direction	-
D	Diffusion Coefficient	$m^2.s^{-1}$
E_a	Apparent activation energy	$J.mol^{-1}$
EtB	Elongation to Break	%
GS	Granular Starch	-
J	Flux	$mol.m^{-2}.s^{-1}$
k_d	Henry constant	$m^3.m^{-3}.Pa^{-1}$
k_f	Mass transfer coefficient on feed side	$mol.s^{-1}.m^{-2}.(mol.m^{-3})^{-1}$
k_m	Mass transfer coefficient in membrane	$mol.s^{-1}.m^{-2}.(mol.m^{-3})^{-1}$
k_p	Mass transfer coefficient on permeate side	$mol.s^{-1}.m^{-2}.(mol.m^{-3})^{-1}$
l	Thickness	m
L	Length	m
L_0	Original Length	m
M_p	Mass permeant	kg
MD	Machine direction	-
p	Pressure	Pa
P	Permeability	Barrer or $g.m^{-2}.day^{-1}$
P_C	Permeability of the continuous phase	Barrer or $g.m^{-2}.day^{-1}$
P_D	Permeability of the disperse phase	Barrer or $g.m^{-2}.day^{-1}$
P_{eff}	Effective permeability	Barrer or $g.m^{-2}.day^{-1}$
p_l	Partial pressure on permeate side	Pa
p_o	Partial pressure on feed side	Pa
R	Gas constant	$J.mol^{-1}.K^{-1}$
S	Solubility Coefficient	$m^3_{(STP)}.m^{-3}.Pa^{-1}$



Symbol	Definition	Unit
SEM	Scanning Electron Microscope	-
t	Thickness	m
T	Temperature	K
TPS	Thermoplastic Starch	-
UTS	Ultimate Tensile Strength	MPa
WVTR	Water vapour Transmission Rate	
x	Position	m
YS	Yield Strength	MPa
Φ_C	Volume fraction of continuous phase	-
Φ_D	Volume fraction of disperse phase	-

1. Introduction

The market for high performance fabrics has been growing over the past two decades. Currently this market is dominated by US and European based companies.

BreatheTex is a South African company that produces laminated fabrics for high end uses. The membranes that are laminated onto the fabrics are all imported and the products are usually exported.

BreatheTex wishes to create a local supply of breathable membranes. This is due to several factors:

- The weaker Rand has increased the price of imported membranes
- Suppliers of membranes are branching out into lamination and may not be willing to supply membranes to their competitors
- There are several membranes available on the market, however the market is dominated by a small group of suppliers who can change their process at any time

The aim of the project is to produce a novel breathable membrane in South Africa. Depending on available technology either BreatheTex or an external South African company will produce the membrane. This dissertation examines the effect of fillers on the properties of polyurethane breathable membranes.

2. Literature review

2.1 The waterproof breathable fabric market

The market for waterproof breathable fabrics (WBF) started to develop in the US at the end of the 70's and in Europe towards the beginning of the 80's [Kramer, 1998]. There has been significant growth in the demand for WBFs over recent times. The European market has shown a significant increase in sales over 1996-2000 as shown in Figure 2.1 [Kramer, 1998]. Volumes of laminates and coated fabrics in the European market are relatively similar however in the UK coated fabrics dominate the market (approximately 70% of market share) and in Germany laminated fabrics dominate the market (approximately 70% of market share) [Kramer, 1998; Painter, 1996].

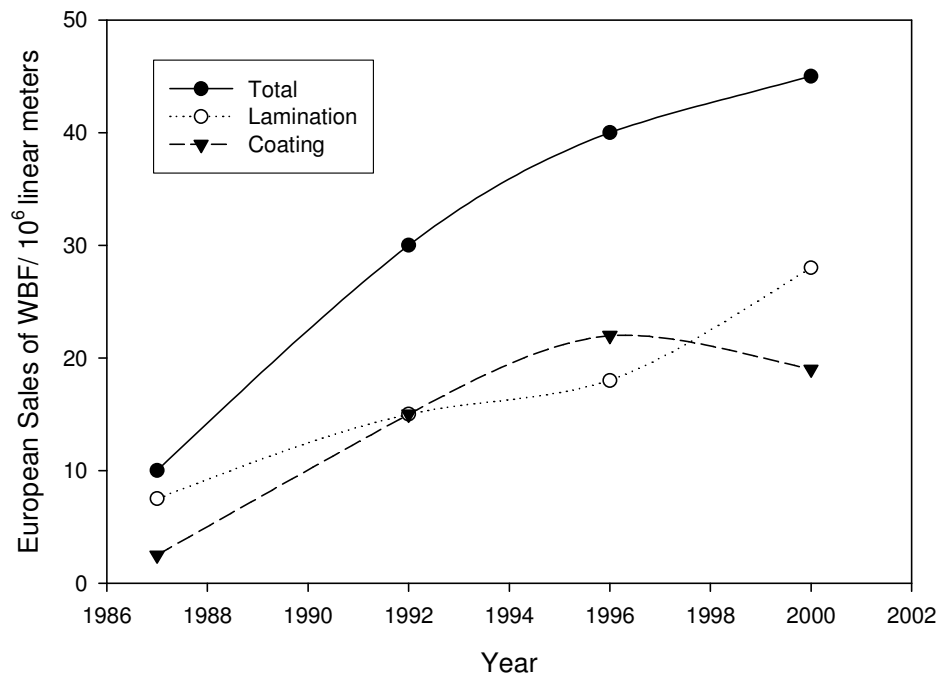


Figure 2.1. European sales Figures for coated and laminated fabrics

The 'branded' market is dominated by six companies. Table 2.1 list the companies and their products.

Table 2.1. The companies that control the branded breathable membrane market [Kramer, 1998; Painter, 1996; BHA Group, s.a; Marmot, s.a; MIC, s.a.]

Company	Branded Product
AKZO Nobel	Sympatex
BHA	eVent
Burlington	Ultrex, Xalt
Gore	Gore-Tex
Mitsubishi	Diaplex
Toray	MemBrain, Entrant, Dermizax

Gore is still dominant with a 60% market share in the US and 50% market share in Europe [Kramer, 1998].

2.2. Requirements of waterproof breathable fabrics

Waterproof, breathable fabrics need to meet requirements other than providing waterproofness and breathability. These requirements are specific to the end uses and may include: [Kramer, 1998; BreatheTex Corp, s.a]

- Windproofness for comfort in varying weather conditions
- Abrasion resistance for increased product life
- Good washability and wash resistance for easy maintenance
- Lightness and packability
- Durability
- Flexibility
- Stretchability
- Handle and look
- Flame retardancy for specific applications like fire fighter suits
- Oil and chemical resistance for applications such as splash coats
- High visibility for applications such as night running clothing

2.3. Applications of waterproof breathable fabrics

Waterproof breathable fabrics have shown various applications in the military sector. These applications include: [BreatheTex Corp, s.a; Toray Industries, 2004]

- Rainwear and cold weather jackets
- Tents
- Sleeping bags
- Trousers
- Overalls
- Socks
- Boot and shoe liners

The medical sector has also shown a large number of applications for waterproof breathable fabrics: [BreatheTex Corp, s.a; Toray Industries, 2004]

- Surgical Gowns
- Operating theatre covers
- Mattress covers
- Insulation gowns for highly contagious diseases
- Prosthetic socks
- Wound coverings

Other markets in which waterproof breathable fabrics are currently used are the sports and leisurewear market and the work-wear market. The sports and leisurewear market focuses on foot wear, golf wear, cycling wear, tents, sleeping bags, gloves and windbreakers. The work-wear market focuses on fire-fighter suits, police uniforms and chemical splash suits. [BreatheTex Corp, s.a; Toray Industries, 2004, Painter; 1996]

2.4. Types of waterproof breathable films

Waterproof breathable films can be grouped into two broad categories: Hydrophilic membranes and microporous membranes. [Van Roey, 1991]

Combining a microporous membrane with a hydrophilic coating results in a bi-component membrane that possesses properties of both microporous and hydrophilic membranes.

The compact nature of hydrophilic films provides water impermeability. Breathability is facilitated by a molecular mechanism of absorption-diffusion-desorption. The driving force for the transport is differences in temperature and humidity. [Jonquieres, 2002; Painter 1996]

Microporous films are made up of a network of permanent air-permeable pores. The large network of micropores allows sufficient penetration of water vapour and other gases while the small size of the pore prevents water penetration. Although some water penetration does occur via diffusion the small pore size stops the bulk of the water droplets from penetrating due to the droplet surface tension effects. The size of a water vapour molecule is estimated to be about 4 Å. Pore sizes are targeted to be between 0.1 and 0.3 µm which are sufficiently large to allow the vapour to pass while stopping larger water drops. [Painter, 1996]

Microporous and hydrophilic film properties vary making them suitable for different applications. Some applications require a combination of the properties. Bi-component membranes consisting of a microporous membrane coated with a hydrophilic membrane satisfy these applications. A comparison of these membranes is shown below.

2.4.1. Hydrophilic films

Advantages of hydrophilic films include: [Painter, 1996]

- Pinhole free films are less sensitive to deterioration
- Laminates are more supple
- Can be engineered to provide greater breathabilities than microporous films with less risk of water leakage
- They are windproof

- They are tougher and more durable

The disadvantages of hydrophilic films include the following: [Painter, 1996]

- Require a reservoir of vapour to start breathing
- Wets out and gives a clammy handle in rainy conditions
- In wet conditions the film swells producing 'noise' effects

2.4.2. Microporous films

Advantages of microporous films include: [Painter, 1996]

- Greater breathability for the same thickness of film
- Greater flexibility and stretch
- Softer handle
- Best air permeability
- Does not require a moisture reservoir to start breathing
- PTFE films cannot melt or burn

The disadvantages of microporous films include: [Painter, 1996]

- Control and consistency of pore size is critical for maintaining breathability and waterproofness
- Less windproofness and wind resistance
- PTFE films tend to creep

2.4.3. Bi-component films

Advantages of bi-component films: [Painter, 1996]

- Hydrophilic layer reduces tendency of water leakage through pinholes or oversized pores
- Added strength
- Reduces stretch which could cause stretching of pores
- Offers improved wind resistance to microporous films
- Offers resistances to certain solvents and oils



- Film swelling of hydrophilic films is lessened due to a more mechanical vapour transmission mechanism

Disadvantages of bi-component films: [Painter, 1996]

- Laminate is stiffer
- Breathability of the microporous film is reduced
- Hydrophilic layer tends to wet out
- Hydrophilic layer requires a moisture reservoir to start breathing
- The additional hydrophilic layer adds cost to the film

Table 2.2 shows a comparison between films that are currently available on the market.

Table 2.2 Properties of current films [Painter, 1996; BHS Group, s.a.; Marmot, s.a; MIC, s.a]

Film Name	Film Producer	Physical description	Chemical Description	Remarks
Sympatex	AKZO	Hydrophilic	Polyester co-block polymer	Sports and leisure, Footwear
Walotex	Bayer	Hydrophilic	Polyurethane	General purpose, Sports and leisure
Porelle	Porvair	Hydrophilic	Polyurethane	General purpose, Sports and leisure
Peebatex	Elf Atochem	Hydrophilic	Polyether co-block amide	General purpose, footwear
Peebamed	Elf Atochem	Hydrophilic	Polyether co-block amide	Medical
Diaplex	Mitsubishi	Hydrophilic	Polyurethane	General purpose, Sports and leisure
Munro	Munro Ltd.	Hydrophilic	Polyether co-block amide	Medical
Goretex	W.L.Gore	Bi-Component	PTFE	General purpose, footwear
Tetratex	Tetratex Corp.	Bi-Component	PTFE	Industrial and Fire market
Grabotter	Graboplast Co.	Microporous	Polyurethane	Industrial and Fire market
MemBrain	Marmot	Hydrophilic	Polyurethane	General purpose, Sports and leisure
Grabotter	Graboplast Co.	Bi-Component	Polyurethane	General purpose, Sports and leisure
eVent	BHA Group	Microporous	PTFE	General purpose, Sports and leisure

2.5. Breathable membranes and resins currently commercially available

2.5.1. Gore

Gore-Tex is a film that is manufactured by bi-directionally stretching a polytetrafluoroethylene (PTFE) sheet. The PTFE micro-fibrillates creating tiny micropores as shown in Figure 2.2. These pores are large enough to let water vapour and air pass but small enough to stop water droplets from passing. [Gore & Allen, 1980]

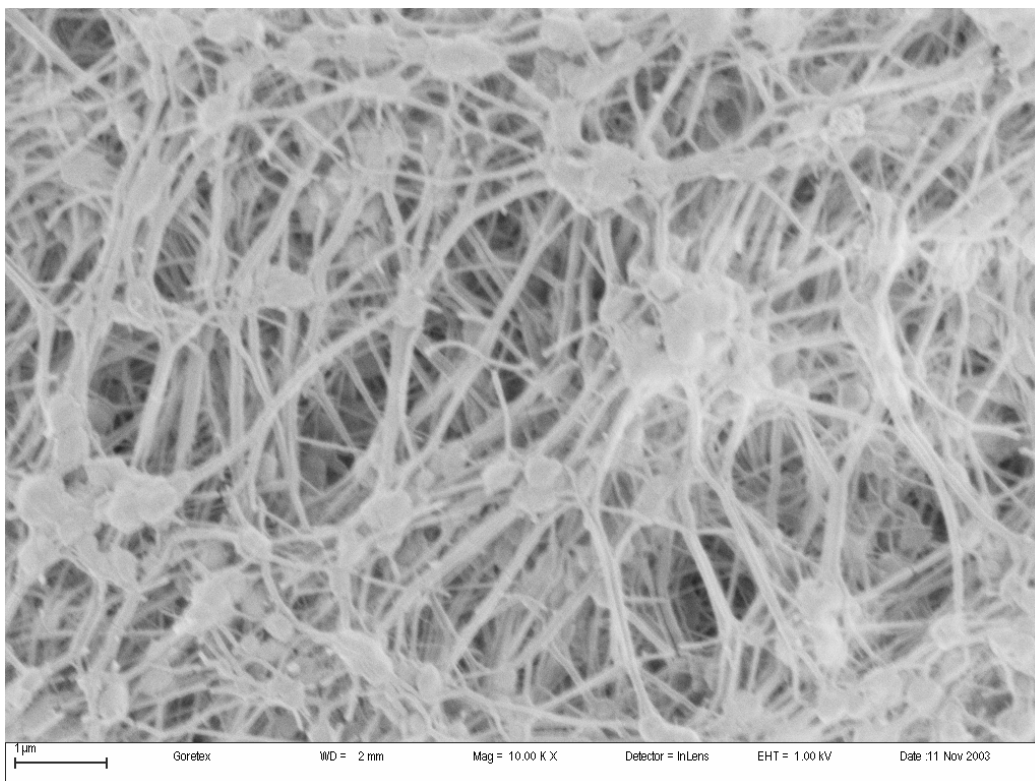


Figure 2.2 SEM photograph of Gore-Tex membrane magnified 10 000 times

2.5.2. Porvair

Porvair produces hydrophilic and microporous membranes. The Porelle membranes are polyether urethane membranes. Figures 2.3 and 2.4 show the Porelle membrane. The membrane is made by compounding the polyether urethane with soluble particulate filler. The membrane is dissolved in

dimethylformamide (DMF) where the particulate filler dissolves leaving micropores. [Pearman & Wright, 1976, Warwicker & Price, 1978]

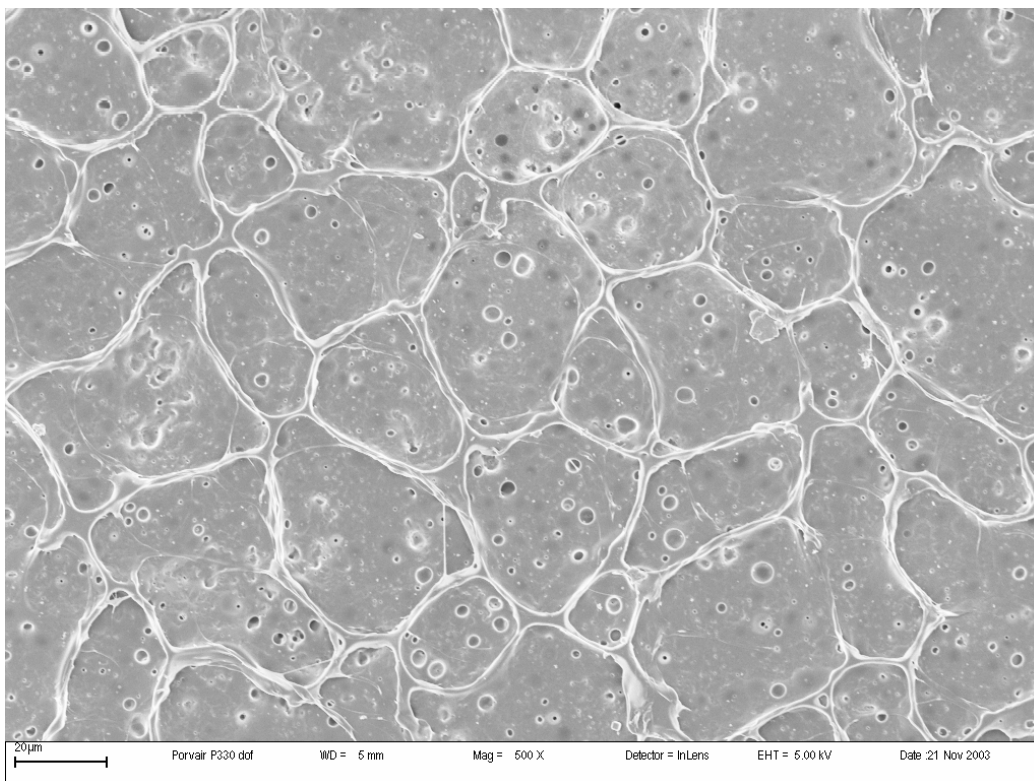


Figure 2.3 Porvair film magnified 500 times. (Side not exposed to DMF)

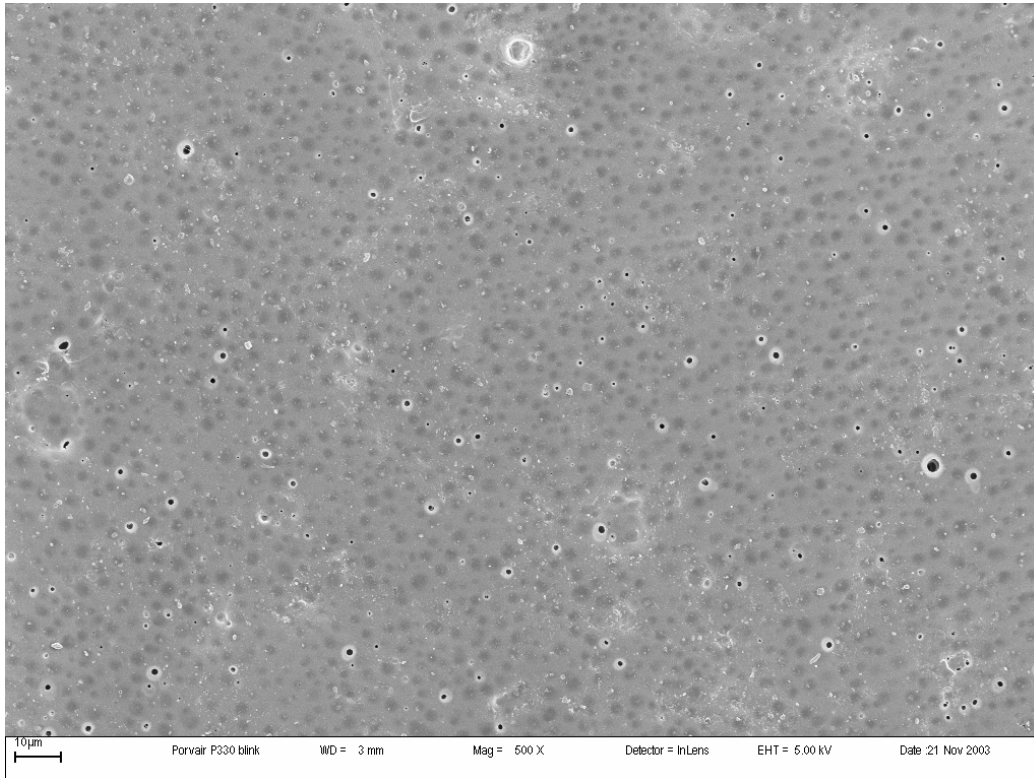


Figure 2.4 Porvair film magnified 500 times. (Side exposed to DMF)

2.5.3. Elf Atochem

Elf Atochem (now called Arkema Inc) manufactures Pebax and Pebaxtex. They are hydrophilic polyether-blockamides that are extensively used in breathable membranes. The Pebax MV 3000 film under magnification is shown in Figure 2.5. [Elf AtoChem, s.a]

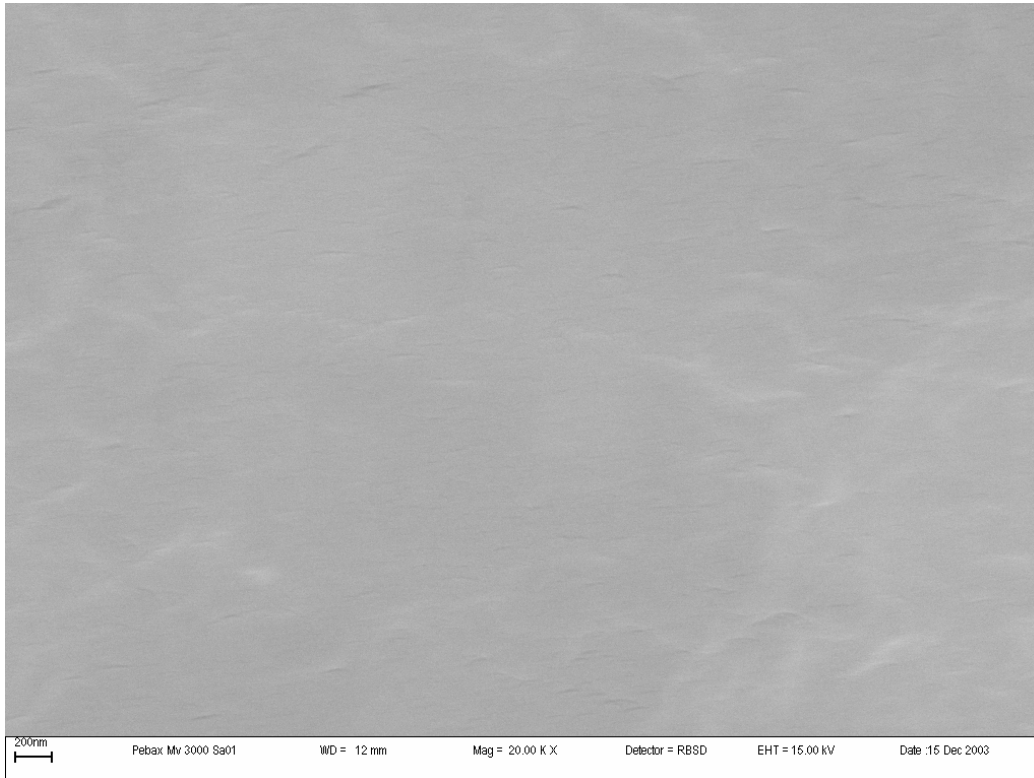


Figure 2.5 SEM photo of Pebax film magnified 20 000 times

2.5.4. Dow Plastics

Dow Plastics manufactures various grades of Pellethane which is hydrophilic thermoplastic polyurethane. Pellethane can be blown or cast into a hydrophilic membrane which will be suitable for clothing applications. [Dow, s.a.] A SEM picture of a Pellethane 2103-70A membrane manufactured at the CSIR shown in Figure 2.6.

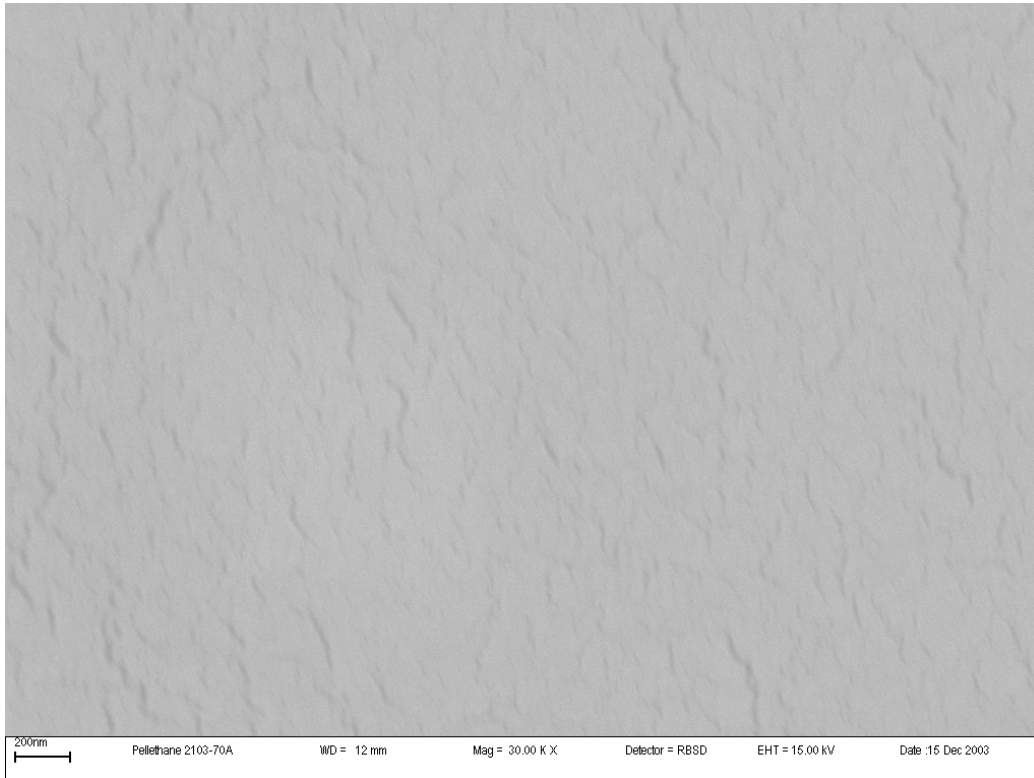


Figure 2.6 SEM photo of Pellethane film (Manufactured at the CSIR)
magnified 30 000 times

2.6. Mass transfer and permeability models

2.6.1 Mass transfer models

Molecular diffusion has been divided into three different categories. These categories are:

- Fickian diffusion
- Knudsen diffusion
- Transition diffusion

Fickian diffusion occurs when the molecules move due to collisions with other molecules. Knudsen diffusion occurs when molecule movement is predominantly due to collisions with the walls of its environment. Transition diffusion is a hybrid model. Figure 2.7 illustrates the difference between these types of diffusion.

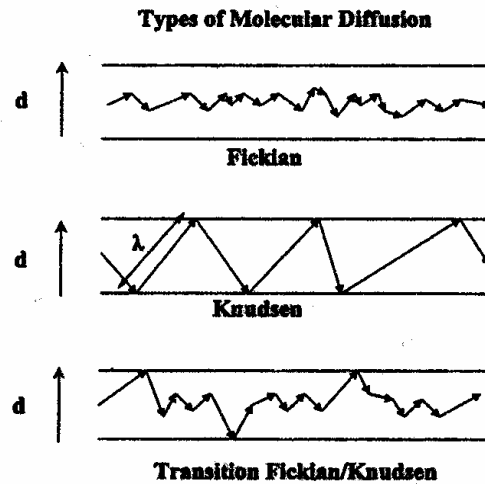


Figure 2.7 The types of molecular diffusion that can occur. [Nguyen et al, 2001]

Mass transport across polymer membranes is well described by Fick's law:

$$J = -D \frac{dc}{dx} \quad (1)$$

At steady state the equation can be reduced to:

$$J = Dk_d \frac{P_o - P_l}{l} \quad (2)$$

Due to the inability of Fick's law to describe the behaviour of glassy polymers various dual mode models have been proposed. In early literature, Meares and Barrer et al. analysed transport through a glassy polymer by classifying the polymer as a heterogeneous structure consisting of a matrix and a micro-void region. [Tsujiita, 2003; Kanehashi et al, 2005; Islam, 2002] This model is shown schematically in Figure 2.8.

Henry gas sorption mechanisms dominate in the matrix region and Langmuir type gas sorption dominates in the micro-void region. [Tsujiita, 2003] The dual-sorption model can be mathematically represented by the sum of the contribution of the Henry sorption and the Langmuir sorption [Tsujiita, 2003]:

$$C = C_D + C_H \quad (3)$$

$$C_D + C_H = k_D p + \frac{C_H' b p}{1 + b p} \quad (4)$$

The dual sorption model may correlate poorly with transport of specific gases, especially if the gas is polar and condensed. Transport of carbon dioxide is an example of this. The carbon dioxide will tend to plasticize the polymer and change the glassy polymer into a rubbery polymer [Tsuji, 2003].

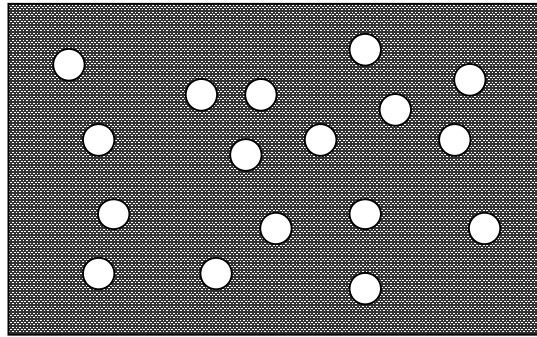


Figure 2.8. Schematic representation of the matrix with micro-void model

Combining equation 1 and 3 results in the following:

$$J = -D_D \frac{\partial C_D}{\partial x} - D_H \frac{\partial C_H}{\partial x} = -D_D \left[1 + \frac{FK}{(1 + b p)^2} \right] \frac{\partial C_D}{\partial x} \quad (5)$$

Where:

$$F = \frac{D_H}{D_D} \quad \text{and} \quad K = \frac{b C_D}{k_D}$$

$$J = -D_D \left[\frac{1 + \frac{FK}{(1+bp)^2}}{1 + \frac{K}{(1+bp)^2}} \right] \frac{\partial C}{\partial x} \quad (6)$$

$$D = D_D \left[\frac{1 + \frac{FK}{(1+bp)^2}}{1 + \frac{K}{(1+bp)^2}} \right] \quad (7)$$

The permeability of a gas through a polymer is governed by a sorption-diffusion mechanism. It is dependant on the gas flux and the driving force gradient. [Clarizia et al, 2004; Gonzo et al, 2005]:

$$P = \frac{J}{\frac{\Delta p}{x}} = DS \quad (8)$$

The addition of filler to a matrix, such that the filler has a higher diffusivity than the matrix, results in an increased diffusion rate and increased permeability.

2.6.2. Permeability models for filled membranes

In order to improve the permeability of polymeric membranes there are three strategies [Clarizia et al., 2004]:

- Synthesis of new polymers or functionalisation of some present polymers
- Use of more selective materials for membrane manufacture
- Use of fillers for the production of composite membranes

The latter option is the cheapest and quickest to market solution. Various authors have investigated various fillers and the effect of fillers on membrane performance [Ji et al., 1995; Bouma et al., 1997; Moggridge et al., 2003; Lape et al., 2004; Clarizia et al., 2004; Wang et al., 2005].

The use of fillers can be used to increase the permeability of a membrane or decrease the permeability of a membrane for the desired application. The incorporation of fillers with permeability higher than that of the matrix is likely to result in improved permeability whereas the incorporation of impermeable fillers will decrease the permeability of the composite. Figure 2.9 and 2.10 illustrate this effect.

The inclusion of impermeable filler will have two effects:

- Reduction in area available for diffusion due to the impermeable filler replacing the matrix
- Due to the impermeable nature of the filler the path length of the molecules travelling through the membrane is increased. [Lape et al, 2004]

This increased path length and reduction in area available for diffusion, due to filler replacing the matrix, reduces the mass flux and the permeability as shown in Figure 2.10 [Lape et al, 2004].

Figure 2.9 shows a spherical particle of higher permeability than the matrix. The matrix area for diffusion is reduced and replaced with regions of higher permeability. Due to the scattered areas of higher permeability, the flux would be higher through the filler particle as discussed above [Bouma et al, 1997; Lape et al, 2004].

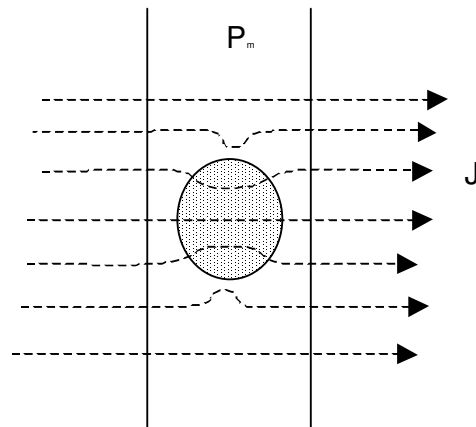


Figure 2.9 Mass flux through a matrix filled with a spherical particle of higher permeability than the matrix [Bouma et al, 1997]

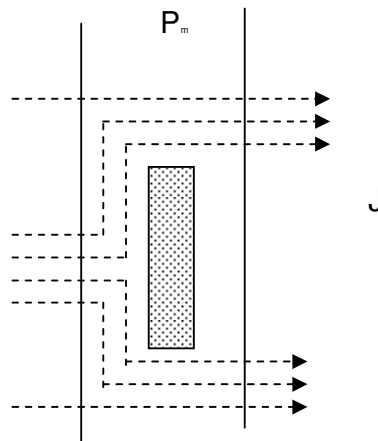


Figure 2.10 Mass flux through a matrix filled with impermeable particle [Lape et al, 2004]

Various models exist to describe the effect of fillers and filler content on permeability. Many of these models have roots in potential theory describing electrical conductivity through heterogeneous substances. The series and parallel models can give the minimum and maximum permeability for a penetrant [Gonzo et al, 2005]:

$$P_{eff}^{min} = \frac{P_C P_D}{\phi_C P_D + \phi_D P_C} \quad (9)$$

$$P_{eff}^{max} = \phi_C P_C + \phi_D P_D \quad (10)$$

Maxwell derived a solution for the conductivity of random non-interacting spheres in a continuous matrix. When applied to permeability of a filled matrix the following equation is obtained [Gonzo et al, 2005; Clarizia et al, 2004]:

$$P_{eff} = P_C \frac{P_D + 2P_C - 2\phi(P_C - P_D)}{P_D + 2P_C + \phi(P_C - P_D)} = P_C \frac{1 + 2\beta\phi}{1 - \beta\phi} \quad (11)$$

The value of α is defined as ratio of the permeability of the particle to that of the matrix, i.e. $\alpha = \frac{P_D}{P_C}$ and $\beta = \frac{\alpha - 1}{\alpha + 2} = \frac{P_D - P_C}{P_D + 2P_C}$

The Maxwell model is only applicable to dilute filler concentration. The model is reliable for filler volume fractions ranging from 0 to about 20% [Gonzo et al, 2005]. The reason for this is that the Maxwell model assumes that the flux around a particle is not influenced by the surrounding particles [Gonzo et al, 2005]. At low volume fractions, if the particles are well dispersed, the assumption hold. At higher volume fractions the flux around the particles will be influenced by the surrounding particles due to the particles being in close proximity. For impermeable spheres equation 11 reduces to:

$$P_{eff} = P_C \frac{1 - \phi}{1 + \phi/2} \quad (12)$$

Applying Maxwell's model to a matrix with particles of significantly higher permeability results in the following relationship:

$$P_{eff} = P_c \frac{1+2\phi}{1-\phi} \quad (13)$$

For the case of dilute dispersions of ellipsoids the Maxwell-Wagner-Sillar equation is [Bouma et al, 1997; Gonzo et al, 2005]:

$$P_{eff} = P_c \frac{nP_D + (1-n)P_c + (1-n)(P_D - P_c)\phi}{nP_D + (1-n)P_c - n(P_D - P_c)\phi} \quad (14)$$

Where n is a shape factor such that $0 \leq n \leq 1/3$ represents prolate ellipsoids, $n=1/3$ represents spherical particles and $1/3 \leq n \leq 1$ represents oblate ellipsoids.

Bruggeman used an equation valid at low filler concentrations and calculated the effect of an infinitesimal increase in filler concentration. Integrating this equation he derived [Gonzo et al, 2005]:

$$\left(\frac{P_{eff}}{P_c} - \alpha \right) \left(\frac{P_{eff}}{P_c} \right)^{-1/3} = (1-\phi)(1-\alpha) \quad (15)$$

The Maxwell model and the Bruggeman model accurately predict behaviour at low filler concentrations. At filler volume fractions higher than 20% the Maxwell model and Bruggeman model deviate [Gonzo et al, 2005]. At high volume fractions the flux near a particle is influenced by the surrounding particles and therefore the Maxwell model predictions are inaccurate.

The permeability is also a function of temperature and displays an Arrhenius type dependence:

$$P = P_o \exp\left(\frac{-E_a}{RT}\right) \quad (16)$$

2.7. Measurement of breathability

Two general types of tests are used to measure breathability. They are gravimetric tests and resistance tests. [Van Roey, 1991]

A direct comparison between breathability results obtained from different methods is unreliable because of the vast difference in the testing methods and the various types of units available as shown in Table 2.3. Even if the test methods result in the same units, comparisons between the different tests are meaningless. [Gretton et al, 1996] A comparison of two different ASTM tests is done below which will explain why there are differences between test methods.

Table 2.3 Units obtained for different breathability tests [Gretton et al, 1996]

Test Type	Units
Resistance to evaporative heat transfer	$m^2 \cdot mbar \cdot W^{-1}$
Percentage permeability index	% of Trul reference. fabric
Resistance in cm of equivalent standard still air	cm ESSA
Water vapour transmission rate	$g \cdot m^{-2} \cdot 24 \text{ hrs}^{-1}$

Gravimetric tests use a cup containing water or desiccant covered by the membrane being tested. The weight loss or gain after a decided time period is a measure of the breathability of the film. [Van Roey, 1991] Water vapour transmission tests are an example of a gravimetric test.

2.7.1. Comparison between methods to determine breathability

The ASTM E96 E and ASTM E96 BW tests are two methods to determine the water vapour transmission rate of a membrane. Figure 2.11 illustrates the different test conditions.

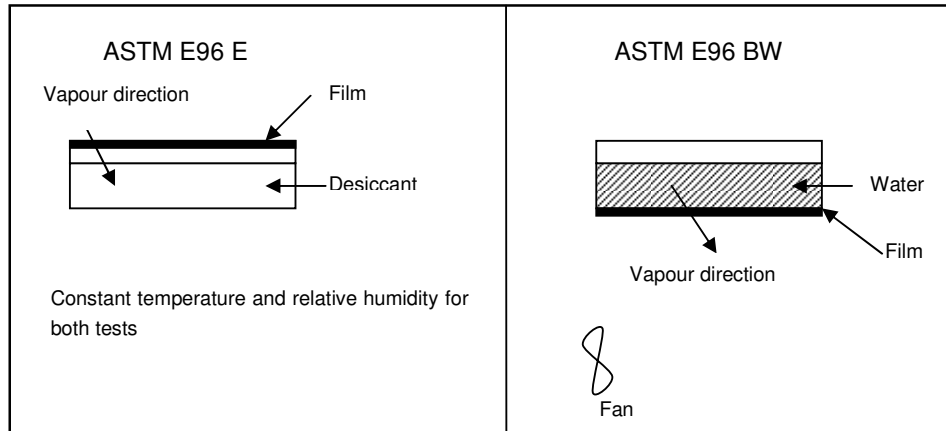


Figure 2.11 Comparison between ASTM E96 E and BW methods

The ASTM E96 E method uses a test cup filled with desiccant and sealed with the membrane being tested. The WVTR is determined by the weight gain of the cup with after a specific amount of time. The weight gain is due to the desiccant absorbing water vapour which is transmitted from the external environment through the membrane and into the cup. The external environment is kept at a constant temperature and relative humidity ~90%. [Nguyen et al, 2001]

The ASTM E96 BW method involves using a test cup filled with water and sealed with the membrane being tested. The cup is then inverted. The WVTR is determined by the weight loss of the cup with after a specific amount of time. The weight loss is due to water vapour being transmitted to the external environment via the membrane. The external environment is kept at a constant temperature and relative humidity ~50%. [Nguyen et al, 2001]

Table 2.4 shows the WVTR that was obtained by these two methods for various films.

Table 2.4 WVTR obtained for Pebax and various other membranes using the ASTM E96 E and BW methods. [Nguyen et al, 2001]

Film	WVTR kg.m ⁻² .day ⁻¹	
	ASTM E96 E	ASTM E96 BW
MV1074	4.7	>20
MV3000	6.6	>15
MV1041	2.7	>10
3533	2.5	2.5
MX1205	1.7	1.7
EVA 040VN4	0.08	0.08
LDPE	0.01	0.0066

At a higher WVTR the values obtained from these methods are unreliable. The ASTM E96 E method tends to level off. This indicates that the boundary resistance governs the transport. The ASTM E96 BW method gives higher WVTR values when there is air circulation. [Nguyen et al, 2001]

This phenomenon can be explained by looking at the mass transfer resistances in series model [Nguyen et al, 2001]. Figure 2.12 illustrates the resistance in series model:

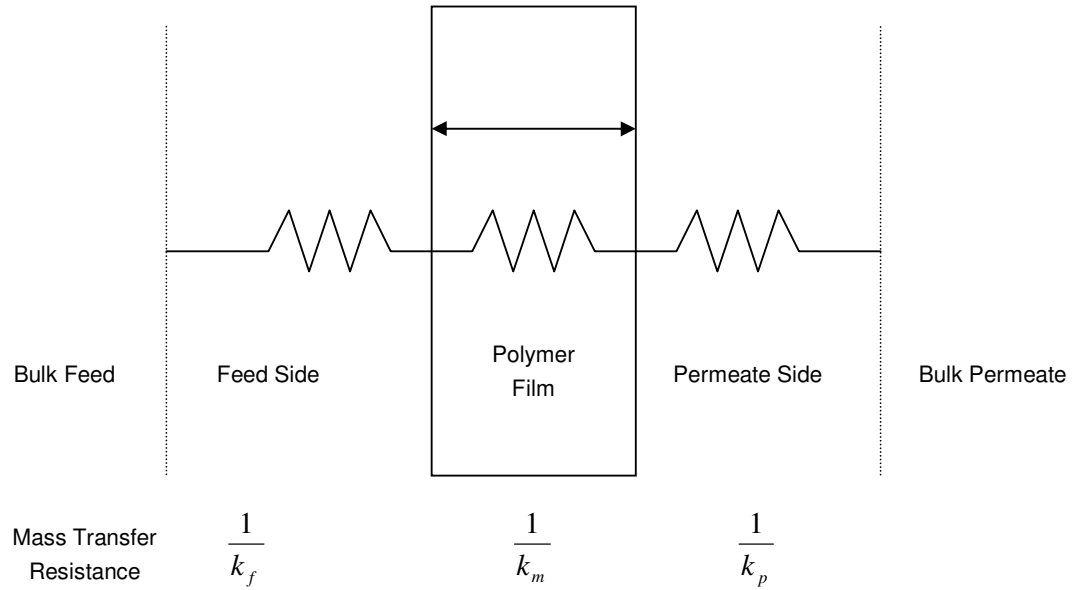


Figure 2.12 Resistances in series model for mass transfer

The total mass transfer resistance is given by the following:

$$\frac{1}{k_t} = \frac{1}{k_f} + \frac{1}{k_m} + \frac{1}{k_p} \quad (17)$$

On the feed side: If there is a liquid in contact with the membrane instead of a gas then the mass transfer resistance on the feed side is negated and there is no concentration gradient between the bulk feed and the membrane, if the liquid itself is diffusing through the material. Generally the mass transfer resistance downstream is negated due to the significantly larger diffusion coefficient of a substance in a gas than in a liquid [Nguyen et al, 2001]. If the bulk liquid is in contact with the membrane then the total mass transfer resistance is reduced to that of the membrane alone and therefore gives a more accurate measure of the permeability of the membrane [Nguyen et al, 2001].

2.8. Standards available to test for breathability

There are various international standards available for the testing of a material's breathability.

2.8.1. British standards

There are three British standards available:

- BS 7209, British Standard Specification for Water vapour permeable apparel fabrics
- BS 3546: Coated fabrics for use in the manufacture of water penetration resistant clothing, Part 4. Specification for water vapour permeable coated fabrics
- BS 3424 Part: 34 Method 37, Testing coated fabrics, Method for determination of water vapour permeability index (WVPI)

These three methods are gravimetric methods. The test membrane is supported on the open mouth of an upright cup containing water. The cup is weighed at specified intervals and the water loss is used to determine the water vapour transmission rate. A reference fabric is tested simultaneously. This is used as a control to minimise the effect of fluctuations in the test conditions.

2.8.2. Canadian standards

- CAN/CGSB2-4.2-M77, Method of Test for Resistance of materials to Water Vapour Diffusion (Control-Dish Method)

This standard is very effective for materials having high water vapour permeability. Six upright cups filled with water are used for the test. Three cups are sealed with a permeable cover while the other three are also sealed with a permeable cover but have the test specimen between the cover and water. The sets of cups are filled with water to three different heights. The

water vapour permeability of the sample is determined from the relationship between the rate of weight loss of water vapour from the test dishes and the thickness of the air layer within these dishes.

- CAN/CGSB 4.2 No. 49-99, Textile Test Method Resistance of materials to Water Vapour Diffusion (the DND Method)

The sample tested is sandwiched between two layers of microporous PTFE membrane. One layer forms the bottom of a dish of water and the other layer is exposed to a stream of dry air. The permeability of the sandwich is determined by the weight loss of the water cell. The PTFE permeability is determined in a separate experiment where the sample is not included in the sandwich. The difference of these values gives the permeability of the sample.

2.8.3. US standards

The methods used are the ASTM E96 methods. These methods are gravimetric methods that have been compared in section 9.2.2. Materials of thickness less than 32mm can be tested using this method.

2.8.4. Italian standards

This standard is called UNI 4818 Parte 26. This test is performed in specially designed cups which should have a mouth of about 1000mm². Three cups are filled with 25ml of distilled water. The sample is preconditioned for 24 hours at 23°C and 60% relative humidity. It is mounted on the cup mouth. The cups are weighed and placed in a desiccators containing silica gel. The cups are reweighed after 24 hours and the weight change of water is used to determine the water vapour transmission rate.

2.8.5. Spanish standards

The Spanish method is called the FNM 817 method. This is another

gravimetric method. The method uses a cup with water in the bottom part. The sample is attached above the water and desiccant is filled in the top part of the cup. The bottom part, filled with water is put in a water bath at 37°C. The top and middle part is exposed to an atmospheric temperature of 20°C. The weight gained by the desiccant is used to determine the water vapour transmission rate of the sample.

2.8.6. Japanese standards

There are three methods used in the Japanese standard JIS L 1099. Methods A-1 and A-2 make use of an upright cup containing water and desiccant. The environment is kept at 40°C. Method B is similar to the ASTM E96 BW method. The specimen is secured on a support floating in a water bath. A cup is sealed with a PTFE film and filled with Potassium acetate. The cup is inverted to make contact with the specimen. The water vapour transmission rate is determined by the change in mass of the test cup.

2.8.7. Sweating Guarded Hot Plate Tests

The evaporative resistance of fabrics is measured using the ISO 11092 or ASTM F 1868 standards using a sweating hot plate. The tests measure the power required to keep the plate heated to skin temperature while water vapour is evaporating from the surface of the plate and diffusing through the fabric [McCullough et al, 2003]. The tests are performed in an environmental chamber in which the relative humidity is maintained at 40%. Figure 2.13 shows the apparatus used for the testing.

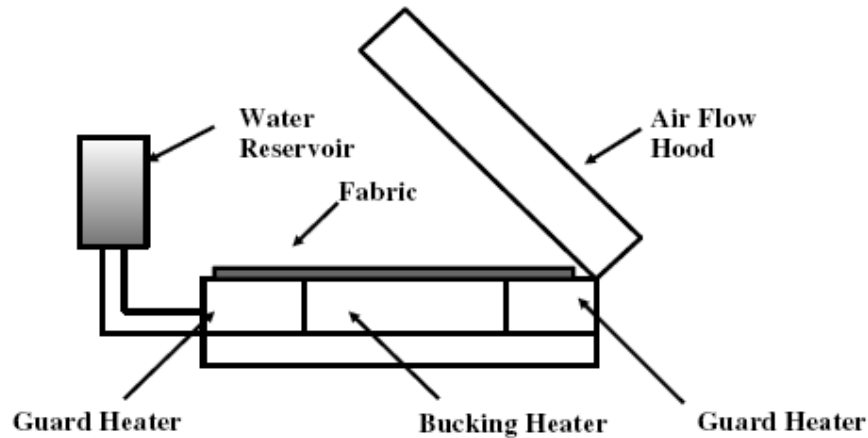


Figure 2.13 Sweating hot plate apparatus [McCullough et al, 2003]

2.9. Blending

Blends constitute over 30% of the polymer market and have experienced an annual growth rate of about 9% over the past 12 years. When blending first began they consisted of only two principle polymers, nowadays commercial blends may contain up to six polymer ingredients. [Utracki, 1989; Utracki, 1991: 86-116] Blends provide the following advantages:

- Better processability.
- Product uniformity is improved
- Products can be tailored to individual consumer needs
- Plants have increased flexibility because formulation changes are quick to implement
- The number of grades that needs to be manufactured and stored is decreased. This results in capital and land savings [Utracki, 1991: 86-116]

Certain polymers have inherent weaknesses. For example, Polycarbonates can stress crack and are susceptible to solvents and chemicals. [Utracki, 1991: 86-116] Blends can be engineered to mitigate the weaknesses of the polymer. By the addition of a lower cost polymer the production costs will decrease giving the process an added benefit. Table 2.5 show how to modify properties by blending and Table 2.6 illustrates the strengths and weaknesses of various polymers.

Table 2.5 Table of Modifying polymers applications [Utracki, 1989]

Property	Matrix	Modifying Polymer
Impact Strength	PVC, PP, PE, PC, PA, PPE, TPE	ABS, ASA, SBS, EPR, EPDM, PBR, SAN, SMA, MBA, HIPS
Stiffness	PC, PA ABS, SAN	TPEs, PEI, PPE PC, PSO
Flame Retardancy	ABS, Acrylics PA, PC	PVC, CPE Aromatics-PA, PSO, copolysiloxanes or phosphazanes
Chemical Resistance	PC, PA, PPE	TPEs, copolysiloxanes polyphosphates
Barrier properties	Polyolefins	PA, EVOH, PVC ₂
Processability	PPE HT thermoplastics PET, PA, PC PVC PSO PO	Styrenics LCP, TPU PE, PBR, MBS, EVOH CPE, Acrylics PA PTFE, SI

Table 2.6 Advantages and Disadvantages of Certain Polymers [Utracki, 1989]

Polymer	Advantages	Disadvantages
Polyamide	Processability, Impact strength, Crystalline	Water absorption, Temperature stability
Polycarbonate	Low-temperature toughness, Temp. stability	Stress cracking, Chemical/Solvent resistance
Polyoxymethylene	Tensile strength	Stress cracking, Impact strength
Polyphenylene ether	Rigidity, Flame retardancy, Temp. stability	Processability, Impact strength
Thermoplastic polyesters	Chemical and solvent resistance	Shrinkage, Low-temp toughness, Processability
High impact polystyrene	Processability, Impact resistance	Temperature stability
Acrylonitrile-butadiene-styrene	Impact strength, Processability, Weatherability	Temperature stability

Not all blends are miscible. In the case of immiscible polymers compatibilization is needed to ensure that the blend is uniform. Compatibilization can be accomplished by a number of different methods:

- The addition of a small amount of co-solvent. The co-solvent will be miscible in both polymer phases. The addition of a di-block copolymer co-solvent tends to be better at reducing interfacial tension whereas the addition of tri-block copolymers tends to improve mechanical behaviour
- The addition of a polymer which has one part that is miscible in one phase and the other part miscible in the other phase. Usually block copolymers are used
- The addition of a large amount (~25-35% w/w) of a core shell copolymer. This method is particularly useful if the blended components have poor impact properties
- Reactive compounding. This is a process in which blends are compounded in the presence of reactants. In this manner compatibilizers are generated in-situ
- Mechano-chemical compounding. Copolymers are generated by chain break-up and recombination [Utracki, 1991: 86-116]

2.9.1. Addition of a copolymer

This method is one of the more popular and better established methods. In addition to affecting the interfacial properties of the blend the rheological properties are also affected. The copolymer can sometimes form micelles. This would reduce its effectiveness at modifying interfacial tension and increase the blend viscosity. An increase in the blend viscosity reduces its processability. [Utracki, 1991: 86-116]

2.9.2. Reactive compatibilization

Reactive compatibilization involves the integration of polymer chemistry and polymer processing. The block or graft polymers are formed in the extrusion or injection phase. Table 2.7 shows the types of copolymer obtained during reactive compatibilization. [Utracki, 1991: 86-116]

Table 2.7 Copolymers formed from various reactions [Utracki, 1989, Utracki, 1991: 86-116]

Type of Reaction	Copolymer Formed
Chain cleavage and recombination	Block and/or Random Copolymers
End group of first polymer reacts with end groups of second polymer	Block Copolymers
Eng group of first polymer react with pendant functionality of second polymer	Graft Copolymers
Covalent crosslinking between reactive groups of two polymers	Graft Copolymer or Cross linked network
Ionic bond formation	Usually Graft but often crosslinked

2.9.3. Methods of blending

A blend can be prepared by a number of techniques: [Utracki, 1989, Utracki, 1991: 86-116]

- Mechanical mixing
- Dissolution in a co-solvent then film casting, freeze or spray drying
- Latex blending
- Fine powder mixing

Mechanical blending is cheaper therefore is the preferred method of blending. The requirements for a compounder/mixer are: [Utracki, 1989, Utracki, 1991: 86-116]

- Shear and elongation stress fields must be uniform
- Control of temperature, pressure and residence time must be easily and flexibly controlled
- Large rheological differences between polymers should not affect homogenization
- Mixing parameters should be easily changed in a controllable manner
- Efficient homogenization before the onset of degradation

These requirements are very difficult to meet. Table 2.8 lists the types of compounders and the advantages and disadvantages of their use.

Table 2.8 Advantages and disadvantages of some mixers [Utracki, 1989]

Machine	Advantages	Disadvantages
Twin screw extruder	Uniform high shear stress flow, Short residence time, Self cleaning, Flexibility.	Capital Cost
Single screw extruder	Cost, Availability, Flexibility.	Poor Control, Low rate of shearing, Long residence time, Dead zones.
Internal mixer	Uniform stress, Control	Capital costs, Operation costs, Long cycle, Batch to batch variations.
Multi stage system	Flexibility, Control, Uniform	Capital Cost

2.10. Starch blends

Starch is a potentially useful polymer that can be used in numerous applications. It is cheap, readily available and a renewable resource. Thus far starch has predominantly been used for the production of biodegradable polymers. [Davis, 2003, Seidenstücker & Fritz, 1998] Starch is also hydrophilic which may improve the WVTR of a hydrophilic membrane. The effect of incorporating starch into breathable membranes has however not been examined yet.

Particulate starch has been incorporated into polymers. [Ha & Broecker, 2002, Santayanan & Wootthikanokkhan, 2003] SEM photographs of starch granules incorporated into polyurethane are shown in Figures 2.13, 2.14 and 2.15.

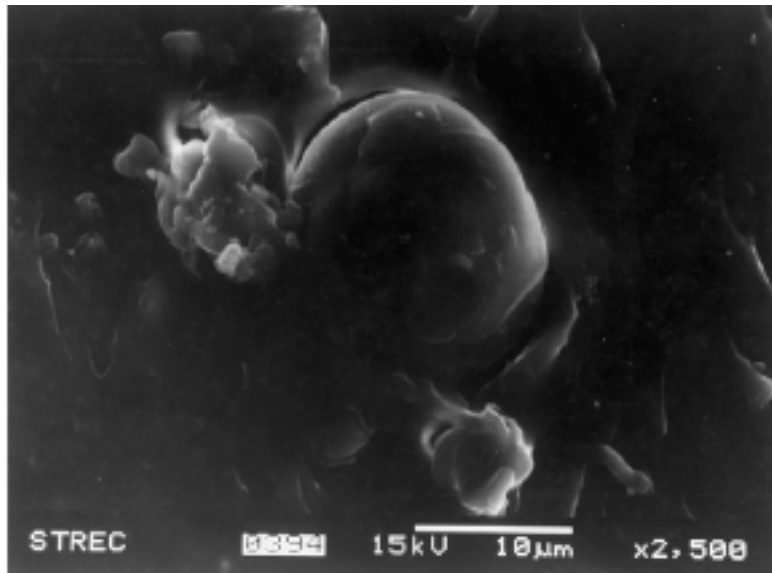


Figure 2.14 SEM photograph of granular starch incorporated into a polyester polyurethane [Santayanan & Wootthikanokkhan, 2003]

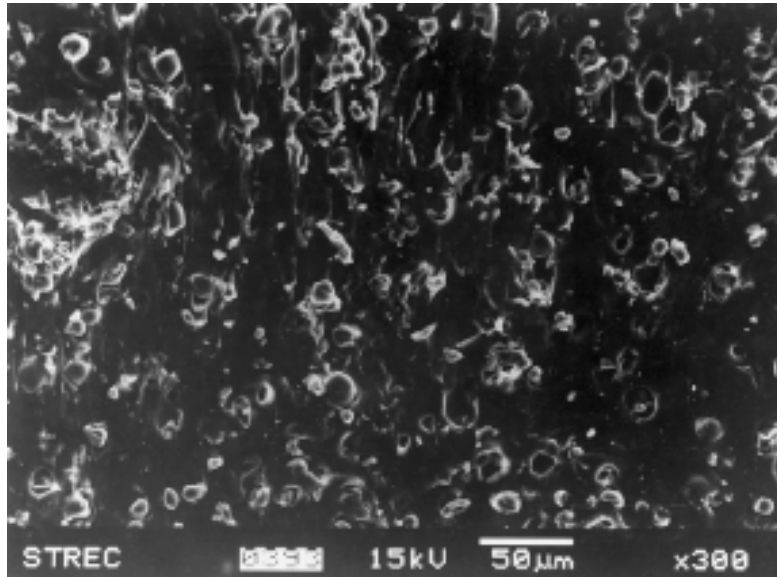


Figure 2.15 SEM photograph of granular starch incorporated into a polyester polyurethane [Santayanan & Wootthikanokkhan, 2003]

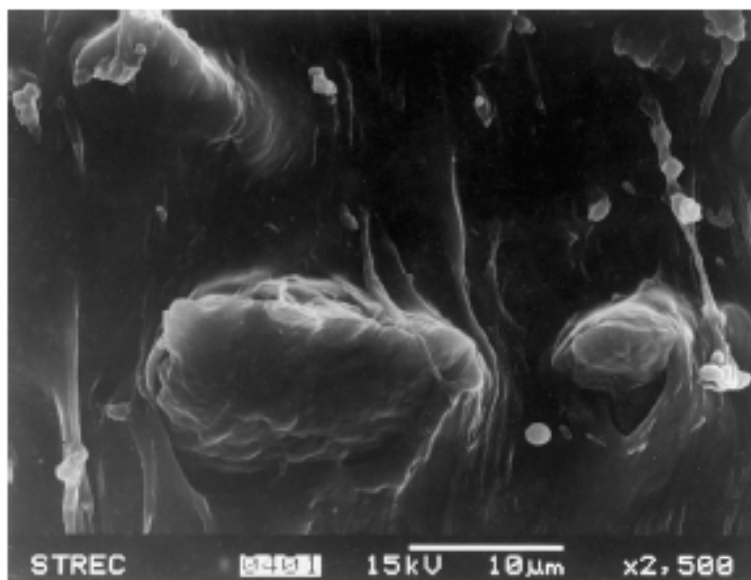


Figure 2.16 SEM photograph of treated granular starch incorporated into a polyester polyurethane [Santayanan & Wootthikanokkhan, 2003]

Starch has been modified in an attempt to increase the amount of starch that can be incorporated into a polymer matrix. In the pursuit for biodegradable materials thermoplastic starch has received a lot of attention [Carvalho et al, 2001; Ishiaku et al, 2002]. Thermoplastic starch is produced by the high temperature shear processing of starch in the presence of a plasticizer.

Research has been focussed on the development of thermoplastic starch in order to obtain materials excluding synthetic polymers [Carvalho et al, 2001].

Thermoplastic starch and granular starch have been investigated as fillers in poly-caprolactone. Granular starch performs better than thermoplastic starch and acts as a rigid particle. Thermoplastic starch preparation utilises water and glycerol for plasticization. During sample fabrication the presence of some water can result in the formation of water vapour which will result in microvoids around the granule. The granular starch acts as a rigid particulate filler with no voids surrounding the granule. This can be used to explain the higher tensile performance of granular starch filled composites [Ishiaku et al, 2002].

Thermoplastic starch blends and filled thermoplastic starch have been investigated for the production of biodegradable materials [Carvalho et al, 2001]. The inclusion of kaolin in a thermoplastic starch matrix has been successfully achieved resulting in polymer composites of improved mechanical properties [Carvalho et al, 2001].

2.11. Recommendations

Microporous membranes generally result in a higher performance than hydrophilic membranes but are more difficult to produce. The production of a microporous membrane may involve solvents or high precision equipment which is very costly. Due to the decreased complexity of producing hydrophilic membranes and the improved mechanical properties the modification of hydrophilic membranes were examined.

Cheap readily available material should be used for the modification of the membrane. Starch is a potentially useful, cheap and renewable resource that can be utilized. The use of starch in membranes results in a cost benefit. Other cheap naturally abundant fillers were also attempted and compared to that of starch. Granular starch when incorporated into polymer results in a dispersion of particles that are considerably larger than 15 μ m. The

breathability of the membrane is improved when the membrane thickness is decreased. Therefore it is desirable that the membrane thickness is approximately $10\mu\text{m}$ - $20\mu\text{m}$. Granular starch is therefore not suitable for the production of a thin breathable membrane. It is desirable for two molten phases to be blended in order to achieve a membrane thickness of less than $20\mu\text{m}$.

The equipment that is used for the manufacture must be readily available. Extruders are used for the blending of the compounds before a film blower is used for membrane manufacture.

The Spanish method is suitable for breathability testing. It is a rigorous method that does not need a humidity chamber.

3. Raw Materials

The thermoplastic polyurethane resin Pellethane 2103-70A based on polytetramethylene glycol ether was obtained from DOW Plastics. The data sheet for Pellethane 210-70A is in Appendix G. The polyethylene resin LDPE Q1388/2 was obtained from Sasol Polymers. The commercially available membranes were also tested. These are summarised in Table 3.1.

The starch than was used is summarised in Table 3.2. Glycerol of 99% purity was supplied by Merck.

Diatomite was supplied by F.R.M. Minerals in Krugersdorp. The grade obtained was Diatomite SF90. As impermeable filler Dicalite was used. It is diatomaceous earth supplied by Chemserve Perlite with 76.2 SiO₂ content.

Stearic acid coated calcium carbonate was supplied by Idwala from Port Shepstone under the trade name Kulucote 2. The particle size of the calcium carbonate was approximately 2.3 µm.

Alumina silicate was supplied by Sarde Chemicals of Johannesburg. The grade obtained was Plasfill 5 which contained 53.5% SiO₂ and 34.3% Al₂O₃. The average particle size was approximately 3.8 µm.

Hydrotalcite Alcamizer 1 was supplied by Kyowa Chemical Industry Co.,Ltd. It is an aluminium-magnesium carbonate hydroxide with the chemical composition of CO₃.2AlH₆O₆.4HO.6Mg.

Sodium bentonite "Bentonite MD" (average particle size 2.85 µm) was supplied by G&W Base Industrial Minerals in Wadeville. Calcium bentonite "Bentonite Calcium 10011" was supplied by G&W Base Industrial Minerals in Wadeville (with 3.9 % particles > 100 µm).

The materials were used as supplied.



Table 3.1 Polymers tested and the class of polymer

Sample Name	Polymer
Elvax 650	Ethyl Vinyl Acetate
Escorene 2285	Ethyl Vinyl Acetate
Pebatex MX 2234	Polyamide
PEBAX MV3000 SA 01	Polyamide
PEBAX MV6100 SL 01	Polyamide
Platilon MX 1389	Polyamide
Arnitel	Polyester
Desmopan 786 (TPU)	Polyurethane
Pearlthane 11T 85 (TPU)	Polyurethane
Pellethane 2103 70A (TPU)	Polyurethane
Polycoating PU Comfort plus F20	Polyurethane
Porell 04	Polyurethane
Porell P3	Polyurethane
Porvair	Polyurethane
Porvair P412 PU	Polyurethane
Porvair PU P330	Polyurethane
PU halopur 4251	Polyurethane
PU hydrophilic comfort plus F25 white	Polyurethane
Texin 950	Polyurethane
Texin 990	Polyurethane
Faitex Polyfix D-2 PU	Polyurethane
Coated Tetratex PTFE TX 4501	PTFE
Goretex	PTFE
Polytetrafluoroethylene commercial film (PTFE)	PTFE



Table 3.2 Starch details

Filler	Trade name	Supplier	Details
High Amylose Starch	Hi-Maize	African Products	70% amylose 30% amylopectin
Low Amylose Starch	Amioca	National Starch and Chemicals	2% amylose 98% amylopectin

4. Experimental

4.1. Sample preparation

The TPS was prepared by mixing starch, glycerol and water. The starch-glycerol-water mixture is allowed to set for a day to ensure that the glycerol has soaked into the starch before the mixture is mixed in a high speed mixer for 10 to 15 minutes until homogeneous. The water content used is 5% on a starch mass basis. After mixing in the high speed mixer the starch-glycerol-water mixture is fed into a single screw extruder. The TPS and filled TPS were melt-processed on a single screw extruder obtained from Rapha Extruders having a 25mm screw diameter and an L/D ratio of 30. The TPS and filled TPS was extruded using a screw speed of 65 rpm and the following temperature profile: 90 °C, 100 °C, 100 °C, 90 °C.

All blends were compounded using a twin screw extruder Berstorff Model: EV 40, Screw configuration: Counter rotating, Screw diameter:30mm, Screw L/D: 25 Screw speed range:0-230Hz. The TPS and Pellethane pellets were fed to the extruder at a feed rate of 20kg.hour⁻¹ and a screw speed of 160 rpm. The following temperature profile was used for the extrusion: (feed) 70 °C, 150 °C, 155 °C, 160 °C, 160 °C, 160 °C, 160 °C, 160 °C, 140 °C (nozzle).

After compounding the TPS/TPU, the resulting blend was pelletized using side cut pelletizer model LSC 108 obtained from LabTech Engineering Company LTD. The target pellet length was between 50-100mm.

Membrane films were blown on a 3-layer film blower (Model LF-400 COEX supplied by LabTech Engineering Company LTD). The support membranes of polyethylene were extruded at a constant temperature profile of 175 °C and a screw speed of 70 rpm. The filled polyurethane membrane was extruded between two sheets of support membranes at a constant temperature profile of 150 °C and a screw speed of 40 rpm.

4.2. Testing of permeability

Permeability tests were carried out using the Spanish FMN 96 method. Commercial and designed samples were tested using the same method. The method is a gravimetric method.

4.2.1. Apparatus used

The testing of the membrane permeability was performed using the following:

- Test cup which is described in 4.2.2.
- A water bath
- Heat circulator
- Balance
- Stop watch

4.2.2. Description of the test method and apparatus

A cup which is made of a non-corroding, water impermeable material was constructed. Detailed drawings of the cup are in Appendix F. The bottom section of the cup is filled with distilled water, the membrane being tested is attached to the middle section of the cup and a desiccant is placed in the upper layer of the cup. The cup is placed in a water bath kept at 37°C while the upper layer of the cup is exposed to the atmosphere where the temperature is kept constant at 20°C ± 2°C. The part of the cup submerged in the water bath is approximately 10cm in height

Depending on the membrane being tested the sample is left for two to 36 hours and the weight loss or gain by the membrane and desiccant is measured and used in the calculation of water vapour transmission rate (WVTR). Generally the membranes were left for two hours to minimise experiment time and because steady state was reached at approximately 2 hours. The starch filled polyurethane membranes should take the longest to

reach equilibrium due to the hydrophilic nature of the starch. Figure 4.1 shows the equilibrium curve obtained Pellethane filled with 20% TPS containing 40% glycerol. Membranes containing less hydrophilic filler will reach equilibrium faster than membranes containing more hydrophilic filler.

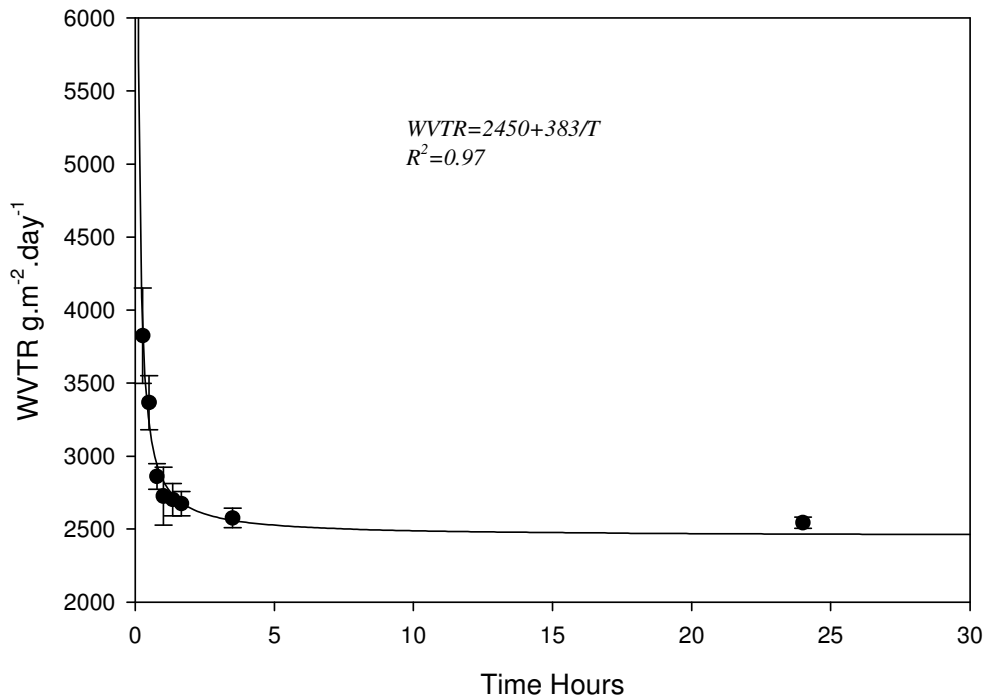


Figure 4.1 Equilibrium curve for TPS filled polyurethane membranes

4.2.3. Calculation of the WVTR

The flux of the water vapour through the membrane was used to determine the WVTR of the membrane. The following equation was used where the increase in the mass of desiccant and the membrane was determined for the duration of the test:

$$WVTR = \frac{\Delta M}{AT} \quad (18)$$

4.3. Blocking Tests

Blocking refers to the tendency of polymer films to self-adhere when pressed together under load for an extended time. Tacky membranes show a strong tendency to block. The ASTM D 1146-00 blocking test was applied at 38°C and 58°C to characterize the cohesive blocking tendency of the membranes. In this test the two membrane sheets are pressed together between two sheets of glass at a pressure of 6.89 kPa for a time of 24 hours at the indicated temperature. The ease of separation, when pulled apart manually, is used to grade the observed behaviour. Samples are categorized as “non-blocking”, 1st degree blocking and 2nd degree blocking depending on the ease of separation. 1st degree blocking describes an adherence between the surfaces under test such that the upper specimen will cling to lower specimen, but may be parted with no evidence of damage to either surface. 2nd degree blocking describes an adherence between the surfaces under test such that the upper specimen will cling to lower specimen and result in damage upon separation. All tests were performed in sextuplet with the blocking reported as the most severe observation of the 6 specimen.

4.4. Scanning Electron Microscope

The morphology of the blends was examined using a scanning electron microscope (SEM) (LEO 1525 Field Emission scanning electron microscope with Oxford's INCA system). The samples were sputtered with gold before examination.

4.5. Software

Sigmaplot 2001 was used for the analysis of the data and the fitting of equations to the experimental data. Sigmaplot was also used to perform the statistical evaluation of the data.

4.6. Tensile Tests

Tensile tests were performed on samples using the LRX Plus tensile tester supplied by Lloyd Instruments. Samples were tested in sextuplets and in both the machine and cross direction. The extension rate for the tests was 50 mm.min⁻¹.

5. Results and discussion

5.1. Commercial membranes

Due to the variability between test-methods all commercial samples obtained were tested for water vapour transmission rate (WVTR) using the Spanish method. The partial pressure gradient in equation 8 can be assumed to be constant for all tests due to the constant conditions being maintained in the cup compartments. Normalizing the flux for varying thickness allows us to compare permeability provided that the membrane is at equilibrium or close to equilibrium.

$$P = \frac{J}{\Delta p/x} \quad (8)$$

The results of the tests are summarized in Figure 5.1. In order to compare all membranes the WVTR was normalized to 20 μm . The relationship between permeability of the membrane and the membrane thickness is a non linear because the diffusion rate is non-linearly related to the diffusion path length. Initially the membranes were normalized linearly. The accuracy of the normalization decreases with an increasing deviation from the 20 μm thickness; therefore the membranes were fabricated such that the thickness is as close as possible to 20 μm .

The average thickness of the membrane was determined by making multiple measurements of thickness on different point of the membrane using a micrometer. On average thirty five measurements were performed and an average of the thickness was used. At least three experiments were performed and an average was used to determine the WVTR.

The WVTR of the Porvair PU P330 and the Porelle P3 membranes performed the best. These polyurethane membranes feature pinholes formed by the dissolution and removal of filler particles from the polymer matrix using DMF a solvent. SEM photographs of the different Porvair membranes are shown in

Appendix B and in Figure 5.2. The SEM photographs clearly show the pinholes that are present in the polyurethane matrix. Due to the pinholes the WVTR is higher than a polyurethane membrane that does not have pinholes. This is because diffusion will occur via Fickian diffusion and via the pinholes. The other polyurethane thermoplastics membranes that were blown did not perform as well as the Porvair membranes because the WVTR was only due to Fickian diffusion.

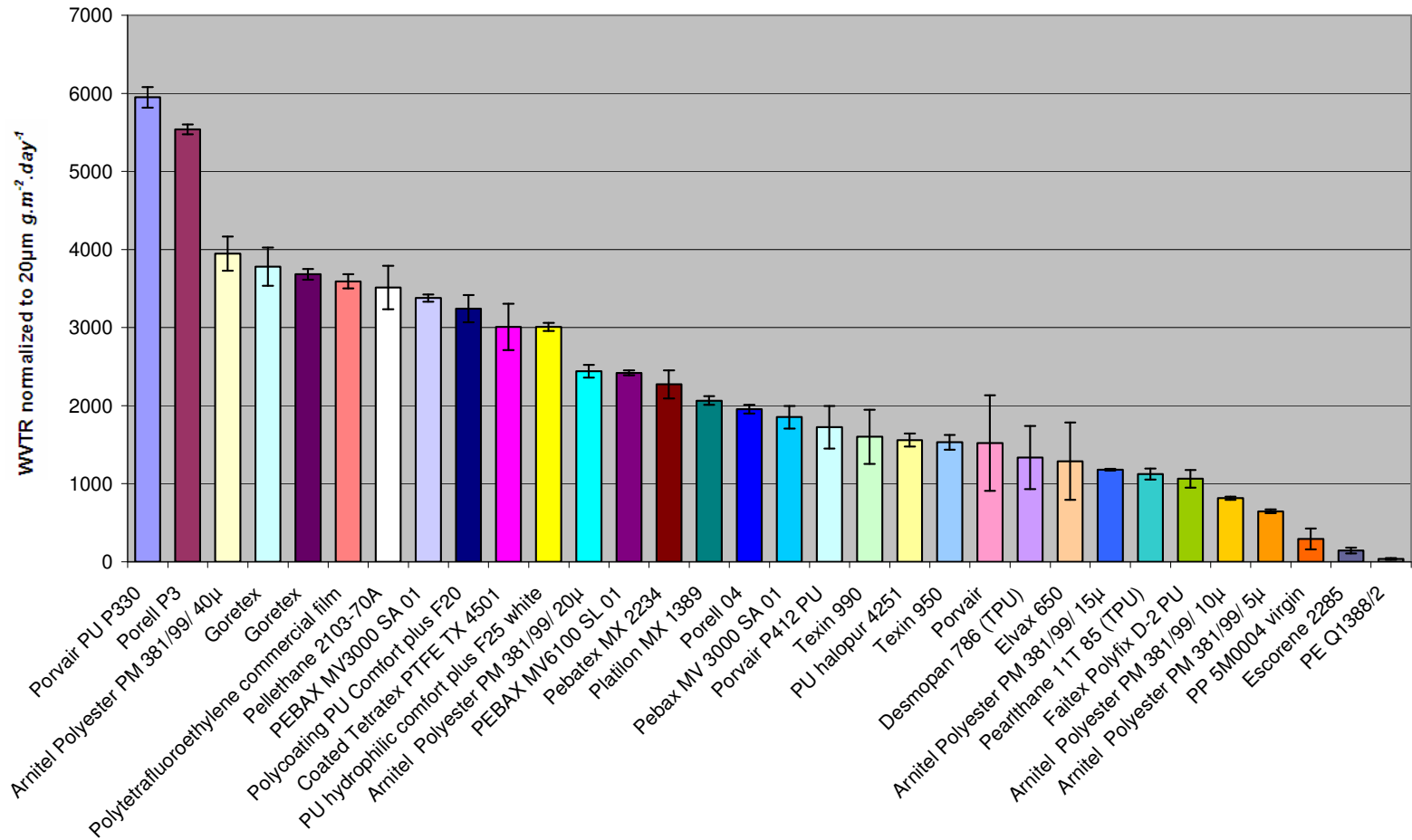


Figure 5.1 WVTR of commercial membranes tested

GoreTex membranes performed relatively poorly compared to the Porvair membranes and other hydrophilic membranes such as the Pebax membrane. GoreTex membranes consist of an interconnected microporous network of PTFE micro-fibrils. The SEM photographs of the GoreTex membranes showing the interconnected porous structure are in Appendix B with the membrane at 10000 times magnification shown in Figure 2.2. Figure 5.3 shows the Pebax membrane. The two membranes perform similarly even though the GoreTex membrane is microporous. It is expected that the permeability through the interconnected porous structure of the PTFE membrane be significantly greater than the permeability of the hydrophilic membranes due to the pinholes. The poor performance observed can be attributed to the polyurethane coating that is applied to the stretched PTFE membranes to give them increased durability and reduced creep. The coating reduces the membrane to a bi-component membrane and therefore the permeability of the membrane is limited to the permeability of the most impermeable layer as suggested in the literature [Painter, 1996].

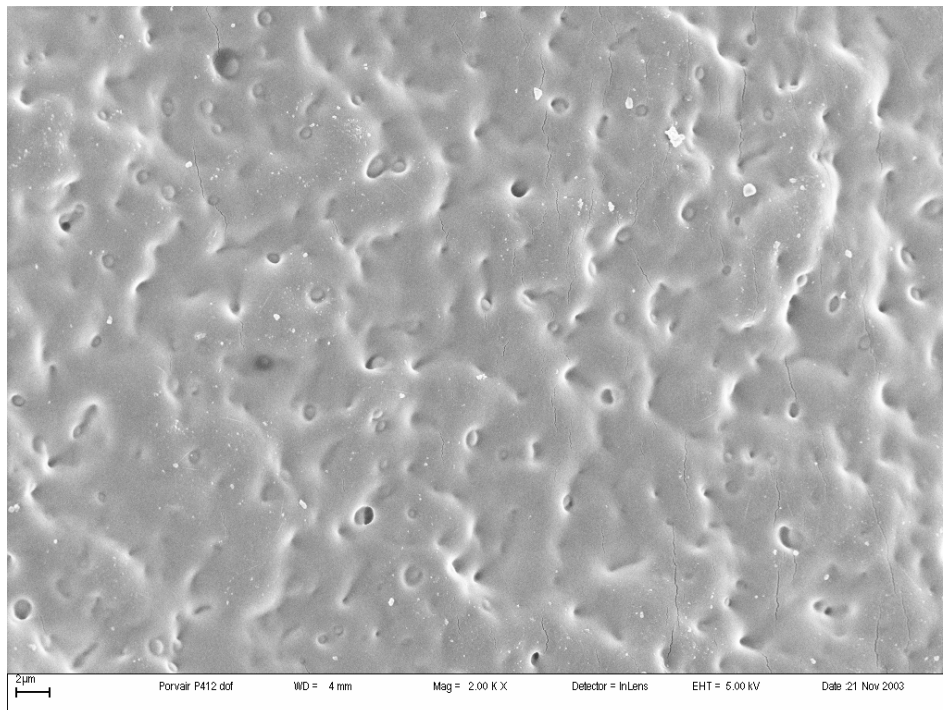


Figure 5.2. Porvair P412 membrane magnified 2000 times (Side not exposed to DMF)

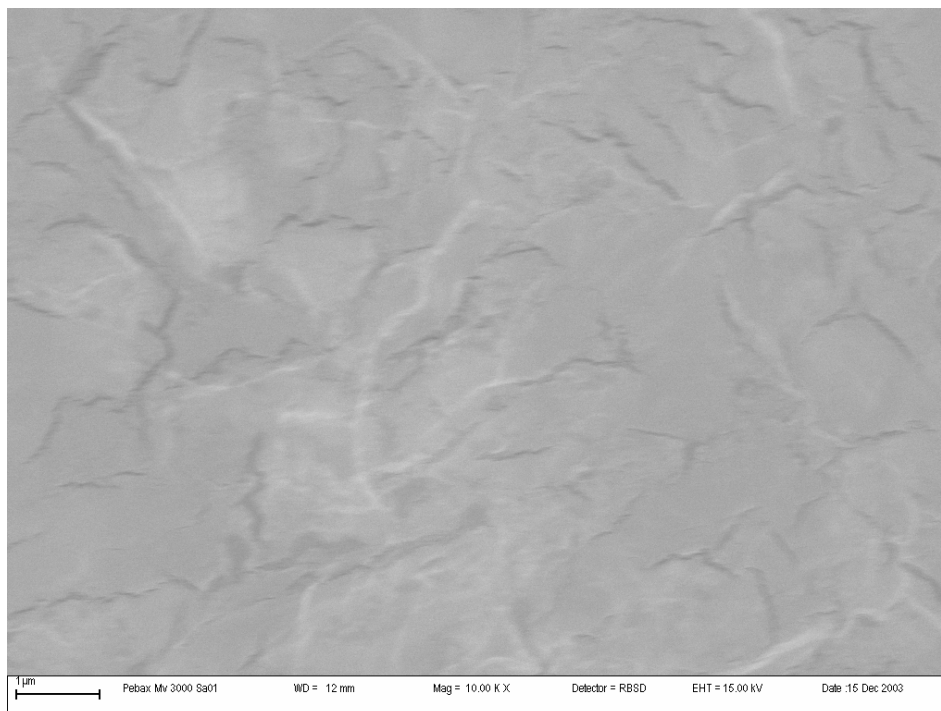


Figure 5.3. Pebax Mv 3000 Sa01 membrane magnified 10 000 times

WVTR results obtained for the Pellethane 2103 70A membrane and the Pebax 3000 MV SA1 membrane showed relatively high performance compared to the other hydrophilic polymers tested. SEM photographs of Pellethane and Pebax are in Appendix B, Figures 7.1 - 8.3. The membranes are hydrophilic with no pinholes. The membrane is a solid barrier to water as can be seen from the SEM photographs. The permeability of the membranes is lower than the porous membranes because mass transfer is only due to Fickian diffusion. Pellethane was chosen as the membrane matrix due to the significant cost reduction compared to Pebax.

The Pellethane 2103 70A membranes produced were very tacky and would tend to stick to it self when blown. Due to the blocking, the membrane is then difficult to separate into a single layer membrane. This makes the membrane undesirable for commercial application because the membrane orientation will be difficult to control. The addition of anti-tack agents helps decrease the tackiness of the membrane.

The relationship between permeability and membrane thickness of Pellethane

membranes is shown in Figure 5.4. The relationship shows that the permeability is inversely proportional to the thickness of the membrane as would be expected from Fick's law.

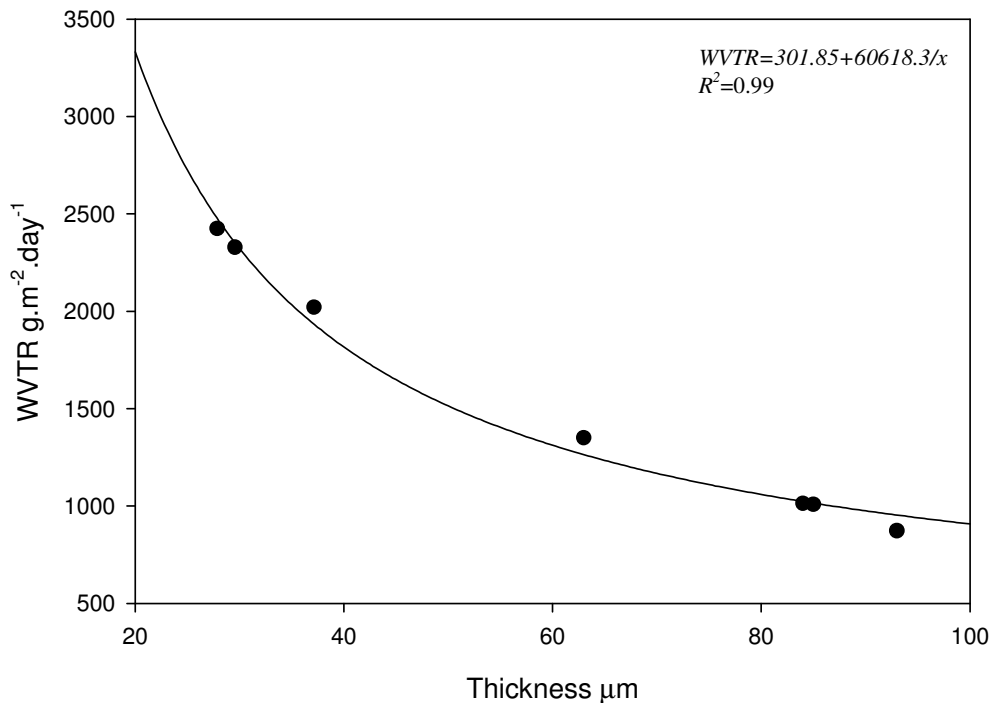


Figure 5.4 WVTR of Pellethane membranes as a function of thickness

5.2. Permeability of filled membranes

5.2.1. TPS filled membranes

Various experiments were performed and the different sets of data were plotted in order to obtain an expression for the relationship between the membrane permeability and thickness. Different expressions were obtained for the membranes of different filler type and concentration to improve the accuracy of the normalization. All data showed similar trends as seen in Figure 5.4. Figure 5.5 shows the permeability of membrane as a function of thickness for Pellethane membranes filled with 20% (m/m) TPS made with 40% (starch mass basis) glycerol. There is an inverse relationship between

thickness and permeability. Table 5.1 summarises the relationship between thickness and permeability for membranes filled with varying starch content made from varying glycerol content.

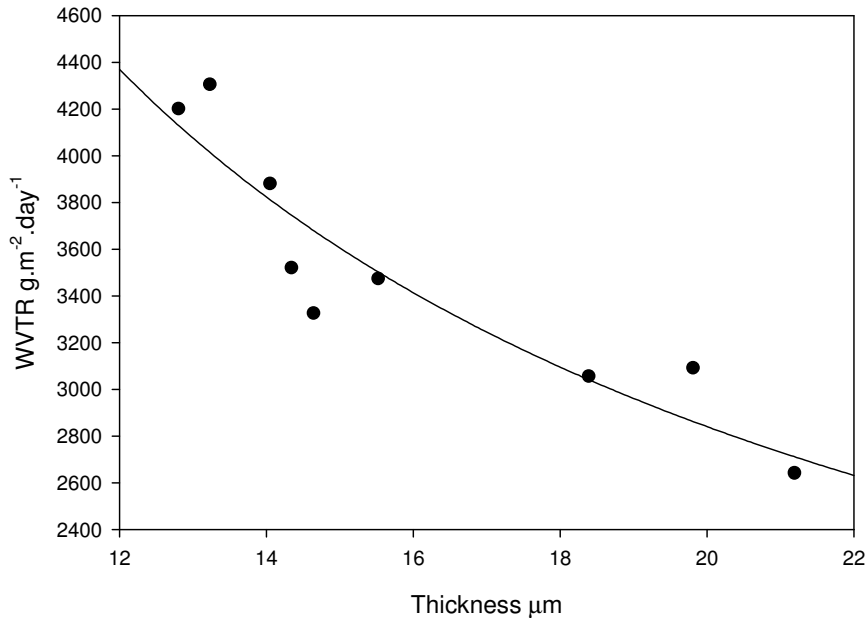


Figure 5.5 WVTR of 20% (m/m) TPS (High Amylose)-Pellethane membranes as a function of thickness. TPS made with 40% glycerol on a starch mass basis.

Table 5.1 Fitted equations for Pellethane filled with TPS (High amylose) at different levels containing varying amounts of glycerol

Formulation	Fitted Equation	R ²
10%TPS(30% Glycerol)	$WVTR = 2122.1 + \frac{17707.2}{x}$	0.59
10%TPS(40% Glycerol)	$WVTR = 1487.1 + \frac{31352.9}{x}$	0.72
20%TPS(30% Glycerol)	$WVTR = 1653.1 + \frac{19893.7}{x}$	0.86
20%TPS(40% Glycerol)	$WVTR = 547.5 + \frac{45865.2}{x}$	0.86

The addition of TPS to the polyurethane matrix resulted in a decrease in the WVTR of the membrane as can be seen in Table 5.2 and Figure 5.5. An increase in the amount of TPS in the composite membrane resulted in a decrease in the WVTR of the membrane as shown in Table 5.2. The starch is therefore less permeable than the TPU matrix and an increase in the amount of starch in the composite membrane will result in a decrease in WVTR.

Table 5.2 The effect of TPS (Hi Maize) and glycerol in TPS on the WVTR of a polyurethane membrane

TPS	Glycerol	WVTR _{Avg}	Std. Deviation
wt %	wt% (Starch Basis)	g.m ⁻² .day ⁻¹	g.m ⁻² .day ⁻¹
20	30	2648	148
20	40	2832	110
10	30	3006	307
10	40	3060	138
0	-	3425	433

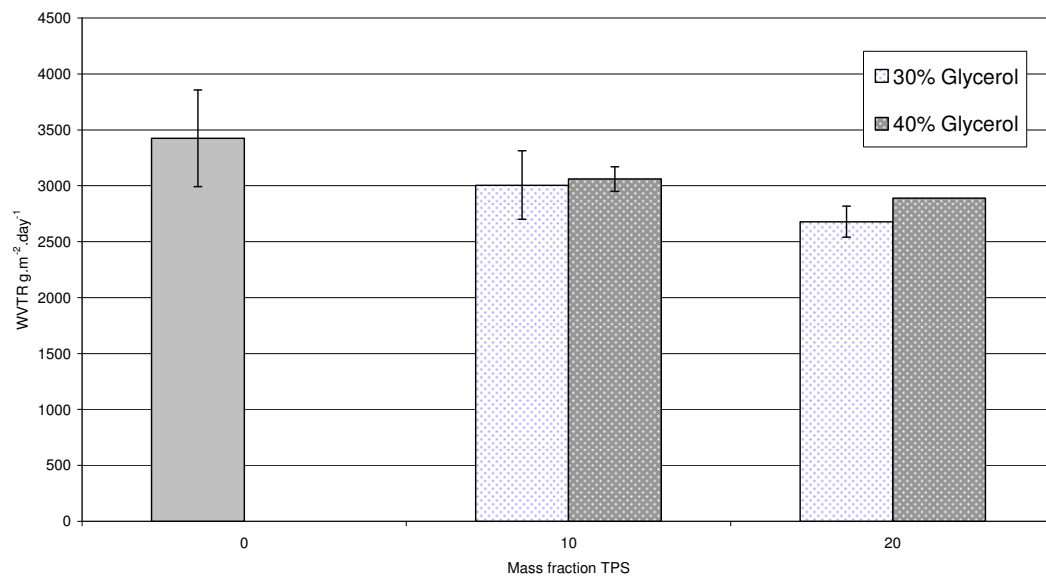


Figure 5.6 WVTR comparison of different TPS blends

TPS with higher plasticizer content performs better than TPS with lower plasticizer content. The TPS-filled membrane results were examined for statistical significance. There was a significant decrease in the permeability of the filled membranes compared to the unfilled membrane. Table 5.3 summarises the results for the unpaired t-test performed between unfilled Pellethane membranes and filled Pellethane membranes. The incorporation of TPS containing 30% or 40% glycerol at 10% and 20% addition levels in Pellethane results in membranes of WVTR significantly different to that of the unfilled Pellethane membranes. At 20% TPS addition the level of glycerol used results in a significant difference between the averages of WVTR obtained for the filled samples while at 10% TPS addition the level of glycerol used does not significantly impact on the averages of WVTR obtained for the filled samples. Table 5.4 summarises the t-test results. The reason for the difference between the 10% and 20% TPS filled membranes can be attributed to the larger difference (2 fold increase) in starch volume fraction at higher TPS addition levels. The starch is less permeable than the matrix. Inclusion of more starch results in a more significant decrease in the permeability of the composite membrane.

Table 5.3 Students t-test results comparing the mean of WVTR for Pellethane membranes with the mean of WVTR for filled Pellethane membranes

Filler	p-value
10% TPS (30% Glycerol)	0.009758
20% TPS(30% Glycerol)	2.99E-05
10% TPS (40% Glycerol)	0.004145
20% TPS(40% Glycerol)	2.53E-05

Table 5.4 Students t-test results comparing the mean of WVTR for filled Pellethane membranes in which the filler addition level is constant but the plasticizer content varies

Membrane 1	Membrane 2	p-value
10% TPS (40% Glycerol)	10% TPS (30% Glycerol)	0.0441
20% TPS(40% Glycerol)	20% TPS(30% Glycerol)	0.7041

The plasticizer may however have no significant impact on the permeability of the composite membrane. Increasing the glycerol content in the TPS represents a decrease in the amount of starch in the TPS. Since starch is less permeable than the TPU matrix, membranes containing lower volumes of starch will perform better than membranes containing higher volumes of starch.

The effective change in permeability for the blends in Table 5.2 was plotted as a function of starch volume fraction in Figure 5.7. The decrease in permeability is a linear function of the starch volume fraction. The increase in glycerol effectively results in decrease in the starch volume fraction and a lesser decrease in the permeability of the composite membrane. Figure 5.7 shows that the change in permeability as a function of filler volume fraction is linear. This suggests that the starch content is the dominant factor in the effective decrease in permeability.

The starch is not impermeable as shown in Figure 5.8 which compares the experimental results to predictions of the Maxwell and Bruggeman models for low volumes of impermeable spheres. The Maxwell equation for impermeable spheres and the Bruggeman equation results in predictions that are identical over very dilute regions. From this plot we can see that the TPS is not completely impermeable. The permeability is however significantly less than that of the matrix.

The Maxwell-Wagner-Sillars model was also compared to the experimental

data. Shape factors of 0.4 and 0.5 were used because the thermoplastic starch is easily deformed. Due to the film blowing process aligning and stretching the starch particles in the direction of the membrane the starch particles will not be spherical. Thermoplastic starch is more easily deformed due to its plastic nature therefore it is expected to align in the plane of the membrane. [Ishiaku et al, 2002] The particles will be oblate ellipsoids as shown in the prior art and SEM pictures in Appendix B [Ishiaku et al, 2002; Santayanan & Wootthikanokkhan, 2003].

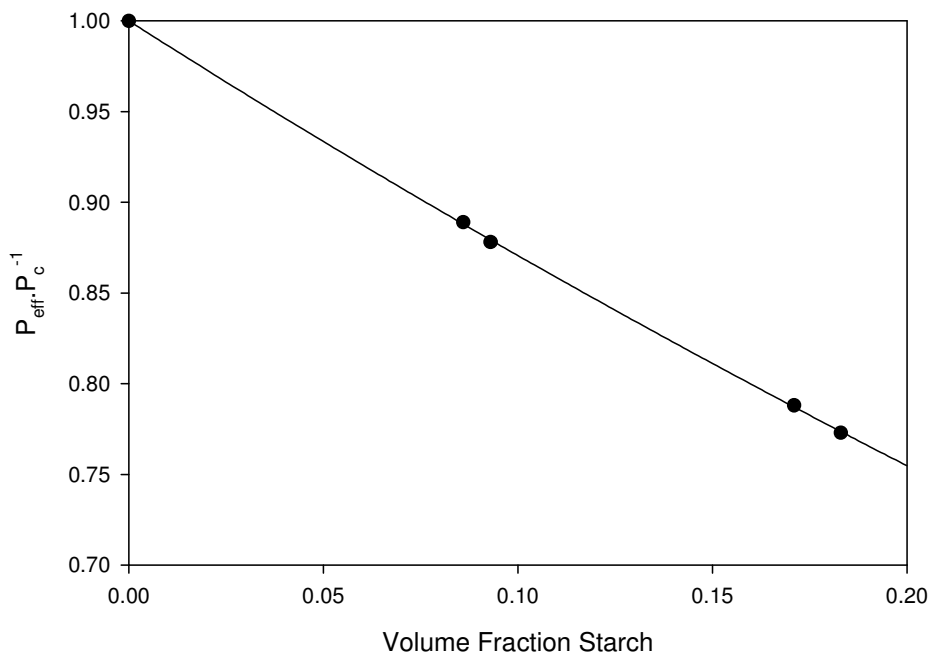


Figure 5.7 The change in permeability as a function of filler volume fraction

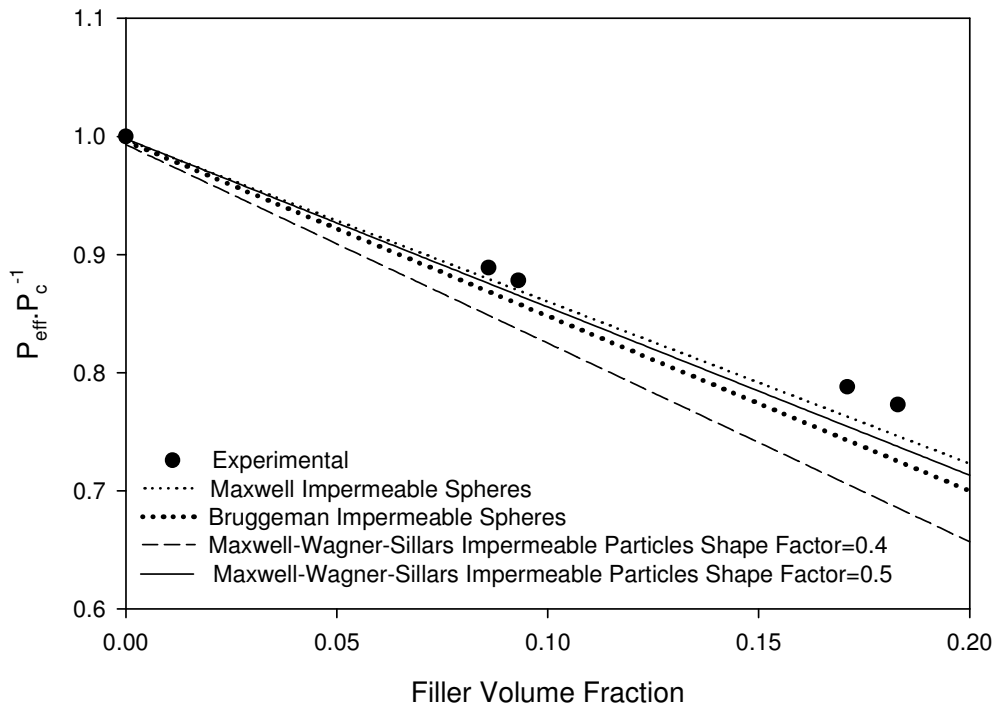


Figure 5.8 Comparison between the experimental change in permeability as a function of filler volume fraction and the change in permeability predicted by the Maxwell model for impermeable spheres

As the concentration increases the deviation between the predictions becomes apparent with the Maxwell equation resulting in an inflated prediction. The Maxwell equation is valid for low filler concentration and the Bruggeman is valid for high filler concentration. Therefore this trend is expected particularly at higher concentrations. Figure 5.9 shows a plot of the Bruggeman equation at varying filler volume fraction and α .

The Maxwell-Sillar-Wagner model was used to determine the permeability of the starch if the granules were slightly deformed and resembled oblate spheres. Thermoplastic starch is more easily deformed due to the plasticization [Ishiaku et al, 2002] and is likely to deform in the machine direction. In the film blowing process there will be some alignment in the machine and cross direction due to stresses induced by the bubble formation and stretching. The alignment expected will be similar to the Alignment A

shown in Figure 5.10.

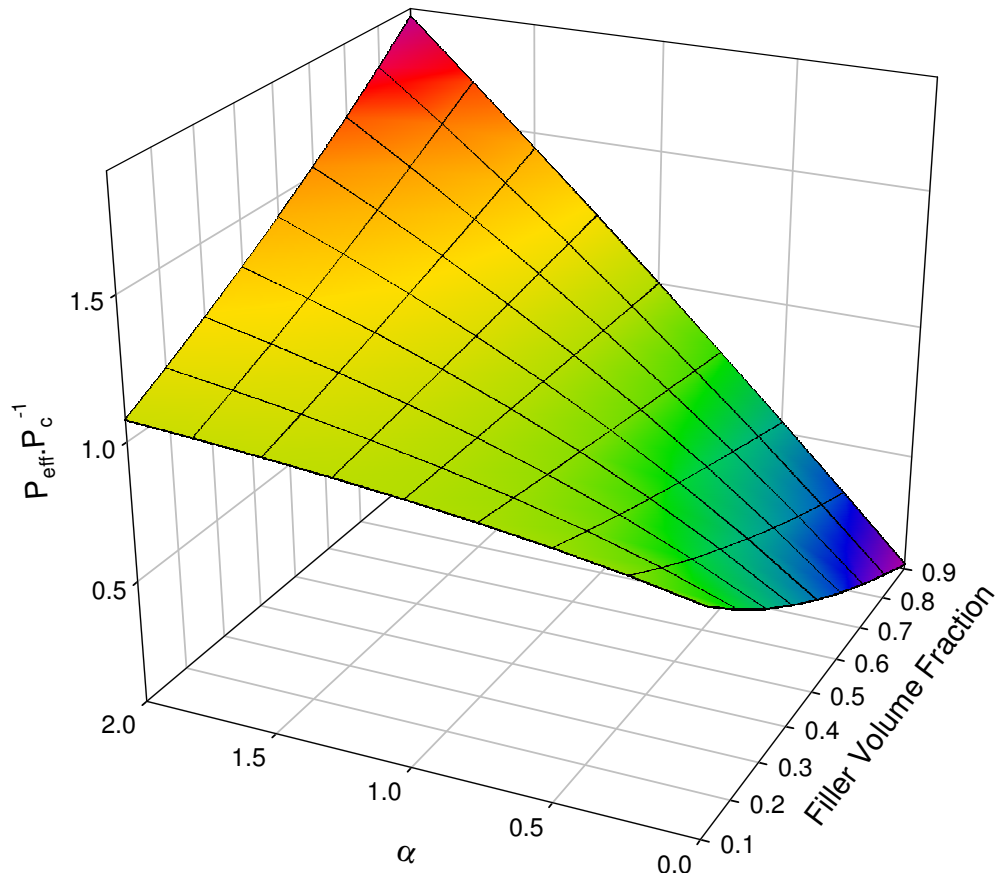


Figure 5.9 The change in permeability as a function of α and filler volume as predicted by the Bruggeman equation

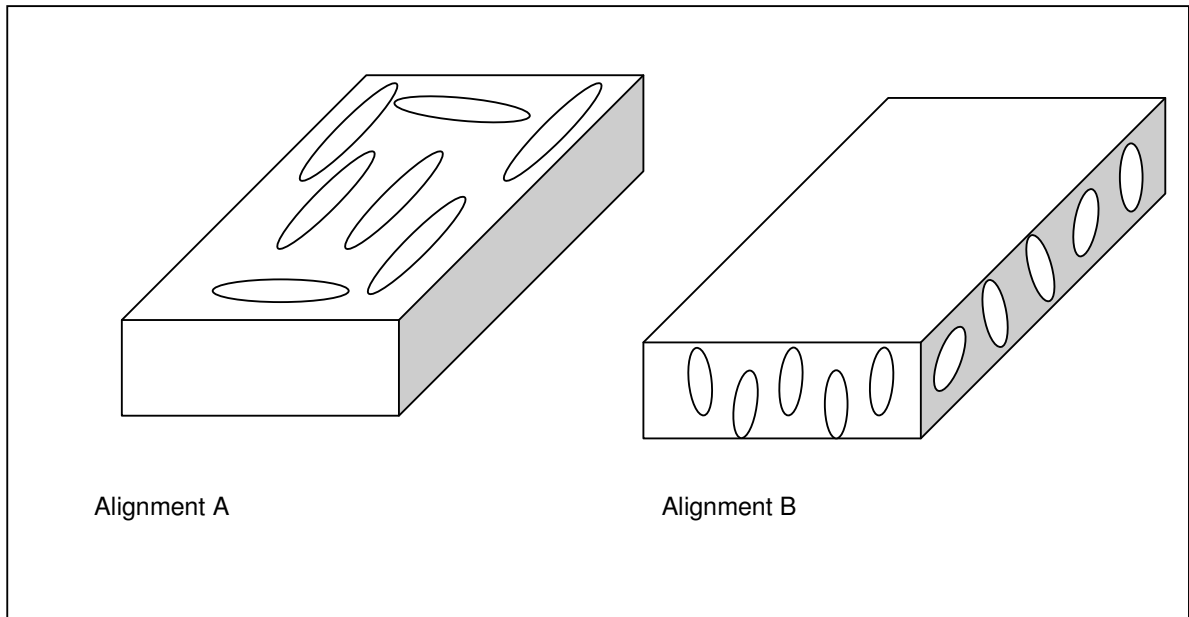


Figure 5.10. Alignment possibilities for the filled membranes

The Maxwell-Wagner-Sillar model was used to generate data to illustrate the effect of shape factor and volume fraction, of the filler, on the relative change in permeability. Figure 5.11 and 5.12 shows this relationship. If the filler is less permeable than the matrix there will be a decrease in permeability with increasing volume fraction and decreasing shape factor. If the filler is more permeable than the matrix there will be a decrease in permeability with a decreasing volume fraction and decreasing shape factor. The dependence on volume fraction is expected because the maximum permeability of the blend is dictated by equation 10:

$$P_{eff}^{max} = \phi_C P_C + \phi_D P_D \quad (10)$$

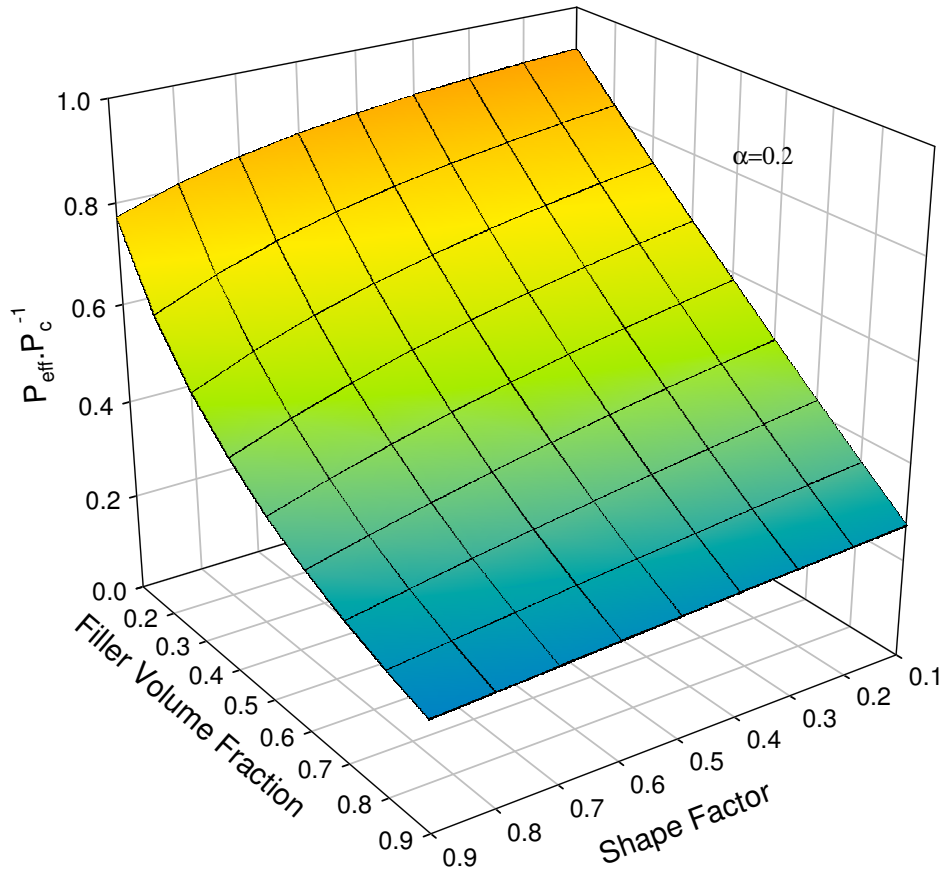


Figure 5.11 The change in permeability as a function of shape factor and filler volume as predicted by the Maxwell-Wagner-Sillar model for $\alpha=0.2$

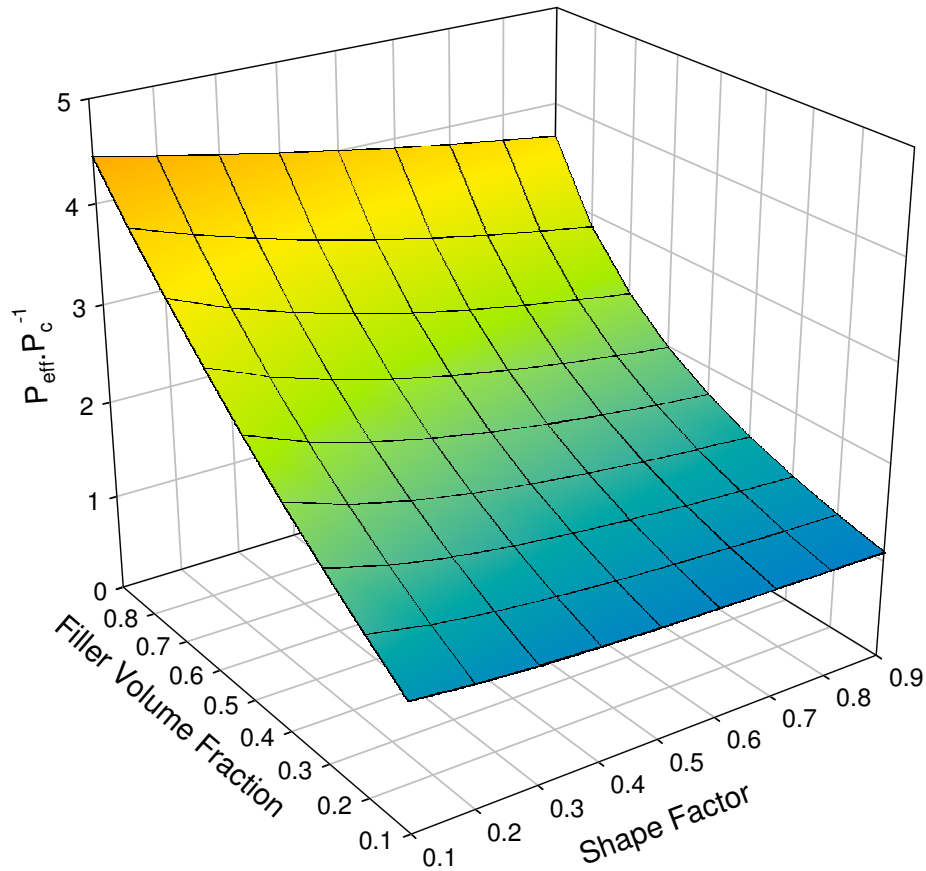


Figure 5.12. The change in permeability as a function of shape factor and filler volume as predicted by the Maxwell-Wagner-Sillar model for $\alpha=5$

The effect of the shape factor is also expected because of the changes in flux as shown in Figures 2.9 and 2.10. In the case of a filler of higher permeability than the matrix the ellipsoid particle will preferentially allow the penetrant to permeate and will do so at a faster rate than the matrix. If the ellipsoid is aligned such that its major axis is perpendicular to the permeation (Alignment A in Figure 5.10) then the penetrant will have a small distance to travel across before re-entering the matrix. If the ellipsoid is aligned such that its minor axis is perpendicular (Alignment B in Figure 5.10) to the permeation then the penetrant will have a larger distance to travel before re-entering the matrix. This would resemble the situation of having pinholes compared to microvoids.

Similarly the alignment of impermeable ellipsoid particle will have similar effects.

Using the Maxwell equation the permeability of the dispersed phase was determined by regression. The ratio of the permeability of the disperse phase permeability to the continuous phase permeability was estimated to be approximately 0.06 implying a water vapour permeability of approximately $205 \text{ g.m}^{-2}.\text{day}^{-1}$.

Using the Maxwell-Wagner-Sillar model and varying the shape factor, the experimental data was fitted to compute the ratio of the permeability of the disperse phase and continuous phase. The thermoplastic starch will be slightly deformed as can be seen in SEM pictures in Appendix B and Figure 5.13. The starch however can be estimated to be close to perfect spheres. Due to the starch being thermoplastic the spheres are more susceptible to deformation which will occur during the film blowing. The granules will be stretched and become oblate ellipsoids.

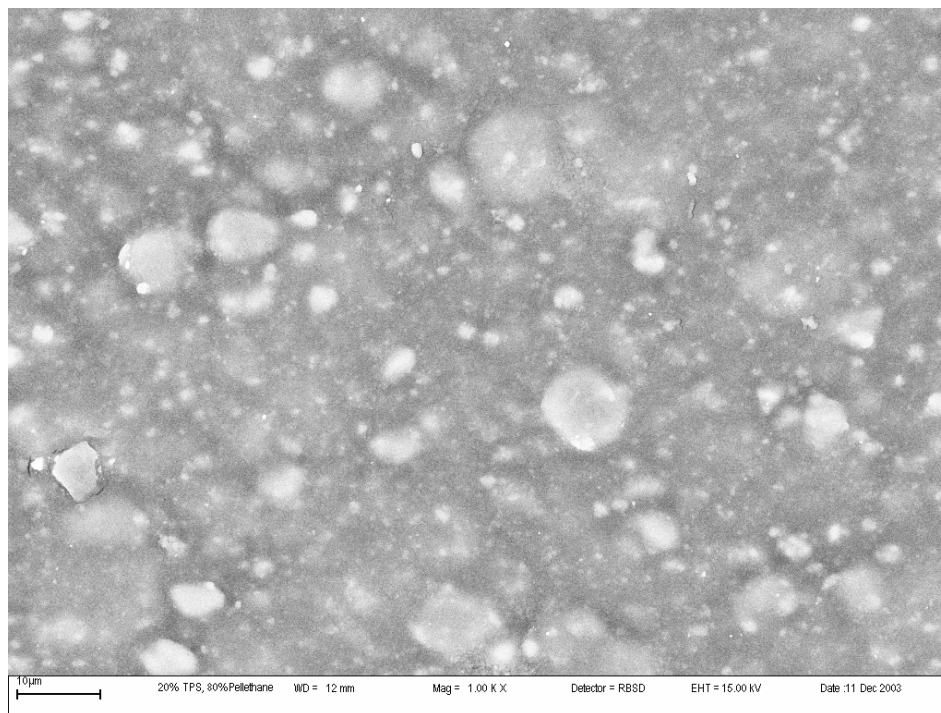


Figure 5.13. 20%TPS containing 30% glycerol and high amylose starch / 80%Pellethane membrane magnified 1000 times

Figure 5.14 shows the comparison between the models and the experimental data. The deviation between the experimental data and the models is very small since the parameters are fitted.

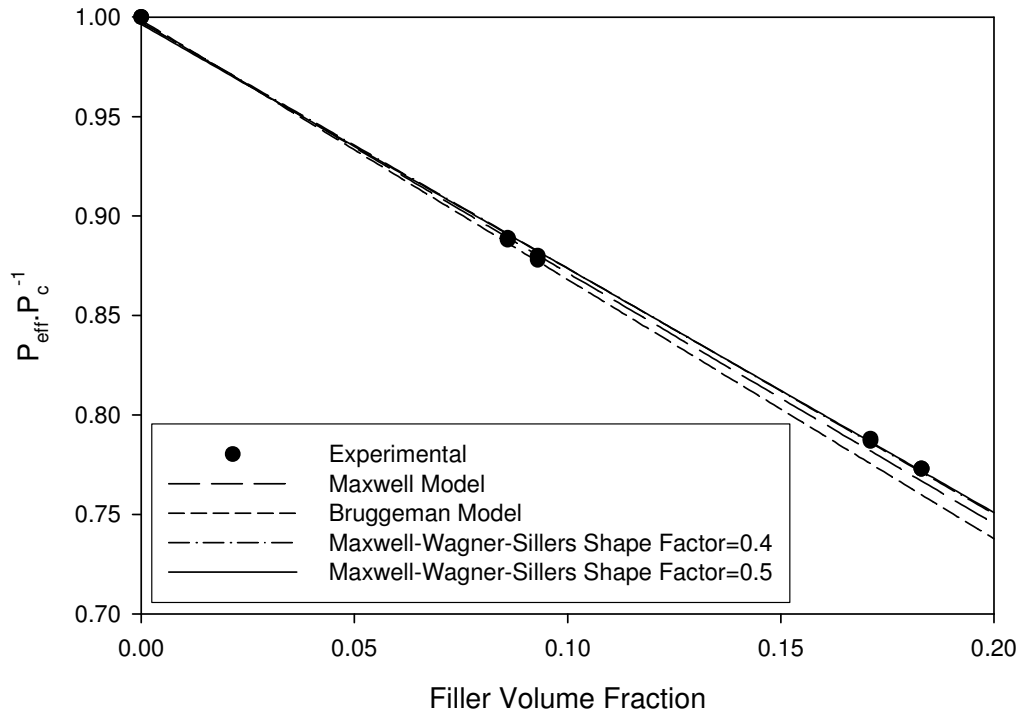


Figure 5.14 Comparison between the experimental change in permeability as a function of filler volume fraction and fitted Maxwell and Bruggeman models

The shape factor is can be estimated from SEM pictures. Assuming that the spherical starch granules are distorted due to the film blowing the shape factors of 0.4 and 0.5 were selected to obtain a more accurate range for the filler permeability. Using these shape factors the WVTR of the thermoplastic starch was approximately $405 \text{ g.m}^{-2}.\text{day}^{-1}$ for a shape factor of 0.4 and $620 \text{ g.m}^{-2}.\text{day}^{-1}$ for a shape factor of 0.5. The expected variation due to the different shape factors is explained in Figure 5.12. A higher shape factor denotes oblate ellipsoids. If a membrane has oblate ellipsoids and performs the same as a membrane containing prolate ellipsoids, the permeability of the oblate ellipsoids will be greater than the permeability of the prolate ellipsoids.

Table 5.5 lists all of the predictions for starch permeability based on the different models. The use of the Maxwell-Sillar-Wagner model results in a prediction of a permeability range that may be more representative of the membrane.

Table 5.5 Predictions of starch permeability based on various models

Model	Starch Permeability $\text{g}\cdot\text{m}^{-2}\cdot\text{day}^{-1}$
Maxwell	206
Bruggeman	206
Maxwell-Sillar-Wagner (Shape Factor =0.4)	407
Maxwell-Sillar-Wagner (Shape Factor =0.5)	621

The effect of amylose content on the permeability is shown in Figure 5.15. An inverse relationship between thickness and permeability similar to that of the other membranes was observed. Table 5.6 summarises the trends observed for these relationships. A student's t-test was performed to determine whether there was a significant difference between the WVTR of TPS filled membranes in which the amylose content varied. There is strong evidence to show that permeability of TPS filled membranes is independent of amylose content ($P=0.4949$).

Table 5.6 Fitted equations for Pellethane filled with TPS (High amylose) at different levels containing varying amounts of glycerol

Formulation	Fitted Equation	R ²
Low Amylose	$WVTR = 1243.9 + \frac{35858.6}{x}$	0.99
High Amylose	$WVTR = 547.5 + \frac{45865.2}{x}$	0.86

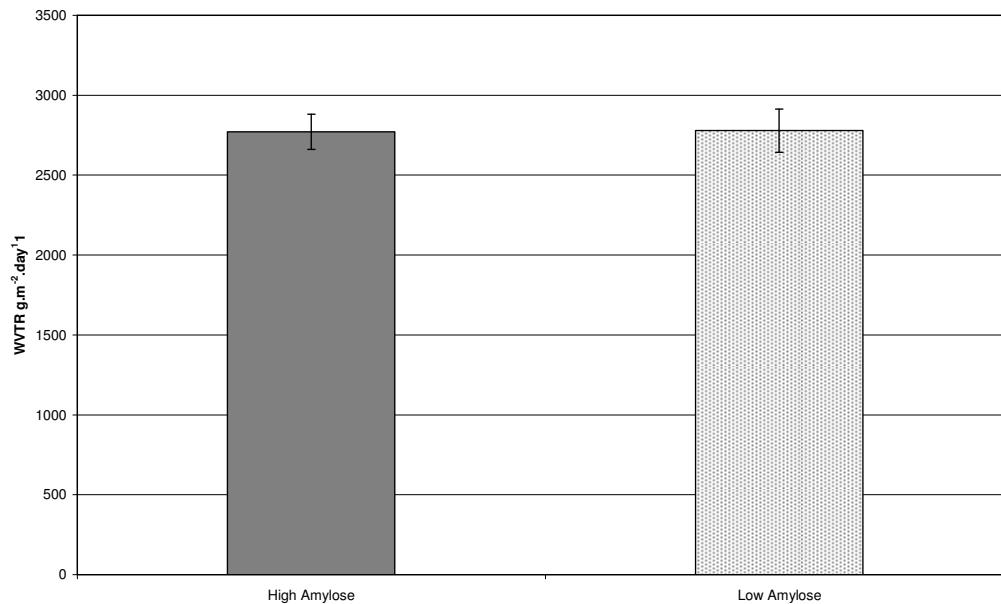


Figure 5.15 Effect of amylose content on permeability of 20% TPS filled made with 40% glycerol and starches of different amylose content

Granular starch was incorporated into the polyurethane matrix. The relative change in permeability of granular starch filled membranes and thermoplastic starch filled membranes are compared in Figure 5.16. SEM picture Figure 5.17 shows the surface of the membrane.

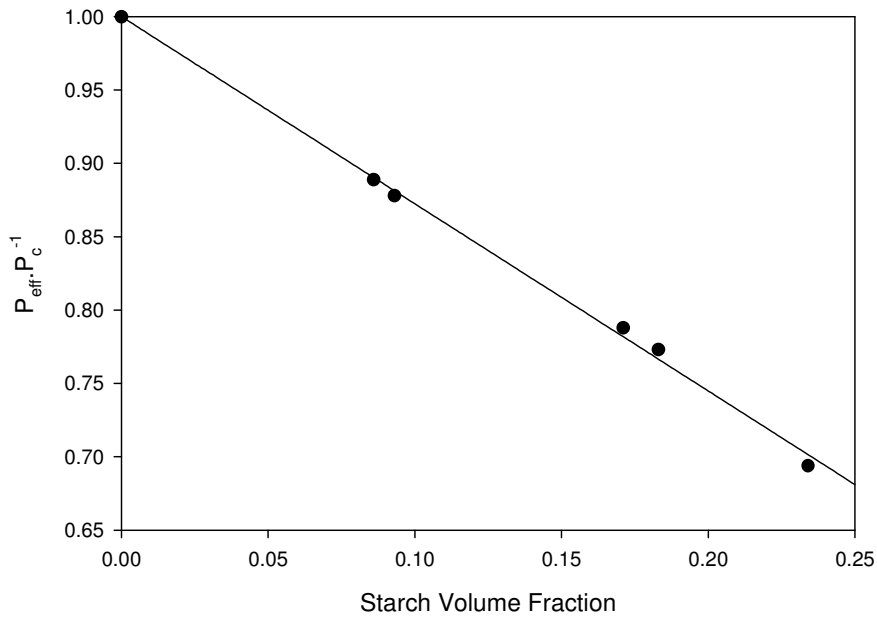


Figure 5.16 Graph of the effective change in permeability as a function of starch volume fraction (irrespective of whether the starch is thermoplastic or granular)

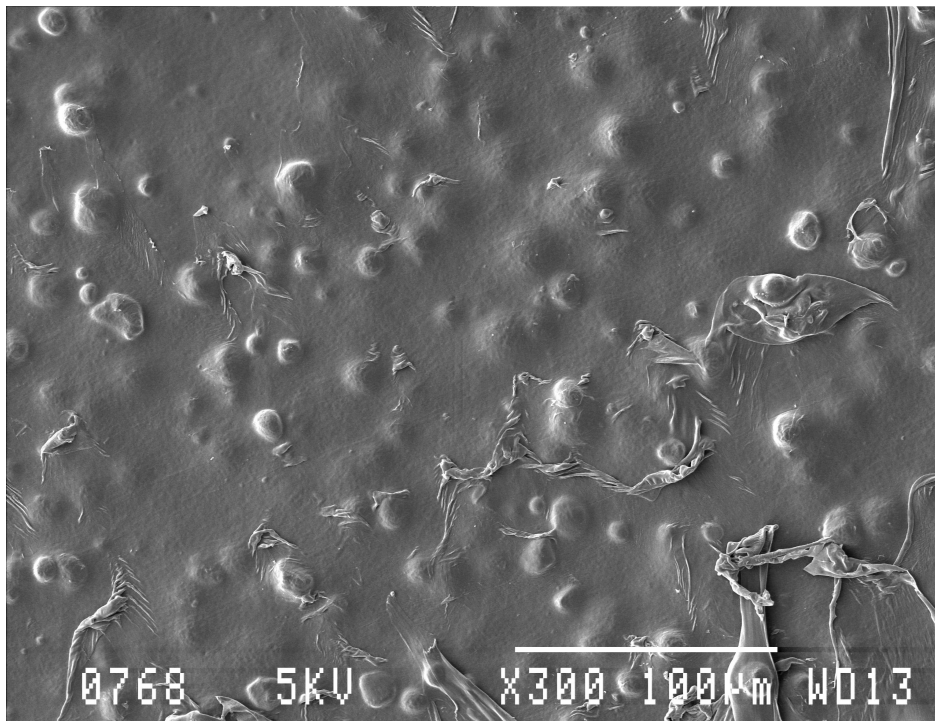


Figure 5.17 SEM picture of granular starch in TPU membrane

Figure 5.18 shows that the granular starch membranes take longer to reach equilibrium than the TPS membranes. The permeability of the granular starch filled membrane after equilibrium was reached compares well with the prediction for the effect of starch volume fraction on the permeability of starch-polyurethane composite membranes as shown in Figure 5.7. Figure 5.16 illustrates that the starch volume fraction is the dominant factor that determines the effective permeability of the composite membrane. This shows that the glycerol in thermoplastic starch has an insignificant effect of the permeability of the composite membrane.

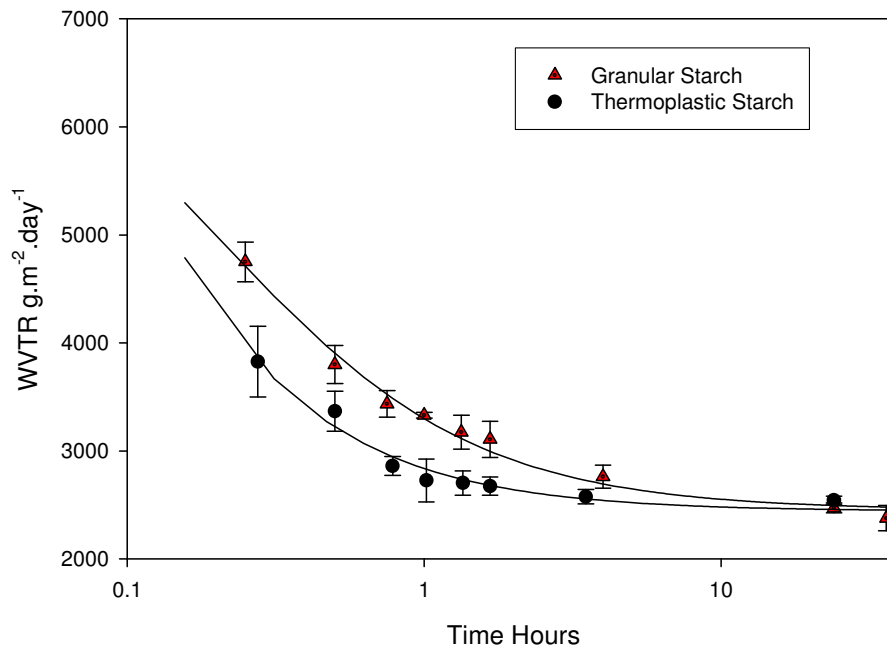


Figure 5.18 Comparison between the time to reach equilibrium between membranes containing 20% granular starch and 20% thermoplastic starch

5.2.2. Other fillers

The effect of mineral fillers was examined to compare results with permeability models and to investigate the effect that the mineral fillers had on the blocking tendency of the membranes. Filler of a known permeability were examined to determine evaluate the various permeability models and in particular the effect

of the shape factors on the effective permeability of the composite membrane. The mineral fillers examined were Dicalite and diatomite. These fillers were platelets which were expected to align in the machine direction and effectively represent a shape factor of $> 1/3$ i.e. oblate ellipsoids. The effect of thickness of membrane permeability of 20% filled Dicalite and 20% diatomite filled membranes is similar to the trends of previous membranes. Both are naturally occurring silica based powders consisting of the fossilized remains of diatoms. Diatomite is porous whereas Dicalite is not. Due to the porosity of Diatomite there will be an apparent permeability observed for the Diatomite. The effect of volume fraction of Dicalite and diatomite on the relative change in permeability was plotted on Figure 5.19. The Maxwell and Bruggeman equations relating the effect of the volume fraction of impermeable sphere on relative change in permeability is also plotted in Figure 5.19. The experimental results deviate from the Maxwell model substantially. This is due to the particle not being spherical but rather resembling ellipsoid platelets. The Maxwell-Wagner-Sillar model will be able to better correlate with the experimental results since a shape factor is incorporated in the model.

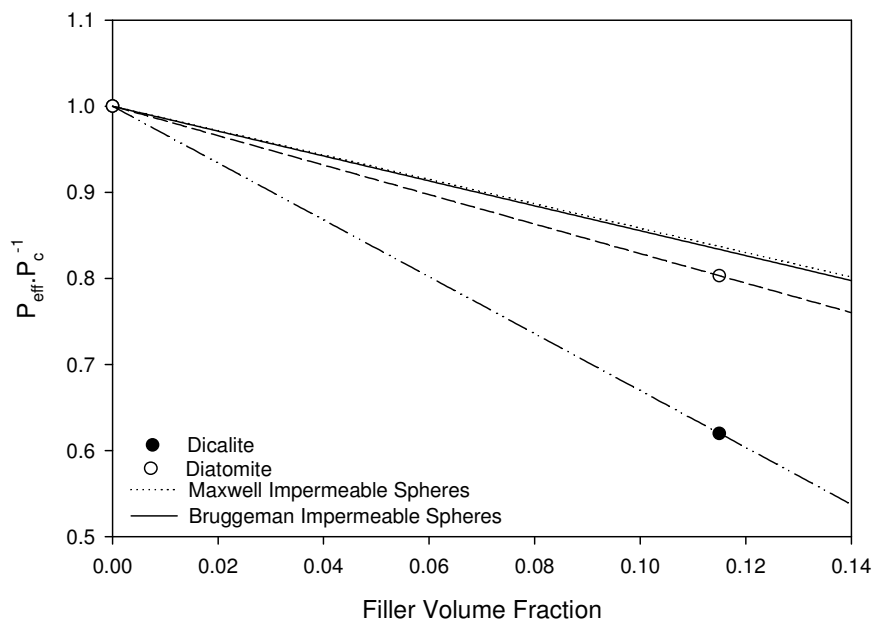


Figure 5.19 Comparison between the experimental change in permeability as a function of filler volume fraction and the change in permeability predicted by the Maxwell model and Bruggeman for impermeable spheres

The Maxwell-Wagner-Sillar model was used to simulate the change in permeability with volume fraction and shape factor of impermeable filler. Figure 5.20 shows the results of the simulation. Comparing the experimental data to the Maxwell-Wagner-Sillar model prediction for impermeable filler like Dicalite the observed change in permeability corresponds to a shape factor of approximately 0.79. This shape factor represents oblate spheroids. The filler is irregularly shaped however the SEM pictures as shown in Figures 5.22 to 5.25, indicate that they are aligned in parallel to the membrane surface. The large number obtained for the shape factor suggests that the ellipsoid major axis is almost parallel to the membrane surface which corresponds to the SEM picture. The alignment experienced can be attributed to the film blowing and stretching process.

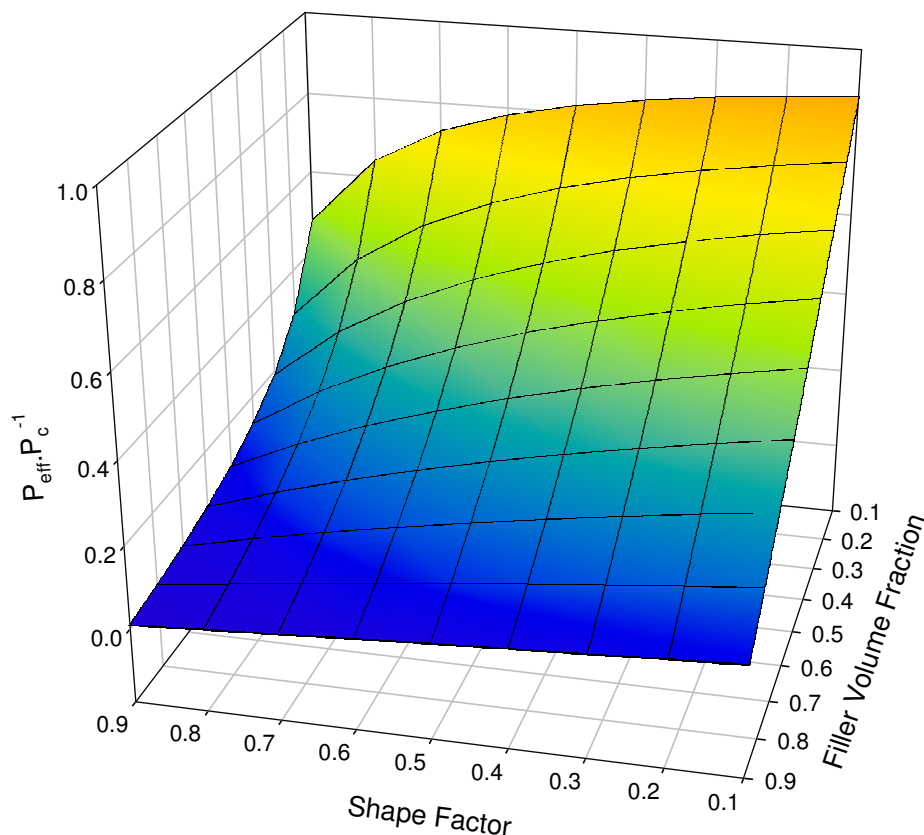


Figure 5.20 The change in permeability as a function of shape factor and filler volume as predicted by the Maxwell-Wagner-Sillar model for impermeable fillers

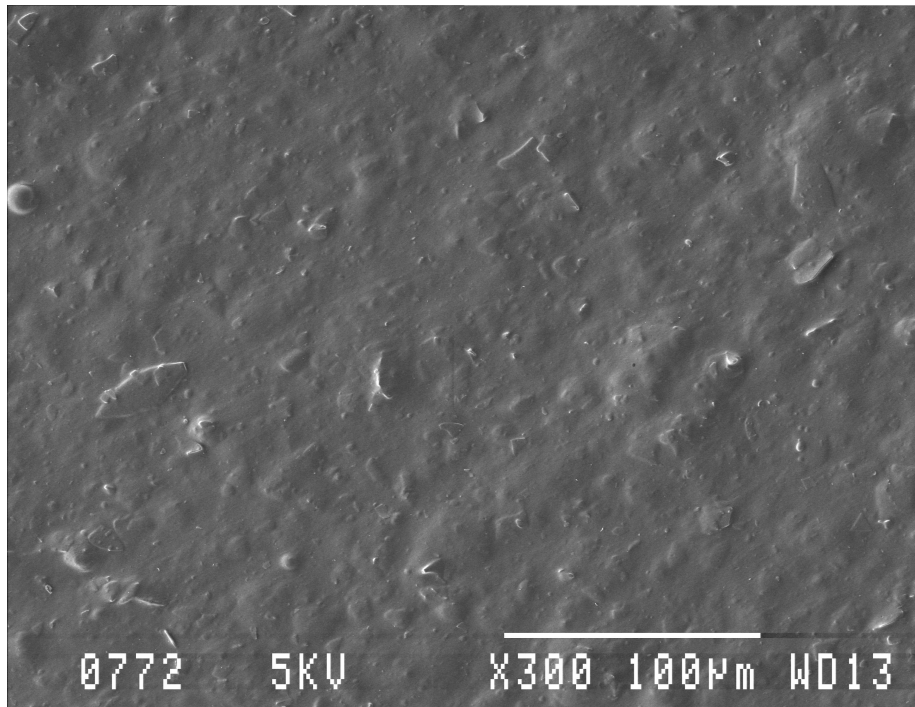


Figure 5.21 SEM picture of Dicalite filled membrane

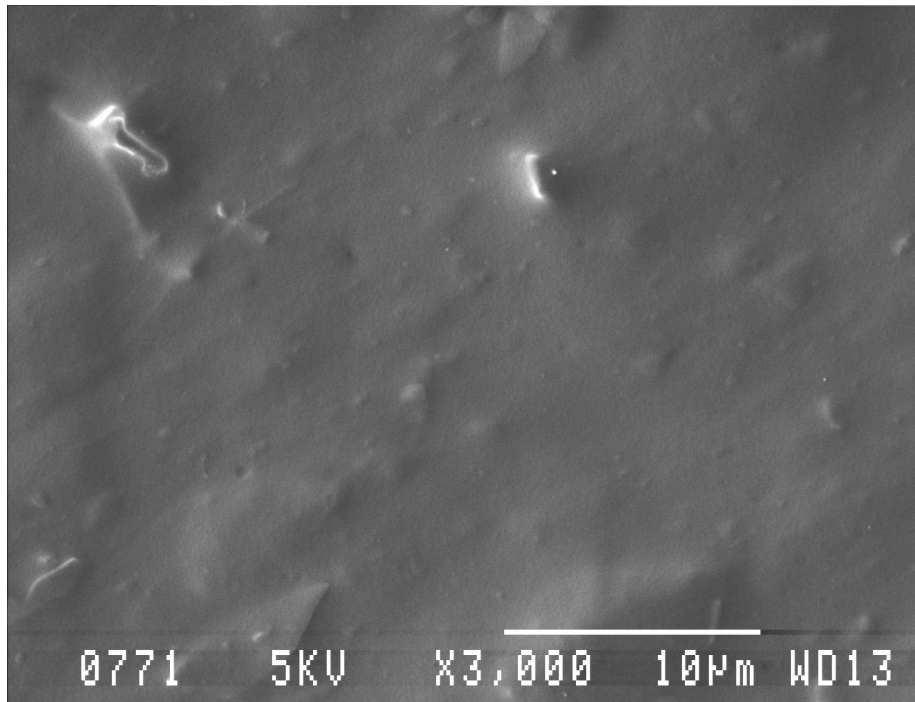


Figure 5.22 SEM picture of Dicalite filled membrane

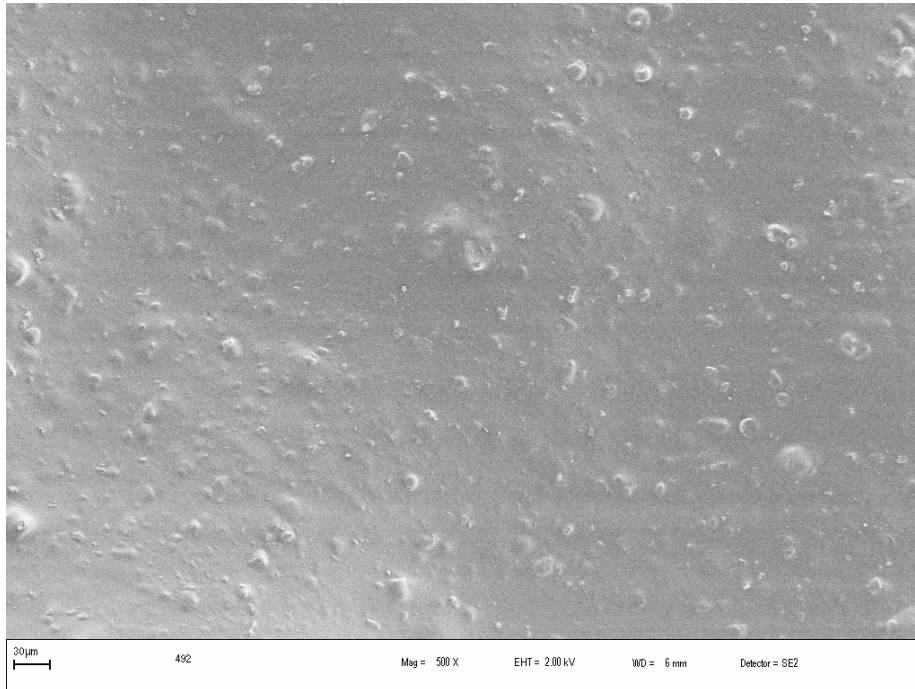


Figure 5.23 SEM picture of Diatomite filled membrane



Figure 5.24 SEM picture of Diatomite filled membrane

The major difference between Dicalite and diatomite is that diatomite is porous whereas Dicalite is not. The porous nature of the diatomite results in its permeability being greater than the permeability of Dicalite. Therefore the

relative decrease in permeability of the Dicalite membranes is greater than that of the diatomite membranes. Assuming that the shape factor for Dicalite filled membranes is approximately the same as that of diatomite filled membranes and that the pores of the diatomite is filled with the matrix the value of α can be estimated to be approximately 0.22, resulting in a water vapour permeability of approximately $755 \text{ g.m}^{-2}.\text{day}^{-1}$. If the diatomite pores are not filled with the matrix there would be air-pockets present in the composite membrane. If there are air-pockets present then the permeability of the membranes should be very high since the diffusivity through the air-pocket is very high. Since the inclusion of diatomite results in a significant decrease in WVTR it can be assumed that there are very few pores that are not filled with the matrix material.

The permeability of the diatomite is a function of the porosity of material. Another factor that will determine the permeability in a composite membrane is the interaction between the filler and the matrix. If the matrix fills the pores of the filler, the permeability of the filler will be a fraction of the matrix (the fraction will be equal to the porosity). Starch filled with diatomite was filled in the polyurethane matrix and is examined in the following section and will be discussed later. The starch when filled with diatomite performed slightly worse compared to unfilled starch however the addition of only diatomite (with no starch) results in similar performance. This was performed at low addition levels.

Figure 5.25 shows the effective change in permeability for TPS filled membranes compared to that of Dicalite and diatomite filled membranes. Diatomite performs better than the Dicalite due to the porosity; however TPS performs better than both fillers. If the diatomite interacts with the matrix such that the pores are not filled with the matrix, there will be air pockets in the membrane which will increase the permeability of the membrane dramatically. The experimental data shows a decrease in the permeability suggesting that the pores are filled with the matrix. The same effect can be inferred from the experiments performed with starch filled with diatomite which will be discussed in the next section.

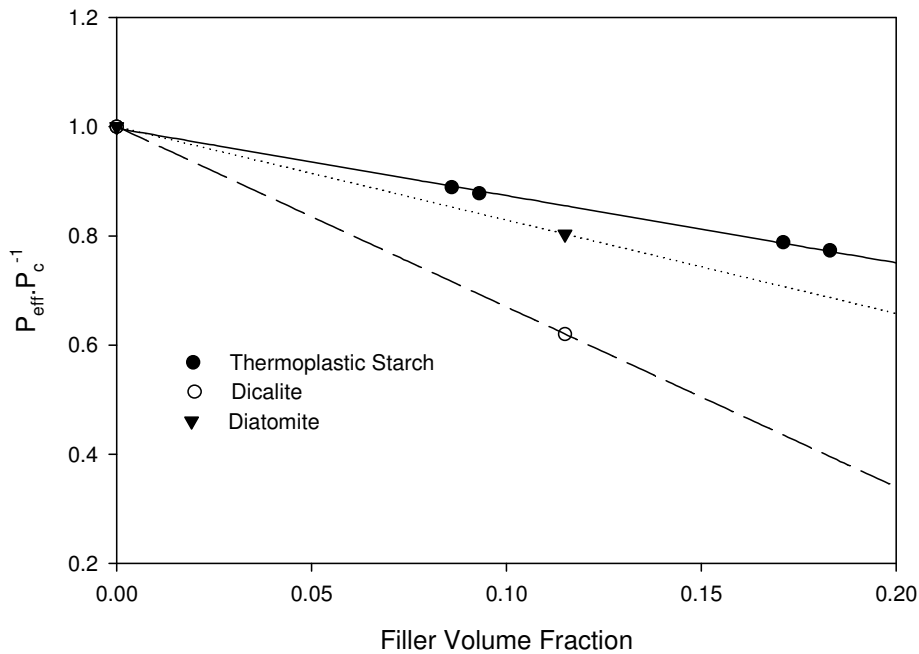


Figure 5.25 Comparison between the experimental change in permeability as a function of filler volume fraction for TPS, Dicalite and diatomite filled membranes

5.2.3. TPS blends with other fillers

Other fillers were incorporated in the TPS before addition to the polyurethane matrix. The fillers used included sodium bentonite, calcium bentonite, hydrotalcite, diatomite, alumina silicate and calcium carbonate. Both bentonites did not result in processible blends. Table 5.8 and Figure 5.26 summarises the WVTR of the filled-TPS filled TPU membranes.

Table 5.8 The effect of fillers in TPS on the WVTR of a polyurethane membrane

Filler	Average WVTR g.m ⁻² .day ⁻¹	Standard Deviation g.m ⁻² .day ⁻¹
None	2832	110
Diatomite	2763	88
Alumina Silicate	2588	27
Hydrotalcite	2754	49
Calcium Carbonate	2836	40

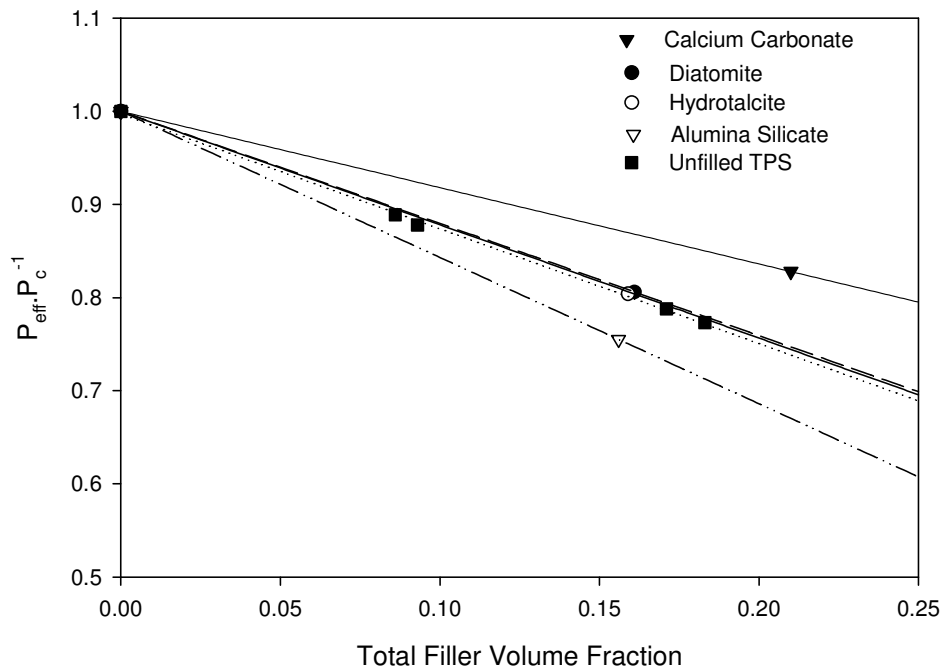


Figure 5.26 Comparison between the experimental change in permeability as a function of filler volume fraction for TPS and filled TPS filled membranes

Incorporation of alumina silicate results in the largest decrease in permeability. This is expected because the filler is non-porous and impermeable.

Hydrotalcite and diatomite addition results in a performance that is almost

identical to the unmodified TPS. Hydrotalcite and diatomite are porous silica based particles. The permeability observed is only due to the porous nature of the material. When incorporated in a matrix, the matrix replaces the void due to the porous nature of the filler. The apparent permeability will therefore be a fraction of the permeability of the matrix. The fraction will be directly related to the porosity.

The addition of these particles is likely to result in a decrease in the permeability of the composite. The extent of the decrease will be dependant on the porosity and the volume fraction of the filler. This effect was modelled with results plotted in Figure 5.27. At low volume fractions the addition of porous fillers does not impact significantly on the permeability of the TPS. The level of addition in experiments was less than 0.02%. At low levels of addition the effect of the filler is insignificant. The minimum and maximum change in permeability of the composite membrane was calculated as a function of porosity and plotted in Figure 5.28. There are no significant differences between the filled and unfilled TPS at low levels of addition. At higher addition levels the change in permeability will be significant as can be seen Figure 5.27. The porosity effects will also become significant.

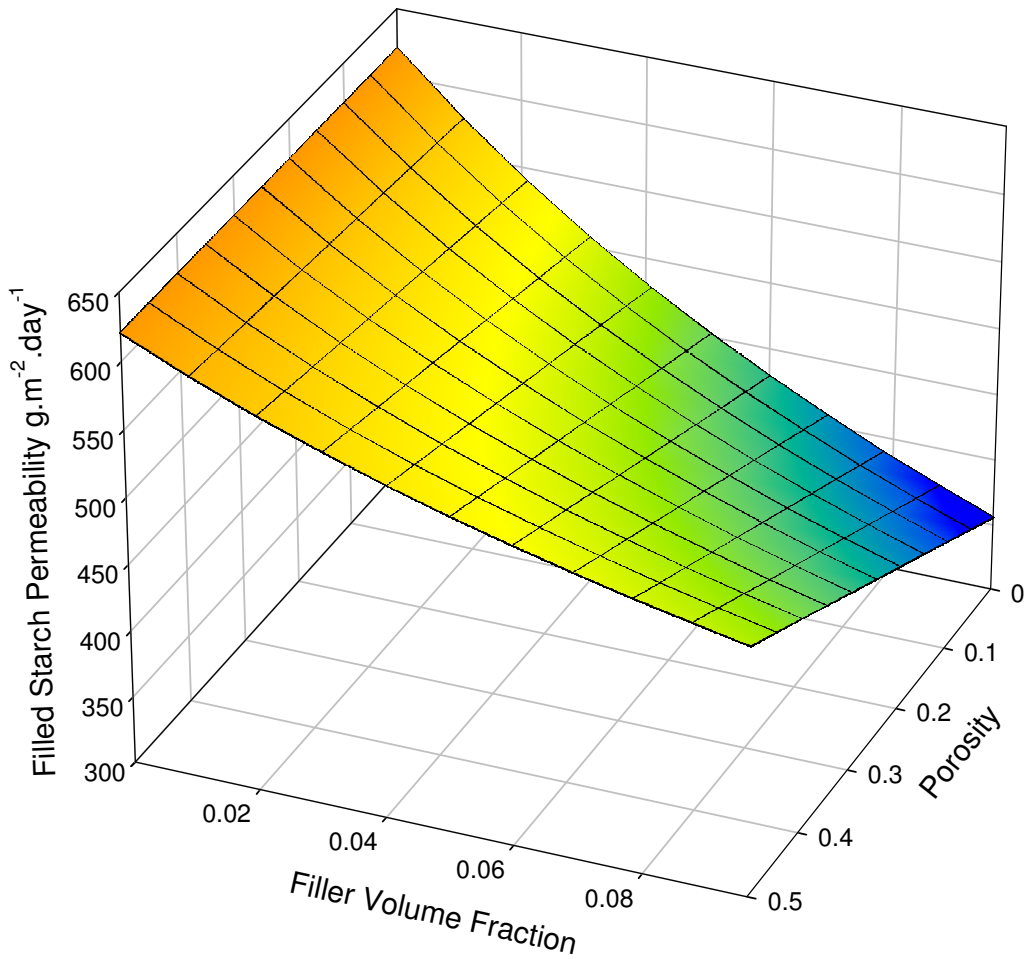


Figure 5.27 The maximum permeability of TPS filled with porous filler as a function of porous filler volume fraction

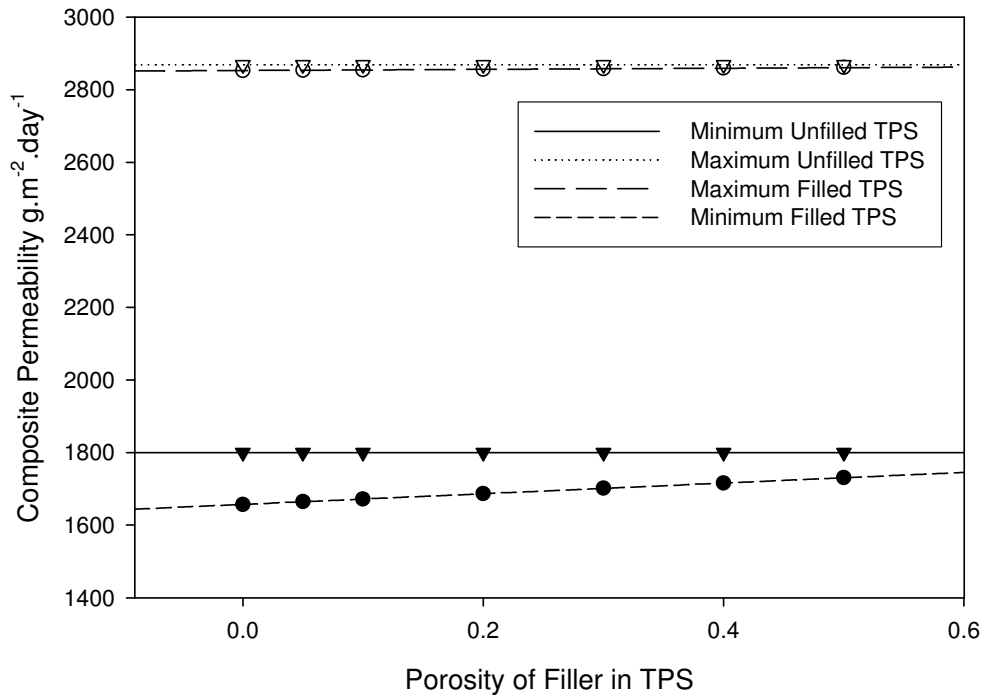


Figure 5.28. Calculated minimum and maximum effective permeability of Diatomite-TPS filled polyurethane membranes as a function of diatomite volume fraction

The addition of calcium carbonate to TPS before incorporation into the TPU matrix results in an increase in the permeability of the composite membrane. A statistical analysis was performed to determine the significance of the difference between the filled TPS composites compared to the unfilled TPS composites. The effect of the addition of diatomite, hydrotalcite or calcium carbonate in the TPS before addition to the polyurethane matrix results in membranes that perform on average similar to unfilled TPS-polyurethane membranes. The addition of alumina silicate in the TPS, even at low levels, does result in a significant decrease in the permeability of the composite membrane compared to the membrane containing unfilled TPS.

Table 5.9 The effect of fillers in TPS on the WVTR of a polyurethane membrane

Filler	p-value
Diatomite	0.8622
Alumina Silicate	0.0473
Hydrotalcite	0.7688
Calcium Carbonate	0.5045

5.3. Blocking and Morphology Results

5.3.1. TPS Blocking and Morphology Results

The addition of TPS to TPU membrane does result in decrease in the blocking of the membrane (Table 5.10). The virgin TPU membrane exhibits severe 2nd degree blocking at both test temperatures. With the addition of TPS the blocking behaviour is no longer exhibited. This can be attributed to the surface roughness introduced by the addition of TPS as shown in SEM pictures of the pure Pellethane membrane and of the membranes filled with 20% TPS(m/m) made with 40% glycerol on starch mass basis (Figures 5.30-5.32). SEM pictures of 20% TPS filled membranes made with 30% glycerol can be found in Appendix B with Figure 5.13 an example thereof. The Pellethane membrane is hydrophilic and does not contain any porosity. The TPS is well distributed in the polyurethane matrix but contains a distribution of particles. The TPS does not form spherical particles but forms ellipsoids with the major axis parallel to the film direction, which is due to the film blowing process resulting in some deformation. Figure 5.13 shows the alignment clearer than Figure 5.30 or 5.32. Figure 5.17 shows a SEM picture of granular starch filled membranes. The starch is evenly distributed in the matrix and retains its spherical shape. It is not plasticized and is expected to retain its shape. The surface roughness created by the addition of granular starch is clearly visibly

in the SEM picture. This roughness results in the membrane showing no blocking.

Table 5.10 The effect of TPS on blocking characteristics of membranes

Filler	Blocking @ 38 °C	Blocking @ 58 °C
None	2 nd Degree blocking	2 nd Degree blocking
20% Granular Starch	No Blocking	No Blocking
20% TPS (30% Glycerol)	No Blocking	No Blocking
20% TPS (40% Glycerol)	No Blocking	No Blocking
10% TPS (30% Glycerol)	No Blocking	No Blocking
10% TPS (40% Glycerol)	No Blocking	No Blocking

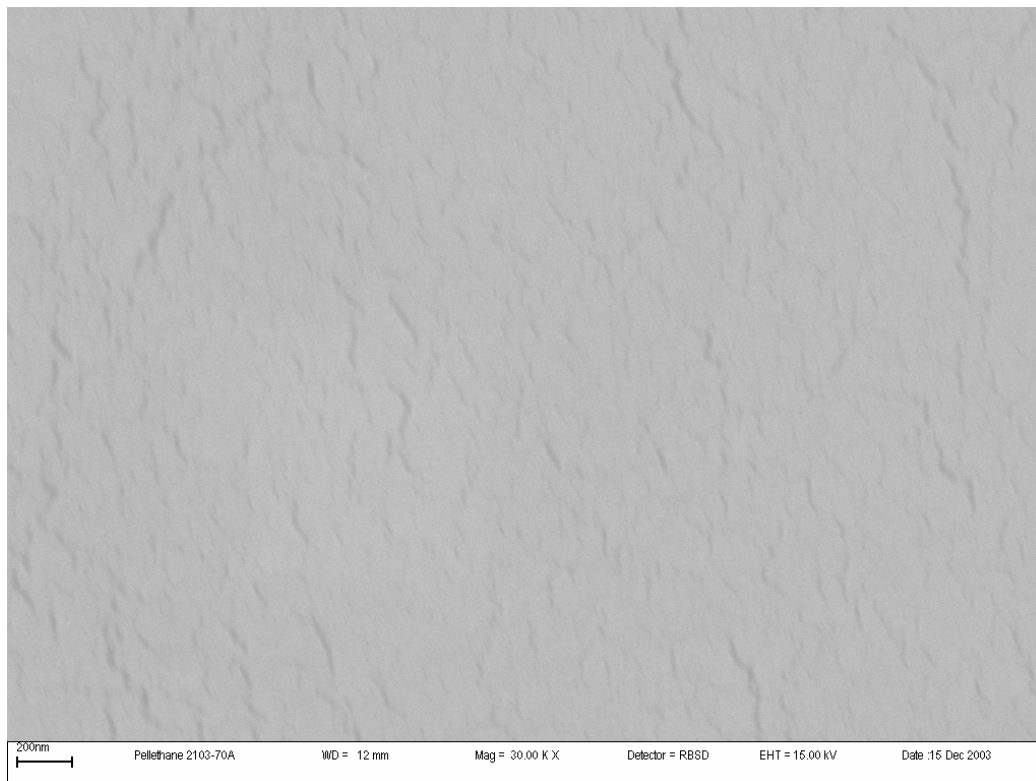


Figure 5.29 Pellethane membrane magnified 30000 times

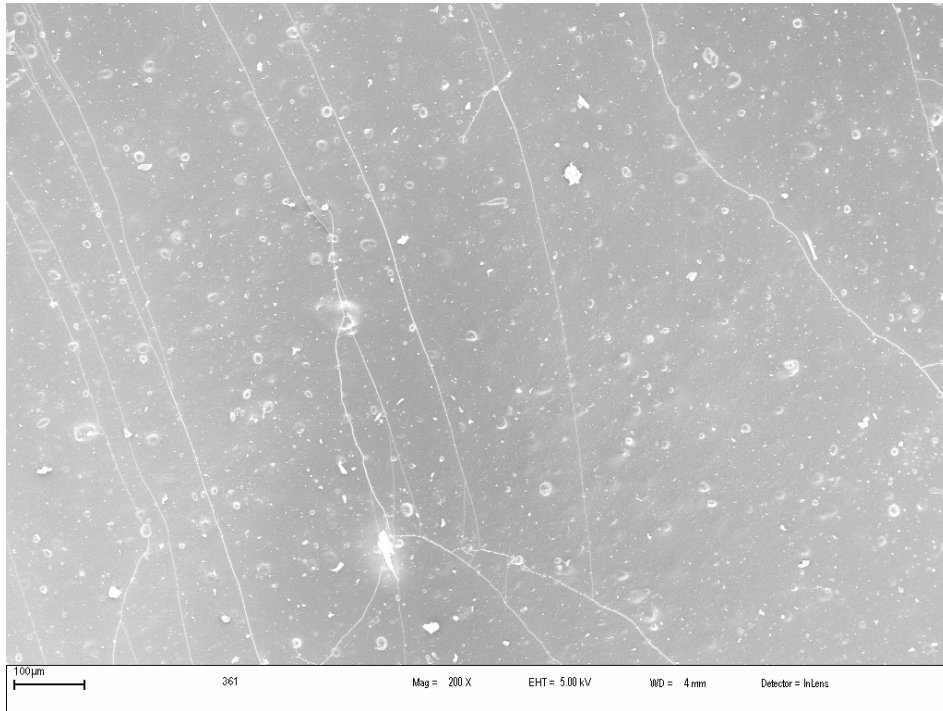


Figure 5.30 20%TPS (containing 40% glycerol and low amylose starch) / 80%Pellethane membrane magnified 200 times

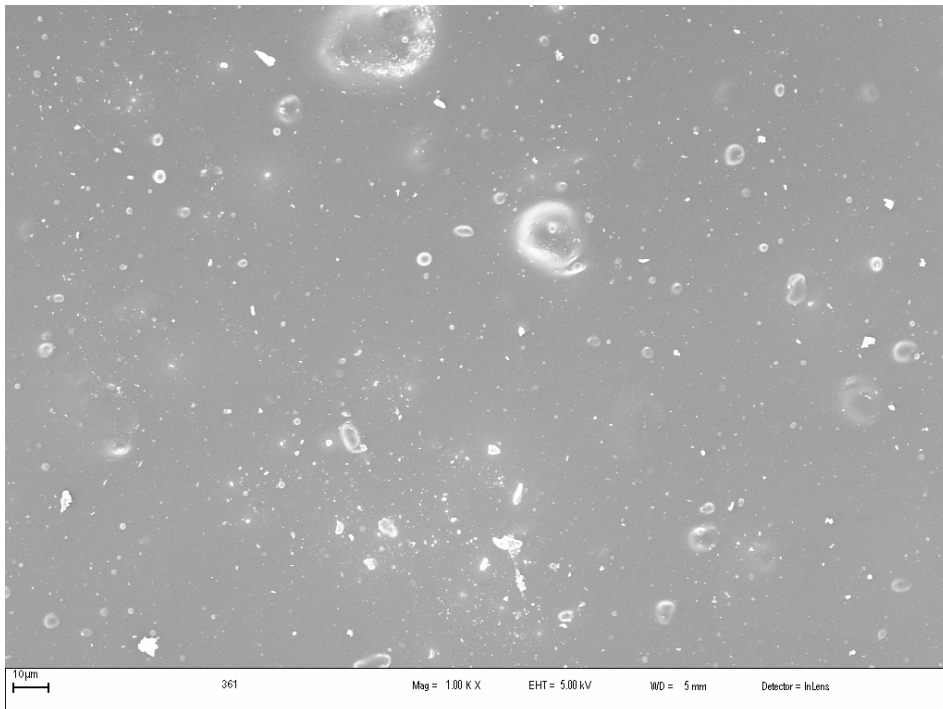


Figure 5.31 20%TPS (containing 40% glycerol and low amylose starch) / 80%Pellethane membrane magnified 1000 times

5.3.2. Other Fillers Blocking and Morphology Results

Figures 5.22-5.25 show the SEM pictures of the Dicalite and diatomite membranes. The flat particles are aligned such that their major axis is parallel to the membrane surface. The surface of the membrane is very rough. The filled membranes show no blocking (Table 5.10) which can be attributed to the large degree of surface roughness.

Table 5.10 The effect of TPS on blocking characteristics of membranes

Filler	Blocking @ 38°C	Blocking @ 58°C
20% Dicalite	No Blocking	No Blocking
20% Diatomite	No Blocking	No Blocking

5.3.3. Filled TPS Blocking and Morphology Results

The blocking tendency of the membrane containing the filled TPS was characterized and is tabulated in Table 5.11. All fillers performed better than the TPU polymer membrane. The SEM pictures of the membranes (Figures 3.33-3.36) show that the membranes all contain some degree of surface roughness. The membrane blocking is more severe when the fillers are incorporated into the TPS compared to membranes only containing TPS however is better than the virgin polymer. The blocking rating can be explained by a combination of the testing procedure and dispersion effects due to the addition of a filler. The blocking rating quoted is the most severe of the 6 samples tested. In most of the tests there was only one sample of the 6 that showed 1st degree blocking with the others showing no blocking; alumina silicate showed 1st degree blocking on all samples and calcium carbonate on two samples. The alumina silicate surface does look smoother than the other samples (Figures 5.22-5.25, 5.32-5.33, 5.34-5.36) when examined using a SEM. The increased smoothness will result in more blocking. The presence of some surface defects will however prevent severe blocking. Poor dispersion

of the filler can explain the higher blocking tendency of some samples containing the other fillers. The sample used for the test is small. If the filler is poorly distributed in the sample the results will vary. Since less than 33% of the samples showed 1st degree blocking there could be some variability in the filler dispersion.

Table 5.11 The effect of Filled-TPS on blocking characteristics of membranes

Filler	Blocking @ 38 °C	Blocking @ 58 °C
Diatomite	No Blocking	1 st Degree blocking
Alumina Silicate	1 st Degree blocking	1 st Degree blocking
Hydrotalcite	1 st Degree blocking	1 st Degree blocking
Calcium Carbonate	1 st Degree blocking	1 st Degree blocking

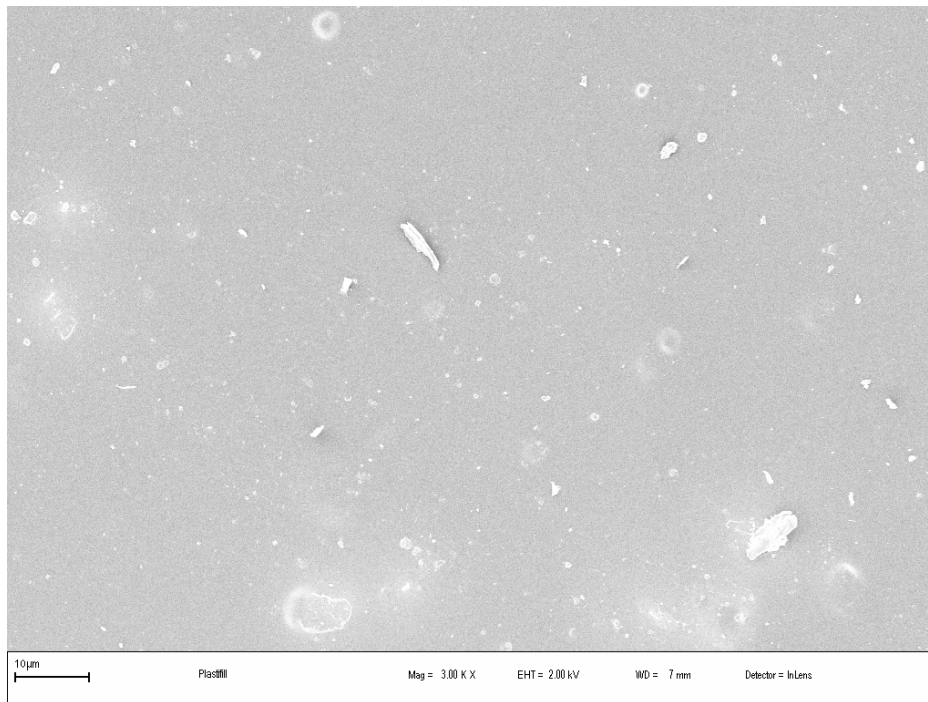


Figure 5.32 20%TPS containing alumina silicate (Plasfill 5) 80%Pellethane membrane magnified 3000 times

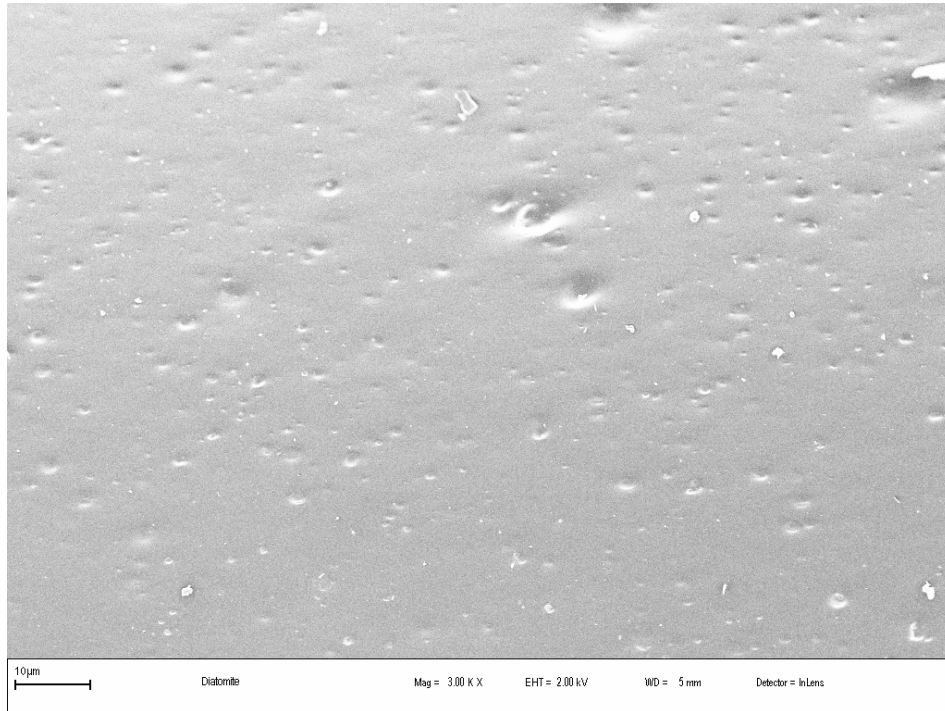


Figure 5.33 20%TPS containing diatomite 80%Pellethane membrane magnified 3000 times

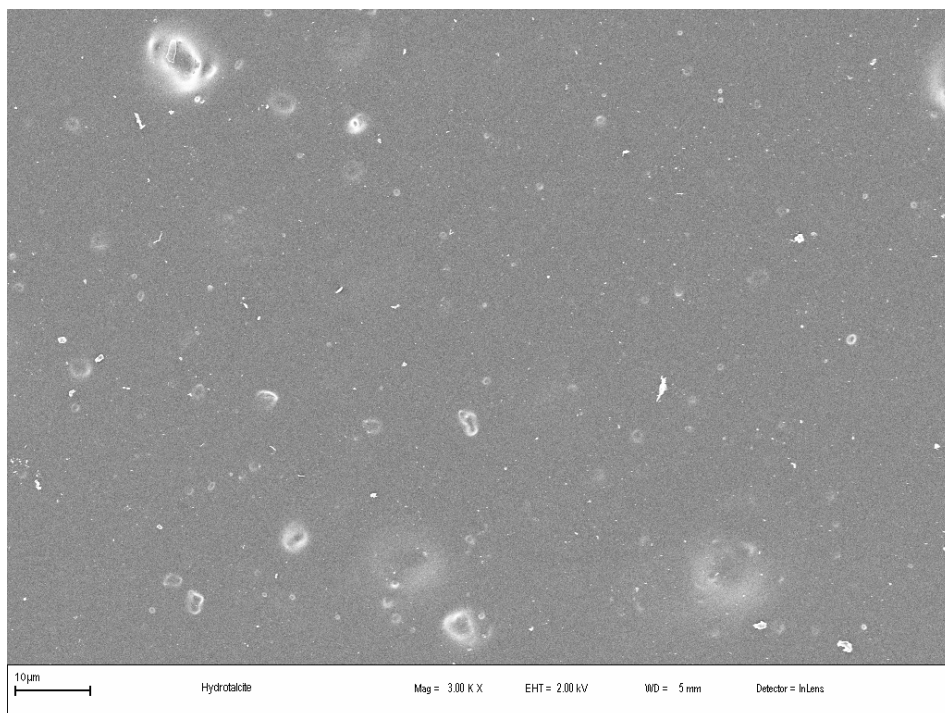


Figure 5.34 20%TPS containing hydrotalcite 80%Pellethane membrane magnified 3000 times

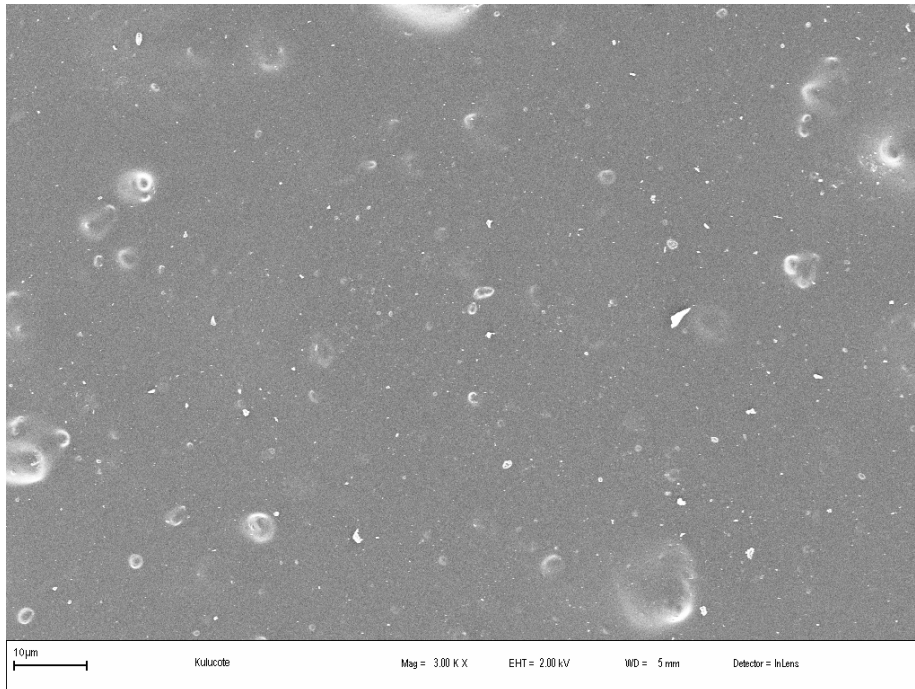


Figure 5.35 20%TPS containing calcium carbonate (Kulucote 2)
80%Pellethane membrane magnified 3000 times

5.4. Tensile Testing

5.4.1. Filled Membranes

The tensile properties of the membranes were examined. Figures 5.37 to 5.40 show the variation between tensile properties between the Pellethane and Pellethane filled with 20% TPS, 20% granular starch, 20% Dicalite and 20% diatomite.

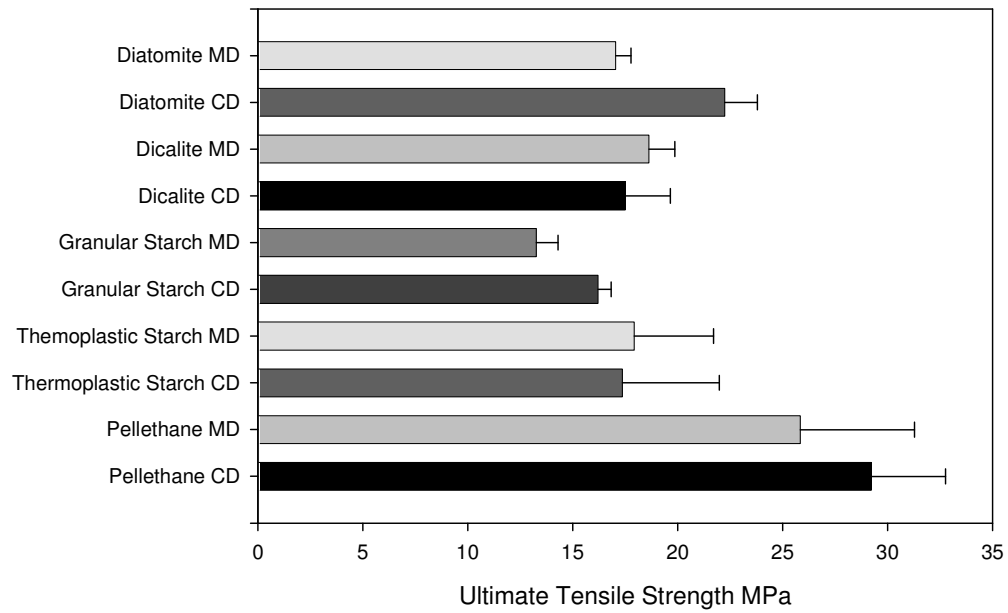


Figure 5.36. Ultimate tensile strength of membranes

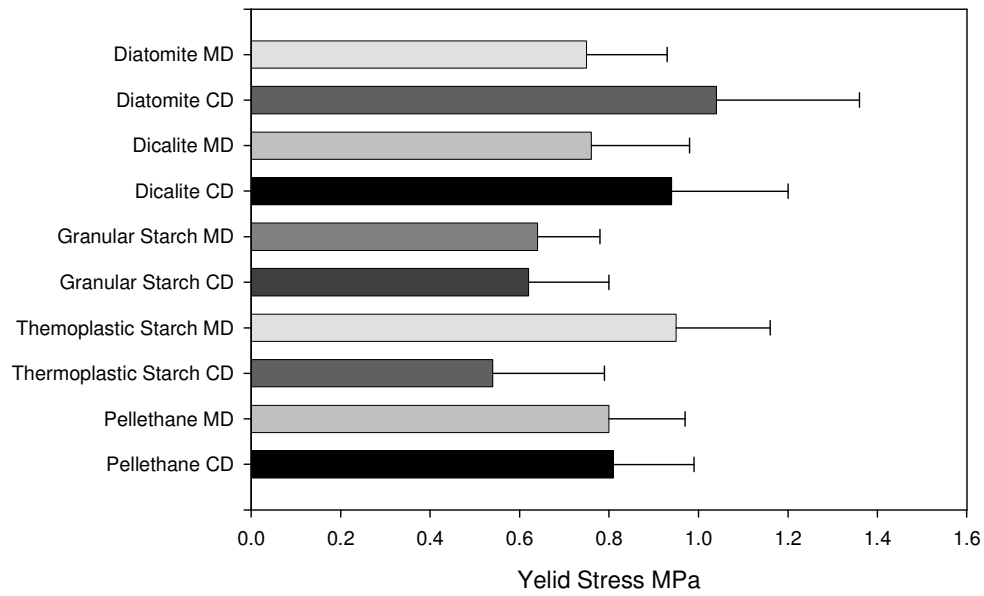


Figure 5.37. Yield stress of membranes

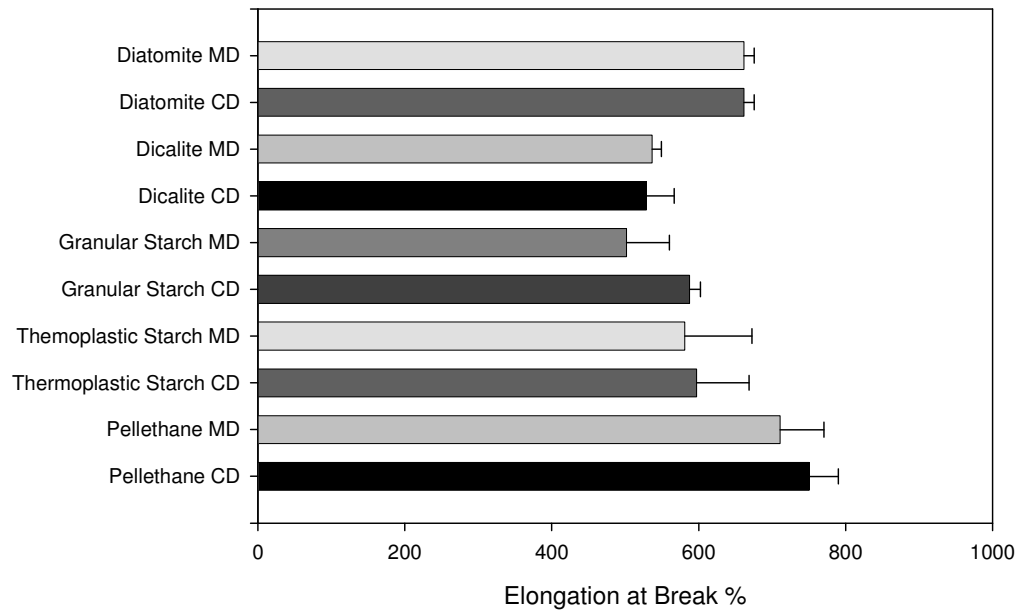


Figure 5.38. Elongation to break of membranes

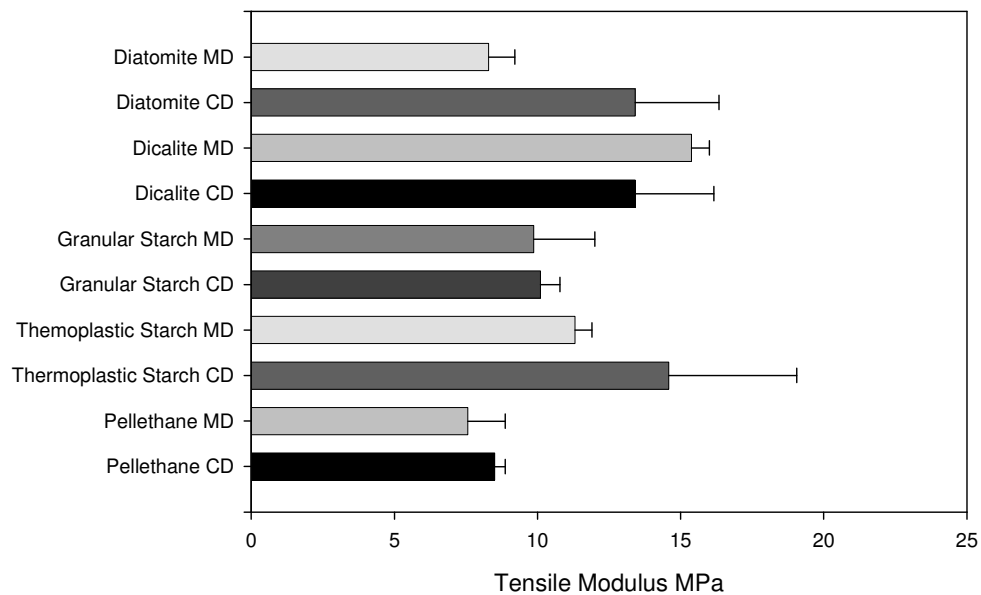


Figure 5.39. Tensile modulus of membranes

Almost all samples tested yielded higher strength properties in the cross direction compared to the machine direction. This indicates that there is more alignment in the cross direction compared to the machine direction. The

increased alignment in the cross direction can be attributed to increased stress during the blowing and formation of the bubble. Figure 5.40 to 5.43 show some pictures of the film blowing apparatus. Figure 5.42 shows the bubble formation. When the bubble is formed the membrane is stretched horizontally before being wound up. The higher tensile properties in the cross direction indicate that there is more alignment in the cross direction compared to the machine direction. The stress caused by the formation of the bubble is responsible for the alignment in the cross direction. The stress induced by the bubble formation is less than the stress induced by the pulling and winding up of the blown membrane, therefore the cross direction strength is greater than the machine direction strength. The standard deviation between samples is however large and a statistical analysis was performed to determine the significance of the difference observed between samples cut in the cross direction and machine direction.



Figure 5.40. Film blowing process



Figure 5.41. Film windup process

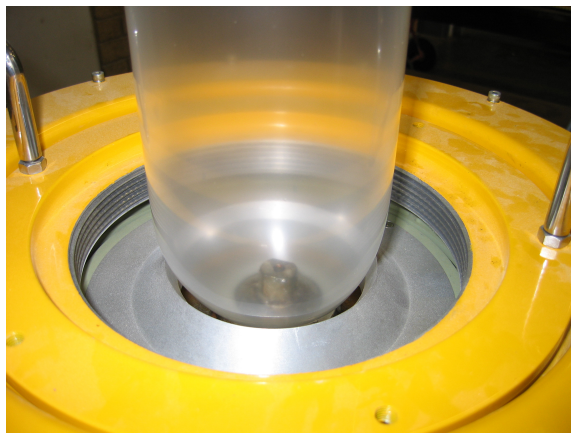


Figure 5.42. Film bubble

Table 5.12 lists the p-values for student t-tests performed to determine the statistical significance of the difference between the machine and cross direction properties. The Pellethane membranes and the diatomite filled membranes show no statistical difference between properties in the machine and cross direction. The other membranes have a significant difference between some of the mechanical properties. This variation can be attributed to different bubble sizes for different blends. A larger bubble would result in more stress in the cross direction. The granular starch and diatomite filled membranes show the significant differences between the strength in the cross direction and machine direction. Diatomite filled membranes are the only membranes to have significant higher modulus in the cross direction compared to the machine direction. All other membranes have a statistically

similar average tensile modulus in the machine and cross direction. Other properties are tabulated in Table 5.12.

Table 5.12. Student t-test results (p-values) for the tensile property differences in the cross and machine direction

Property	Pellethane	TPS	GS	Dicalite	Diatomite
Ultimate Tensile Strength	0.320	0.825	0.000	0.285	0.000
Yield Strength	0.947	0.017	0.842	0.228	0.087
Elongation to Break	0.292	0.760	0.006	0.632	0.855
Tensile Modulus	0.211	0.105	0.805	0.119	0.002

The effect of the incorporation of the fillers on the properties of the matrix was examined with a similar statistical evaluation. The results are tabulated in Table 5.13 and 5.14. The incorporation of the fillers results in significant decrease in the ultimate tensile strength of the samples, a significant increase in tensile modulus and a significant decrease in elongation to break. The use of the fillers resulted in membranes that were stiffer and possessing poorer tensile properties.

These results correspond to work undertaken by Ishiaku et al, 2002 in which the incorporation of thermoplastic starch and granular starch in polycaprolactone was examined. In the before mentioned study the use of thermoplastic starch resulted in poorer properties when compared to granular starch. This was explained by a combination of poorer interaction between the matrix and the TPS compared to the granular starch and the formation of water vapour which creates microvoids when TPS is blended with the matrix.

In this exercise there was no significant difference between the ultimate tensile strength, yield strength and elongation to break achieved in the cross direction when comparing the granular starch filled membranes and the thermoplastic starch filled membranes. In the cross direction there the thermoplastic starch filled membranes are significantly stiffer than the granular

starch filled membranes. The other properties are on average similar when using granular starch or thermoplastic starch. The higher modulus obtained when using thermoplastic starch compared to granular starch is different from work performed by Ishiaku et al, 2003. The difference can be attributed to the fabrication procedure. The blends were dried before blowing films to ensure that there was no moisture present. It should be expected that the thermoplastic starch blends perform better than the granular starch blends since the thermoplastic starch is easily deformed. The thermoplastic starch will have a greater surface area and will have more contact with the matrix than the granular starch. The presence of micro-voids will decrease the performance of membrane negatively. All membranes produced did not contain any fish-eyes and it can be inferred that there was no moisture present. The absence of moisture resulted in no void formation and a stronger composite. Therefore the thermoplastic starch performed better than the granular starch.

Table 5.13. Student t-test results (p-values) for the tensile property differences between Pellethane and filled Pellethane (MD)

Property	TPS	GS	Dicalite	Diatomite
Ultimate Tensile Strength	0.0191	0.0003	0.0110	0.0032
Yield Strength	0.2317	0.1153	0.7541	0.6681
Elongation to Break	0.0242	0.0002	0.0001	0.0832
Tensile Modulus	0.0001	0.0654	0.0000	0.3096

Table 5.14. Student t-test results (p-values) for the tensile property differences between Pellethane and filled Pellethane (CD)

Property	TPS	GS	Dicalite	Diatomite
Ultimate Tensile Strength	0.0039	0.0000	0.0002	0.0024
Yield Strength	0.1221	0.1394	0.4075	0.2328
Elongation to Break	0.0066	0.0000	0.0000	0.0009
Tensile Modulus	0.0313	0.0028	0.0082	0.0113

Table 5.15. Student t-test results (p-values) for the tensile property differences granular starch filled membranes and thermoplastic starch filled membranes (CD)

Property	p-value
Ultimate Tensile Strength	0.559
Yield Strength	0.561
Elongation to Break	0.755
Tensile Modulus	0.036

5.4.2. Filled Starch-Pellethane Membranes

The properties obtained in the cross direction for the filled starch-Pellethane membranes were greater than the properties in the machine direction similar to the other membranes tested. The tensile properties of the membranes are shown in Figures 5.44 to 5.47.

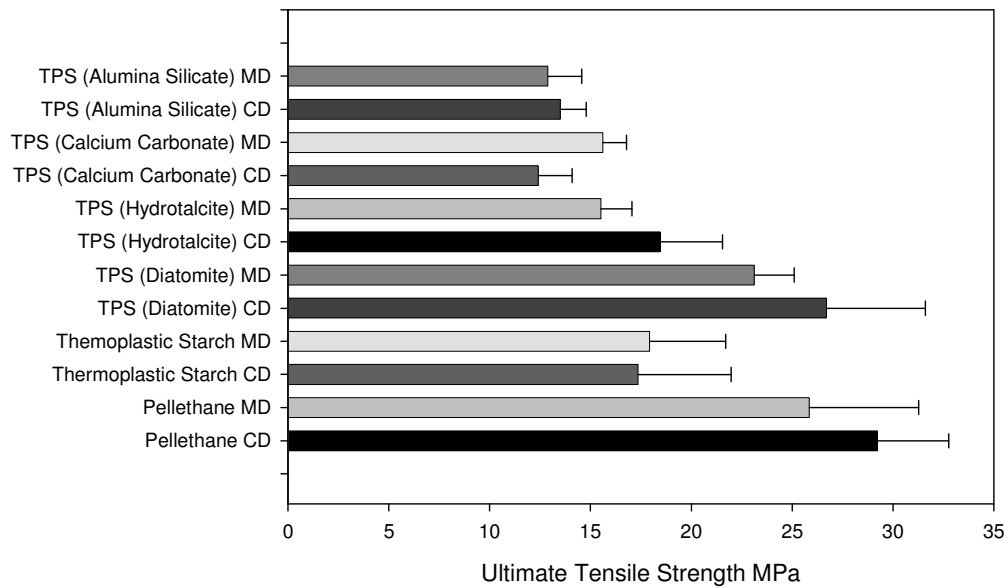


Figure 5.43. Ultimate tensile strength of membranes containing filled starch

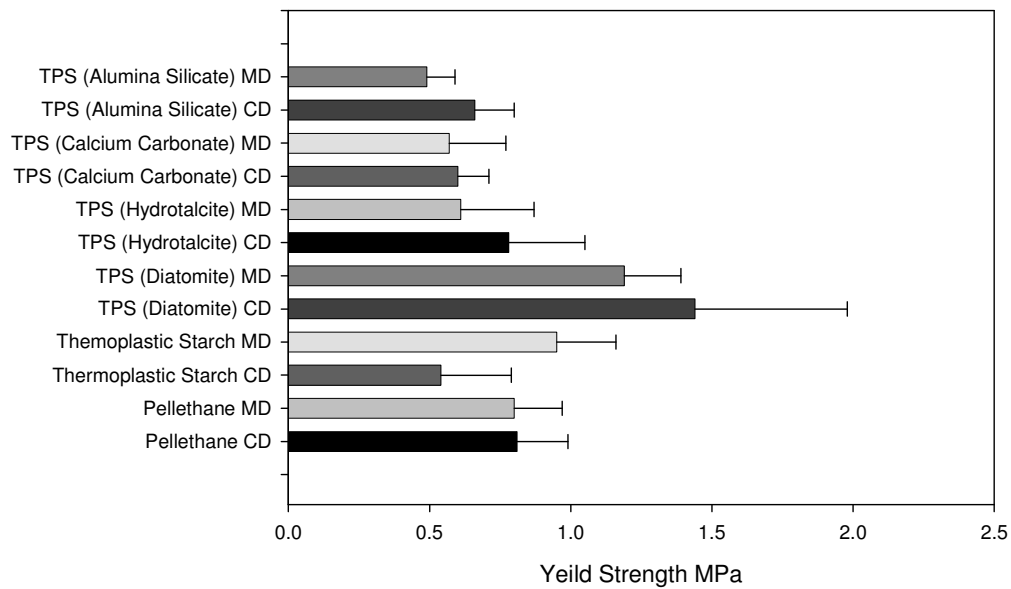


Figure 5.44. Yield strength of membranes containing filled starch

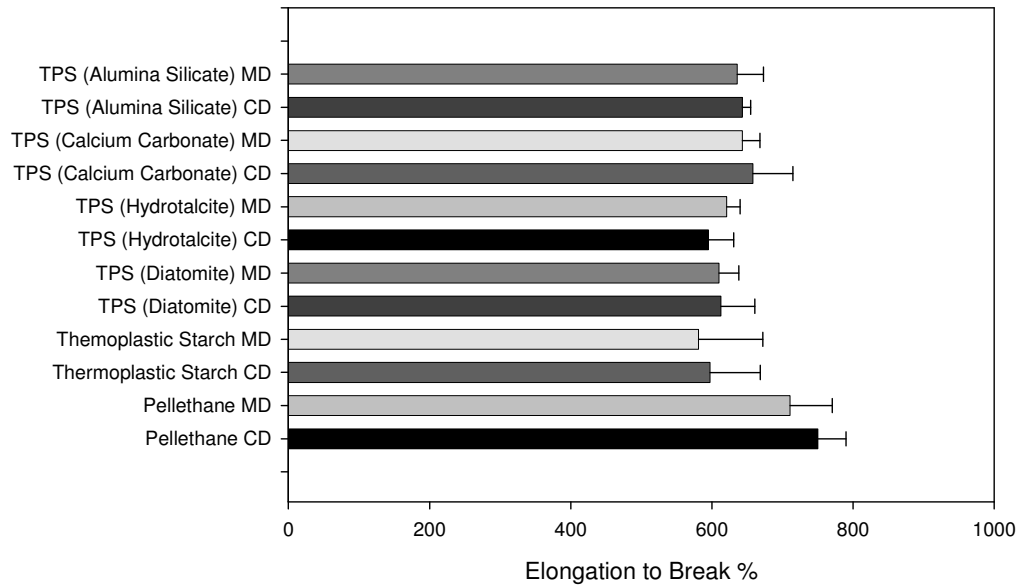


Figure 5.45. Elongation to break of membranes containing filled starch

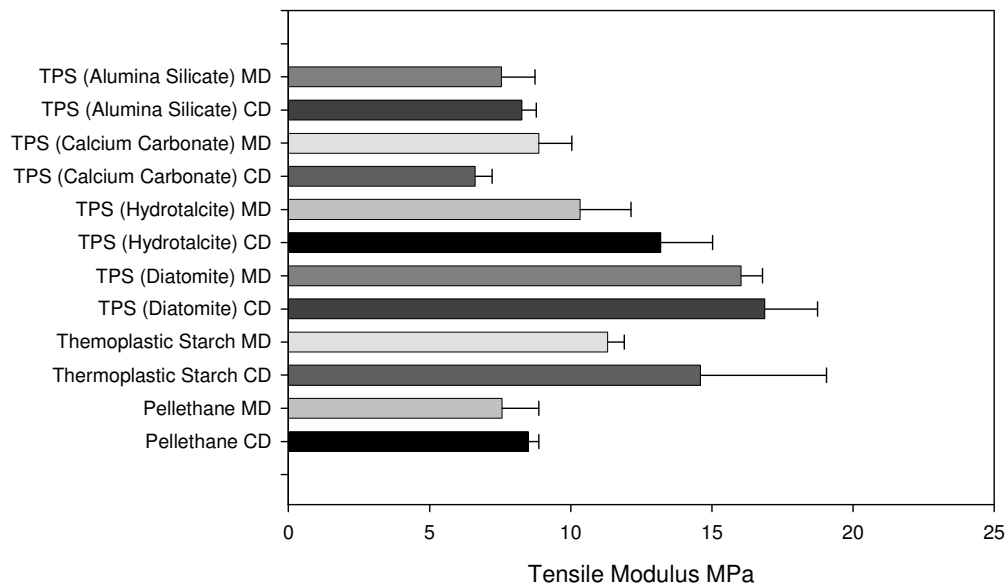


Figure 5.46. Tensile modulus of membranes containing filled starch

A statistical analysis shows that the variation between properties in the machine and cross direction is only significant for membranes containing starch filled with hydrotalcite or calcium carbonate. The p-values for student t-

test performed examining the differences between the machine and cross direction properties is tabulated in Table 5.16. The inclusion of calcium carbonate and alumina silicate results in a significant decrease in stiffness (when compared to unfilled starch-Pellethane membranes) which is not observed in the other membranes. The statistical analysis results are tabulated in Table 5.17. In inclusion of diatomite in the starch filled membrane results in a significant improvement in the ultimate tensile strength and yield strength compared to unfilled starch-Pellethane membranes. Other fillers did not show a significant improvement to the UTS or YS compared to the unfilled membranes. The use the diatomite in also results in an ultimate tensile strength that is statistically similar to that of the unfilled membrane. This is the only filler combination that does not shows decrease in the ultimate tensile properties of the composite (Refer to Table 5.18). The use of diatomite in combination with starch results in a higher yield strength compared to the unfilled membrane. The material is also significantly stiffer compared to the unfilled membrane. The diatomite may act similar to a mechanical compatibilizer. The pores of the diatomite are filled with the TPS and polyurethane matrix. This increases the contact surface area between the matrix and the reinforcement. Since the TPS is also present in the pores the contact surface area between the TPS and diatomite is also increased. The larger contact surface area can account for the improvement in the properties.

Table 5.16. Student t-test results (p -values) for the tensile property differences in the cross and machine direction

Property	Diatomite	Hydrotalcite	Calcium Carbonate	Alumina Silicate
Ultimate Tensile Strength	0.17	0.04	0.00	0.49
Yield Strength	0.36	0.33	0.79	0.04
Elongation to Break	0.93	0.20	0.58	0.92
Tensile Modulus	0.38	0.04	0.00	0.52

Table 5.17. Student t-test results (p-values) for the tensile property differences between Starch-Pellethane membranes and filled Starch-Pellethane (CD)

Property	Diatomite	Hydrotalcite	Calcium Carbonate	Alumina Silicate
Ultimate Tensile Strength	0.01	0.67	0.04	0.15
Yield Strength	0.01	0.19	0.62	0.42
Elongation to Break	0.69	0.96	0.15	0.25
Tensile Modulus	0.32	0.53	0.00	0.03

Table 5.18. Student t-test results (p-values) for the tensile property differences between Diatomite-Starch-Pellethane membranes and unfilled Pellethane (CD)

Property	Dicalite-TPS
Ultimate Tensile Strength	0.4177
Yield Strength	0.0617
Elongation to Break	0.0025
Tensile Modulus	0.0001

5.5. Cost Benefit

The commercial viability of the production of the developed membrane was examined in a cost model. Film blowing plants usually do not operate continuously. The model was therefore based on a batch film blowing plant. Two options were looked at:

1. A plant that used a single screw extruder for the compounding of the TPS and a twin screw extruder for the compounding of the polymer blend. These units would have separate pelletizers and will run

simultaneously.

2. A plant that used twin screw extruder for the compounding of the TPS and the compounding of the polymer blend. Batches of TPS would have to be produced first and stored. After sufficient TPS pellets are produced a batch of the polymer blend is produced and stored for blowing.

Although the second plant needs attention to logistics to ensure that the supply of pellets to the film blower is not interrupted it will result in a saving of capital equipment. Generally the cost of extruders increases at a decreasing rate with an increase in extruder capacity. Higher capacity extruders will allow flexibility for expansion and using more than one material on the machine. The disadvantage of a higher capacity extruder is that there is larger waste during purging.

The following assumptions were made when performing the cost analysis

1. Selling price will be estimated to be a maximum of R14/linear meter
2. Exchange rates are taken from x-rates.com
3. A batch process cost will be estimated where one extruder and pelletizer will be required
4. This process must be equivalent to running a plant with two extruders
5. Therefore a contingency of 50% equipment costs is incorporated into the model
6. Four operators and one supervisor is accounted for in the model as well as two cleaners and a clerk
7. Estimates for the direct and indirect costs are obtained from Peters et al, 2003 with a few exceptions
8. Working capital is estimated as one month of raw materials supply
9. Overheads are assumed to be approximately 100% cost of labour
10. It is assumed that the plant will be constructed on vacant land that will be bought and not in rented space (Rent=0)
11. Construction fees are assumed to be slightly lower for plastics plants

than other plants therefore this was reduced from 25% to 15% direct costs

12. BreathTex will purchase the complete amount of membrane produced. The growth rate in sales has been ignored to illustrate a worst case scenario. Sales to companies other than BreathTex have also been ignored. The incorporation of these factors will increase the profitability and sustainability of the plant.
13. For the DCF analysis depreciation was ignored

The resulting analysis shows that the plant can produce membranes at approximately R5 per linear meter. BreatheTex Corp supplied market information stating that membranes with similar performance are sold at approximately R18 per linear meter.

A sensitivity analysis of the IRR and break even point was performed. The primary factors examined were the operating costs, capital investment and sales. The results are displayed below. The analysis was performed for a 20% TPS blend which was made using 40% glycerol on a starch basis and sold at R16 per linear meter. Figure 5.47 shows the sensitivity analysis.

The capital investment is not a dominant factor unless it has been poorly underestimated. This is unlikely due to the large contingency that is planned for. The effect sales greatly influence the eventual profitability of the plant when compared to operating costs. Since the membranes have been developed in conjunction BreatheTex Corp and as an import replacement for BreatheTex Corp the base line sales are unlikely to decrease. An IRR of more than 30% is highly probable. A copy of the analysis is attached at the back of the dissertation in Appendix C.

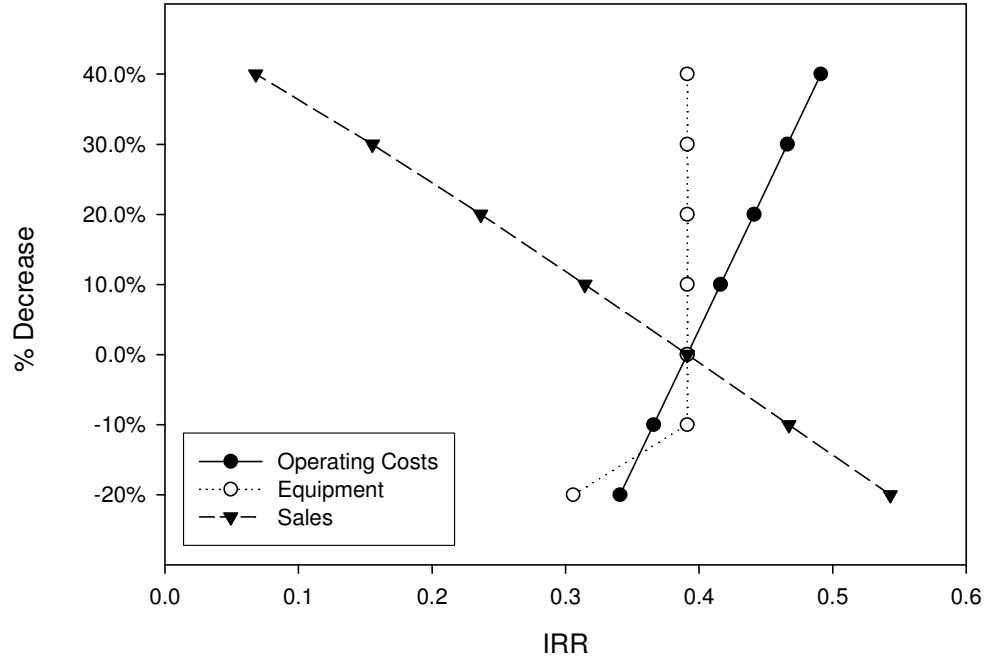


Figure 5.47 Sensitivity analyses performed on the IRR for a proposed plant examining the effect of operating costs, capital and sales fluctuations

6. Conclusion

The inclusion of fillers is the quickest and cheapest method to alter the properties of polymer membranes. The inclusion of TPS in a polyurethane matrix has resulted in a decrease in the permeability of the membrane. The decrease follows the trend that can be predicted by the Maxwell and Bruggeman equation. These equations are only valid for spherical particles or particles that can be approximated to be spheres. The Maxwell-Wagner-Sillars model better describes the effect of non-spherical fillers on the permeability of a composite and was used to calculate the starch permeability since thermoplastic starch is deformed in the parallel to the membrane surface as seen in the SEM pictures and in prior art [Santayanon & Wootthikanokkhan, 2003; Carvalho et al, 2001; Ishiaku et al, 2002]. The effect of thermoplastic starch on breathability of membranes has not been previously examined in literature and therefore cannot be compared to prior art. Thermoplastic starch filled membranes perform the same as granular starch filled membrane if the volume fraction of starch in the membrane is the same. The granular starch membranes do however take significantly longer to reach equilibrium than the thermoplastic starch membranes. The amylose content of the starch has no significant effect on the permeability of the composite membrane.

The inclusion of Dicalite in membranes resulted in a decrease in the effective permeability of the composite membrane. This is expected since the Dicalite particles are impermeable. The Dicalite particles were arranged parallel to the membrane surface and the Maxwell-Wagner-Sillars model described the phenomena well when the shape factor represented oblate spheres. This corresponded to the arrangement of particles and is expected since the film blowing procedure stretches the membrane thus aligning the particles parallel to the membrane.

The inclusion of diatomite in the membranes also resulted in a decrease in the permeability of the membrane. The porous nature of the diatomite resulted in a lower decrease as experienced with the inclusion of Dicalite. This apparent

permeability is due to the porosity of the diatomite. Manipulation of the shape factors reveal that the arrangement of filler particles impact dramatically on the permeability of the composite membrane. A summary of all filled membranes is tabulated below.

Table 6.1 Summary of WVTR results

Starch wt %	Glycerol wt% (Starch Basis)	Other Filler	WVTR _{Avg} g.m ⁻² day ⁻¹	Std. Deviation g.m ⁻² day ⁻¹
0	-	-	3425	433
10	30	-	3006	307
10	40	-	3060	138
20	30	-	2648	148
20	40	-	2832	110
20	0	-	2409	96
20	40	Diatomite	2832	110
20	40	Alumina Silicate	2763	88
20	40	Hydrotalcite	2588	27
20	40	Calcium Carbonate	2754	49
-	-	Dicalite(20% wt)	2151	88
-	-	Diatomite(20% wt)	2750	72

The degree of blocking is a vital factor in the use of the membrane commercially. If the membranes display strong blocking the membrane will stick to itself making unwinding from a reel and lamination impossible. Blowing the membrane with a backing film will not be an alternative since the membrane will be difficult to delaminate from the backing film.

Despite the decrease in the permeability caused by the inclusion of starch and other fillers, the filled membranes are easier to handle. The blocking tendency of each of the filled membranes is reduced by the addition of filler. The reduction in blocking can be attributed to surface roughness created by the filler and some surface modification caused by the filler. The best performing filler was the starch, however all fillers resulted in a decrease in the blocking tendency of the membranes. The superior performance by the starch can be attributed to a combination of surface roughness and chemical effects due to the presence of hydroxyl groups from the starch. The other fillers provide surface roughness only.

The use of the fillers in the matrix results in a composite that is stiffer than the unfilled polymer. There is however a decrease in the ultimate tensile properties and elongation to break of the filled membranes when compared to the unfilled membranes. The use of thermoplastic starch and granular starch does not yield composites of significantly different ultimate tensile strength or elongation to break. The thermoplastic starch filled membrane does result in a significantly stiffer composite when compared to the granular starch filled membranes. This does not correspond to prior art.

The use of starch as a filler results in a significant decrease in the production costs. The cost of starch is approximately 15 times less than the cost of the Pellethane resin. Incorporation of at 10% and 20% m/m levels results in a raw material cost saving of 10% and 20% respectively. A techno-economic model showed that the membranes would cost approximately ZAR5 per linear meter to produce and performs in the category of membranes that usually cost approximately ZAR16 per linear meter. If a plant is built to manufacture the membranes the internal rate of return for the plant is approximately 40%.

The use of the fillers examined in this study for modification of Pellethane results in membranes with the following properties:

1. Decreased WVTR

2. Improved blocking characteristics
3. Improved tensile modulus
4. Decrease ultimate tensile strength
5. Decreased elongation to break
6. Significant financial benefit

The decrease in WVTR falls within the performance range for other membranes in its class. The tensile properties are not of vital importance for application in clothing lamination since the membrane will be laminated onto a fabric which will act as a support. However if a more durable membrane is required the use of diatomite filled TPS will provide better tensile properties compared to the unfilled membrane. The improved anti-block characteristics are vital for the use of the membranes in a commercial environment. With a decrease in manufacturing cost the membrane will be a viable option for replacement of currently imported membranes.

The starch filled membranes resulted in the best performance. The Dicalite filled membranes resulted in poor performance. The diatomite filled membranes resulted in performance which was comparable to some of the starch filled membranes. The inclusion of calcium carbonate with the starch in the polyurethane matrix results in similar permeability when compared to membranes filled with starch alone. The fillers examined are all low cost fillers. The cost saving enjoyed from the use of these fillers depends on the level of addition. There is a trade-off between the performance achieved and the cost saving. At low addition levels the use of starch results in membranes that perform greater than required. At an addition level of approximately 17.5% (v/v) a techno-economic cost model indicates that an internal rate of return of 40% will be achieved. The performance achieved from these membranes is approximately $2700 \text{ g}\cdot\text{m}^{-2}\cdot\text{day}^{-1}$ which is within the specification of the application.

In concluding, the use of starch for modification of Pellethane membranes will result in a composite membrane that has great potential for replacement of currently imported products.

7. Acknowledgments

I would like to acknowledge and thank the following individuals:

- The mentorship and guidance of Dr Heidi Rolfes throughout the duration of this project is gratefully acknowledged.
- Prof Walter Focke for guidance, advice and supervision.
- Special thanks to the Innovation Fund, BreatheTex Corp and CSIR for the funding as part of IF project 32445 and for allowing the use of some results of the project in this dissertation.
- Charlene Fourie, Thilo van der Merwe and Robert Kwindu for sample preparation
- Viktoria Varga for formulation advice and guidance with regard to the completion of this dissertation

8. References

1. Barton, A. F. M., (1991) Handbook of solubility parameters and other cohesion parameters 2nd Editions, CRC Press, 55-69 369-446
2. BHA Group., (s.a) eVent product literature, www.eventfabrics.com [2006-08-28]
3. Bouma, R.H.B., Checchetti, A., Chidichimo, G. & Drioli, E., (1997) Permeation through a heterogeneous membrane: the effect of the dispersed phase, Journal of Membrane Science 128, 141-149
4. Breathetex Corp., (s.a) Introducing BreathteTex Corporation (Pty) Ltd ECMAC, www.namactech.co.za/6g-ECMAC.pdf [2004-01-8]
5. Carvalho, A. J. F., Curvelo, A. A. S. & Agnelli J. A. M. (2001) A first insight on composites of thermoplastic starch and kaolin, Carbohydrate Polymers 45, 189-194
6. Clarizia, G., Algieri, C. & Drioli, E., (2004) Filler-Polymer combination: a route to modify gas transport properties of a polymeric membrane, Polymer 45, 5671-5681
7. Davis, G. (2003) Characterization and characteristics of degradable polymer sacks, Material Characterization, 147-157
8. Dow, (s.a) Pellethane Polyurethane Thermoplastic Elastomers (s.a) www.dow.com [2004-01-30]
9. Elf Atochem (s.a) Product information brochure: Pebax and Pebatex, Elf Autochem, France
10. George, S. C. & Thomas, S., (2001) Transport phenomena through polymeric systems, Progress in Polymer Science Vol 26, 985-1017
11. Gonza, E.E., Parentis, M.L. & Gottifredi, J.C., (2005) Estimating models for predicting effective permeability of mixed matrix membranes, Journal of membrane Science
12. Gore, R. W. & Allen. S. B. (1980) Waterproof laminate, U.S. Patent 4194041 assigned to W. L. Gore & Associates Inc, USA
13. Gretton, J. C., Brook, D. B., Dyson, H. M. & Harlock, S. C., (1996) A correlation between test methods used to measure MVT through fabrics, Journal of Coated Fabrics Vol 25, 301-310

14. Ha, S., Broecker, H. C., (2002) Characteristics of polyurethanes incorporating starch granules, *Polymer* 43, 5227-5234
15. Hale, W. R., Dohrer, K. K., Tant, M. R. & Sand, I. D., (2001) A diffusion model for water vapor transmission through microporous polyethylene/CaCO₃ films, *Colloids and Surfaces A: Physicochem. Eng. Aspects* 187-188, 483-491
16. Ishiaku, U.S., Pang, K. W., Lee W. S. & Mohd. Ishak Z. A. (2002) Mechanical properties and enzymic degradation of thermoplastic and granular sago starch filled poly(ϵ -caprolactone) *European Polymer Journal* 38, 393-401
17. Islam, M.A. & Buschatz, H., (2002) Gas permeation through a glassy polymer: chemical potential gradient or dual mobility mode, *Chemical Engineering Science* 57, 2089-2099
18. Jena, A. & Gupta, K., (2002) Characterization of water vapor permeable membranes, *Desalination* 149, 471-476
19. Ji, W., Sikdar, S.K. & Hwang, S., (1995) Sorption, diffusion and permeation of 1,1,1-trichloroethane through absorbent-filled polymeric membranes, *Journal of Membrane Science* 103, 243-255
20. Jonquière, A., Clément, R. & Lochon, P., (2002) Permeability of block copolymers to vapors and liquids, *Progress in Polymer Science* 27, 1803-1877
21. Kanehashi, S. & Nagai, K., (2005) analysis of dual-mode model parameters for gas sorption in glassy polymers, *Journal of Membrane Science* 253, 117-138
22. Kramar, L., (1998) Recent and future trends for high performance fabrics providing breathability and waterproofness, *Journal of Coated Fabrics* Volume 28, 106-115
23. Lape, N.K., Nuxoll, E.E. & Cussler, E.L., (2004) Polydisperse flakes in barrier films, *Journal of Membrane Science* 236, 29-37
24. Marmot., (s.a) MemBrain®, www.marmotmountain.com/membrain.htm [2006-08-28]
25. McCormack, A. L. & Haffner. W. B., (2004) Breathable multilayer films with breakable skin layers, U.S. Patent 6682803 assigned to Kimberly Clark Worldwide Inc, USA

26. McCullough, E.A., Kwon, M. & Shim, H., (2003) A comparison of standard methods for measuring water vapour permeability of fabrics, *Measurement Science and Technology* 14, 1402-1408
27. MIC., (s.a) Diaplex: The intelligent material, www.diaplex.com [2006-08-27]
28. Moggridge, G.D., Lape, N.K., Yang, C. & Cussler, E.L. (2003) Barrier films using flakes and reactive additives, *Progress in Organic Coatings* 46, 231-240
29. Nguyen, Q.T. Germain, Y. Clément, R. & Hirata, Y. Pervaporation, a novel technique for the measurement of vapour transmission rate of highly permeable films *Polymer Testing* Vol. 20 2001 pp 901-911
30. Painter, C. J., (1996) Waterproof, breathable fabric laminates: A perspective from film to market place, *Journal of Coated Fabrics* Volume 26, 107-130
31. Pearman, A. W. & Wright, S. J. (1976) Water vapour permeable sheet, U.S. Patent 3968292, assigned to Porvair Inc, UK
32. Peters, M.S., Timmerhaus, K.D., West, R.E. and Peters, M. "Plant Design and Economics for Chemical Engineers", McGraw Hill, 2003
33. Santayanon, R. & Wootthikanokkhan, J (2003). Modification of cassava starch by using propionic anhydride and properties of the starch-blended polyeter polyurethane. *Carbohydrate Polymers* 51, 17-24
34. Seidenstücker, T. & Fritz, H. G. (1998) Innovative biodegradable materials based upon starch and thermoplastic poly(ester-urethane) (TPU), *Polymer Degradation and Stability* 59, 279-285
35. Stroeks, A. & Dijkstra, K., (2001) Modelling the moisture vapour transmission rate through segmented block co-poly(ether-ester) based breathable films, *Polymer* 42, 117-127
36. Technicare Services Ltd., (2000) Physical Tests for Knitted and Woven Textiles, http://www.technicare-services.com/pricelist/physical_tests_for_knitted_and_w.htm [2004-02-16]
37. Toray Industries Inc., (2004) Comfort factors for activesports fabrics <http://www.torayentrant.com/comfort/comf.html> [2004-02-16]
38. Tsujit, Y., (2003) Gas sorption and permeation of glassy polymers with microvoids, *Progress in Polymer Science* 28, 1377-1401
39. Utracki, L. A., (1989) Polymer alloys and blends, Hanser
40. Utracki, L. A., (1991) Commercial polymer blends, Chapman & Hall, 86-116

41. Van Roey, M., (1991) Water resistant breathable fabrics, Journal of coated fabrics Vol 21, 20-31
42. Wang, Z.F., Wang, B., Qi, N., Zangh, H.F. & Zangh, L.Q., (2005) Influence of fillers on free volume and gas barrier properties in styrene-butadiene rubber studied by positrons, Polymer 46, 719-724
43. Warwicker, E. A. & Price, D. (1978) Water vapor permeable microporous sheet materials and their method of manufacture, U.S. Patent 4090010, assigned to Porvair Inc, UK
44. Weder, M., (1997) Performance of breathable rainwear materials with respect to protection, durability and ecology, Journal of Coated fabrics Vol 27, 146-168



Starch Membranes																	
% Glycerol	Sample name	Thickness µm	Lid gram	Sample detail		Lid with silica gel (After) gram	Film after gram	Testing time Hours	Water absorbed gram	WVTR Calculated			Normalized WVTR				
				Silica gel in lid gram	Film before gram					Individual values g/m ² .day	Average g/m ² .day	Std Dev g/m ² .day	Co. Var. %	Individual values g/m ² .day	Normalized to 20 micron g/m ² .day	Std Dev g/m ² .day	Co. Var. %
40	80% Pellethane 2103-70A + 20% TPS (Low Amylose)	27.03	172.6323	16.1909	0.14855	189.0922	0.14948	2	0.26993	2643.3	2836.0	341.8	12.05%	2904.2	2778.9	135.7	4.88%
40		21.86	172.9208	16.0582	0.12785	189.2648	0.12818	2	0.28613	2802.0				2886.8			
40		24.37	172.0294	16.106	0.13551	188.3945	0.1355	2	0.25909	2537.2				2704.7			
40		25.26	174.3893	16.1584	0.14117	190.8007	0.14137	2	0.2532	2479.5				2671.7			
40		13.38	172.6326	16.1864	0.08487	189.1734	0.08518	2	0.35471	3473.5				2966.5			
40		16.52	174.3893	15.9368	0.09415	190.6208	0.0944	2	0.29495	2888.3				2692.4			
40		13.85	174.5827	16.1455	0.09059	191.0372	0.09085	2	0.30926	3028.5				2625.7			
40	80% Pellethane 2103-70A + 20% TPS (High Amylose)	14.05	172.633	16.1037	0.08896	189.1336	0.08842	2	0.39636	3881.4	3443.5	513.1	14.90%	2878.1	2770.6	121.6	4.39%
40		21.19	172.9209	16.0806	0.13089	189.2709	0.13131	2	0.26982	2642.2				2770.3			
40		14.34	174.3891	16.1377	0.08367	190.886	0.08404	2	0.35957	3521.1				2657.7			
40		12.806	172.0311	16.4004	0.0667	188.8603	0.067	2	0.4291	4202.0				2873.3			
40		18.39	172.6326	16.1956	0.08633	189.1405	0.08618	2	0.31215	3056.8				2851.3			
40		15.52	172.9211	16.0209	0.07826	189.2967	0.07838	2	0.35482	3474.6				2807.5			
40		14.64	174.3894	16.0636	0.07106	190.7926	0.07116	2	0.3397	3326.5				2556.2			
40	90% Pellethane 2103-70A + 10% TPS (High Amylose)	18.12	172.6337	15.8781	0.0823	188.8435	0.08272	2	0.33212	3252.3	3213.6	260.6	8.11%	3093.9	3060.0	137.8	4.50%
40		20	172.9218	16.5184	0.10942	189.7396	0.10959	2	0.29957	2933.6				2933.6			
40		19.86	174.3915	16.0358	0.10068	190.7228	0.10103	2	0.29585	2897.1				2887.1			
40		17.14	172.6318	16.103	0.08827	189.0745	0.09818	2	0.34961	3423.6				3163.1			
40		14.83	172.0295	16.2429	0.08744	188.6353	0.08737	2	0.36283	3553.0				3031.4			
40		20.37	172.9206	16.1675	0.15239	189.4173	0.1522	2	0.32901	3221.9				3251.0			
30		80% Pellethane 2103-70A + 20% TPS (High Amylose)	39.27	172.037	15.3318	0.1857	187.5972	0.1858	2	0.2285				2237.6			
30	19.81		174.3961	15.3667	0.14497	190.0064	0.14685	2	0.24548	2403.9	2395.3						
30	15.03		172.6387	15.2868	0.07622	188.2506	0.07643	2	0.32531	3185.6	2833.7						
30	15.24		172.9259	15.2182	0.07899	188.4456	0.07922	2	0.30173	2954.7	2644.5						
30	15.48		172.0349	15.0771	0.08435	187.4141	0.08445	2	0.3022	2959.3	2666.8						
30	12.08		174.3942	15.1717	0.07065	189.8974	0.07092	2	0.33177	3248.9	2606.9						
30	90% Pellethane 2103-70A + 10% TPS (High Amylose)		13.23	172.643	15.4622	0.07805	188.4907	0.07818	2	0.38563	3776.3	3062.4	522.7	17.07%	3281.9	3006.4	306.9
30		17.27	172.9299	15.5626	0.09655	188.8602	0.09653	2	0.36768	3600.5	3440.4						
30		32.5	174.3988	15.9261	0.14307	190.5904	0.14331	2	0.26574	2602.3	2934.6						
30		19.25	172.6367	15.6	0.11318	188.5276	0.11315	2	0.29087	2848.4	2816.1						
30		12.73	172.9243	15.4186	0.09858	188.6522	0.09771	2	0.31043	3039.9	2602.4						
30		41.93	172.0332	15.388	0.12899	187.6783	0.12888	2	0.25599	2506.8	2963.0						
30		Pellethane 2103-70A	37.15	172.6434	15.5952	0.24573	188.4439	0.24676	2	0.20633	2020.5				3068.83		
30	16.48		172.9303	15.5283	0.18136	188.8785	0.1818	2	0.42034	4116.2	3446.7						
30	27.8		174.3988	15.5313	0.28342	190.2434	0.2836	2	0.31348	3069.8	4121.4						
30	85		172.6428	16.3855	0.48485	189.1261	0.48999	2	0.10294	1008.0	3309.8						
30	84		172.9293	16.6346	0.37998	189.6573	0.39006	2	0.10348	1013.3	3299.6						
30	63		172.0401	16.3103	0.40243	188.469	0.42169	2	0.13786	1350.0	3482.6						
30	93		174.3978	16.0934	0.45511	190.5693	0.4661	2	0.08909	872.4	3446.7						

Filled Starch Membranes																
Sample name	Thickness µm	Lid gram	Sample detail		Lid with silica gel (After) gram	Film after gram	Testing time Hours	Water absorbed gram	WVTR Calculated			Normalized WVTR				
			Silica gel in lid gram	Film before gram					Individual values g/m ² .day	Average g/m ² .day	Std Dev g/m ² .day	Co. Var. %	Individual values g/m ² .day	Normalized to 20 micron g/m ² .day	Std Dev g/m ² .day	Co. Var. %
80% Pellethane 2103-70A + 20% TPS (Diatomite)	27	172.6332	16.1656	0.14153	189.0518	0.14198	2	0.25345	2481.9	4290.7	3527.6	82.21%	2806.6	2763.3	88.0	3.18%
	23	172.0307	16.0616	0.12978	188.3635	0.1299	2	0.27132	2656.9				2821.1			
	27.46	172.1922	16.2691	0.15721	189.4394	0.15742	2	0.97832	9580.3							
	24.5	174.3902	16.0169	0.11232	190.6564	0.11258	2	0.24956	2443.8				2662.0			
80% Pellethane 2103-70A + 20% TPS (Plasfill 5)	22.3	172.6326	16.4161	0.11734	189.3071	0.11758	2	0.25864	2532.8	2482.3	43.8	1.76%	2607.3	2587.8	27.0	1.04%
	25	172.0303	16.2729	0.13645	188.5538	0.13654	2	0.25069	2454.9				2599.0			
	23.2	172.9212	16.1198	0.1294	189.2921	0.12943	2	0.25113	2459.2				2557.0			
	22.6	174.3895	16.1194	0.12397	190.7571	0.12414	2	0.24837								
80% Pellethane 2103-70A + 20% TPS (Hydrotalcite)	13.91	172.6327	16.2176	0.08579	189.1784	0.08629	2	0.3286	3217.8	3204.3	313.4	9.78%	2810.0	2753.9	48.7	1.77%
	13.19	172.0303	16.1082	0.08901	188.4943	0.08931	2	0.3561	3487.1							
	11.81	172.9215	16.258	0.09565	189.5214	0.09566	2	0.34191	3348.2				2722.3			
	19.26	174.3899	16.1408	0.13105	190.8123	0.13171	2	0.28226	2764.1				2729.3			
80% Pellethane 2103-70A + 20% TPS (Kulucote 2)	15.66	172.6337	16.3173	0.12028	189.273	0.12211	2	0.32383	3171.1	3178.8	189.0	5.95%	2810.7	2836.2	40.0	1.41%
	16.77	172.0311	16.308	0.12397	188.6882	0.1245	2	0.34963	3423.8							
	16.58	172.9221	16.0992	0.11924	189.3434	0.11957	2	0.32243	3157.4				2882.3			
	17.97	174.3902	16.0554	0.12603	190.7477	0.12648	2	0.30255	2962.7				2815.6			

Other Fillers																
Sample name	Thickness µm	Lid gram	Sample Details		Lid with silica gel (After) gram	Film after gram	Testing time Hours	Water absorbed gram	WVTR Calculated			Normalized WVTR				
			Silica gel in lid gram	Film before gram					Individual values g/m ² .day	Average g/m ² .day	Std Dev g/m ² .day	Co. Var. %	Individual values g/m ² .day	Normalized to 20 micron g/m ² .day	Std Dev g/m ² .day	Co. Var. %
80% Pellethane 2103-70A + 20% Dicalite	19.5	172.6285	16.0096	0.11082	188.8678	0.11173	2	0.23061	2258.3	2180.1	104.0	4.77%	2233.7	2150.5	88.4	4.11%
	20	172.027	16.0348	0.12699	188.2871	0.12745	2	0.22576	2210.8				2210.8			
	16.13	172.9178	16.1531	0.10352	189.3088	0.10394	2	0.23832	2333.8				2037.7			



	19.37	174.3857	16.0564	0.11219	190.6607	0.11278	2	0.21919	2146.4									2105.0
	21.16	172.0285	16.0436	0.09477	188.2813	0.09512	2	0.20935	2050.1									2120.5
	19.73	172.6297	16.0566	0.0984	188.9047	0.09988	2	0.21966	2151.2									2133.6
	20.72	172.9196	16.0326	0.09538	189.1823	0.0957	2	0.23022	2254.4									2302.9
	20.55	174.3872	16.0246	0.11042	190.6194	0.11075	2	0.20793	2036.2									2069.7
80% Pellethane 2103-70A + 20% Diatomite	29.52	172.0286	16.0987	0.13267	188.3331	0.13313	2	0.20626	2019.8	2196.8	133.3	4.72%						2692.0
	26.92	172.6298	16.0773	0.13999	188.9228	0.14023	2	0.21594	2114.6									2640.0
	29.6	172.9202	16.0015	0.1447	189.136	0.14493	2	0.21653	2120.4									2831.3
	26.69	174.3877	16.0442	0.12455	190.6625	0.1251	2	0.23115	2263.6									2808.6
	25.82	174.3902	16.0542	0.14873	190.6776	0.14885	2	0.23332	2284.8									2767.8
	24.32	174.5843	16.0195	0.15115	190.8464	0.15137	2	0.24282	2377.8									2757.0

Starch Kinetics											
Sample Details							WVTR Calculated				
Sample name	Lid	Silica gel in lid	Film before	Lid with silica gel (After)	Film after	Testing time	Water absorbed	Individual values	Average	Std Dev	
	gram	gram	gram	gram	gram	Hours	gram	g/m ² .day	g/m ² .day	g/m ² .day	
Thermoplastic Starch	174.3259	187.282	0.1196	187.3306	0.13	0.275	0.059	4201.91	3824.45	327.0641	
	174.6086	189.0317	0.1192	189.0751	0.1267	0.275	0.0509	3625.04			
	174.415	188.039	0.1392	188.0866	0.1428	0.275	0.0512	3646.40			
	174.5174	190.4609	0.1161	190.5403	0.1175	0.500	0.0808	3164.96	3366.04	185.0704	
	172.6561	187.4378	0.113	187.5148	0.1229	0.500	0.0869	3403.90			
	172.0558	188.2848	0.1338	188.3662	0.1425	0.500	0.0901	3529.25			
	172.9566	187.252	0.1285	187.3584	0.1326	0.783	0.1105	2762.76	2860.27	87.72225	
	172.3379	185.8656	0.1217	185.9808	0.1219	0.783	0.1154	2885.27			
	174.4876	186.716	0.1345	186.8289	0.1389	0.783	0.1173	2932.77			
	174.3259	187.3306	0.1305	187.5567	0.1321	1.667	0.2277	2675.73	2674.16	83.44386	
	174.6086	189.0751	0.1305	189.2841	0.1419	1.667	0.2204	2589.94			
	174.415	188.0866	0.1612	188.2779	0.2045	1.667	0.2346	2756.81			
	174.5174	190.5403	0.1276	190.7272	0.1294	1.350	0.1887	2737.57	2702.27	110.9265	
	172.6561	187.5148	0.1525	187.6972	0.1625	1.350	0.1924	2791.25			
	172.0558	188.3662	0.1537	188.5437	0.1539	1.350	0.1777	2577.99			
	172.9566	187.3584	0.117	187.511	0.11747	1.017	0.15307	2948.76	2724.71	198.9137	
	172.3379	185.9808	0.1581	186.1174	0.1594	1.017	0.1379	2656.52			
	174.4876	186.8289	0.129	186.962	0.12925	1.017	0.13335	2568.87			
	174.5168	191.6543	0.1404	194.7155	0.1503	24.000	3.0711	2506.17	2543.60	37.49758	
	172.6551	189.626	0.1382	192.7207	0.16033	24.000	3.11683	2543.49			
	172.0581	190.2842	0.1142	193.4438	0.1176	24.000	3.163	2581.16			
	174.5174	190.7272	0.1566	191.1917	0.16502	3.500	0.47292	2646.35	2575.95	66.96115	
	172.6561	187.6972	0.1802	188.1363	0.1902	3.500	0.4491	2513.06			
	172.0558	188.5437	0.1416	188.9995	0.1448	3.500	0.459	2568.46			

Starch Kinetics											
Sample Details							WVTR Calculated				
Sample name	Lid	Silica gel in lid	Film before	Lid with silica gel (After)	Film after	Testing time	Water absorbed	Individual values	Average	Std Dev	
	gram	gram	gram	gram	gram	Hours	gram	g/m ² .day	g/m ² .day	g/m ² .day	
Granular Starch	174.3276	188.8606	0.1023	188.9183	0.1029	0.250	0.0583	4567.26	4750.06	184.1145	
	174.6078	189.6926	0.102	189.7548	0.1028	0.250	0.063	4935.46			
	174.4135	186.5272	0.1022	186.5867	0.1033	0.250	0.0606	4747.45			
	172.9468	189.4592	0.0909	189.5394	0.1114	0.500	0.1007	3944.45	3799.52	176.0052	
	172.3372	188.2178	0.1147	188.3075	0.117	0.500	0.092	3603.67			
	174.4875	188.8426	0.1187	188.9177	0.1419	0.500	0.0983	3850.44			



174.3276	188.9083	0.1223	189.0501	0.1489	1.000	0.1684	3298.14	3330.13	27.85871
174.6078	189.7448	0.0896	189.9096	0.0955	1.000	0.1707	3343.19		
174.4135	186.5767	0.1072	186.715	0.1399	1.000	0.171	3349.06		
172.9468	189.5354	0.1078	189.7357	0.112	1.333	0.2045	3003.88	3173.29	156.9741
172.3372	188.2975	0.1053	188.5219	0.1065	1.333	0.2256	3313.81		
174.4875	188.9077	0.1023	189.0978	0.1302	1.333	0.218	3202.18		
174.5168	189.628	0.1232	189.8991	0.1219	1.667	0.2698	3170.45	3106.60	168.5549
172.6551	187.7129	0.1093	187.982	0.1154	1.667	0.2752	3233.90		
172.0581	188.43	0.1006	188.5168	0.2619	1.667	0.2481	2915.45		
172.9457	187.5578	0.1166	188.1036	0.1184	4.000	0.5476	2681.21	2761.02	106.1344
172.3367	187.7896	0.1032	188.3077	0.1736	4.000	0.5885	2881.47		
174.4869	189.2519	0.1117	189.8072	0.112	4.000	0.5556	2720.38		
174.3253	190.6375	0.097	190.7457	0.1226	0.750	0.1338	3493.99	3434.80	123.4355
174.6071	189.8279	0.1187	189.9469	0.1344	0.750	0.1347	3517.50		
174.4122	189.3311	0.112	189.446	0.1232	0.750	0.1261	3292.92		
174.3253	190.7807	0.12031	193.7486	0.1272	24.000	2.97479	2427.57	2471.43	47.13083
174.6071	189.3407	0.1038	192.4284	0.1057	24.000	3.0896	2521.26		
174.4122	190.8714	0.1159	193.8793	0.1292	24.000	3.0212	2465.45		
174.3241	189.9592	0.1299	193.966	0.1965	36.000	4.0734	2216.06	2376.91	116.3531
174.6058	190.9337	0.1346	195.0639	0.1561	36.000	4.1517	2258.66		
174.4117	192.1476	0.1068	196.654	0.1633	36.000	4.5629	2482.37		
174.5152	191.2112	0.0895	195.6151	0.1345	36.000	4.4489	2420.35		
172.6539	189.2888	0.1056	193.6175	0.1621	36.000	4.3852	2385.69		
172.0541	190.3921	0.1131	194.9195	0.178	36.000	4.5923	2498.36		



Summary of Tensile Tests

Sample 1: Dicalite CD	At Max Slope			At Break		Dimensions				MPa		%	MPa
	Maximum Slope	Load	Elongation	Load	Elongation	Thickness	Width	Area	Gauge Length	Ultimate Tensile Strength	Yield Stress	Elongation at Break	Tensile Modulus
1	0.027119678	0.13535	4.7582	2.2053	324.36	0.000019	0.0067	1.273E-07	65	17.32364493	1.06323645	4.99	14.52
2	0.030619031	0.096002	3.2191	2.6573	367.86	0.000019	0.0067	1.273E-07	65	20.87431265	0.75413983	5.66	15.23
3	0.022498385	0.097414	4.6072	2.1	358.05	0.000019	0.0067	1.273E-07	65	16.49646504	0.76523174	5.51	10.80
4	0.021554019	0.12472	6.6922	1.8781	320.69	0.000019	0.0067	1.273E-07	65	14.75333857	0.97973291	4.93	9.52
5	0.033401601	0.1747	5.3258	2.4215	320.69	0.000019	0.0067	1.273E-07	65	19.02199529	1.37234878	4.93	16.75
6	0.025615295	0.087706	3.2773	2.1037	371.41	0.000019	0.0067	1.273E-07	65	16.52553024	0.68897093	5.71	13.66
Average										17.49921445	0.93727677	5.29	13.41299276
Standare Deviation										2.155661181	0.25758511	0.38	2.747952049

Sample 2: Dicalite MD	At Max Slope			At Break		metre				MPa		%	MPa
	Maximum Slope	Load	Elongation	Load	Elongation	Thickness	Width	Area	Gauge Length	Ultimate Tensile Strength	Yield Stress	Elongation at Break	Tensile Modulus
1	0.03948595	0.16472	4.5486	2.9696	352.08	0.000022	0.0067	1.474E-07	65	20.14654003	1.11750339	5.42	15.97
2	0.037151756	0.078607	2.2965	2.521	339.2	0.000022	0.0067	1.474E-07	65	17.10312076	0.53329037	5.22	15.09
3	0.036083543	0.10808	3.256	2.8621	362.6	0.000022	0.0067	1.474E-07	65	19.41723202	0.73324288	5.58	14.64
4	0.037433521	0.10023	3.0046	2.5373	345.52	0.000022	0.0067	1.474E-07	65	17.21370421	0.67998643	5.32	14.71
5	0.03927578	0.085851	2.3795	2.7991	349.32	0.000022	0.0067	1.474E-07	65	18.98982361	0.58243555	5.37	15.91
6	0.040193158	0.13454	3.7246	2.7979	344.49	0.000022	0.0067	1.474E-07	65	18.9816825	0.91275441	5.30	15.93
Average										18.64201719	0.75986884	5.37	15.37515804
Standare Deviation										1.225493291	0.21963014	0.12	0.634078929

Sample 3: Diatomite MD	At Max Slope			At Break		metre				MPa		%	MPa
	Maximum Slope	Load	Elongation	Load	Elongation	Thickness	Width	Area	Gauge Length	Ultimate Tensile Strength	Yield Stress	Elongation at Break	Tensile Modulus
1	0.027087682	0.16911	7.1417	3.3576	420.25	0.000029	0.0067	1.943E-07	65	17.28049408	0.87035512	6.47	7.92
2	0.026678335	0.16042	7.2234	3.3016	421.14	0.000029	0.0067	1.943E-07	65	16.99227998	0.82563047	6.48	7.43
3	0.028536298	0.13728	6.1465	3.4138	412.9	0.000029	0.0067	1.943E-07	65	17.56973752	0.70653628	6.35	7.47
4	0.026209732	0.18243	7.5771	3.0929	442.29	0.000029	0.0067	1.943E-07	65	15.91816778	0.9389089	6.80	8.05
5	0.030127987	0.14392	5.0121	3.2071	450.61	0.000029	0.0067	1.943E-07	65	16.50591868	0.74071024	6.93	9.61
6	0.030506038	0.083259	3.0133	3.4888	426.04	0.000029	0.0067	1.943E-07	65	17.95573855	0.42850746	6.55	9.24
Average										17.0370561	0.75177475	6.60	8.28773895
Standare Deviation										0.737971803	0.17955826	0.22	0.92109433

Sample 4: Diatomite CD	At Max Slope			At Break		metre				MPa		%	MPa
	Maximum Slope	Load	Elongation	Load	Elongation	Thickness	Width	Area	Gauge Length	Ultimate Tensile Strength	Yield Stress	Elongation at Break	Tensile Modulus
1	0.039276522	0.14832	3.8346	4.0605	427.83	0.000029	0.0067	1.943E-07	65	20.89809573	0.76335564	6.58	12.94
2	0.063947877	0.1207	2.1138	4.8873	423.85	0.000029	0.0067	1.943E-07	65	25.15337108	0.62120432	6.52	19.10
3	0.038378199	0.17082	4.681	4.1486	423.41	0.000029	0.0067	1.943E-07	65	21.35151827	0.87915594	6.51	12.21
4	0.044520278	0.25959	6.4287	4.1388	428.09	0.000029	0.0067	1.943E-07	65	21.3010808	1.33602676	6.59	13.51
5	0.038570931	0.25884	7.295	4.3346	429.74	0.000029	0.0067	1.943E-07	65	22.30880082	1.33216675	6.61	11.87
6	0.036216523	0.24991	7.7016	4.3649	447.9	0.000029	0.0067	1.943E-07	65	22.46474524	1.2862069	6.89	10.86
Average										22.24626866	1.03635272	6.62	13.41389402
Standare Deviation										1.550123565	0.31978868	0.14	2.931744554

Sample 5: Granular Starch CD	At Max Slope			At Break		metre				MPa		%	MPa
	Maximum Slope	Load	Elongation	Load	Elongation	Thickness	Width	Area	Gauge Length	Ultimate Tensile Strength	Yield Stress	Elongation at Break	Tensile Modulus
1	0.032571123	0.13519	4.1358	3.419	377.36	0.000033	0.0067	2.211E-07	65	15.46359114	0.61144279	5.81	9.61
2	0.031832796	0.16948	5.0709	3.5017	389.34	0.000033	0.0067	2.211E-07	65	15.83763003	0.76653098	5.99	9.83
3	0.034275661	0.072662	1.867	3.6247	382.74	0.000033	0.0067	2.211E-07	65	16.39393939	0.32863863	5.89	11.44
4	0.033399612	0.16952	5.0937	3.825	394.81	0.000033	0.0067	2.211E-07	65	17.29986431	0.7667119	6.07	9.78
5	0.035982146	0.11162	3.2412	3.5831	367.32	0.000033	0.0067	2.211E-07	65	16.20578924	0.50483944	5.65	10.12
6	0.033790584	0.16306	4.8859	3.5525	379.4	0.000033	0.0067	2.211E-07	65	16.06739032	0.73749435	5.84	9.81
Average										16.21136741	0.61927635	5.87	10.09938709
Standare Deviation										0.622537958	0.17608187	0.15	0.67815854



Sample 6: Granular Starch MD	At Max Slope			At Break		metre			MPa			Elongation at Break	MPa
	Maximum Slope	Load	Elongation	Load	Elongation	Thickness	Width	Area	Gauge Length	Ultimate Tensile Strength	Yield Stress		
1	0.024032456	0.13635	5.767	2.6372	344.1	0.000029	0.0067	1.943E-07	65	13.57282553	0.70174987	5.29	7.91
2	0.032889699	0.14613	4.3497	2.4582	299.89	0.000029	0.0067	1.943E-07	65	12.65156974	0.75208441	4.61	11.24
3	0.033171702	0.15469	4.6507	1.8339	228.48	0.000029	0.0067	1.943E-07	65				
4	0.022395543	0.11012	4.9559	2.8693	381.44	0.000029	0.0067	1.943E-07	65	14.76737005	0.56675244	5.87	7.43
5	0.033776901	0.09725	2.6286	2.6817	310.3	0.000029	0.0067	1.943E-07	65	13.8018528	0.50051467	4.77	12.38
6	0.035012231	0.088784	2.4196	3.36	355.05	0.000029	0.0067	1.943E-07	65				
7	0.024919755	0.095464	3.7161	2.5296	345.39	0.000029	0.0067	1.943E-07	65	13.01904272	0.4913227	5.31	8.59
8	0.033783306	0.15844	4.5485	2.2785	275.6	0.000029	0.0067	1.943E-07	65	11.72671127	0.81544004	4.24	11.65
Average										13.25656202	0.63797735	5.02	9.867543205
Standare Deviation										1.043338865	0.1371546	0.59	2.132871964

Sample 7: Polymer CD	At Max Slope			At Break		metre			MPa			Elongation at Break	MPa
	Maximum Slope	Load	Elongation	Load	Elongation	Thickness	Width	Area	Gauge Length	Ultimate Tensile Strength	Yield Stress		
1	0.024699097	0.23138	9.7576	1.7275	231.2	0.000036	0.0067	2.412E-07	65				
2	0.032786795	0.16903	5.46	7.036	489.26	0.000036	0.0067	2.412E-07	65	29.1708126	0.70078773	7.53	8.34
3	0.032742103	0.17517	5.5335	8.0077	493.3	0.000036	0.0067	2.412E-07	65	33.19941957	0.72624378	7.59	8.53
4	0.035891847	0.2591	7.7578	5.9418	453.14	0.000036	0.0067	2.412E-07	65	24.63432836	1.07421227	6.97	9.00
5	0.034220545	0.17512	5.8043	7.2122	515.56	0.000036	0.0067	2.412E-07	65	29.9013267	0.72603648	7.93	8.13
6	0.033363612	0.23449	7.4827	4.3059	359.58	0.000036	0.0067	2.412E-07	65				
Average										29.22647181	0.80682007	7.50	8.501170678
Standare Deviation										3.527540335	0.17866167	0.40	0.370863689

Sample 8: Polymer MD	At Max Slope			At Break		metre			MPa			Elongation at Break	MPa
	Maximum Slope	Load	Elongation	Load	Elongation	Thickness	Width	Area	Gauge Length	Ultimate Tensile Strength	Yield Stress		
1	0.034641555	0.19618	5.7814	6.7403	443.8	0.000038	0.0067	2.546E-07	65	26.47407698	0.77054203	6.83	8.66
2	0.031139379	0.15975	5.3992	6.7317	481.96	0.000038	0.0067	2.546E-07	65	26.44029851	0.62745483	7.41	7.55
3	0.025315303	0.23989	10.326	4.6677	409.57	0.000038	0.0067	2.546E-07	65	18.33346426	0.9422231	6.30	5.93
4	0.029123883	0.25555	9.7605	6.2309	461.42	0.000038	0.0067	2.546E-07	65	24.47329144	1.00373134	7.10	6.68
5	0.036973825	0.16547	4.6893	8.5319	512.95	0.000038	0.0067	2.546E-07	65	33.51099764	0.64992145	7.89	9.01
Average										25.84642577	0.79877455	7.11	7.568241519
Standare Deviation										5.427300928	0.1694768	0.60	1.297666481

Sample 9: TPS CD	At Max Slope			At Break		metre			MPa			Elongation at Break	MPa
	Maximum Slope	Load	Elongation	Load	Elongation	Thickness	Width	Area	Gauge Length	Ultimate Tensile Strength	Yield Stress		
1	0.040850802	0.19009	3.1848	3.5349	360.24	0.00004	0.0067	2.211E-07	65	15.98778833	0.85974672	5.54	17.55
2	0.047369374	0.080689	1.2128	4.6959	411.77	0.00004	0.0067	2.211E-07	65	21.23880597	0.36494346	6.33	19.56
3	0.046259845	0.071587	1.3598	4.7449	437.64	0.00004	0.0067	2.211E-07	65	21.46042515	0.32377657	6.73	15.48
4	0.037293538	0.084237	2.0525	3.9613	409.48	0.00004	0.0067	2.211E-07	65	17.91632745	0.3809905	6.30	12.07
6	0.030001329	0.17131	6.0494	2.252	321.84	0.00004	0.0067	2.211E-07	65	10.18543645	0.77480778	4.95	8.33
Average										17.35775667	0.54085301	5.97	14.59473289
Standare Deviation										4.623997841	0.25497569	0.71	4.467752912

Sample 10: TPS MD	At Max Slope			At Break		metre			MPa			Elongation at Break	MPa
	Maximum Slope	Load	Elongation	Load	Elongation	Thickness	Width	Area	Gauge Length	Ultimate Tensile Strength	Yield Stress		
1	0.034110933	0.12956	3.8711	3.7062	429.25	0.000035	0.0067	1.943E-07	65	19.07462687	0.66680391	6.60	11.20
2	0.036865728	0.18664	5.3559	2.0466	264.03	0.000035	0.0067	1.943E-07	65	10.53319609	0.96057643	4.06	11.66
3	0.035431582	0.19142	5.9452	3.6877	396.52	0.000035	0.0067	1.943E-07	65	18.97941328	0.98517756	6.10	10.77
4	0.038123092	0.15628	4.5325	4.141	409.97	0.000035	0.0067	1.943E-07	65	21.3124035	0.80432321	6.31	11.53
5	0.033973532	0.19119	6.0649	3.8136	401	0.000035	0.0067	1.943E-07	65	19.62738034	0.98399382	6.17	10.55
6	0.039454119	0.25071	6.9058	3.5118	365.69	0.000035	0.0067	1.943E-07	65	18.0741122	1.29032424	5.63	12.15
Average										17.93352204	0.9485332	5.81	11.30846261
Standare Deviation										3.780650588	0.20963508	0.91	0.592591376



Sample 1: TPS Diatomite CD	At Max Slope			At Break		Metre				MPa		%	MPa
	Maximum Slope	Load	Elongation	Load	Elongation	Thickness	Width	Area	Gauge Length	Ultimate Tensile Strength	Yield Stress	Elongation at Break	Tensile Modulus
1	0.041117069	0.15048	4.2481	3.4192	389.18	0.000019	0.0067	1.273E-07	65	26.85938727	1.18208955	5.99	18.09
2	0.040709209	0.18638	5.4409	3.7388	414.87	0.000019	0.0067	1.273E-07	65	29.36999214	1.46410055	6.38	17.49
3	0.036948499	0.096504	2.9886	2.313	347.93	0.000019	0.0067	1.273E-07	65	18.16967793	0.75808327	5.35	16.49
4	0.032085608	0.28236	10.441	3.7054	416.08	0.000019	0.0067	1.273E-07	65	29.1076198	2.21806756	6.40	13.81
5	0.042287738	0.19825	5.4762	3.8183	423.68	0.000019	0.0067	1.273E-07	65	29.99450118	1.55734485	6.52	18.48
6	0.029301879	0.16152	6.382	2.617	377.84	0.000019	0.0067	1.273E-07	65				
Average										26.70023566	1.43593716	6.13	16.87186152
Standare Deviation										4.913527955	0.53646656	0.48	1.870428169

Sample 2: TPS Diatomite MD	At Max Slope			At Break		Metre				MPa		%	MPa
	Maximum Slope	Load	Elongation	Load	Elongation	Thickness	Width	Area	Gauge Length	Ultimate Tensile Strength	Yield Stress	Elongation at Break	Tensile Modulus
1	0.040968717	0.15667	4.1003	3.1388	377.44	0.000022	0.0067	1.474E-07	65	21.29443691	1.06289009	5.81	16.85
2	0.040250814	0.1653	4.3635	3.4371	398.14	0.000022	0.0067	1.474E-07	65	23.31818182	1.12143826	6.13	16.71
3	0.031923297	0.15822	5.4572	2.8494	417.34	0.000022	0.0067	1.474E-07	65				
4	0.039790695	0.19611	5.556	3.8416	425.87	0.000022	0.0067	1.474E-07	65	26.0624152	1.33046133	6.55	15.57
5	0.037352414	0.14297	4.1886	3.1301	386.17	0.000022	0.0067	1.474E-07	65	21.23541384	0.96994573	5.94	15.05
6	0.040838768	0.21335	5.8859	3.4856	395.54	0.000022	0.0067	1.474E-07	65	23.64721845	1.44742198	6.09	15.98
Average										23.11153324	1.18643148	6.10	16.03123798
Standare Deviation										1.991169863	0.1969856	0.28	0.758670064

Sample 3: TPS Hydrotalcite CD	At Max Slope			At Break		Metre				MPa		%	MPa
	Maximum Slope	Load	Elongation	Load	Elongation	Thickness	Width	Area	Gauge Length	Ultimate Tensile Strength	Yield Stress	Elongation at Break	Tensile Modulus
1	0.037286472	0.13563	3.8534	3.081	356.56	0.000029	0.0067	1.943E-07	65	15.85692229	0.69804426	5.49	11.77
2	0.033919046	0.14402	5.1679	3.0477	398.23	0.000029	0.0067	1.943E-07	65				
3	0.039842422	0.14125	3.6105	3.6609	402.31	0.000029	0.0067	1.943E-07	65	18.84148224	0.72696861	6.19	13.09
4	0.038504927	0.18431	5.3821	3.3072	366.02	0.000029	0.0067	1.943E-07	65	17.02110139	0.94858466	5.63	11.46
5	0.052642849	0.21534	4.4792	4.5964	405.69	0.000029	0.0067	1.943E-07	65	23.65620175	1.10828616	6.24	16.08
6	0.0448297	0.079263	1.9569	3.28	402.98	0.000029	0.0067	1.943E-07	65	16.88111168	0.40794133	6.20	13.55
Average										18.45136387	0.777965	5.95	13.19031042
Standare Deviation										3.101813967	0.26651858	0.36	1.838364161

Sample 4: TPS Hydrotalcite MD	At Max Slope			At Break		Metre				MPa		%	MPa
	Maximum Slope	Load	Elongation	Load	Elongation	Thickness	Width	Area	Gauge Length	Ultimate Tensile Strength	Yield Stress	Elongation at Break	Tensile Modulus
1	0.029849863	0.036487	1.2492	2.7317	417.64	0.000029	0.0067	1.943E-07	65	14.05918682	0.18778693	6.43	9.77
2	0.043385787	0.1727	4.4185	3.7583	403.45	0.000029	0.0067	1.943E-07	65				
3	0.028397284	0.13475	5.2075	2.672	403.49	0.000029	0.0067	1.943E-07	65	13.75193001	0.69351518	6.21	8.66
4	0.032593099	0.15504	5.2071	3.1144	405.24	0.000029	0.0067	1.943E-07	65	16.02882141	0.79794133	6.23	9.96
5	0.031206135	0.15573	5.2793	3.2021	407.55	0.000029	0.0067	1.943E-07	65	16.48018528	0.80149254	6.27	9.87
6	0.046570962	0.10652	2.6586	3.3529	383.6	0.000029	0.0067	1.943E-07	65	17.25630468	0.5482244	5.90	13.40
Average										15.51528564	0.60579207	6.21	10.33199544
Standare Deviation										1.537493453	0.25542009	0.19	1.796469751

Sample 5: TPS Kuluocote CD	At Max Slope			At Break		Metre				MPa		%	MPa
	Maximum Slope	Load	Elongation	Load	Elongation	Thickness	Width	Area	Gauge Length	Ultimate Tensile Strength	Yield Stress	Elongation at Break	Tensile Modulus
1	0.024972196	0.15379	7.13	2.8854	419.19	0.000033	0.0067	2.211E-07	65	13.05020353	0.69556762	6.45	6.34
2	0.029469037	0.10286	4.0338	3.3323	450.26	0.000033	0.0067	2.211E-07	65	15.07146088	0.46521936	6.93	7.50
3	0.025871459	0.14914	6.8244	2.7843	450.49	0.000033	0.0067	2.211E-07	65	12.59294437	0.67453641	6.93	6.42
4	0.023705711	0.1019	5.1685	2.7682	468.27	0.000033	0.0067	2.211E-07	65	12.52012664	0.46087743	7.20	5.80
5	0.025175083	0.13668	6.1958	2.3737	412	0.000033	0.0067	2.211E-07	65	10.73586612	0.61818182	6.34	6.49
6	0.025747488	0.15033	6.185	2.3166	366.27	0.000033	0.0067	2.211E-07	65	10.47761194	0.67991859	5.63	7.15
Average										12.40803558	0.5990502	6.58	6.614857727
Standare Deviation										1.677835258	0.10855589	0.57	0.609436963



Sample 6: TPS Kulucote MD	At Max Slope			At Break		Metre				MPa		%	MPa
	Maximum Slope	Load	Elongation	Load	Elongation	Thickness	Width	Area	Gauge Length	Ultimate Tensile Strength	Yield Stress	Elongation at Break	Tensile Modulus
1	0.024155043	0.11777	5.4901	2.7144	422.2	0.000029	0.0067	1.943E-07	65	13.97014925	0.60612455	6.50	7.18
2	0.030462292	0.036272	1.3213	3.1487	435.2	0.000029	0.0067	1.943E-07	65	16.20535255	0.18668039	6.70	9.18
3	0.031539091	0.12988	4.2629	2.7944	388.53	0.000029	0.0067	1.943E-07	65	14.38188369	0.66845085	5.98	10.19
4	0.034641907	0.11072	3.7762	3.1564	415.12	0.000029	0.0067	1.943E-07	65	16.24498199	0.56984045	6.39	9.81
5	0.029435548	0.12428	4.5795	3.2941	420.2	0.000029	0.0067	1.943E-07	65	16.95367988	0.63962944	6.46	9.08
6	0.02605025	0.14909	6.4137	3.0899	428.15	0.000029	0.0067	1.943E-07	65	15.90272774	0.76731858	6.59	7.78
Average										15.60979585	0.57300738	6.43	8.8693376
Standare Deviation										1.170144591	0.20082834	0.25	1.169330961

Sample 7: TPS PlasFill CD	At Max Slope			At Break		Metre				MPa		%	MPa
	Maximum Slope	Load	Elongation	Load	Elongation	Thickness	Width	Area	Gauge Length	Ultimate Tensile Strength	Yield Stress	Elongation at Break	Tensile Modulus
1	0.029180025	0.15816	5.5157	3.2574	427.21	0.000036	0.0067	2.412E-07	65	14.91500829	0.74411277	6.47	8.82
2	0.034072606	0.17948	5.4847	3.5975	420.33	0.000036	0.0067	2.412E-07	65	14.17827529	0.79382255	6.47	8.16
3	0.033070451	0.19147	6.3224	3.4198	420.82	0.000036	0.0067	2.412E-07	65	12.10033167	0.47014925	6.25	8.49
4	0.03281429	0.1134	3.5977	2.9186	406.33	0.000036	0.0067	2.412E-07	65	12.79311774	0.64303483	6.51	7.62
5	0.028537419	0.1551	5.4845	3.0857	423.45	0.000036	0.0067	2.412E-07	65	13.49668325	0.66277985	6.43	8.273754851
6	0.032861069	0.23773	8.0491	3.8069	420.28	0.000036	0.0067	2.412E-07	65	1.280757039	0.14292614	0.12	0.511285388
Average										13.49668325	0.66277985	6.43	8.273754851
Standare Deviation										1.280757039	0.14292614	0.12	0.511285388

Sample 8: TPS PlasFill MD	At Max Slope			At Break		Metre				MPa		%	MPa
	Maximum Slope	Load	Elongation	Load	Elongation	Thickness	Width	Area	Gauge Length	Ultimate Tensile Strength	Yield Stress	Elongation at Break	Tensile Modulus
1	0.033837059	0.14438	4.6725	3.3799	423.5	0.000038	0.0067	2.546E-07	65	13.27533386	0.56708562	6.52	7.89
2	0.027840283	0.15892	6.3603	3.2022	423.85	0.000038	0.0067	2.546E-07	65	12.57737628	0.62419482	6.52	6.38
3	0.038559266	0.11809	3.3791	3.0926	383.47	0.000038	0.0067	2.546E-07	65	12.14689709	0.46382561	5.90	8.92
4	0.039865506	0.10098	3.1101	3.9439	442.51	0.000038	0.0067	2.546E-07	65	15.49057345	0.39662215	6.81	8.29
5	0.026854414	0.10497	4.2774	2.7901	393.5	0.000038	0.0067	2.546E-07	65	10.95875884	0.41229379	6.05	6.27
6	0.035957527	0.07238	2.1227	3.0329	430.92	0.000036	0.0067	2.412E-07	65	12.57421227	0.30008292	6.63	9.19
Average										12.8897879	0.4928044	6.36	7.548904067
Standare Deviation										1.680111021	0.09918908	0.37	1.179576983

Appendix B: SEM Photographs

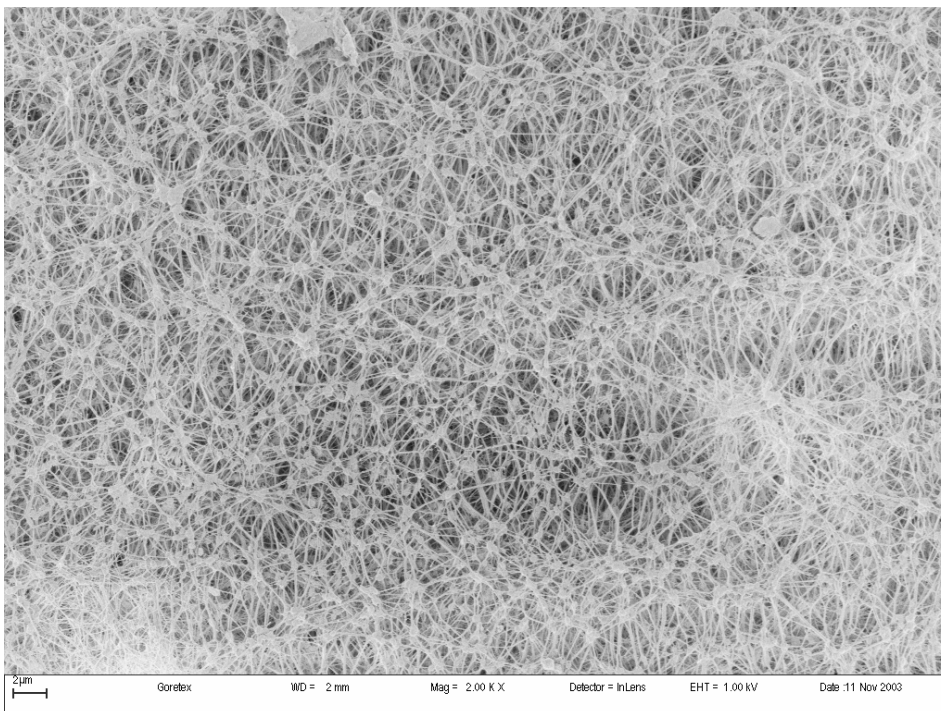


Figure B.1.1.Goretex membrane magnified 2000 times

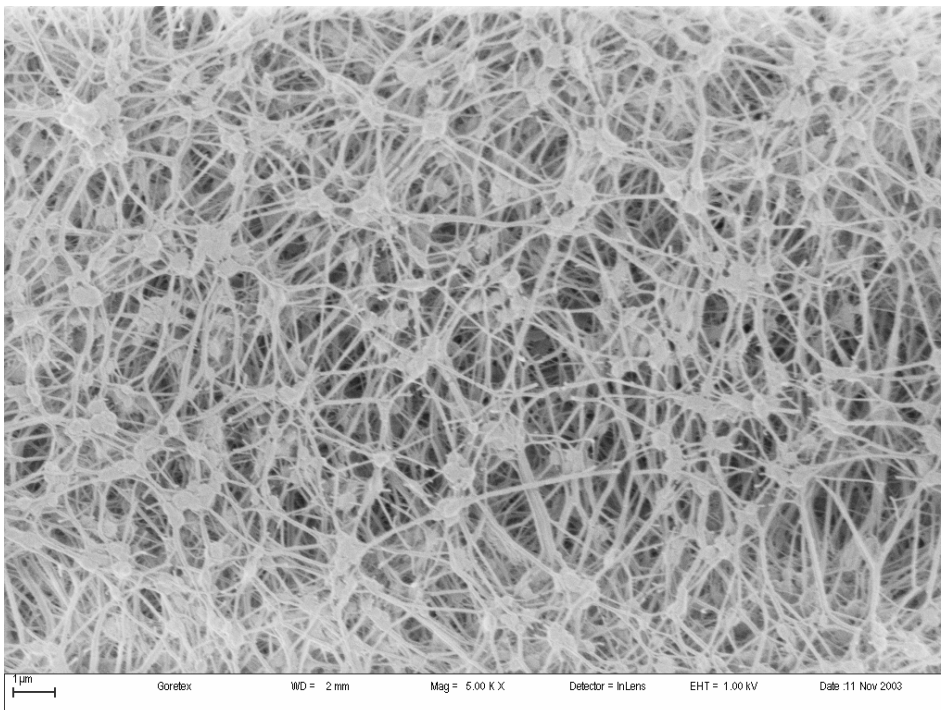


Figure B.1.2.Goretex membrane magnified 5000 times

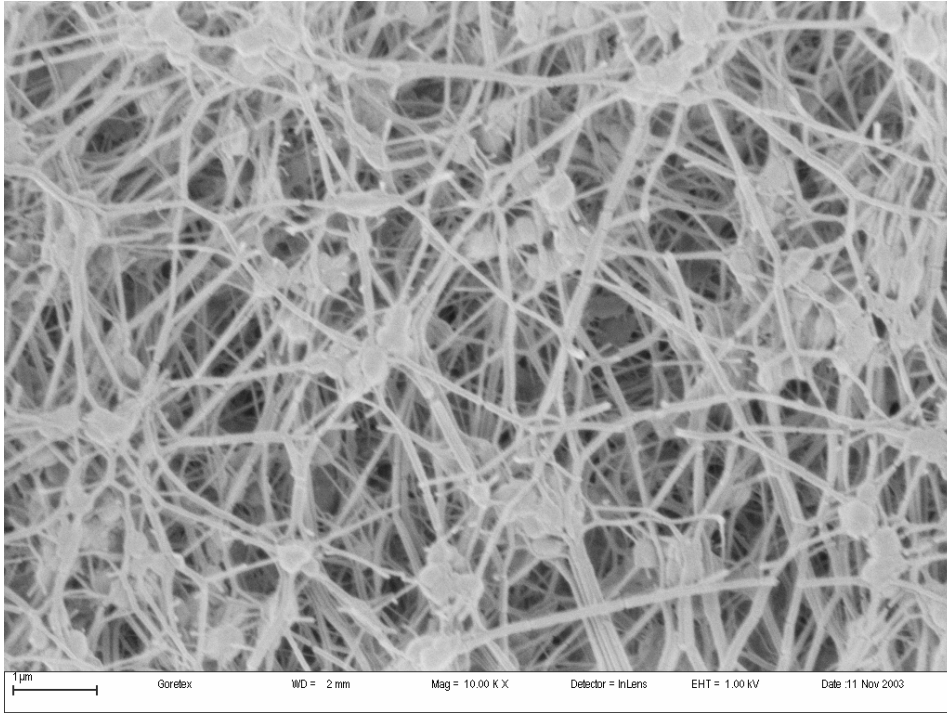


Figure B.1.3.Goretex membrane magnified 10 000 times

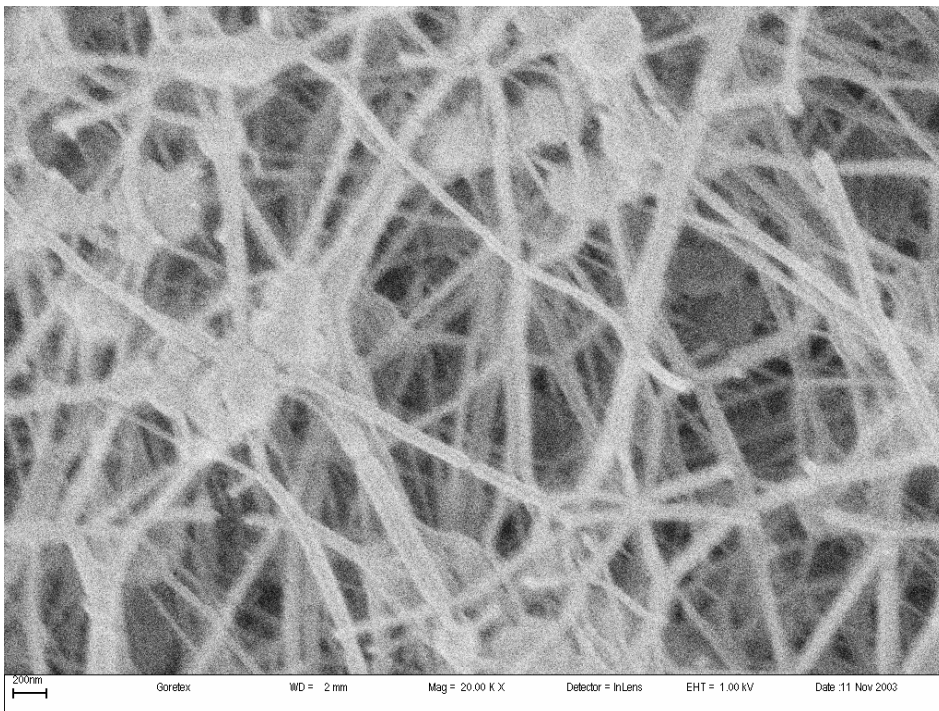


Figure B.1.4.Goretex membrane magnified 20 000 times

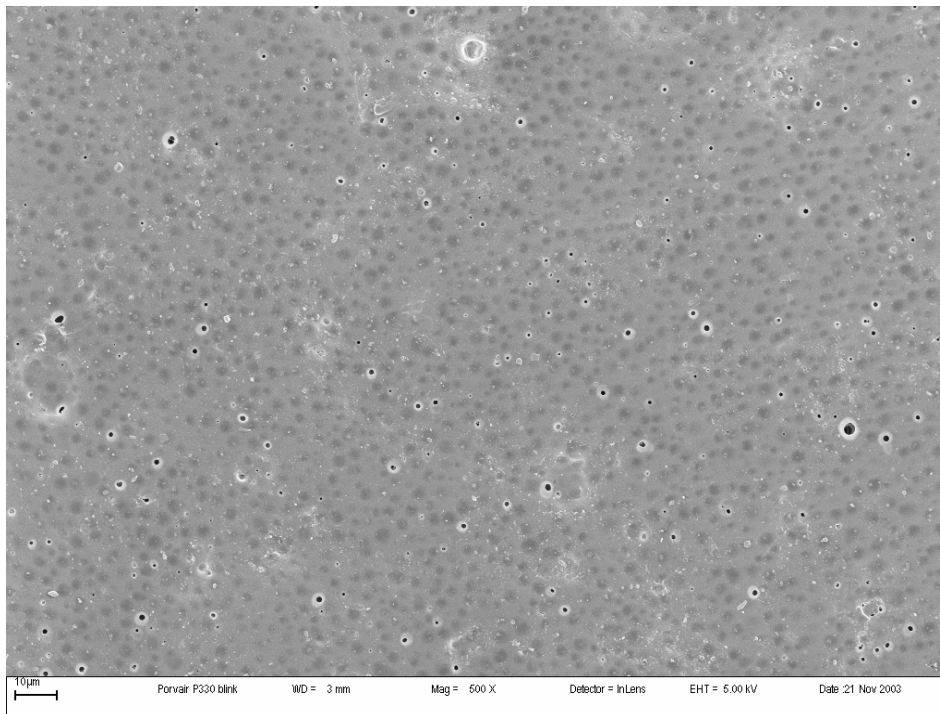


Figure B.2.1.Porvair P330 membrane magnified 500 times (Side not exposed to DMF)

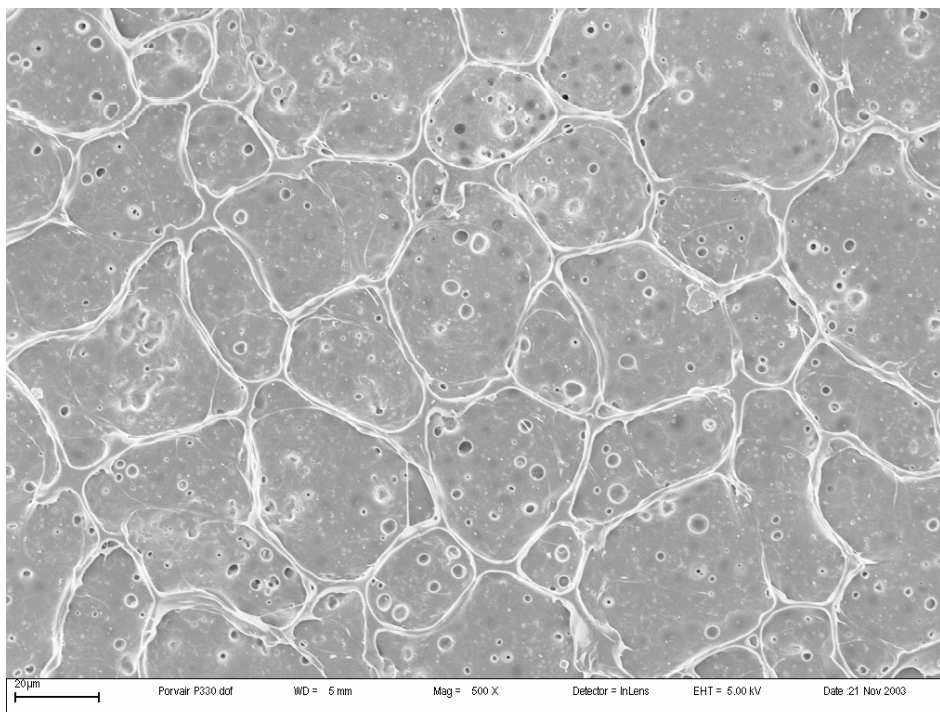


Figure B.2.2.Porvair P330 membrane magnified 500 times (Side exposed to DMF)

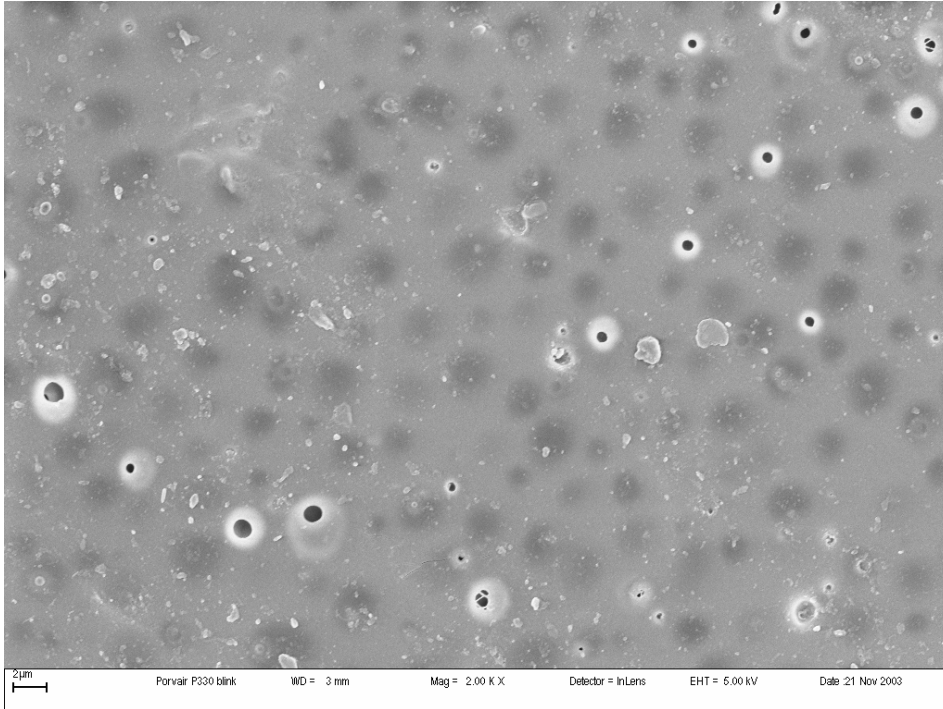


Figure B.2.3. Porvair P330 membrane magnified 2000 times (Side not exposed to DMF)

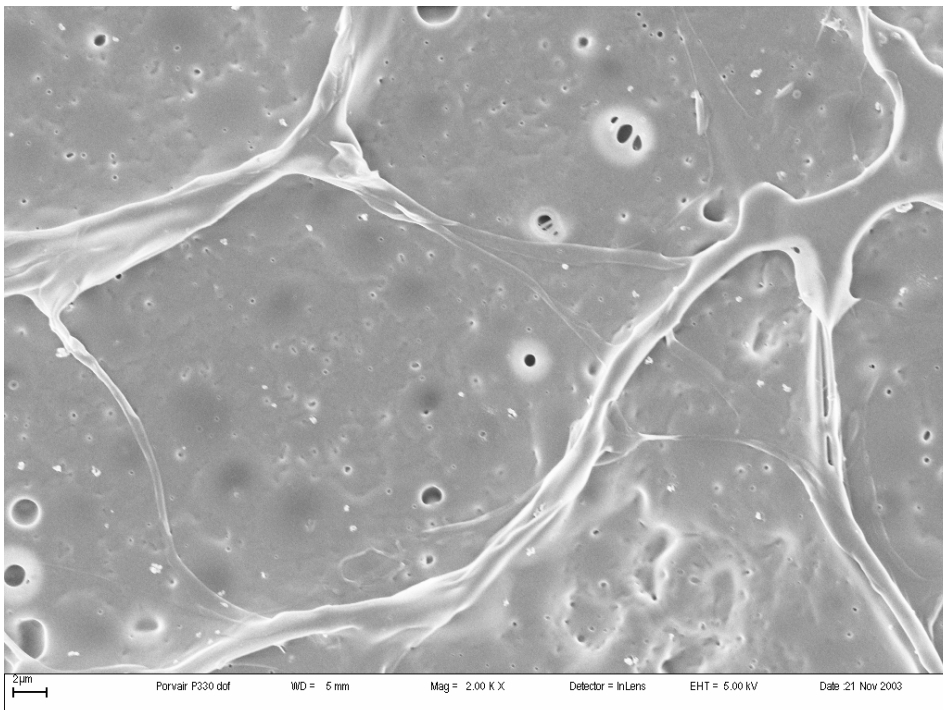


Figure B.2.4. Porvair P330 membrane magnified 2000 times (Side exposed to DMF)

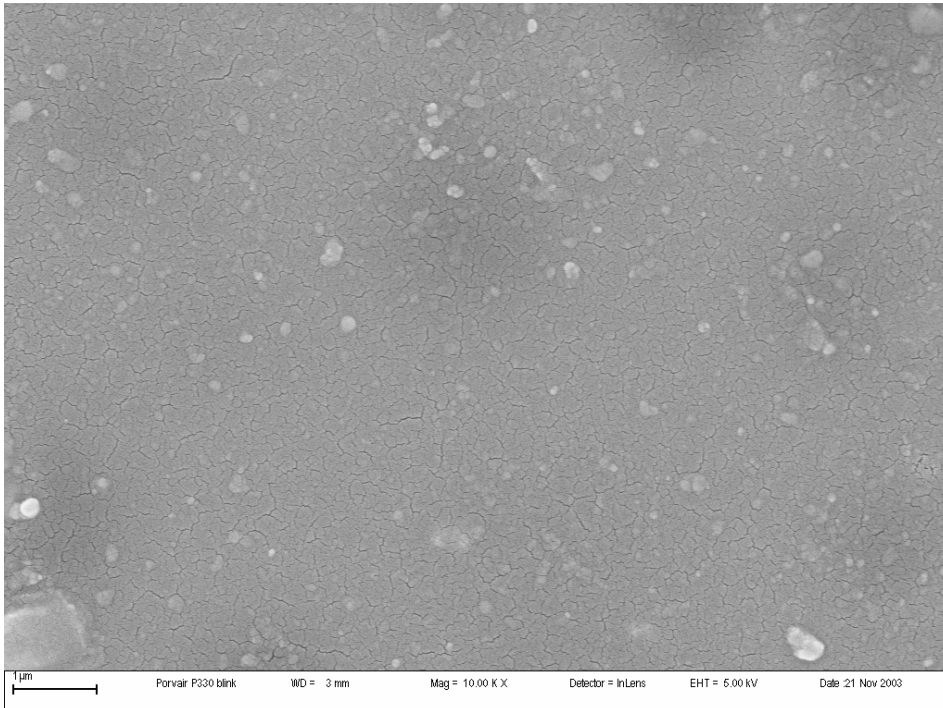


Figure B.2.5. Porvair P330 membrane magnified 10 000 times (Side not exposed to DMF)

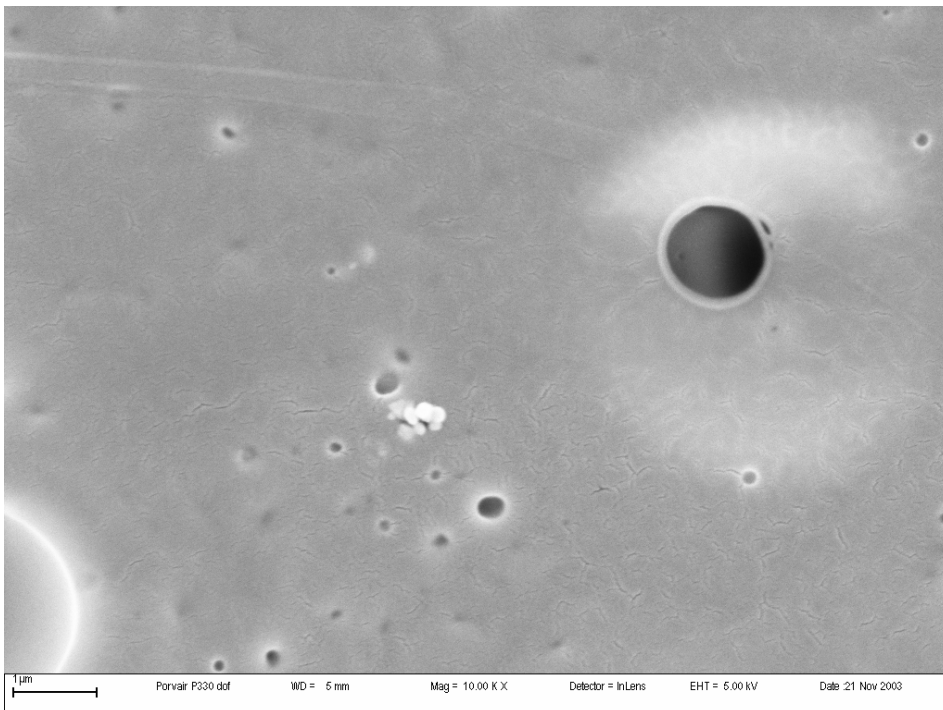


Figure B.2.6. Porvair P330 membrane magnified 10 000 times (Side exposed to DMF)

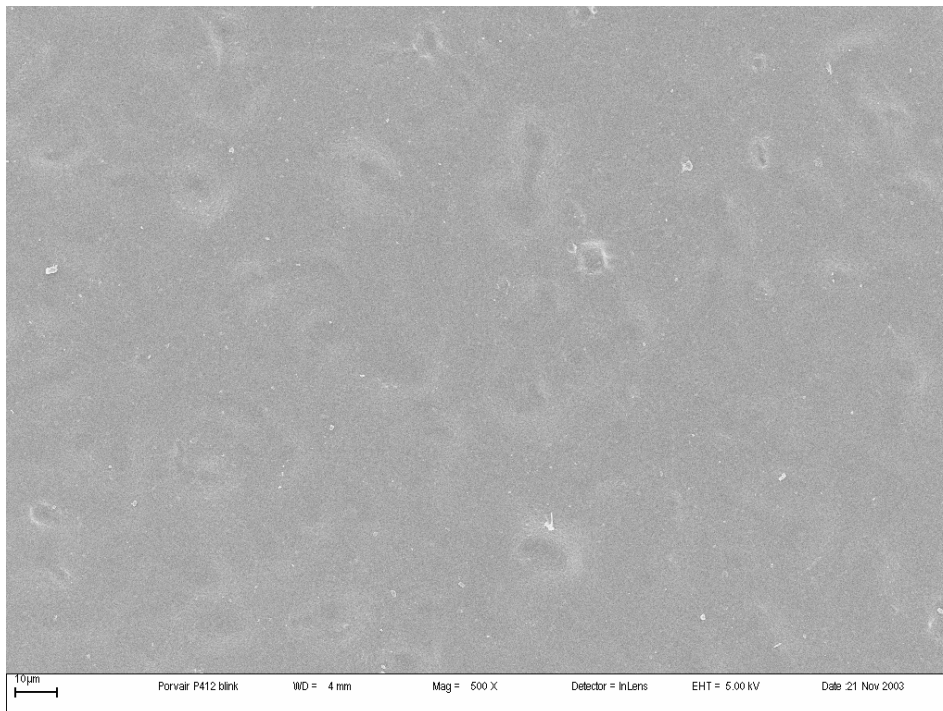


Figure B.3.1. Porvair P412 membrane magnified 500 times (Side not exposed to DMF)

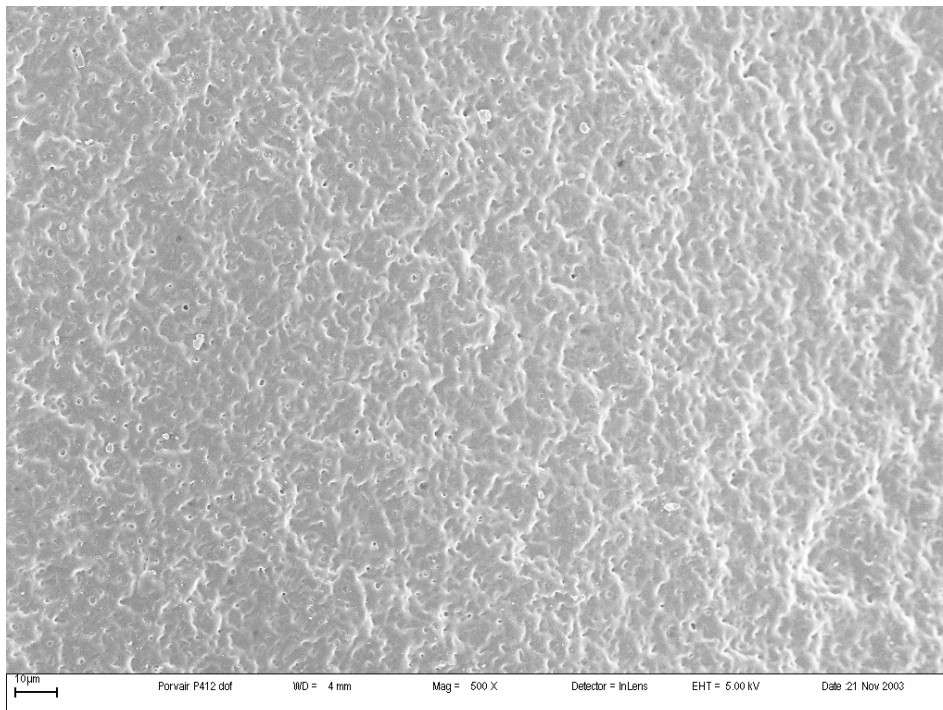


Figure B.3.2. Porvair P412 membrane magnified 500 times (Side not exposed to DMF)

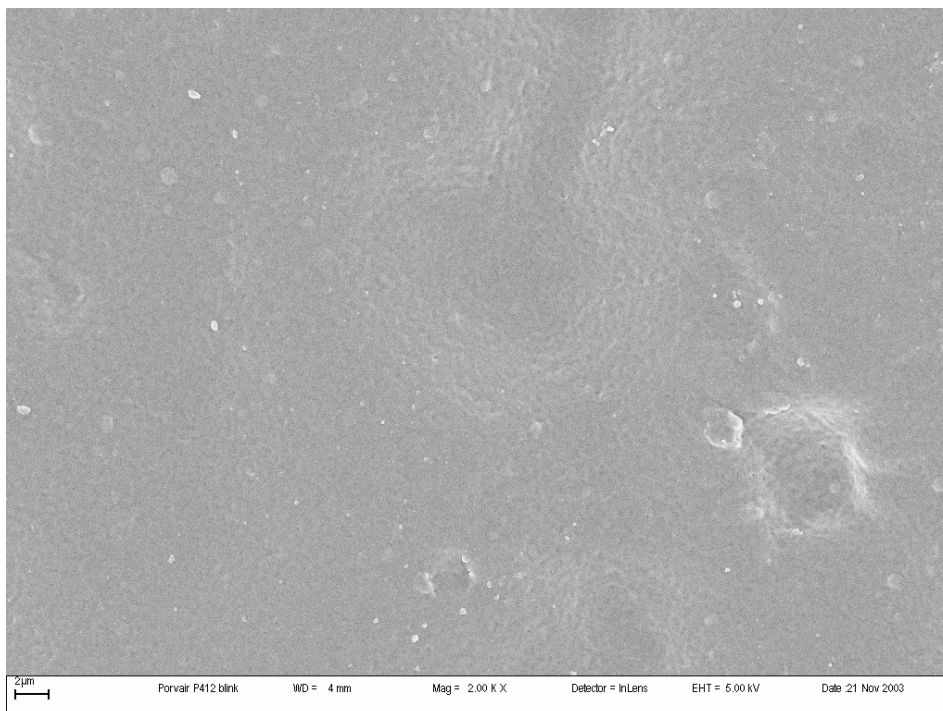


Figure B.3.3. Porvair P412 membrane magnified 2000 times (Side not exposed to DMF)

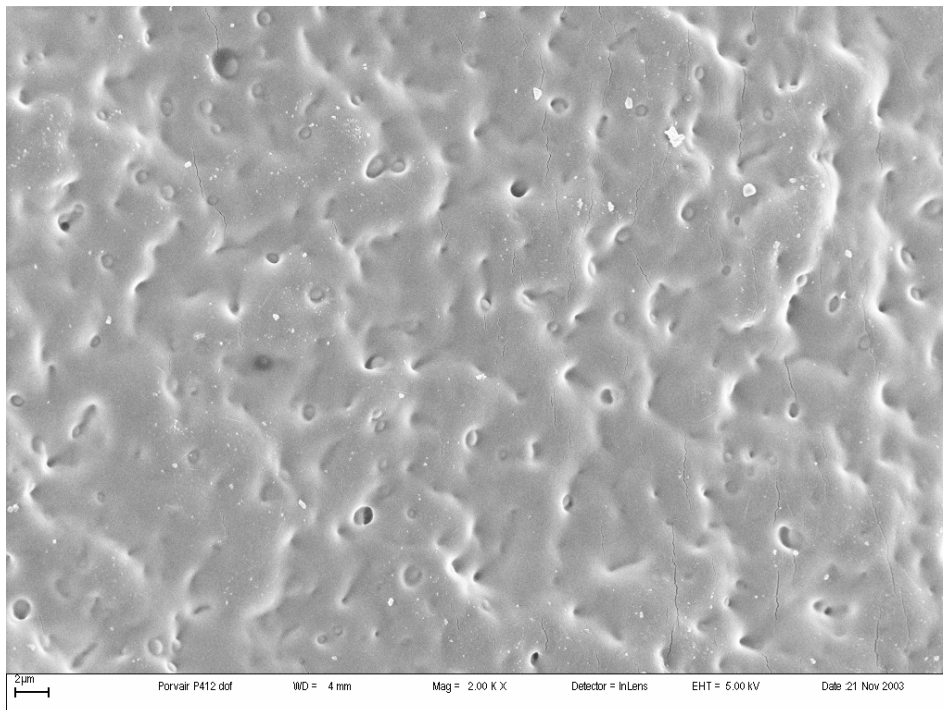


Figure B.3.4. Porvair P412 membrane magnified 2000 times (Side not exposed to DMF)

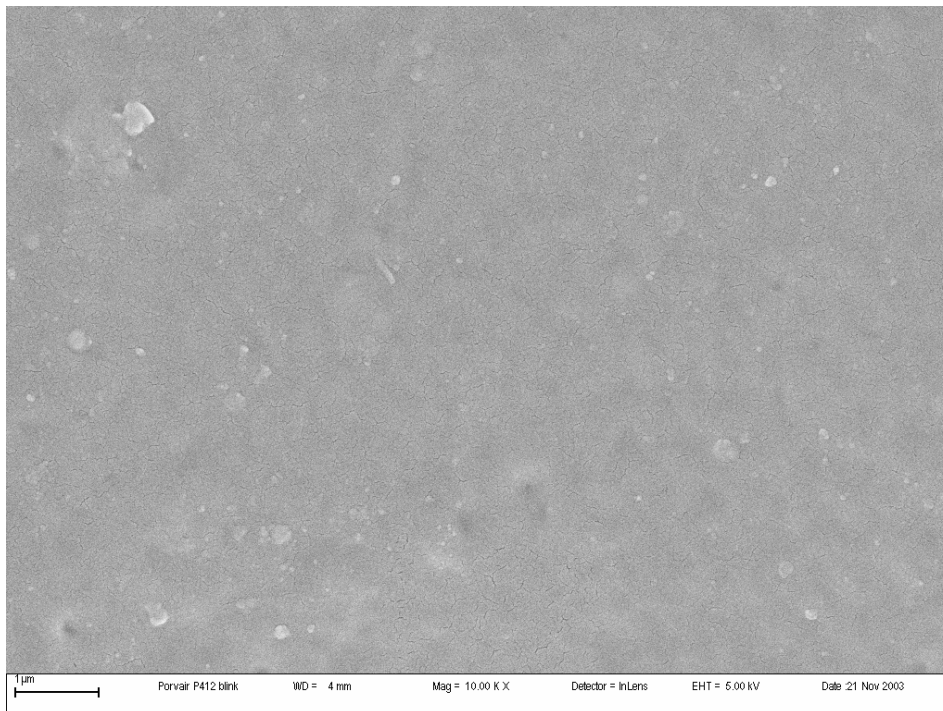


Figure B.3.5. Porvair P412 membrane magnified 10 000 times (Side not exposed to DMF)

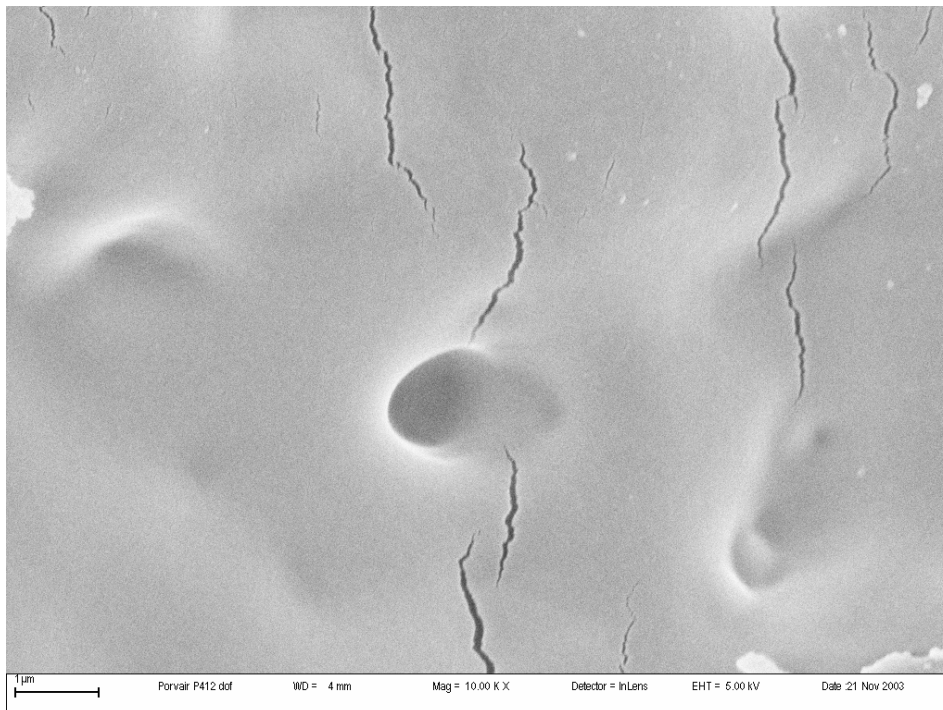


Figure B.3.6. Porvair P412 membrane magnified 10 000 times (Side exposed to DMF)

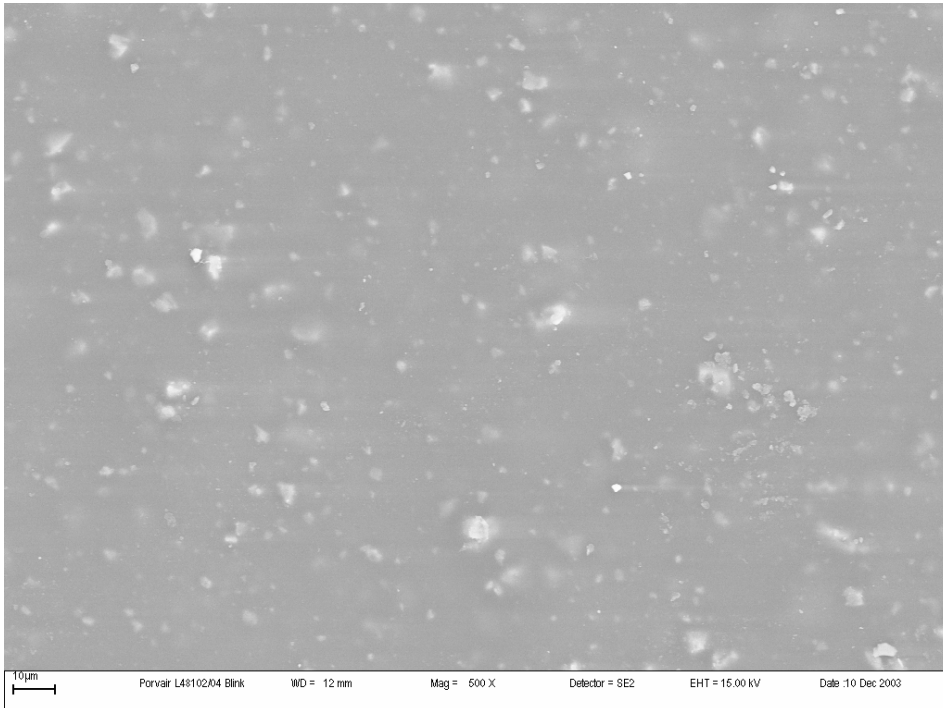


Figure B.4.1. Porvair L48102/04 membrane magnified 500 times (Side not exposed to DMF)

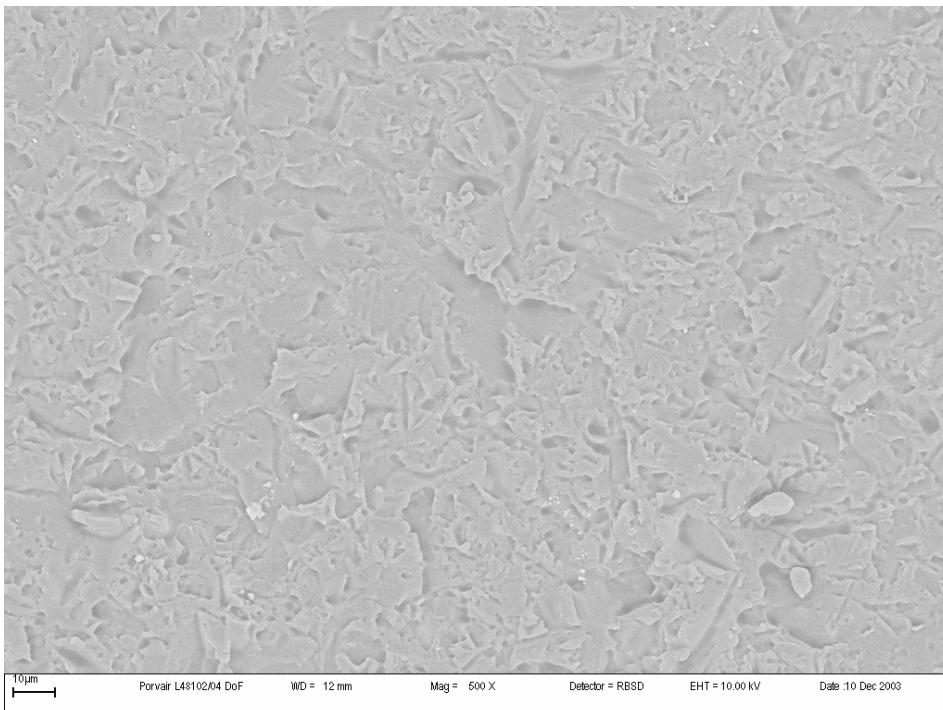


Figure B.4.2. Porvair L48102/04 membrane magnified 500 times (Side exposed to DMF)

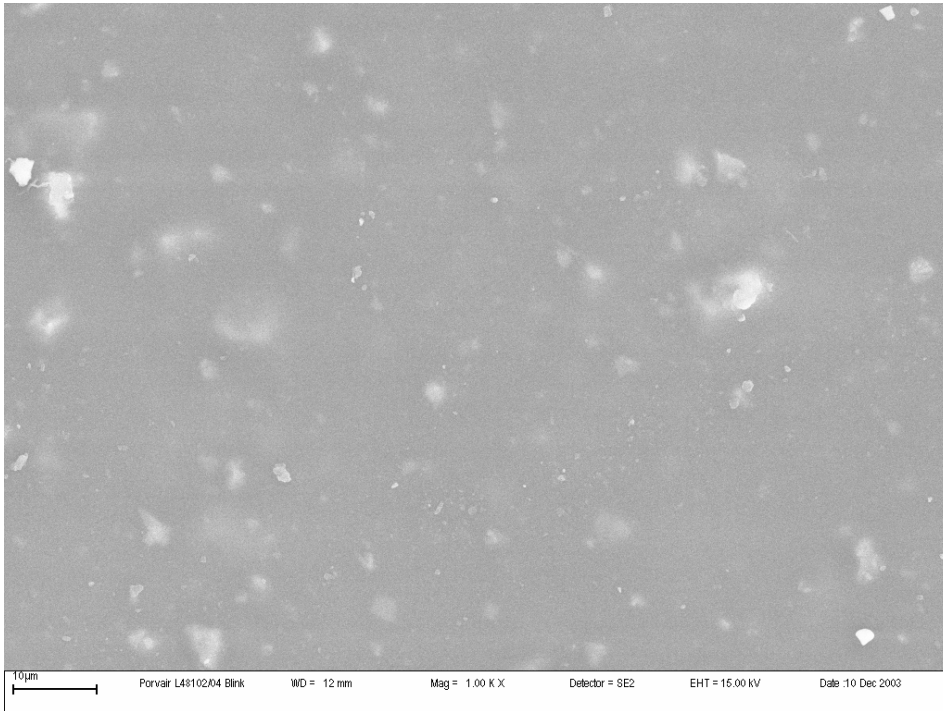


Figure B.4.3.Porvair L48102/04 membrane magnified 1000 times (Side not exposed to DMF)

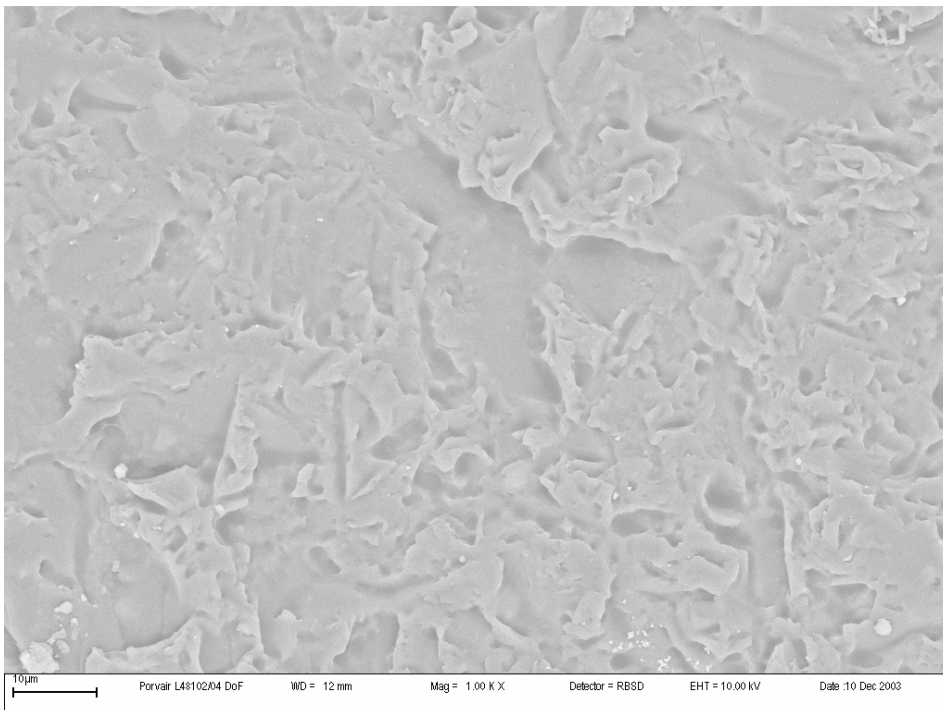


Figure B.4.4.Porvair L48102/04 membrane magnified 1000 times (Side exposed to DMF)

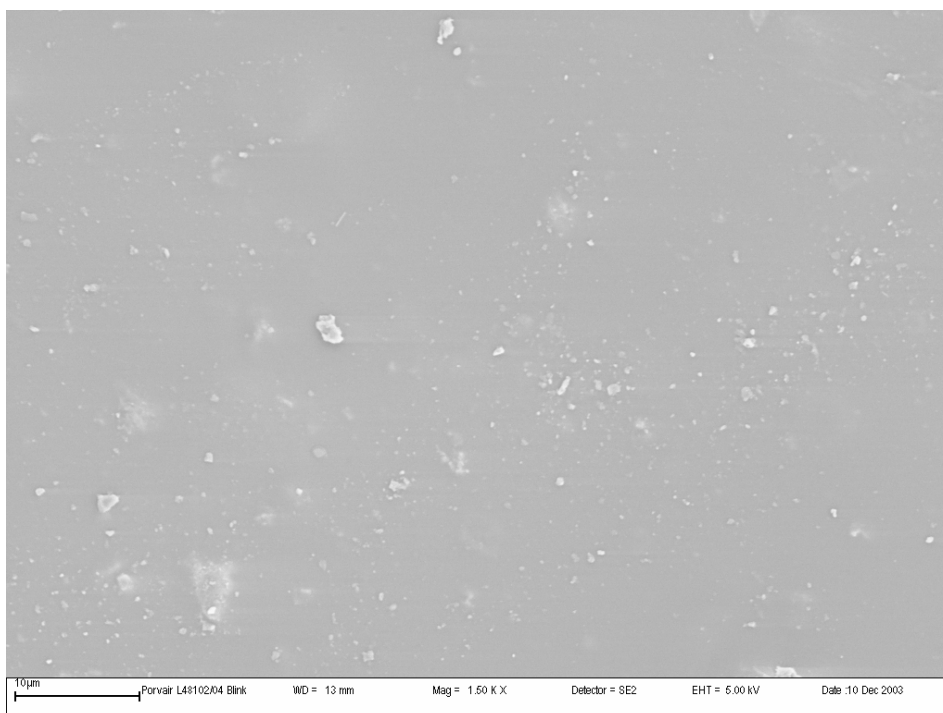


Figure B.4.5. Porvair L48102/04 membrane magnified 1500 times (Side not exposed to DMF)

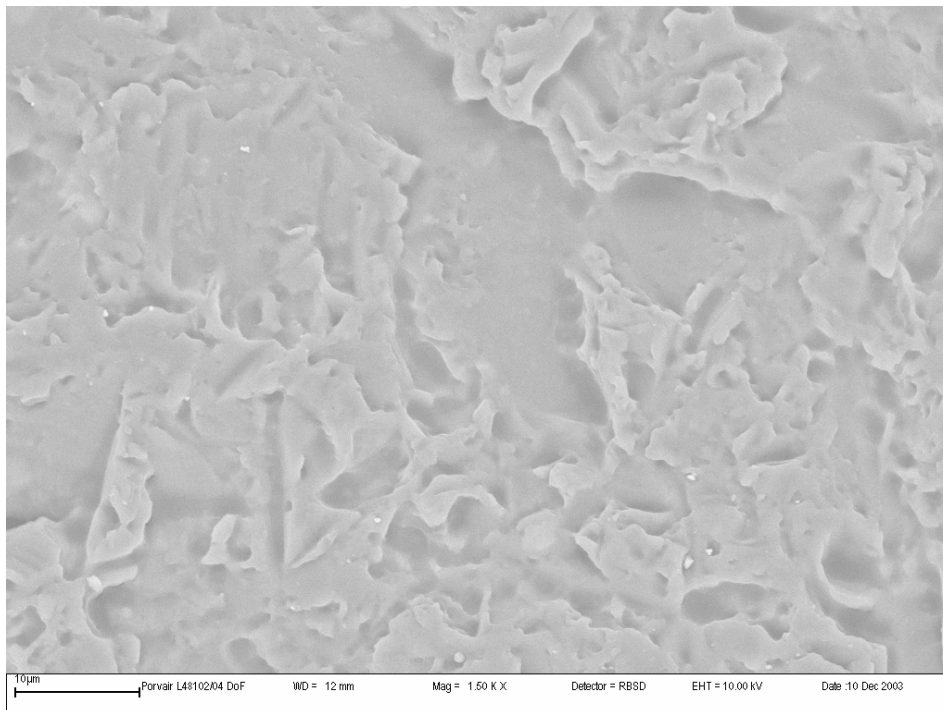


Figure B.4.6. Porvair L48102/04 membrane magnified 1500 times (Side exposed to DMF)

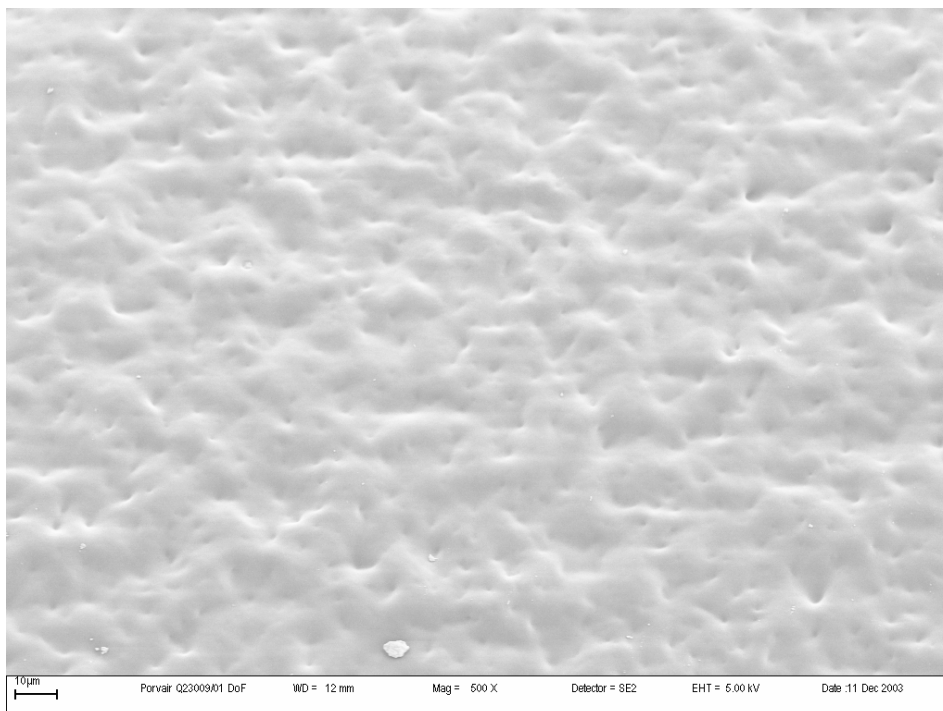


Figure B.5.1.Porvair Q23009/01 membrane magnified 500 times (Side exposed to DMF)

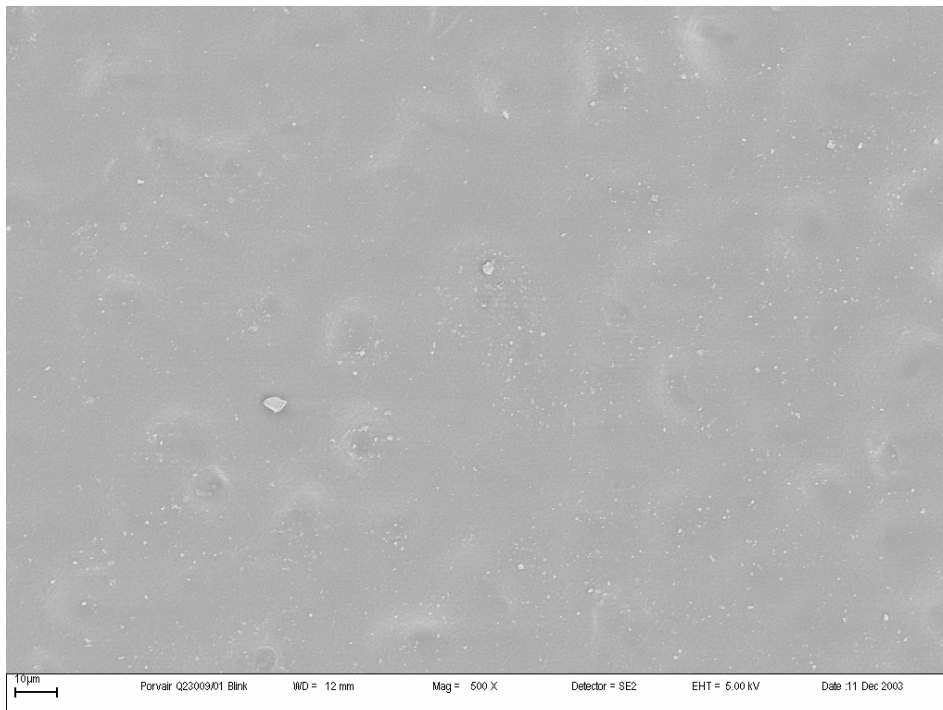


Figure B.5.2.Porvair Q23009/01 membrane magnified 500 times (Side not exposed to DMF)

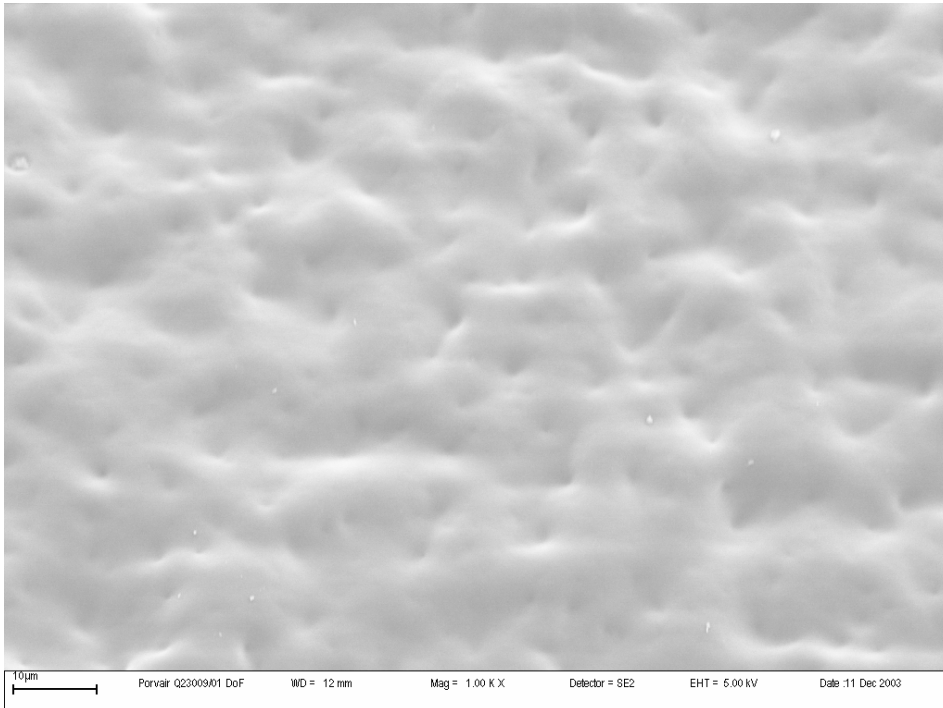


Figure B.5.3.Porvair Q23009/01 membrane magnified 1000 times (Side exposed to DMF)

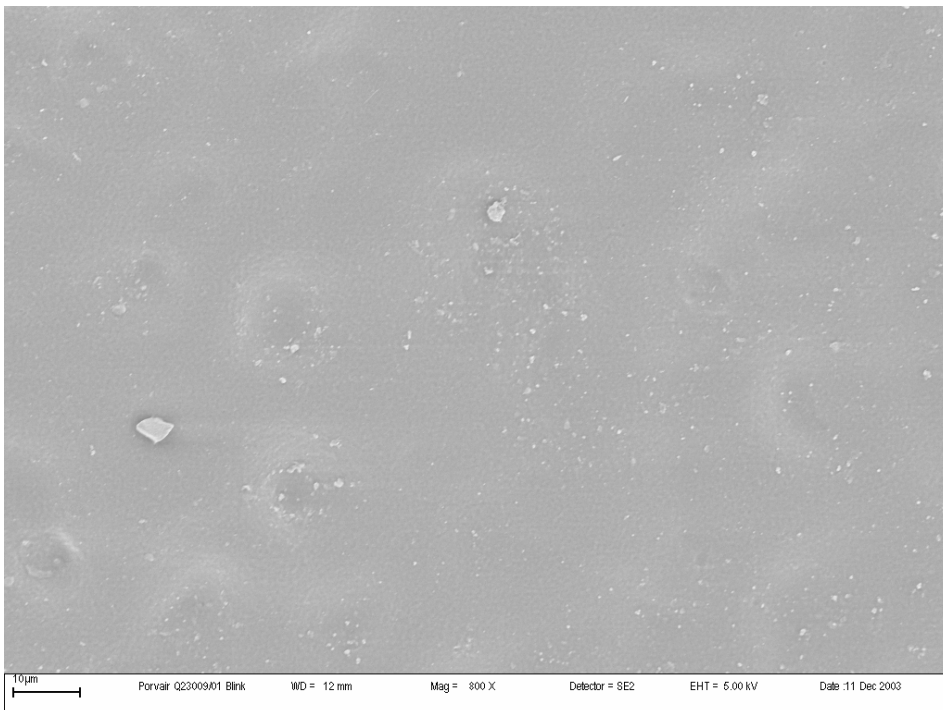


Figure B.5.4.Porvair Q23009/01 membrane magnified 800 times (Side not exposed to DMF)

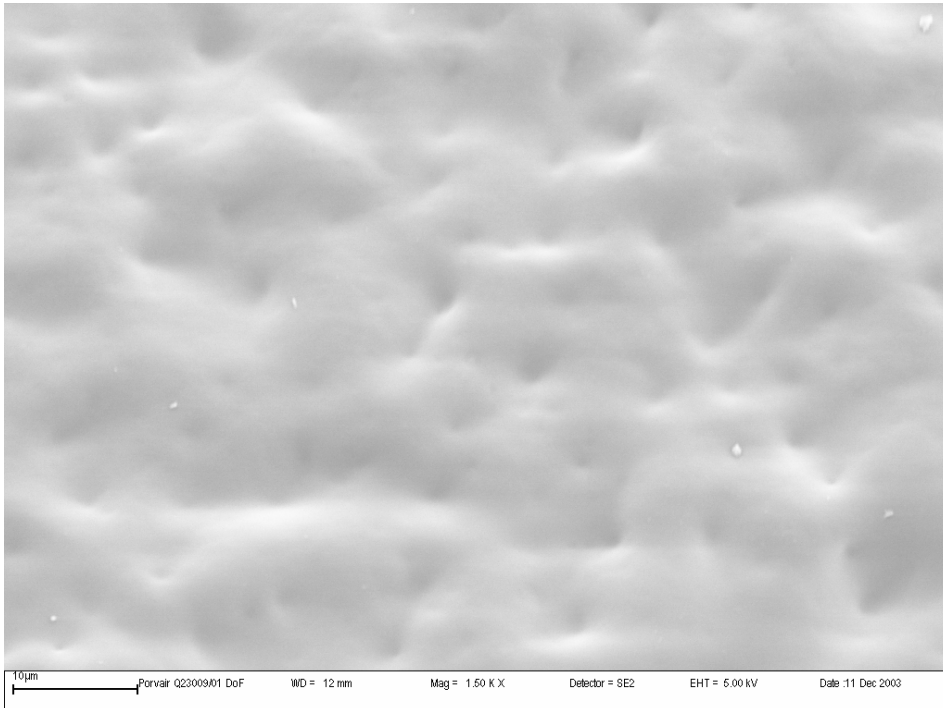


Figure B.5.5.Porvair Q23009/01 membrane magnified 1500 times (Side exposed to DMF)

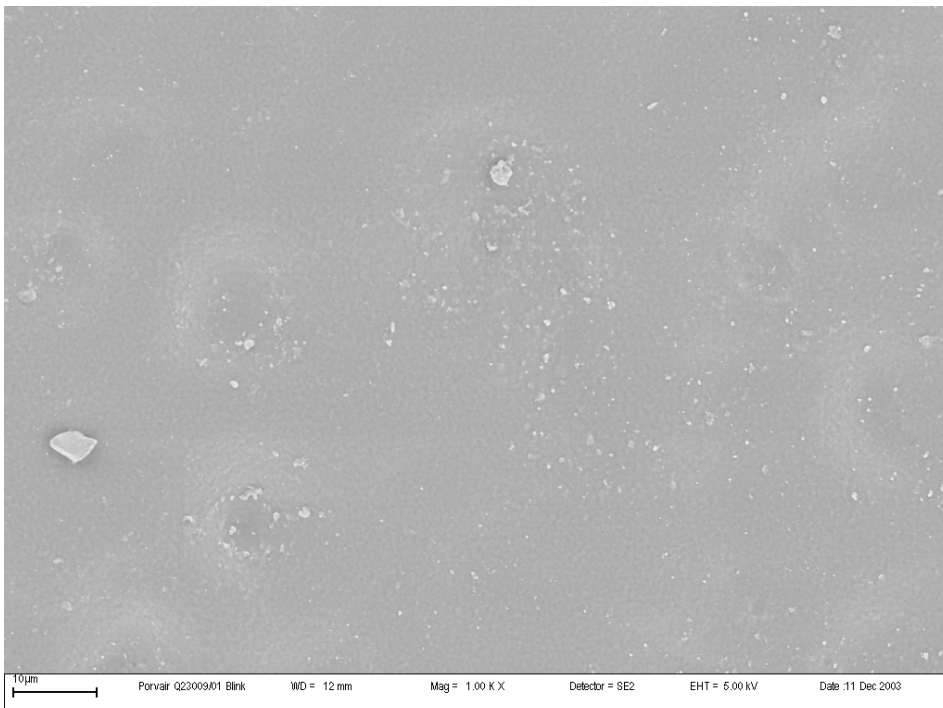


Figure B.5.5.Porvair Q23009/01 membrane magnified 1000 times (Side not exposed to DMF)

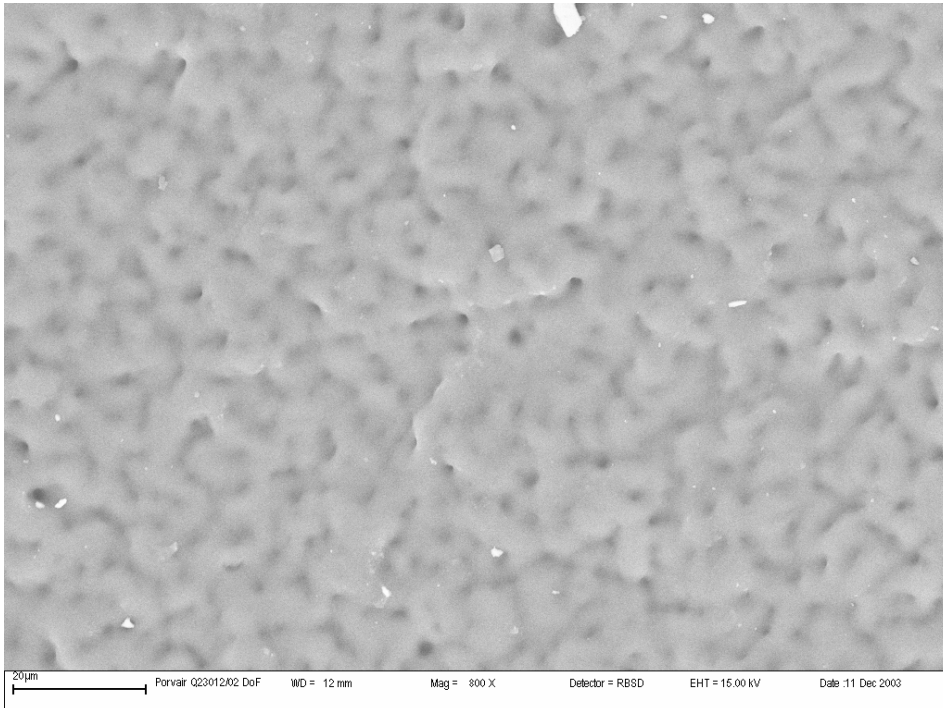


Figure B.6.1.Porvair Q23012/02 membrane magnified 800 times (Side exposed to DMF)

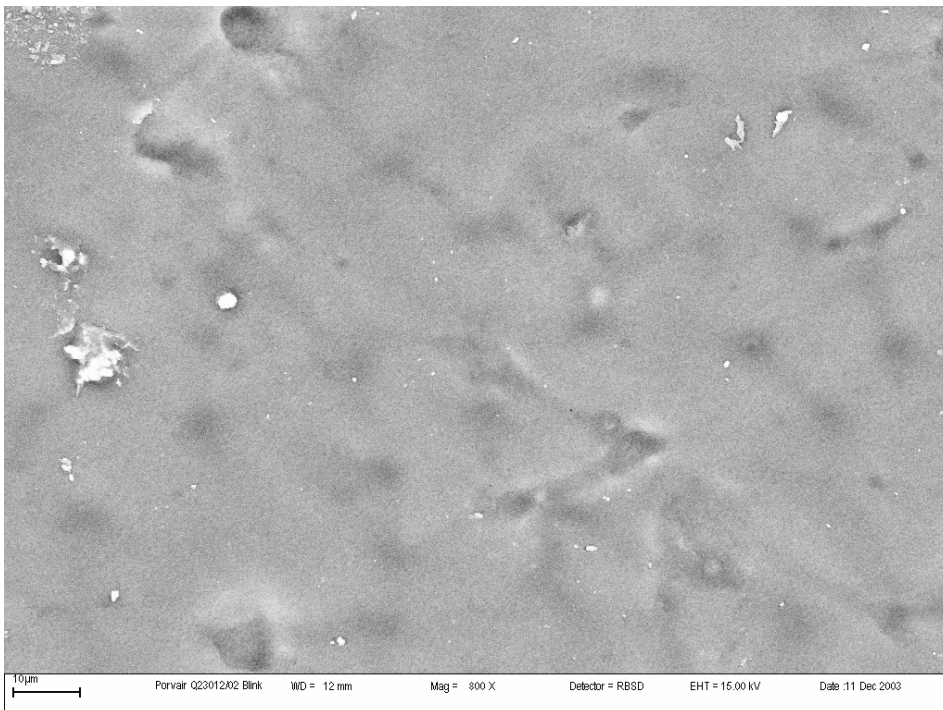


Figure B.6.2.Porvair Q23012/02 membrane magnified 800 times (Side not exposed to DMF)

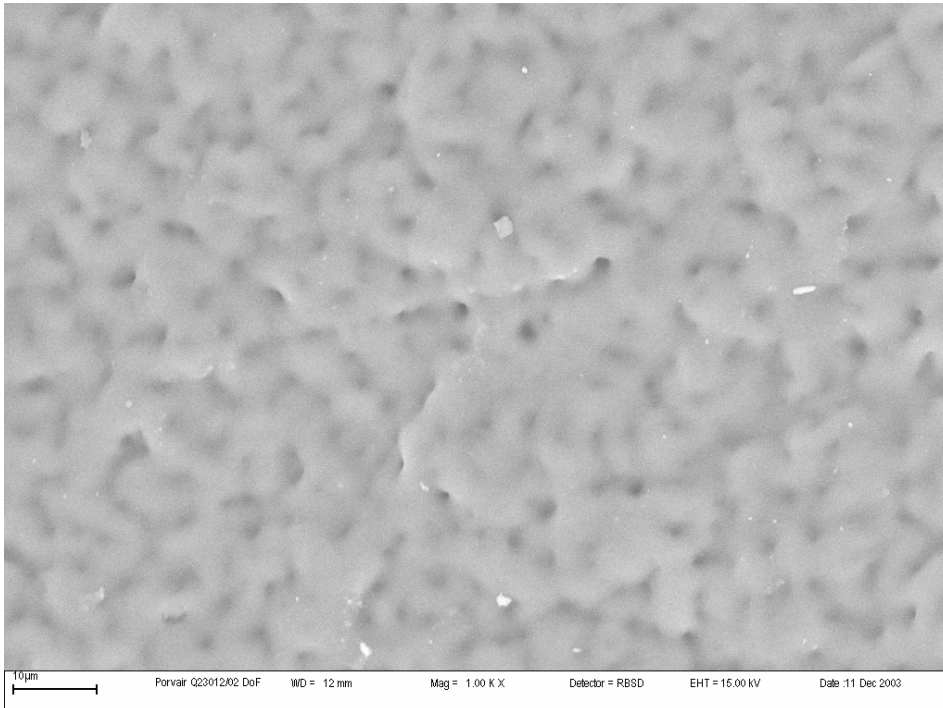


Figure B.6.3.Porvair Q23012/02 membrane magnified 1000 times (Side exposed to DMF)

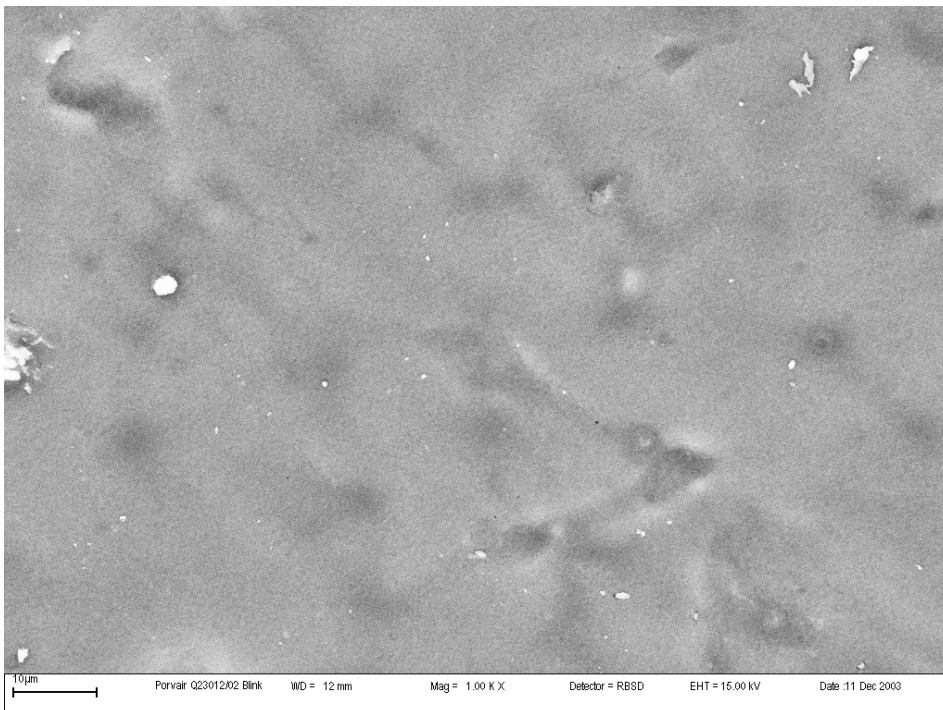


Figure B.6.4.Porvair Q23012/02 membrane magnified 1000 times (Side not exposed to DMF)

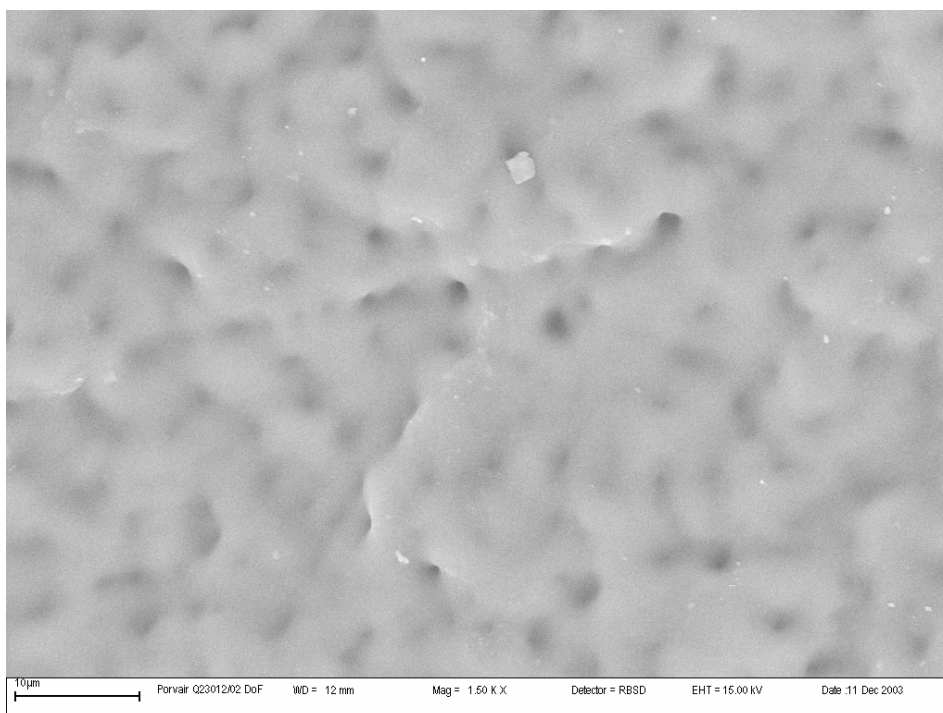


Figure B.6.5.Porvair Q23012/02 membrane magnified 1500 times (Side exposed to DMF)

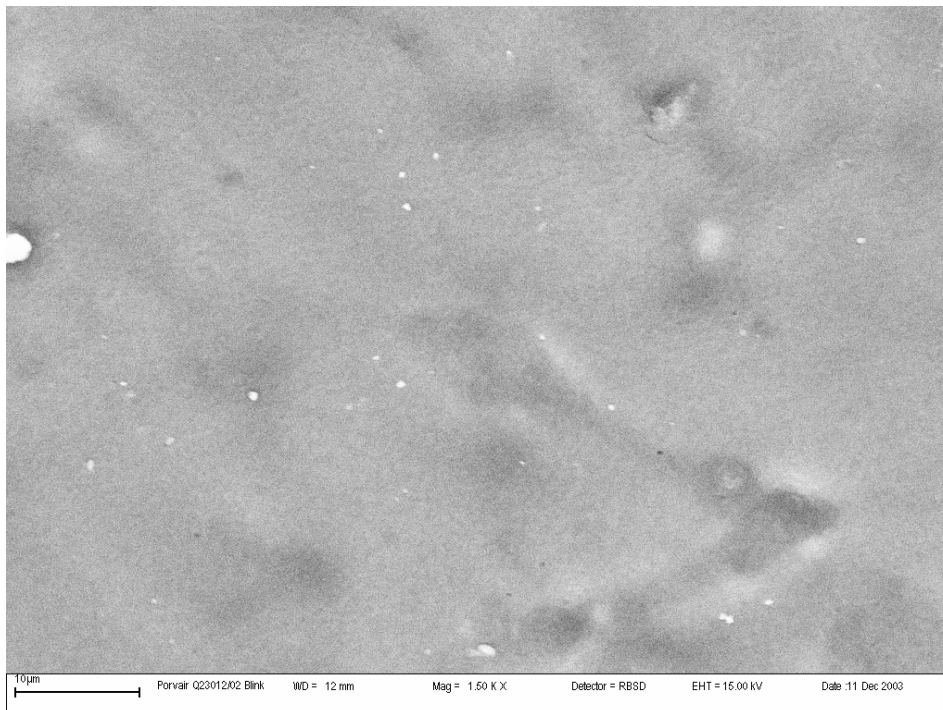


Figure B.6.6.Porvair Q23012/02 membrane magnified 1500 times (Side not exposed to DMF)

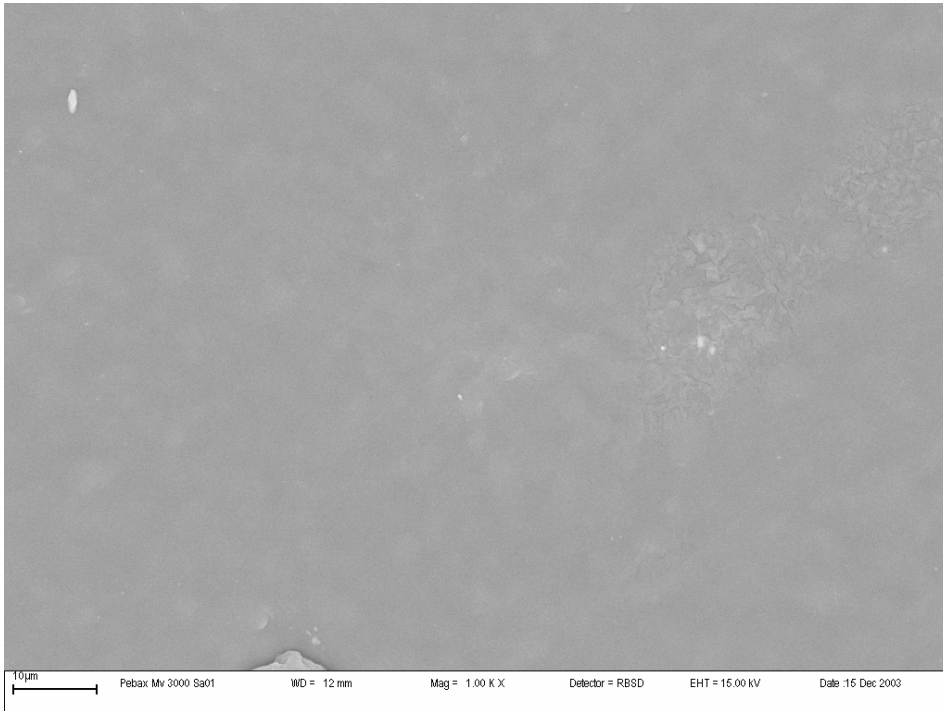


Figure B.7.1.Pebax Mv 3000 Sa01 membrane magnified 1000 times

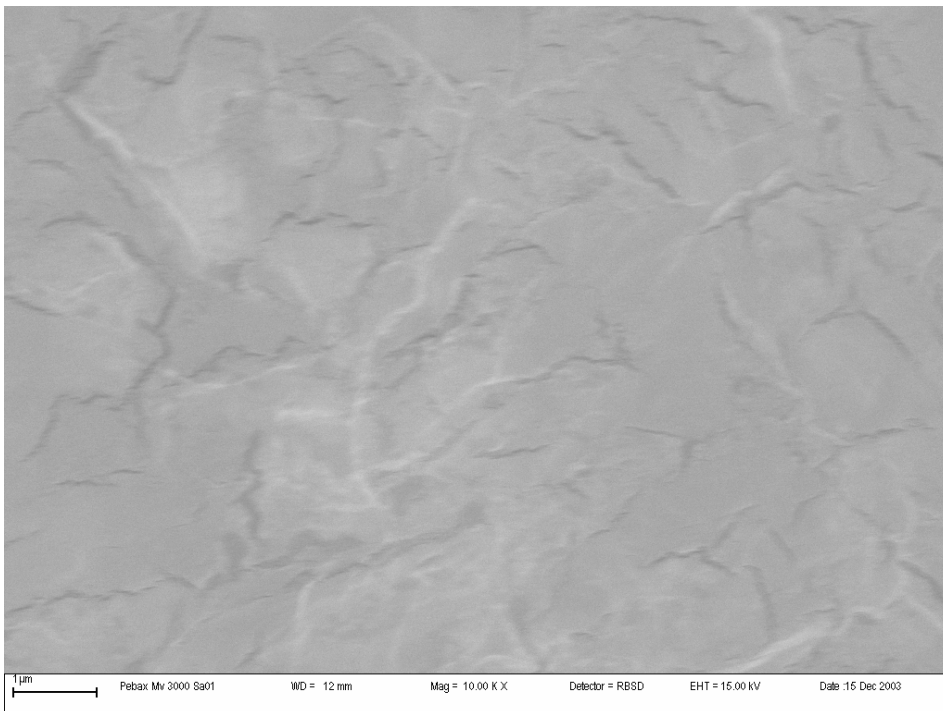


Figure B.7.2.Pebax Mv 3000 Sa01 membrane magnified 10 000 times

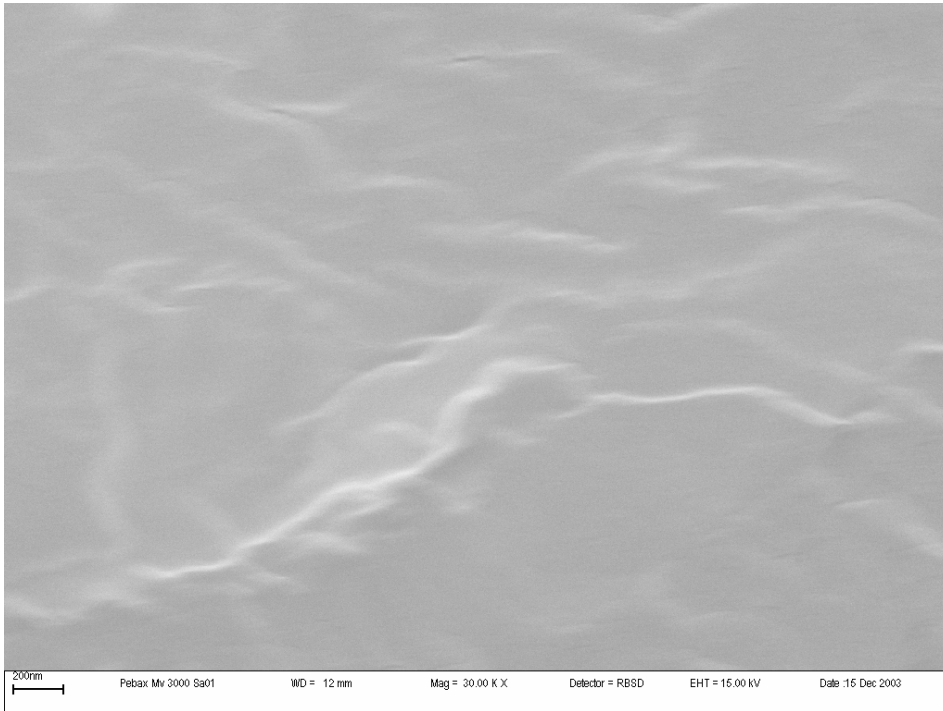


Figure B.7.3. Pebax Mv 3000 Sa01 membrane magnified 30 000 times

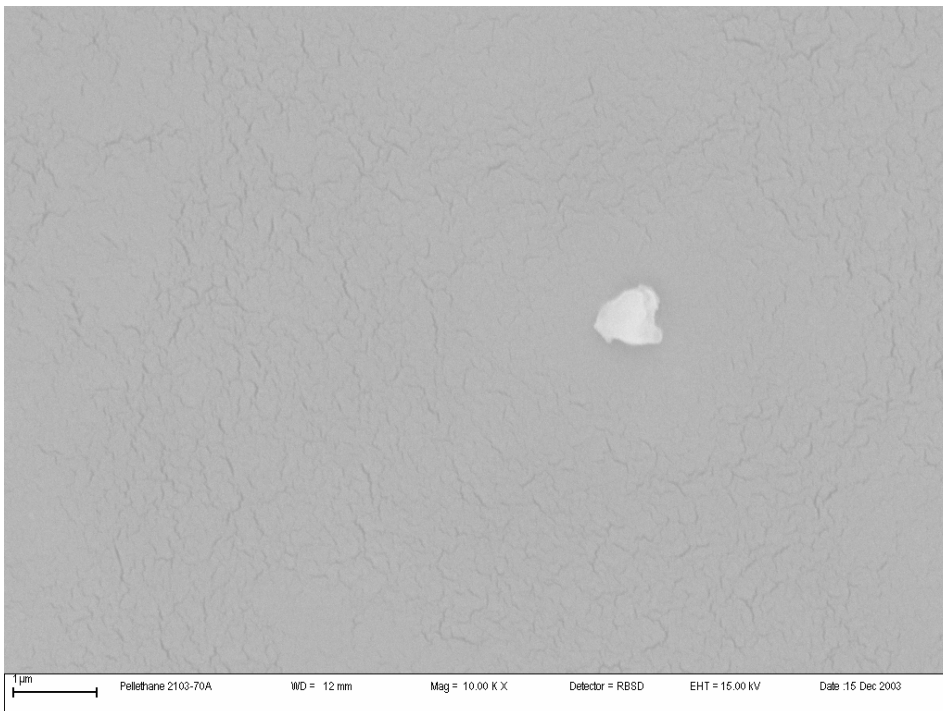


Figure B.8.1. Pellethane 2103-70A membrane magnified 10 000 times

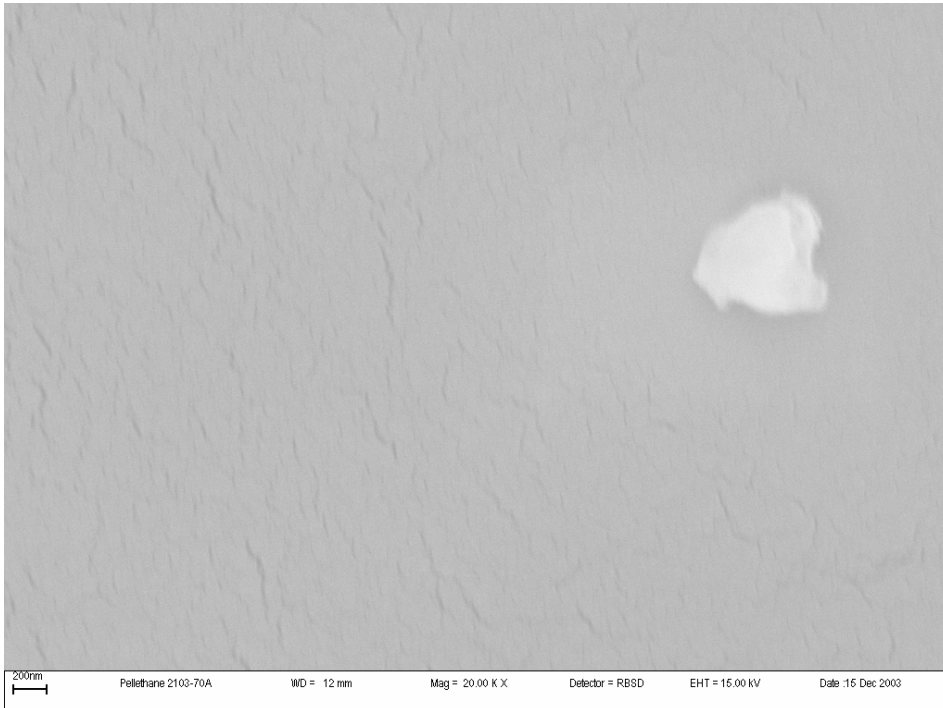


Figure B.8.2. Pellethane 2103-70A membrane magnified 20 000 times

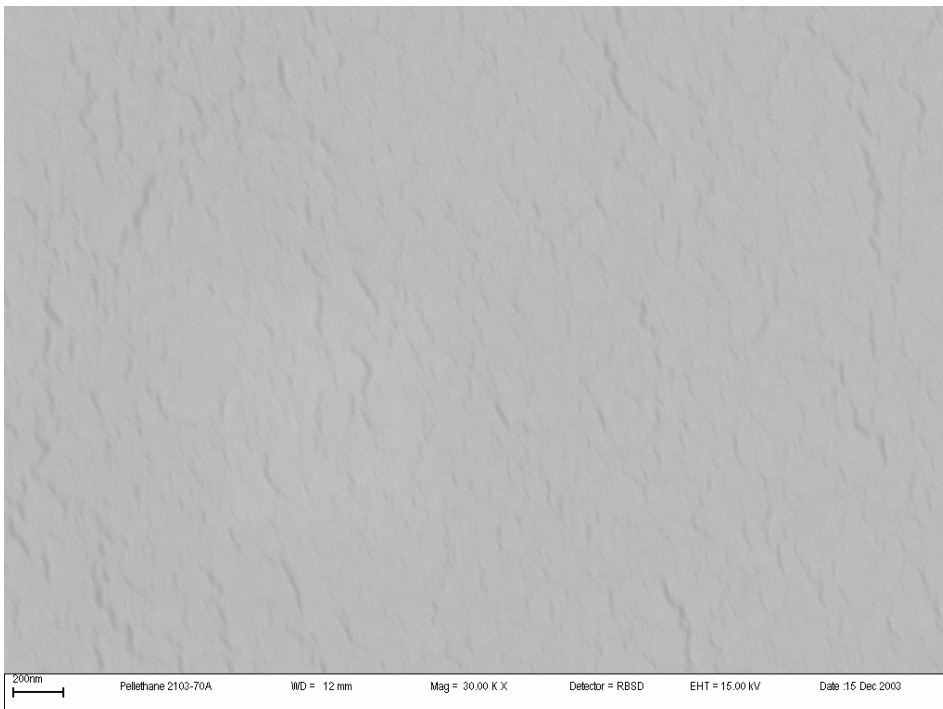


Figure B.8.3. Pellethane 2103-70A membrane magnified 30 000 times

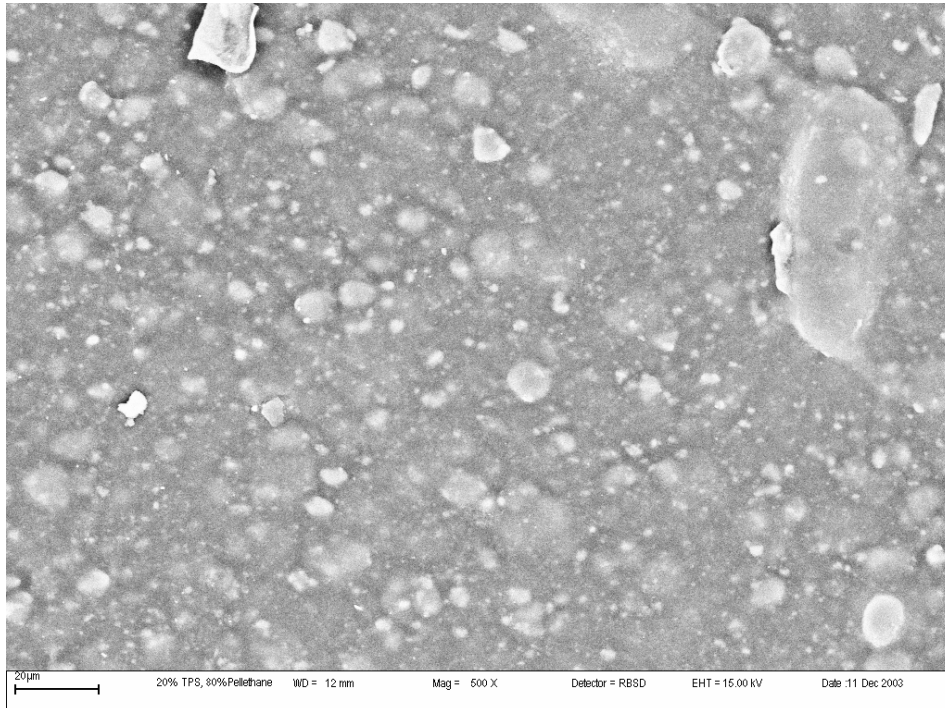


Figure B.9.1. 20%TPS containing 30% glycerol and high amylose starch / 80%Pellethane membrane magnified 500 times

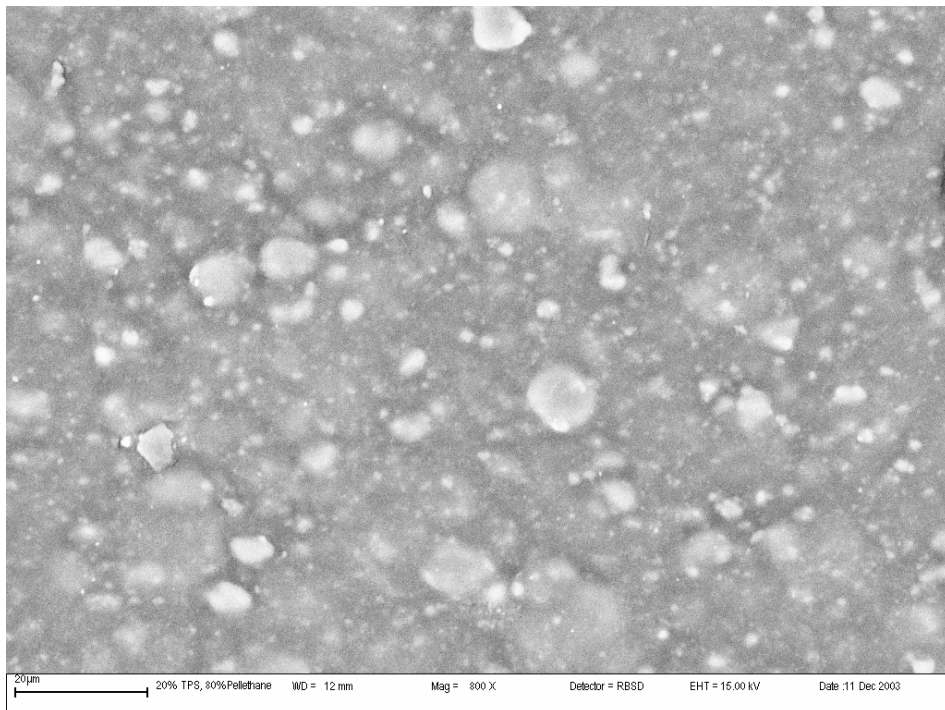


Figure B.9.2. 20%TPS containing 30% glycerol and high amylose starch / 80%Pellethane membrane magnified 800 times

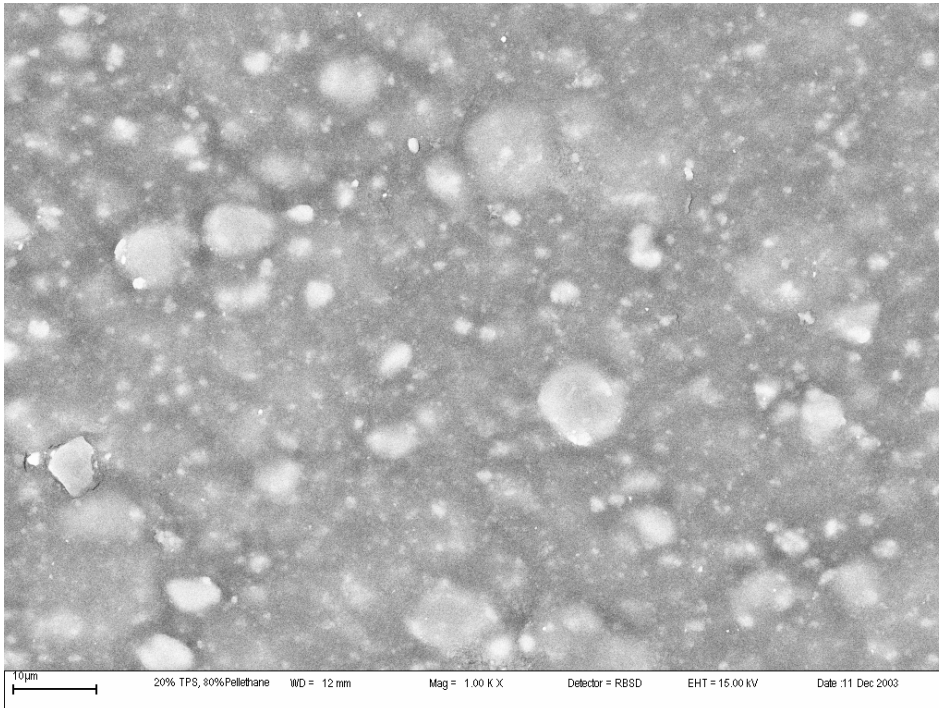


Figure B.9.3. 20%TPS containing 30% glycerol and high amylose starch / 80%Pellethane membrane magnified 1000 times

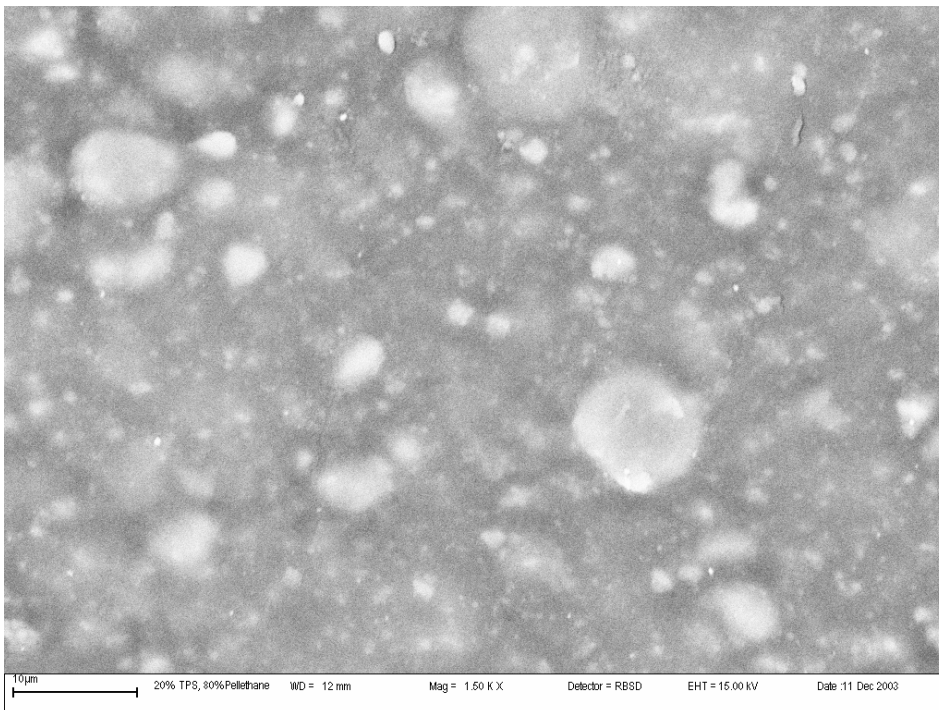


Figure B.9.4. 20%TPS containing 30% glycerol and high amylose starch / 80%Pellethane membrane magnified 1500 times

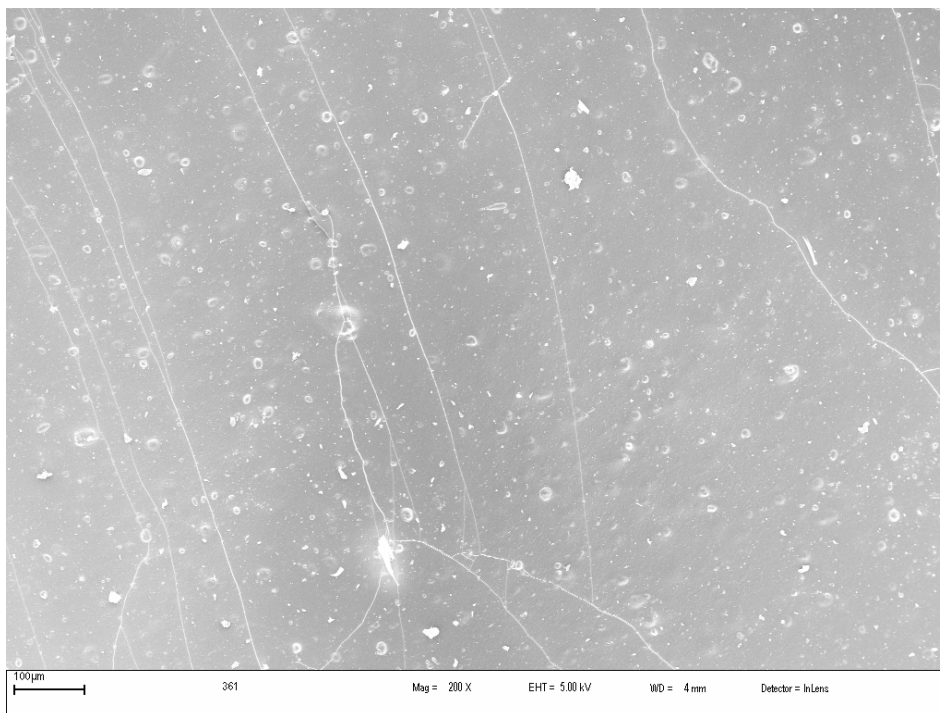


Figure B.10.1. 20%TPS containing 40% glycerol and low amylose starch / 80%Pellethane membrane magnified 200 times

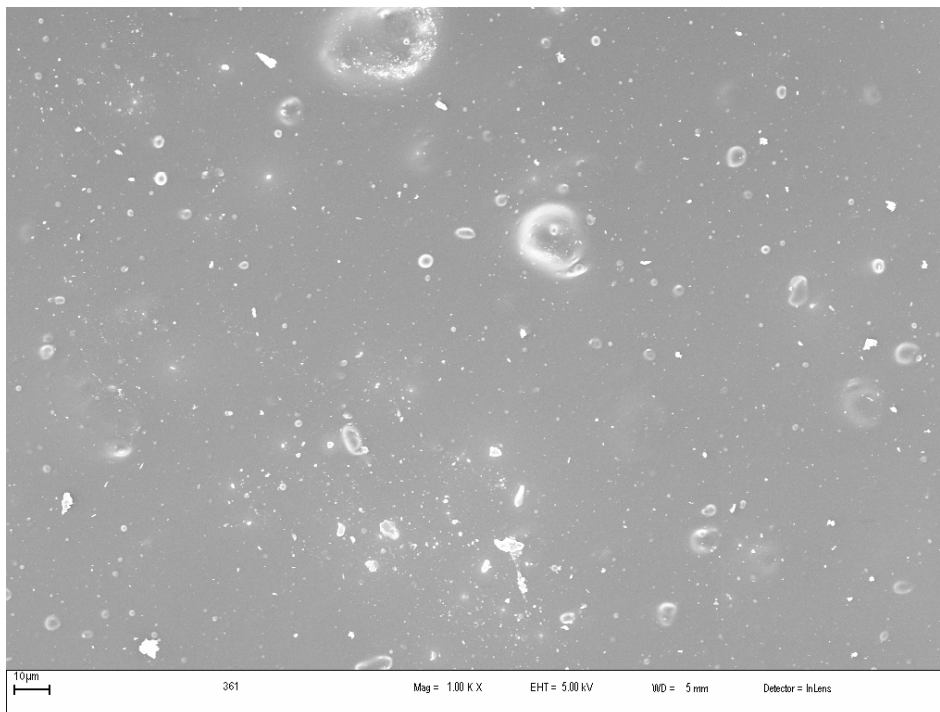


Figure B.10.2. 20%TPS containing 40% glycerol and low amylose starch / 80%Pellethane membrane magnified 1000 times

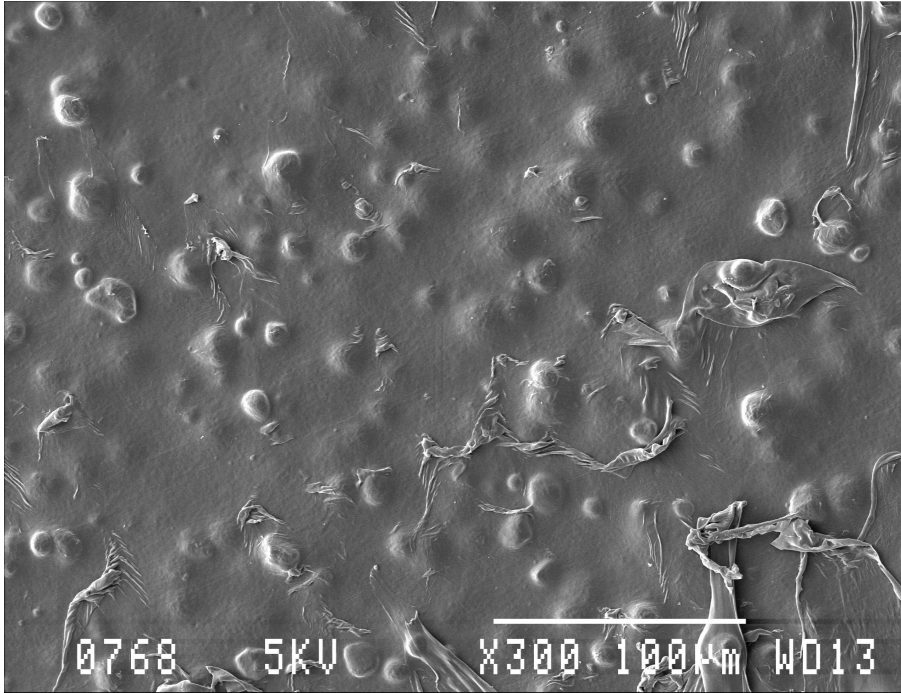


Figure B.11.1. 20% Granular starch / 80%Pellethane membrane magnified 300 times

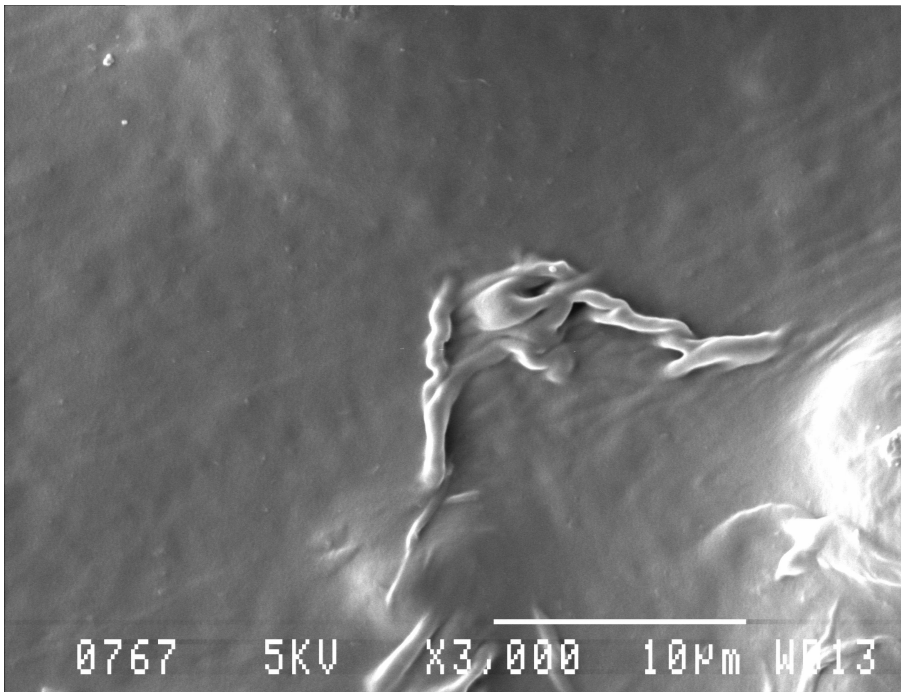


Figure B.11.2. 20% Granular starch / 80%Pellethane membrane magnified 3000 times

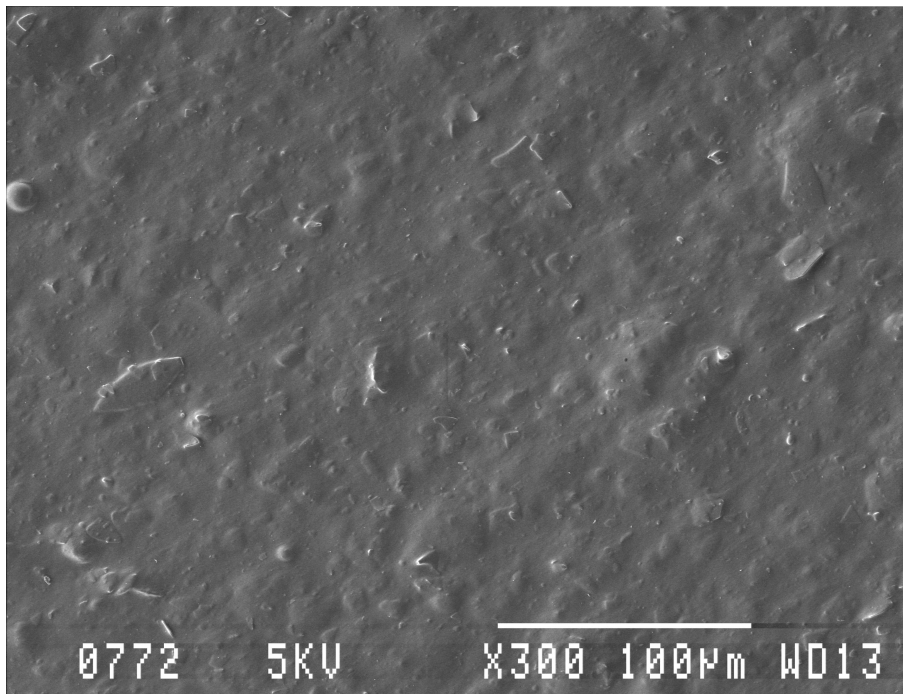


Figure B.12.1. 20% Dicalite / 80%Pellethane membrane magnified 300 times

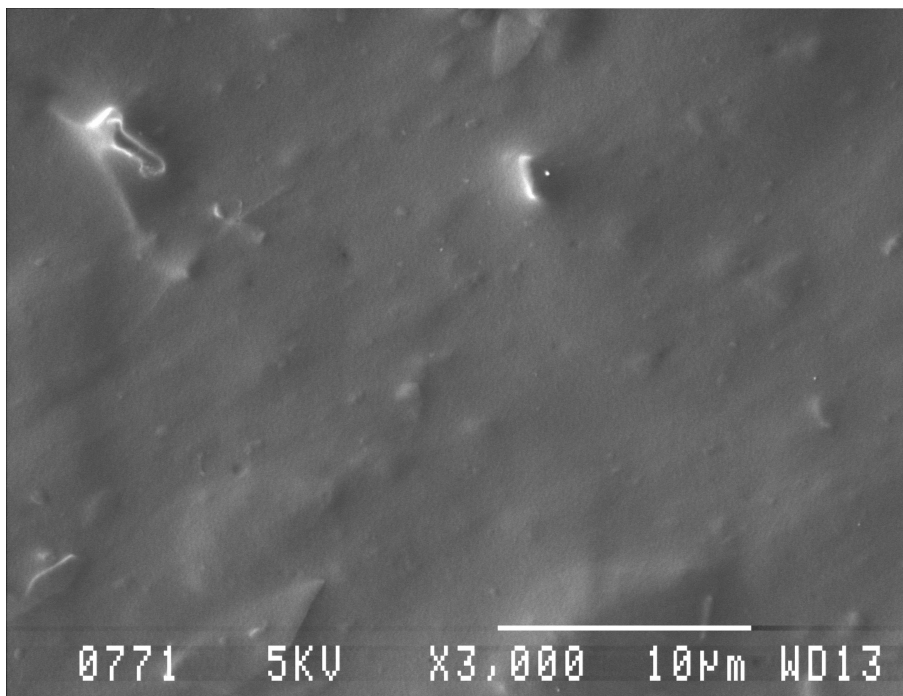


Figure B.12.2. 20% Dicalite / 80%Pellethane membrane magnified 3000 times

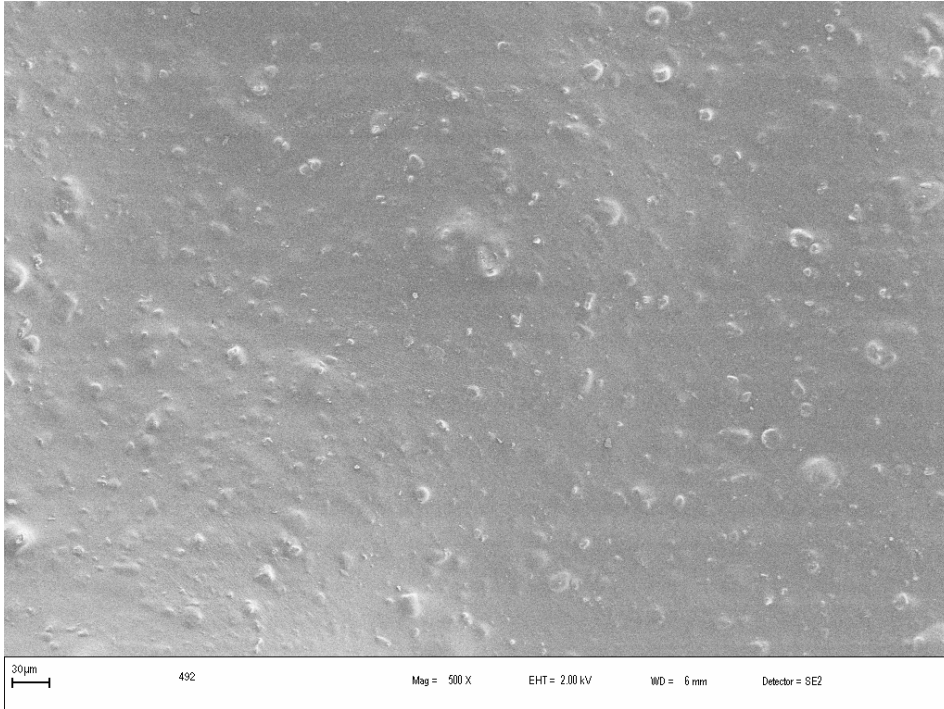


Figure B.13.1. 20% Diatomite / 80%Pellethane membrane magnified 500 times

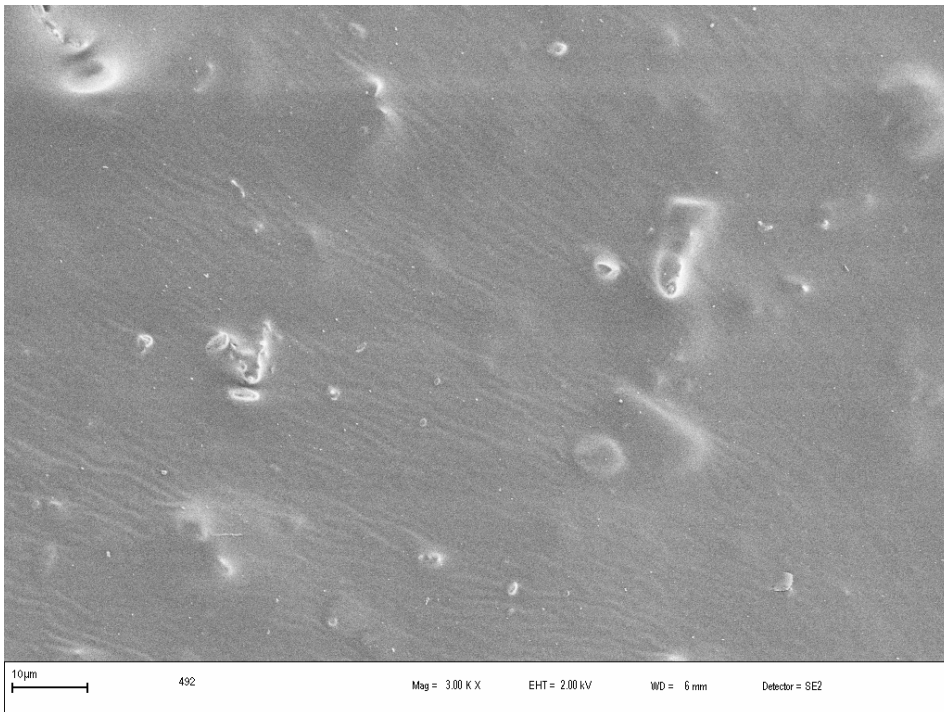


Figure B.13.2. 20% Diatomite / 80%Pellethane membrane magnified 500 times



UNIVERSITEIT VAN PRETORIA
UNIVERSITY OF PRETORIA
YUNIBESITHI YA PRETORIA



Appendix C: Sample Calculations

WVTR Calculations:

The WVTR of calculated using the following formula:

$$WVTR = \frac{(M_{Final}^{Membrane} + M_{Final}^{Dessicant} - M_{Initial}^{Membrane} - M_{Initial}^{Dessicant})}{At}$$

Using data from Appendix A for 10% low amylose thermoplastic starch containing 40% glycerol filled Pellethane:

Mass of the membrane and silica gel before and after test:

$$M_{Final}^{Membrane} = 0.07818g$$

$$M_{Final}^{Dessicant} = M_{Final}^{Lid+Silica} - M^{Lid} = 188.4907 - 172.643 = 15.8477g$$

$$M_{Initial}^{Membrane} = 0.07805g$$

$$M_{Initial}^{Dessicant} = 15.4622g$$

Internal cross-sectional area of the cup (Area of membrane being tested):

$$r = 0.02m$$

$$\frac{1}{A} = \frac{1}{\pi r^2} = \frac{1}{\pi(0.02)^2} \approx 795.77m^{-2}$$

WVTR of the membrane:

$$WVTR = \frac{795.77(0.07818 + 15.8477 - 0.07805 - 15.4622)}{2.00} = 157.3 \text{ g.m}^{-2} \text{ .hr}^{-1}$$

Convert the WVTR to standard units

$$WVTR = 157.3 \text{ g.m}^{-2} \text{ .hr}^{-1} \times 24 \text{ hr.day}^{-1} = 3776.3 \text{ g.m}^{-2} \text{ .day}^{-1}$$

After obtaining a relationship between thickness and WVTR the values were normalized to 20µm. The relationship obtained was using SigmaPlot

$$WVTR = A + \frac{B}{t} \text{ where } A = 2122.0823 \text{ and } B = 17707.2335$$

Normalising to 20µm using a linear normalisation:

$$WVTR_{Normalised} = WVTR_{Original} \times \frac{A + \frac{B}{20}}{A + \frac{B}{t}}$$

$$WVTR_{Normalised} = 3776.3 \times \frac{2122.0823 + \frac{17707.2335}{20}}{2122.0823 + \frac{17707.2335}{13.23}} = 3281.9 \text{ g.m}^{-2} \text{ .day}^{-1}$$

Tensile Tests Calculations:

The tensile properties were calculated as follows:

The ultimate tensile strength was calculated using the following formula:

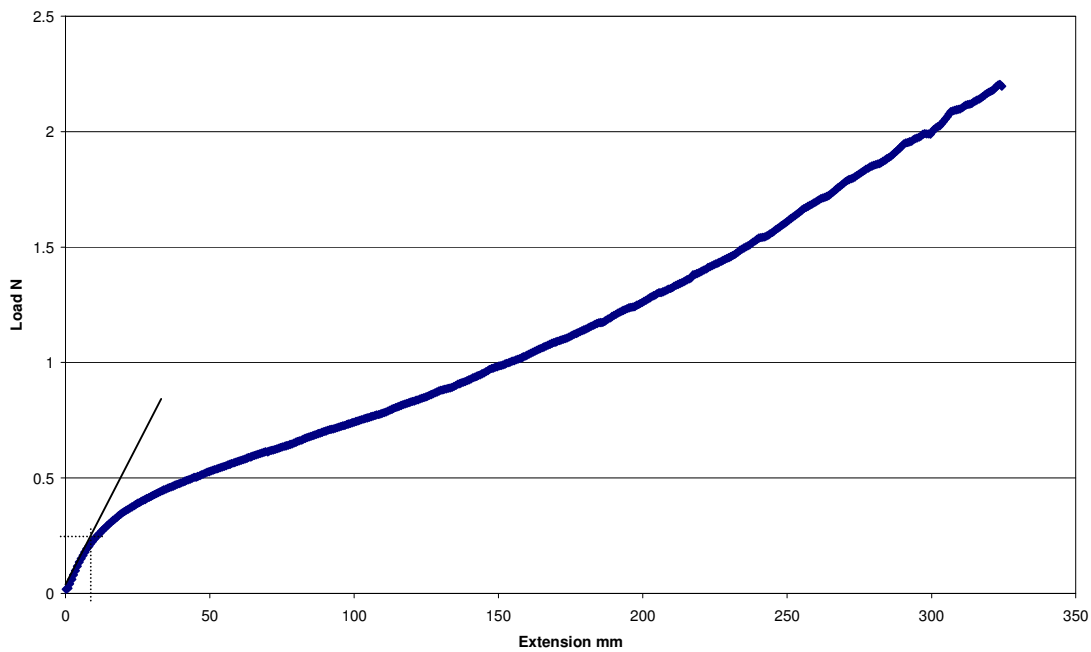
$$UTS = \frac{Load_{Break}}{A}$$

The elongation to break was read of the curve and converted to % using:

$$EtB = \frac{L - L_0}{L_0} \times 100$$

The yield strength was determined using the following formula:

$$YS = \frac{Load_{yield}}{A}$$



The figure above shows an approximation of the point when the material yields.

The tensile modulus was calculated using the following:

$$TM = \frac{Load_{yield} / A}{L_{Yield} - L_0 / L_0}$$

Using Dicalite in the cross direction as an example:

$$UTS = \frac{2.205}{0.00019 \times 0.0067} \times 10^{-6} = 17.3 MPa$$

$$EtB = \frac{(324.36 + 65) - 65}{65} \times 100 = 499\%$$



$$YS = \frac{0.13535}{0.00019 \times 0.0067} \times 10^{-6} = 1.1 \text{ MPa}$$

$$TM = \frac{\left(\frac{0.13535}{0.00019 \times 0.0067} \times 10^{-6} \right)}{\left(\frac{(4.76 + 65) - 65}{65} \right)} = 14.5 \text{ MPa}$$

Summary of DCF Sensitivity Results

The effect on IRR

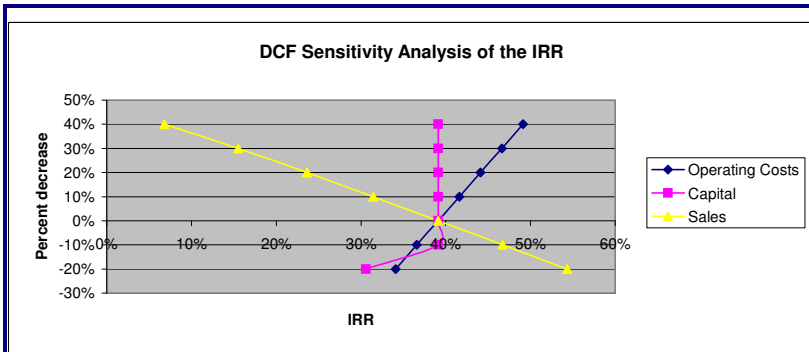
	-20.0%	-10.0%	0.0%	10.0%	20.0%	30.0%	40.0%
Operating Costs	34%	37%	39%	42%	44%	47%	49%
Capital	31%	39%	39%	39%	39%	39%	39%
Sales	54%	47%	39%	31%	24%	16%	7%

The effect on the break-even point

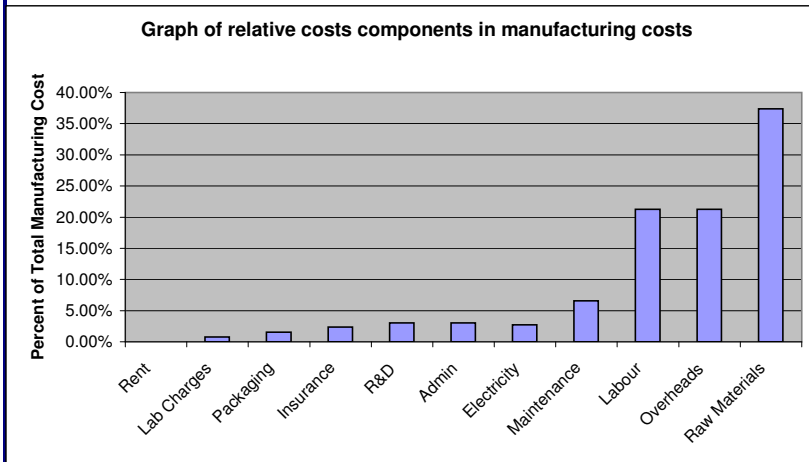
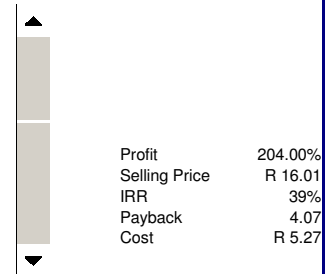
	-20.0%	-10.0%	0.0%	10.0%	20.0%	30.0%	40.0%
Operating Costs	4.08	4.08	4.07	3.09	3.08	3.08	3.07
Capital	4.07	4.07	4.07	4.07	4.07	4.07	4.07
Sales	3.07	3.08	4.07	4.09	5.11	6.14	8.19

The effect on the break-even point

	-20.0%	-10.0%	0.0%	10.0%	20.0%	30.0%	40.0%
Operating Costs	4.08	4.08	4.07	3.09	3.08	3.08	3.07
Capital	4.07	4.07	4.07	4.07	4.07	4.07	4.07
Sales	3.07	3.08	4.07	4.09	5.11	6.14	8.19

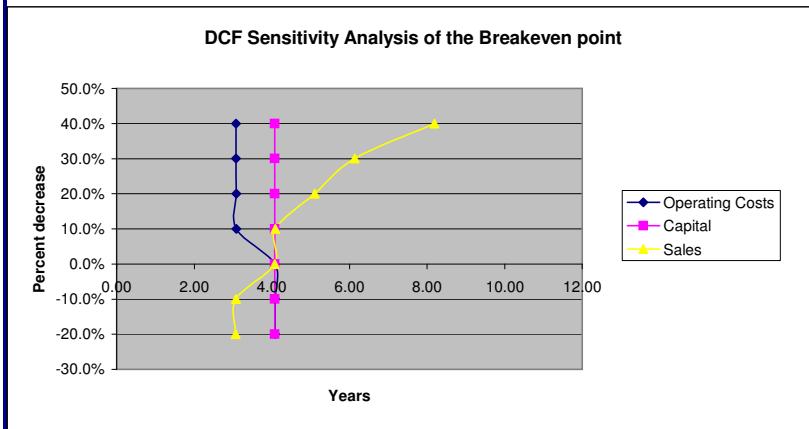


Adjust profit



Payback Period 4.07 years
Cost per meter R 5.27

Formulation:
% Starch 20%
% Glycerol 50%
% Water 10%





Input Block

Blowing

Polymer Feed Rate	91.08615124	kg.h ⁻¹	
Water Feed Rate	2.277153781	kg.h ⁻¹	
Starch Feed Rate	22.77153781	kg.h ⁻¹	
Glycerol Feed Rate	11.3857689	kg.h ⁻¹	
Polymer:Starch Ratio	4		
Water Ratio (Starch Basis)	10.00%		
Glycerol Ratio (Starch Basis)	50.00%		
Starch Density	0.65	g.cm ⁻³	650 kg.m ⁻³
Polymer Density	1.06	g.cm ⁻³	1060 kg.m ⁻³
Glycerol Density	1.2161	g.cm ⁻³	1216.1 kg.m ⁻³

Desired Annual Production Rate(Blowing)	1000000	m/year	1
Hours Production per year	2000	hours	
Hours Extrusion:Hours Blowing Ratio	0.14		
Time Spent Extruding	280	hours	
Hours Extrusion Starch:Hours Extrusion Blend	0.2		
Time Extruding Starch	56	hours	If only one extruder is used
Time Extruding Blend	224	hours	
Time Spent Blowing	1720	hours	
Number of cycle per month	1		

Mass balance complete

Mass balance complete

Final Film Thickness	20	μm
Final Film Width	1.6	m
Exit Line Speed(Blowing)	0.161498708	m.s ⁻¹

Wastage of Extruders	4	%	
Wastage of Pelletizers	1	%	
Wastage of Blower	2	%	Estimated startup losses
Wastage of Stretcher	2.5	%	For sheet extrusion only. Losses when cutting
Wastage of Haul Off	0.5	%	Estimated losses for unexpected tears

Exchange Rate R:\$	6	R/\$	Rates for 22/06/2004 from www.x-rates.com
Exchange Rate R:€	7.7		
Cost of Electricity	0.46	R/kWh	
Admin electricity costs	14484	R	
Cost of Water	10	R/kL	
Cost of Glycerol	9.8	R/kg	
Cost of Starch	7.88	R/kg	
Cost of Pellethane	74	R/kg	

Number of Operators	4
Number of Cleaners	2
Number of Support Staff	1
Number of Supervisors	1

Rate of Operators	50	R/hour
Rate of Cleaners	30	R/hour
Rate of Support Staff	50	R/hour
Rate of Supervisors	150	R/hour

Cost of Operators	400000	R
Cost of Cleaners	120000	R
Cost of Support Staff	100000	R
Cost of Supervisors	300000	R

Profit percentage	204.00%
Estimated Selling Price	R 16.01 /m
Estimated Sales per Annum	R 16,008,967
Equipment Maintenance Estimate	0.1 % of Capital

Mixer Residence Time	20	min
Mixer Required Capacity	63.02890294	kg
Mixer Design Capacity	70	kg
Mixer Design Capacity	0.08247119	m ³
Radius	0.5	m
Height	0.5	m
Turbine Speed	10	m.s ⁻¹
Turbine Speed	7.853981634	s ⁻¹
Mixture Density	848.78125	kg.m ⁻³
Mixture Viscosity	0.09616	kg.m ⁻¹ .s ⁻¹
g	9.81	m.s ⁻²
Reynolds Number	1.73E+04	



K Turbulent	4.1
K Viscous	70
Material	Carbon Steel
Power from Peters & Timmerhaus	1393.303125 W
Power from Re vs Power Number	171862.1619 W

Single Screw Extruder Throughput	36.4344605 kg.h ⁻¹
Extruder Design Throughput	100 kg.h ⁻¹
Material	Carbon Steel
Power	25000 W

Twin Screw Extruder Throughput	148.2591066 kg.h ⁻¹
Extruder Design Throughput	150 kg.h ⁻¹
Material	Carbon Steel
Power	W

Primary Pelletizer Throughput	32.79101445 kg.h ⁻¹
Pelletizer Design Throughput	50 kg.h ⁻¹
Material	Carbon Steel
Power	W

Secondary Pelletizer Throughput	148.2591066 kg.h ⁻¹
Pelletizer Design Throughput	150 kg.h ⁻¹
Material	Carbon Steel
Power	W

Storage Tank Capacity	2739.828291 kg
Density of Pellets	1001.852462 kg.m ⁻³
Volume Pellets	2.734762247 m ³
Porosity	0.3
Volume Tank	3.555190921 m ³
Design Volume	4 m ³
Height	3 m
Radius	0.652 m
Material	Carbon Steel
Power	0 W

Blower Throughput	42.11906439 kg.h ⁻¹
Pellet Density	1001.852462 kg.m ⁻³
Blower Throughput	0.042041185 m ³ .h ⁻¹
Design Throughput	0.043 m ³ .h ⁻¹
Material	Carbon Steel
Power	15000 W

Reference: Plant Design and Economics for Chemical Engineers 5th Edition page 532 - Estimated

Film Blower Throughput	42.11906439 kg.h ⁻¹
Design Throughput	50 kg.h ⁻¹
Material	Carbon Steel
Power	W

Stretcher Throughput	18.63911558 kg.h ⁻¹
Design Throughput	20 kg.h ⁻¹
Material	Carbon Steel
Power	W

Exit Pellet Temp	170 °C
Desired Temp	40 °C
Pellet Flow Rate	117.4212125 kg.h ⁻¹
Est Area Pellets/hour	35.16122888 m ²
Est Heat Capacity Pellet	1.3 J.g ⁻¹ .K ⁻¹
Entry Water Temp	20 °C
Heat Capacity	4.1801 J.g ⁻¹ .K ⁻¹
Exit Water Temp	30 °C
Heat per pellet	1424.189726 L/hour
Energy for cooling	59532.55472 KJ/h

Pellet Radius	0.01 m
Pellet Height	0.01 m

<http://www2.eng.cam.ac.uk/~amw33/foams/node8.html>



Energy for cooling	16.53682076 kW
Hours of operation	280 hours
Energy per year	4630.309812 kWh

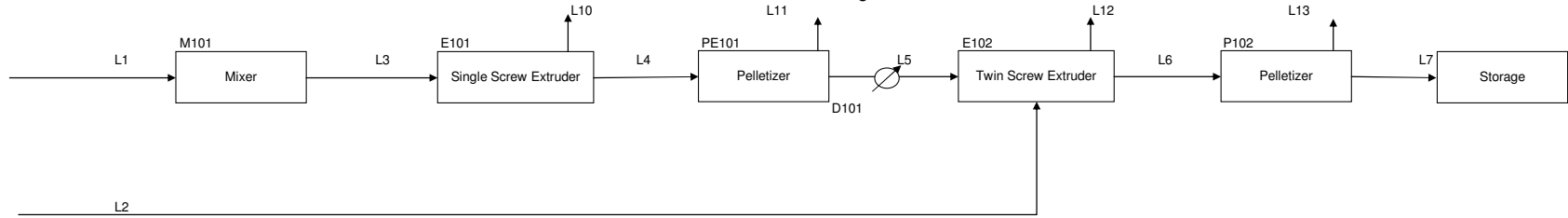
Pump 1 Capacity	2.277153781 L.hr ⁻¹
Pump 1 Capacity	0.002277154 m ³ .hr ⁻¹
Design Capacity	0.003 m ³ .hr ⁻¹
Pump 2 Capacity	1424.189726 L.hr ⁻¹
Pump 2 Capacity	1.424189726 m ³ .hr ⁻¹
Max capacity of pump	250 L.hr ⁻¹
Number of Pumps	6
Design Capacity	0.25 m ³ .hr ⁻¹
Power for Pump 1	W
Power for each of Pumps 2	W
Total Power	0 W

Assume each pump max 250L.hr⁻¹

Refer to Unit Ops page

Refer to Unit Ops page

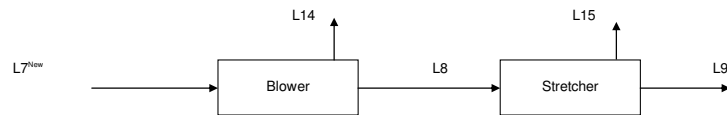
Mass Balance for a Batch Film Blowing Plant



Input/ kg.h ⁻¹	L1	L2	L3	L4	L5	L6	L7	L10	L11	L12	L13
Starch	22.77154		22.77154	21.86068	21.64207	20.77639	20.56862	0.910862	0.218607	0.865683	0.207764
Water	2.277154		2.277154	0	0	0	0	2.277154	0	0	0
Glycerol	11.38577		11.38577	10.93034	10.82103	10.38819	10.28431	0.455431	0.109303	0.432841	0.103882
Polymer		91.08615				87.44271	86.56828			3.643446	0.874427

IN	-	OUT	=	
22.77154		22.77154		0
2.277154		2.277154		0
11.38577		11.38577		0
91.08615		91.08615		0

Hours of Operation 280 hours
Pellets Produced 32877.94 kg/year 2739.828 kg/month



Input/ kg.h ⁻¹	L7 ^{new}	L8	L9	L14	L15
Starch	3.34838	3.281413	3.265006	0.066968	0.016407
Water	0	0	0	0	0
Glycerol	1.67419	1.640706	1.632503	0.033484	0.008204
Polymer	14.09251	13.81066	13.74161	0.28185	0.069053

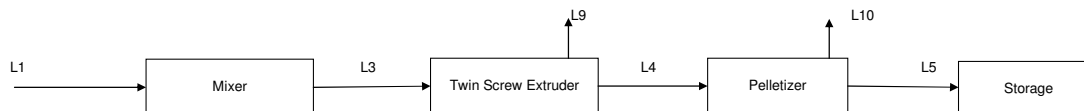
IN	-	OUT	=	
3.34838		3.34838		0
0		0		0
1.67419		1.67419		0
14.09251		14.09251		0

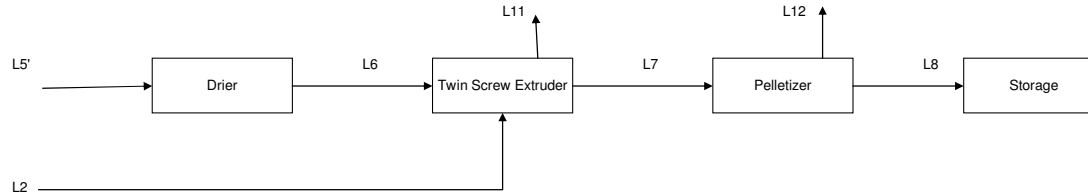
Recalculated L7	
3.34838047	Recalculated due to batch process
0	
1.674190235	
14.09251039	

Hours of Operation	1720 hours
Amount Film Produced	18.63912 kg.h ⁻¹
Amount Film Produced	32059.28 kg
Density of Film	1.001852 g.cm ⁻³ 1001.852 kg.m ⁻³
Film Thickness	20 μm 0.00002 m
Film Width	1.6 m
Exit Line Speed	0.161499 m.s ⁻¹

Desired Line Speed	0.161499 m.s ⁻¹
Difference	0 m.s ⁻¹

Sheet 1. A plant based on two extruders and two pelletizers





Input/ kg.h ⁻¹	L1	L2	L3	L4	L5	L5'	L6	L7	L8	L9	L10	L11	L12
Starch	118.1792		118.1792	113.452	112.3175	28.07938	28.07938	26.9562	26.68664	4.727168	1.13452	1.123175	0.269562
Water	11.81792		11.81792	0	0	0	0	0	0	11.81792	0	0	0
Glycerol	59.0896		59.0896	56.72601	56.15875	14.03969	14.03969	13.4781	13.34332	2.363584	0.56726	0.561588	0.134781
Polymer		112.3175						107.8248	106.7466			4.4927	1.078248

Extruding Starch

IN	-	OUT	=	
118.1792		118.1792		0
11.81792		11.81792		0
59.0896		59.0896		0
0		0		0

Extruding Blend

IN	-	OUT	=	
28.07938		28.07938		0
0		0		0
14.03969		14.03969		0
112.3175		112.3175		0

Starch Produced 9434.67 Required 9434.67 Difference 0.000

Hours of Operation 56 hours
Starch Pellets produced 9434.67 kg/year 786.2225 kg/month

Hours of Operation 224 hours
Pellets produced 32877.94 kg/year 2739.828 kg/month

Pellets Produced with two Extruders 32877.94 kg/year 2739.828 kg/month

Difference 0.000

Sheet 2. A plant based on one extruders and one pelletizers

Extruders	2 kg.h ⁻¹	1 kg.h ⁻¹
Mixer	36.43446	189.0867
Single Screw Extruder	36.43446	-
Pelletizer	32.79101	-
Drier	32.79101	42.11906
Twin Screw Extruder	123.5493	189.0867
Pelletizer	118.6073	170.178
Storage Tank	2739.828	2739.828



Operating Labour Costs

Number of Operators	Hours	Rate	Cost/Oper	Total Cost
4	2000	50	100000	R 400,000.00
				R 400,000.00

Cost of Clerical Labour/Support Staff

Number of Operators	Hours	Rate	Cost/Oper	Total Cost
3	2000	50	100000	R 300,000.00
2	2000	30	60000	R 120,000.00 Cleaners, etc
				R 420,000.00

Cost of Supervisory Staff

Number of Operators	Hours	Rate	Cost/Oper	Total Cost
1	2000	150	300000	R 300,000.00 Plant manager
				R 300,000.00

Total cost of labour R 1,120,000.00

Raw Material Costs

Material	Amount/year	Amount/mnt	Cost/kg	Cost/month	Cost/year
Polymer	25504.12235	2125.343529	74	157275.4211	1887305.054
Starch	6376.030587	531.3358822	7.88	4186.926752	50243.12102
Glycerol	3188.015293	265.6679411	9.8	2603.545823	31242.54987
Water	2061.792784	171.8160654	0.01	1.718160654	20.61792784
Total				<u>164067.6119</u>	<u>1968811.342</u>



<i>Direct Costs Estimation</i>		
	Percentage of Equipment Cost	Cost
Equipment Cost	-	R 3,468,146.20
Installation, including insulation and painting	30.00%	R 1,040,443.86
Instrumentation and controls	25.00%	R 867,036.55
Piping	10.00%	R 346,814.62
Electrical	30.00%	R 1,040,443.86
Building, Process and Auxiliary	20.00%	R 693,629.24
Service, Facilities and Yard improvements	25.00%	R 867,036.55
Land	1.50%	R 52,022.19
<i>Total Direct Costs</i>		<i>R 8,375,573.08</i>
<i>Indirect Costs Estimation</i>		
	Percentage of Direct Costs	
Engineering and Supervision	25.00%	R 2,093,893.27
Construction and Contractors fee	15.00%	R 1,256,335.96
Contingency	10.00%	R 837,557.31
<i>Total Indirect Costs</i>		<i>R 4,187,786.54</i>
<i>Fixed Capital Costs</i>	-	<i>R 12,563,359.63</i>
	Percent of Fixed Capital	
<i>Working Capital</i>	Based on a month of raw material	<i>R 164,067.61</i>
Total Capital Investment		R 12,727,427.24
Reference:	Peters and Timmerhaus 3 rd Edition Pages 207-208	



Estimation of Manufacturing Costs

Direct Production Costs

	Percent of Operating Labour	Cost
Raw Materials		R 1,968,811.34
Operating Labour		R 400,000.00
Supervisory Labour		R 300,000.00
Clerical Labour		R 420,000.00
Maintenance		R 346,814.62
Water		<i>Included in the raw materials</i>
Electricity		R 144,623.71
Laboratory Charges	10.00%	R 40,000.00

Total Direct Production Costs R 3,620,249.67

Fixed Charges

	Percent of Fixed Capital	
Insurance	1.00%	R 125,633.60
Rent	0.00%	R 0.00
Percent of Labour		
Overheads	100.00%	R 1,120,000.00

Total Fixed Charges R 1,245,633.60

General Costs

	Percent of Product Sales	
Admin Costs	1.00%	160089.6659
Packaging costs	0.50%	80044.83295
R&D Costs	1.00%	160089.6659

Total Manufacturing Costs R 5,266,107.43

Cost per meter R 5.27

Item	Cost	Percentage
Rent	R 0.00	0.00%
Lab Charges	R 40,000.00	0.76%
Packaging	R 80,044.83	1.52%
Insurance	R 125,633.60	2.39%
R&D	R 160,089.67	3.04%
Admin	R 160,089.67	3.04%
Electricity	R 144,623.71	2.75%
Maintenance	R 346,814.62	6.59%
Labour	R 1,120,000.00	21.27%
Overheads	R 1,120,000.00	21.27%
Raw Materials	R 1,968,811.34	37.39%

DCF Calculation for Breathable Membrane Film Blowing Plant
Amounts are expressed in Sount African R mil

Years	0	1	2	3	4	5	6	7	8	9	10
Capital Investment	-12.7274272										
Working Capital	-0.08203381										
Sales		16.008967	16.00897	16.00897	16.00897	16.00897	16.00897	16.00897	16.00897	16.00897	16.00897
Operating Costs		-5.266107	-5.26611	-5.26611	-5.26611	-5.26611	-5.26611	-5.26611	-5.26611	-5.26611	-5.26611
Net Income Before Tax		10.742859	10.74286	10.74286	10.74286	10.74286	10.74286	10.74286	10.74286	10.74286	10.74286
Tax Allowance of 33% on investment		-4.200051	-4.20005	-4.20005							
Taxable Income		6.5428082	6.542808	6.542808	10.74286	10.74286	10.74286	10.74286	10.74286	10.74286	10.74286
Tax at 35% p.a.		-2.289983	-2.28998	-2.28998	-3.76	-3.76	-3.76	-3.76	-3.76	-3.76	-3.76
Nett income after tax		4.2528253	4.252825	4.252825	6.982858	6.982858	6.982858	6.982858	6.982858	6.982858	6.982858
Cash flow	-12.809461	4.2528253	4.252825	4.252825	6.982858	6.982858	6.982858	6.982858	6.982858	6.982858	6.982858
IRR	39%										
Discount Factor % p.a.	39.10899157										
Discount Factor	1	0.990099	0.980296	0.97059	0.96098	0.951466	0.942045	0.932718	0.923483	0.91434	0.905287
Present Value	-12.809461	4.2107181	4.169028	4.12775	6.71039	6.64395	6.578169	6.513038	6.448553	6.384706	6.321491
Nett Present Value	-12.809461	-8.598743	-4.42972	-0.30196	6.408425	13.05238	19.63054	26.14358	32.59213	38.97684	45.29833
		0	0	0	4.074882	0	0	0	0	0	0
Payback Period		4.07 years									

Cash flow	-12.80946104	3.910528	3.910528	3.910528	6.640561	6.640561	6.640561	6.640561	6.640561	6.640561	6.640561
IRR	37%										
Discount Factor % p.a.	36.59823204										
Discount Factor	1	0.990099	0.980296	0.97059	0.96098	0.951466	0.942045	0.932718	0.923483	0.91434	0.905287
Present Value	-12.80946104	3.87181	3.833475	3.79552	6.381449	6.318266	6.255709	6.193772	6.132447	6.07173	6.011614
Net Present Value	-12.80946104	-8.93765	-5.10418	-1.30866	5.072794	11.39106	17.64677	23.84054	29.97299	36.04472	42.05633

4.078742

Years	0	1	2	3	4	5	6	7	8	9	10
Capital Investment	-12.72742724										
Working Capital	-0.082033806										
Sales		16.00897	16.00897	16.00897	16.00897	16.00897	16.00897	16.00897	16.00897	16.00897	16.00897
Operating Costs		-5.26611	-5.26611	-5.26611	-5.26611	-5.26611	-5.26611	-5.26611	-5.26611	-5.26611	-5.26611
Net Income Before Tax		10.74286	10.74286	10.74286	10.74286	10.74286	10.74286	10.74286	10.74286	10.74286	10.74286
Tax Allowance of 33% on investment		-4.20005	-4.20005	-4.20005							
Taxable Income		6.542808	6.542808	6.542808	10.74286	10.74286	10.74286	10.74286	10.74286	10.74286	10.74286
Tax at 35% p.a.		-2.28998	-2.28998	-2.28998	-3.76	-3.76	-3.76	-3.76	-3.76	-3.76	-3.76
Nett income after tax		4.252825	4.252825	4.252825	6.982858	6.982858	6.982858	6.982858	6.982858	6.982858	6.982858
Cash flow	-12.80946104	4.252825	4.252825	4.252825	6.982858	6.982858	6.982858	6.982858	6.982858	6.982858	6.982858
IRR	39%										
Discount Factor % p.a.	39.10899157										
Discount Factor	1	0.990099	0.980296	0.97059	0.96098	0.951466	0.942045	0.932718	0.923483	0.91434	0.905287
Present Value	-12.80946104	4.210718	4.169028	4.12775	6.71039	6.64395	6.578169	6.513038	6.448553	6.384706	6.321491
Net Present Value	-12.80946104	-8.59874	-4.42972	-0.30196	6.408425	13.05238	19.63054	26.14358	32.59213	38.97684	45.29833

Operating Cost Increase 0%

R 4.07

Years	0	1	2	3	4	5	6	7	8	9	10
Capital Investment	-12.72742724										
Working Capital	-0.082033806										
Sales		16.00897	16.00897	16.00897	16.00897	16.00897	16.00897	16.00897	16.00897	16.00897	16.00897
Operating Costs		-4.7395	-4.7395	-4.7395	-4.7395	-4.7395	-4.7395	-4.7395	-4.7395	-4.7395	-4.7395
Net Income Before Tax		11.26947	11.26947	11.26947	11.26947	11.26947	11.26947	11.26947	11.26947	11.26947	11.26947

Operating Cost Increase 10%

Tax Allowance of 33% on investment		-4.20005	-4.20005	-4.20005							
Taxable Income		7.069419	7.069419	7.069419	11.26947	11.26947	11.26947	11.26947	11.26947	11.26947	11.26947
Tax at 35% p.a.		-2.4743	-2.4743	-2.4743	-3.94431	-3.94431	-3.94431	-3.94431	-3.94431	-3.94431	-3.94431
Nett income after tax		4.595122	4.595122	4.595122	7.325155	7.325155	7.325155	7.325155	7.325155	7.325155	7.325155
Cash flow	-12.80946104	4.595122	4.595122	4.595122	7.325155	7.325155	7.325155	7.325155	7.325155	7.325155	7.325155
IRR	42%										
Discount Factor % p.a.	41.61442124										
Discount Factor	1	0.990099	0.980296	0.97059	0.96098	0.951466	0.942045	0.932718	0.923483	0.91434	0.905287
Present Value	-12.80946104	4.549626	4.50458	4.45998	7.03933	6.969634	6.900628	6.832305	6.764658	6.697681	6.631368
Nett Present Value	-12.80946104	-8.25984	-3.75525	0.704726	7.744056	14.71369	21.61432	28.44662	35.21128	41.90896	48.54033

0 0 3.086962 0 0 0 0 0 0 0

3.086962

Years	0	1	2	3	4	5	6	7	8	9	10
Capital Investment	-12.72742724										
Working Capital	-0.082033806										
Sales		16.00897	16.00897	16.00897	16.00897	16.00897	16.00897	16.00897	16.00897	16.00897	16.00897
Operating Costs		-4.21289	-4.21289	-4.21289	-4.21289	-4.21289	-4.21289	-4.21289	-4.21289	-4.21289	-4.21289
Net Income Before Tax		11.79608	11.79608	11.79608	11.79608	11.79608	11.79608	11.79608	11.79608	11.79608	11.79608
Tax Allowance of 33% on investment		-4.20005	-4.20005	-4.20005							
Taxable Income		7.59603	7.59603	7.59603	11.79608	11.79608	11.79608	11.79608	11.79608	11.79608	11.79608
Tax at 35% p.a.		-2.65861	-2.65861	-2.65861	-4.12863	-4.12863	-4.12863	-4.12863	-4.12863	-4.12863	-4.12863
Nett income after tax		4.937419	4.937419	4.937419	7.667452	7.667452	7.667452	7.667452	7.667452	7.667452	7.667452
Cash flow	-12.80946104	4.937419	4.937419	4.937419	7.667452	7.667452	7.667452	7.667452	7.667452	7.667452	7.667452
IRR	44%										
Discount Factor % p.a.	44.1165986										
Discount Factor	1	0.990099	0.980296	0.97059	0.96098	0.951466	0.942045	0.932718	0.923483	0.91434	0.905287
Present Value	-12.80946104	4.888534	4.840133	4.792211	7.368271	7.295318	7.223087	7.151571	7.080764	7.010657	6.941245
Nett Present Value	-12.80946104	-7.92093	-3.08079	1.711416	9.079687	16.375	23.59809	30.74966	37.83043	44.84108	51.78233

0 0 3.082234 0 0 0 0 0 0 0

3.082234

Years	0	1	2	3	4	5	6	7	8	9	10
-------	---	---	---	---	---	---	---	---	---	---	----

Operating Cost Increase 20%

DCF Calculation for Breathable Membrane Film Blowing Plant
Amounts are expressed in Sount African R mil

Years	0	1	2	3	4	5	6	7	8	9	10	
Capital Investment	-15.27291268											
Working Capital	-0.082033806											
Sales		16.00897	16.00897	16.00897	16.00897	16.00897	16.00897	16.00897	16.00897	16.00897	16.00897	16.00896659
Operating Costs		-5.26611	-5.26611	-5.26611	-5.26611	-5.26611	-5.26611	-5.26611	-5.26611	-5.26611	-5.26611	-5.266107431
Net Income Before Tax		10.74286	10.74286	10.74286	10.74286	10.74286	10.74286	10.74286	10.74286	10.74286	10.74286	10.74285916
Tax Allowance of 33% on investment		-5.04006	-5.04006	-5.04006								
Taxable Income		5.702798	5.702798	5.702798	10.74286	10.74286	10.74286	10.74286	10.74286	10.74286	10.74286	10.74285916
Tax at 35% p.a.		-1.99598	-1.99598	-1.99598	-3.76	-3.76	-3.76	-3.76	-3.76	-3.76	-3.76	-3.760000706
Nett income after tax		3.706819	3.706819	3.706819	6.982858	6.982858	6.982858	6.982858	6.982858	6.982858	6.982858	6.982858453
Cash flow	-15.35494649	3.706819	3.706819	3.706819	6.982858	6.982858	6.982858	6.982858	6.982858	6.982858	6.982858	6.982858453
IRR	31%											
Discount Factor % p.a.	30.56780039											
Discount Factor	1	0.990099	0.980296	0.97059	0.96098	0.951466	0.942045	0.932718	0.923483	0.91434	0.905286955	0.905286955
Present Value	-15.35494649	3.670118	3.633378	3.597802	6.71039	6.64395	6.578169	6.513038	6.448553	6.384706	6.321490664	6.321490664
Nett Present Value	-15.35494649	-11.6848	-8.05105	-4.45325	2.257142	8.901092	15.47926	21.9923	28.44085	34.82556	41.14704791	41.14704791

Capital Increase by -20%

Years	0	1	2	3	4	5	6	7	8	9	10	
Capital Investment	-12.72742724											
Working Capital	-0.082033806											
Sales		16.00897	16.00897	16.00897	16.00897	16.00897	16.00897	16.00897	16.00897	16.00897	16.00897	16.00896659
Operating Costs		-5.26611	-5.26611	-5.26611	-5.26611	-5.26611	-5.26611	-5.26611	-5.26611	-5.26611	-5.26611	-5.266107431
Net Income Before Tax		10.74286	10.74286	10.74286	10.74286	10.74286	10.74286	10.74286	10.74286	10.74286	10.74286	10.74285916
Tax Allowance of 33% on investment		-4.20005	-4.20005	-4.20005								
Taxable Income		6.542808	6.542808	6.542808	10.74286	10.74286	10.74286	10.74286	10.74286	10.74286	10.74286	10.74285916
Tax at 35% p.a.		-2.28998	-2.28998	-2.28998	-3.76	-3.76	-3.76	-3.76	-3.76	-3.76	-3.76	-3.760000706
Nett income after tax		4.252825	4.252825	4.252825	6.982858	6.982858	6.982858	6.982858	6.982858	6.982858	6.982858	6.982858453

4.074882

Capital Increase by -10%



Cash flow	-12.80946104	4.252825	4.252825	4.252825	6.982858	6.982858	6.982858	6.982858	6.982858	6.982858	6.982858453
IRR	39%										
Discount Factor % p.a.	39.10899157										
Discount Factor	1	0.990099	0.980296	0.97059	0.96098	0.951466	0.942045	0.932718	0.923483	0.91434	0.905286955
Present Value	-12.80946104	4.210718	4.169028	4.12775	6.71039	6.64395	6.578169	6.513038	6.448553	6.384706	6.321490664
Net Present Value	-12.80946104	-8.59874	-4.42972	-0.30196	6.408425	13.05238	19.63054	26.14358	32.59213	38.97684	45.29833078

		0	0	0	4.074882	0	0	0	0	0	4.074882	
Years		0	1	2	3	4	5	6	7	8	9	10
Capital Investment	-12.72742724											
Working Capital	-0.082033806											
Sales		16.00897	16.00897	16.00897	16.00897	16.00897	16.00897	16.00897	16.00897	16.00897	16.00897	16.00896659
Operating Costs		-5.26611	-5.26611	-5.26611	-5.26611	-5.26611	-5.26611	-5.26611	-5.26611	-5.26611	-5.26611	-5.266107431
Net Income Before Tax		10.74286	10.74286	10.74286	10.74286	10.74286	10.74286	10.74286	10.74286	10.74286	10.74286	10.74285916
Tax Allowance of 33% on investment		-4.20005	-4.20005	-4.20005								
Taxable Income		6.542808	6.542808	6.542808	10.74286	10.74286	10.74286	10.74286	10.74286	10.74286	10.74286	10.74285916
Tax at 35% p.a.		-2.28998	-2.28998	-2.28998	-3.76	-3.76	-3.76	-3.76	-3.76	-3.76	-3.76	-3.760000706
Nett income after tax		4.252825	4.252825	4.252825	6.982858	6.982858	6.982858	6.982858	6.982858	6.982858	6.982858	6.982858453
Cash flow	-12.80946104	4.252825	4.252825	4.252825	6.982858	6.982858	6.982858	6.982858	6.982858	6.982858	6.982858	6.982858453
IRR	39%											
Discount Factor % p.a.	39.10899157											
Discount Factor	1	0.990099	0.980296	0.97059	0.96098	0.951466	0.942045	0.932718	0.923483	0.91434	0.905286955	
Present Value	-12.80946104	4.210718	4.169028	4.12775	6.71039	6.64395	6.578169	6.513038	6.448553	6.384706	6.321490664	
Net Present Value	-12.80946104	-8.59874	-4.42972	-0.30196	6.408425	13.05238	19.63054	26.14358	32.59213	38.97684	45.29833078	

4.074882

Capital Increase by 0%

		0	0	0	4.074882	0	0	0	0	0	4.074882	
Years		0	1	2	3	4	5	6	7	8	9	10
Capital Investment	-12.72742724											
Working Capital	-0.082033806											
Sales		16.00897	16.00897	16.00897	16.00897	16.00897	16.00897	16.00897	16.00897	16.00897	16.00897	16.00896659
Operating Costs		-5.26611	-5.26611	-5.26611	-5.26611	-5.26611	-5.26611	-5.26611	-5.26611	-5.26611	-5.26611	-5.266107431
Net Income Before Tax		10.74286	10.74286	10.74286	10.74286	10.74286	10.74286	10.74286	10.74286	10.74286	10.74286	10.74285916

4.074882

Capital Increase by 10%



Tax Allowance of 33% on investment		-4.20005	-4.20005	-4.20005								
Taxable Income		6.542808	6.542808	6.542808	10.74286	10.74286	10.74286	10.74286	10.74286	10.74286	10.74286	10.74285916
Tax at 35% p.a.		-2.28998	-2.28998	-2.28998	-3.76	-3.76	-3.76	-3.76	-3.76	-3.76	-3.76	-3.760000706
Nett income after tax		4.252825	4.252825	4.252825	6.982858	6.982858	6.982858	6.982858	6.982858	6.982858	6.982858	6.982858453
Cash flow	-12.80946104	4.252825	4.252825	4.252825	6.982858	6.982858	6.982858	6.982858	6.982858	6.982858	6.982858	6.982858453
IRR	39%											
Discount Factor % p.a.	39.10899157											
Discount Factor	1	0.990099	0.980296	0.97059	0.96098	0.951466	0.942045	0.932718	0.923483	0.91434	0.905286955	
Present Value	-12.80946104	4.210718	4.169028	4.12775	6.71039	6.64395	6.578169	6.513038	6.448553	6.384706	6.321490664	
Nett Present Value	-12.80946104	-8.59874	-4.42972	-0.30196	6.408425	13.05238	19.63054	26.14358	32.59213	38.97684	45.29833078	

0 0 0 4.074882 0 0 0 0 0 0 0

4.074882

Years	0	1	2	3	4	5	6	7	8	9	10
Capital Investment	-12.72742724										
Working Capital	-0.082033806										
Sales		16.00897	16.00897	16.00897	16.00897	16.00897	16.00897	16.00897	16.00897	16.00897	16.00896659
Operating Costs		-5.26611	-5.26611	-5.26611	-5.26611	-5.26611	-5.26611	-5.26611	-5.26611	-5.26611	-5.266107431
Net Income Before Tax		10.74286	10.74286	10.74286	10.74286	10.74286	10.74286	10.74286	10.74286	10.74286	10.74285916
Tax Allowance of 33% on investment		-4.20005	-4.20005	-4.20005							
Taxable Income		6.542808	6.542808	6.542808	10.74286	10.74286	10.74286	10.74286	10.74286	10.74286	10.74285916
Tax at 35% p.a.		-2.28998	-2.28998	-2.28998	-3.76	-3.76	-3.76	-3.76	-3.76	-3.76	-3.760000706
Nett income after tax		4.252825	4.252825	4.252825	6.982858	6.982858	6.982858	6.982858	6.982858	6.982858	6.982858453
Cash flow	-12.80946104	4.252825	4.252825	4.252825	6.982858	6.982858	6.982858	6.982858	6.982858	6.982858	6.982858453
IRR	39%										
Discount Factor % p.a.	39.10899157										
Discount Factor	1	0.990099	0.980296	0.97059	0.96098	0.951466	0.942045	0.932718	0.923483	0.91434	0.905286955
Present Value	-12.80946104	4.210718	4.169028	4.12775	6.71039	6.64395	6.578169	6.513038	6.448553	6.384706	6.321490664
Nett Present Value	-12.80946104	-8.59874	-4.42972	-0.30196	6.408425	13.05238	19.63054	26.14358	32.59213	38.97684	45.29833078

0 0 0 4.074882 0 0 0 0 0 0 0

4.074882

Years	0	1	2	3	4	5	6	7	8	9	10
-------	---	---	---	---	---	---	---	---	---	---	----

Capital Increase by 20%



Discount Factor	1	0.990099	0.980296	0.97059	0.96098	0.951466	0.942045	0.932718	0.923483	0.91434	0.905286955
Present Value	-12.80946104	4.210718	4.169028	4.12775	6.71039	6.64395	6.578169	6.513038	6.448553	6.384706	6.321490664
Nett Present Value	-12.80946104	-8.59874	-4.42972	-0.30196	6.408425	13.05238	19.63054	26.14358	32.59213	38.97684	45.29833078

0 0 0 4.074882 0 0 0 0 0 0 0 4.074882

DCF Calculation for Breathable Membrane Film Blowing Plant
Amounts are expressed in Sount African R mil

Years	0	1	2	3	4	5	6	7	8	9	10
Capital Investment	-12.72742724										
Working Capital	-0.082033806										
Sales		19.21076	19.21076	19.21076	19.21076	19.21076	19.21076	19.21076	19.21076	19.21076	19.21076
Operating Costs		-5.26611	-5.26611	-5.26611	-5.26611	-5.26611	-5.26611	-5.26611	-5.26611	-5.26611	-5.26611
Net Income Before Tax		13.94465	13.94465	13.94465	13.94465	13.94465	13.94465	13.94465	13.94465	13.94465	13.94465
Tax Allowance of 33% on investment		-4.20005	-4.20005	-4.20005							
Taxable Income		9.744601	9.744601	9.744601	13.94465	13.94465	13.94465	13.94465	13.94465	13.94465	13.94465
Tax at 35% p.a.		-3.41061	-3.41061	-3.41061	-4.88063	-4.88063	-4.88063	-4.88063	-4.88063	-4.88063	-4.88063
Nett income after tax		6.333991	6.333991	6.333991	9.064024	9.064024	9.064024	9.064024	9.064024	9.064024	9.064024
Cash flow	-12.80946104	6.333991	6.333991	6.333991	9.064024	9.064024	9.064024	9.064024	9.064024	9.064024	9.064024
IRR	54%										
Discount Factor % p.a.	54.32304654										
Discount Factor	1	0.990099	0.980296	0.97059	0.96098	0.951466	0.942045	0.932718	0.923483	0.91434	0.905287
Present Value	-12.80946104	6.271278	6.209186	6.147709	8.710349	8.624108	8.538721	8.454179	8.370474	8.287598	8.205543
Nett Present Value	-12.80946104	-6.53818	-0.329	5.818713	14.52906	23.15317	31.69189	40.14607	48.51654	56.80414	65.00968

Sales Decreases by -20%

0 0 3.067304 0 0 0 0 0 0 0 0 3.067304

Years	0	1	2	3	4	5	6	7	8	9	10
Capital Investment	-12.72742724										
Working Capital	-0.082033806										
Sales		17.60986	17.60986	17.60986	17.60986	17.60986	17.60986	17.60986	17.60986	17.60986	17.60986
Operating Costs		-5.26611	-5.26611	-5.26611	-5.26611	-5.26611	-5.26611	-5.26611	-5.26611	-5.26611	-5.26611
Net Income Before Tax		12.34376	12.34376	12.34376	12.34376	12.34376	12.34376	12.34376	12.34376	12.34376	12.34376
Tax Allowance of 33% on investment		-4.20005	-4.20005	-4.20005							
Taxable Income		8.143705	8.143705	8.143705	12.34376	12.34376	12.34376	12.34376	12.34376	12.34376	12.34376
Tax at 35% p.a.		-2.8503	-2.8503	-2.8503	-4.32031	-4.32031	-4.32031	-4.32031	-4.32031	-4.32031	-4.32031

Sales Decreases by -10%



Nett income after tax		5.293408	5.293408	5.293408	8.023441	8.023441	8.023441	8.023441	8.023441	8.023441	8.023441
Cash flow	-12.80946104	5.293408	5.293408	5.293408	8.023441	8.023441	8.023441	8.023441	8.023441	8.023441	8.023441
IRR	47%										
Discount Factor % p.a.	46.71724769										
Discount Factor	1	0.990099	0.980296	0.97059	0.96098	0.951466	0.942045	0.932718	0.923483	0.91434	0.905287
Present Value	-12.80946104	5.240998	5.189107	5.13773	7.710369	7.634029	7.558445	7.483609	7.409513	7.336152	7.263517
Nett Present Value	-12.80946104	-7.56846	-2.37936	2.758374	10.46874	18.10277	25.66122	33.14483	40.55434	47.89049	55.15401

0 0 0 3.077833 0 0 0 0 0 0 0 0

3.077833

Years	0	1	2	3	4	5	6	7	8	9	10
Capital Investment	-12.72742724										
Working Capital	-0.082033806										
Sales		16.00897	16.00897	16.00897	16.00897	16.00897	16.00897	16.00897	16.00897	16.00897	16.00897
Operating Costs		-5.26611	-5.26611	-5.26611	-5.26611	-5.26611	-5.26611	-5.26611	-5.26611	-5.26611	-5.26611
Net Income Before Tax		10.74286	10.74286	10.74286	10.74286	10.74286	10.74286	10.74286	10.74286	10.74286	10.74286
Tax Allowance of 33% on investment		-4.20005	-4.20005	-4.20005							
Taxable Income		6.542808	6.542808	6.542808	10.74286	10.74286	10.74286	10.74286	10.74286	10.74286	10.74286
Tax at 35% p.a.		-2.28998	-2.28998	-2.28998	-3.76	-3.76	-3.76	-3.76	-3.76	-3.76	-3.76
Nett income after tax		4.252825	4.252825	4.252825	6.982858	6.982858	6.982858	6.982858	6.982858	6.982858	6.982858
Cash flow	-12.80946104	4.252825	4.252825	4.252825	6.982858	6.982858	6.982858	6.982858	6.982858	6.982858	6.982858
IRR	39%										
Discount Factor % p.a.	39.10899157										
Discount Factor	1	0.990099	0.980296	0.97059	0.96098	0.951466	0.942045	0.932718	0.923483	0.91434	0.905287
Present Value	-12.80946104	4.210718	4.169028	4.12775	6.71039	6.64395	6.578169	6.513038	6.448553	6.384706	6.321491
Nett Present Value	-12.80946104	-8.59874	-4.42972	-0.30196	6.408425	13.05238	19.63054	26.14358	32.59213	38.97684	45.29833

0 0 0 0 4.074882 0 0 0 0 0 0 0

4.074882

Years	0	1	2	3	4	5	6	7	8	9	10
Capital Investment	-12.72742724										
Working Capital	-0.082033806										
Sales		14.40807	14.40807	14.40807	14.40807	14.40807	14.40807	14.40807	14.40807	14.40807	14.40807
Operating Costs		-5.26611	-5.26611	-5.26611	-5.26611	-5.26611	-5.26611	-5.26611	-5.26611	-5.26611	-5.26611

Sales Decreases by 10%



Net Income Before Tax		9.141962	9.141962	9.141962	9.141962	9.141962	9.141962	9.141962	9.141962	9.141962	9.141962
Tax Allowance of 33% on investment		-4.20005	-4.20005	-4.20005							
Taxable Income		4.941912	4.941912	4.941912	9.141962	9.141962	9.141962	9.141962	9.141962	9.141962	9.141962
Tax at 35% p.a.		-1.72967	-1.72967	-1.72967	-3.19969	-3.19969	-3.19969	-3.19969	-3.19969	-3.19969	-3.19969
Nett income after tax		3.212242	3.212242	3.212242	5.942276	5.942276	5.942276	5.942276	5.942276	5.942276	5.942276
Cash flow	-12.80946104	3.212242	3.212242	3.212242	5.942276	5.942276	5.942276	5.942276	5.942276	5.942276	5.942276
IRR	31%										
Discount Factor % p.a.	31.44865193										
Discount Factor	1	0.990099	0.980296	0.97059	0.96098	0.951466	0.942045	0.932718	0.923483	0.91434	0.905287
Present Value	-12.80946104	3.180438	3.148949	3.117771	5.71041	5.653871	5.597892	5.542468	5.487592	5.433259	5.379465
Nett Present Value	-12.80946104	-9.62902	-6.48007	-3.3623	2.348107	8.001978	13.59987	19.14234	24.62993	30.06319	35.44265

0 0 0 4.087995 0 0 0 0 0

4.087995

Years	0	1	2	3	4	5	6	7	8	9	10
Capital Investment	-12.72742724										
Working Capital	-0.082033806										
Sales		12.80717	12.80717	12.80717	12.80717	12.80717	12.80717	12.80717	12.80717	12.80717	12.80717
Operating Costs		-5.26611	-5.26611	-5.26611	-5.26611	-5.26611	-5.26611	-5.26611	-5.26611	-5.26611	-5.26611
Net Income Before Tax		7.541066	7.541066	7.541066	7.541066	7.541066	7.541066	7.541066	7.541066	7.541066	7.541066
Tax Allowance of 33% on investment		-4.20005	-4.20005	-4.20005							
Taxable Income		3.341015	3.341015	3.341015	7.541066	7.541066	7.541066	7.541066	7.541066	7.541066	7.541066
Tax at 35% p.a.		-1.16936	-1.16936	-1.16936	-2.63937	-2.63937	-2.63937	-2.63937	-2.63937	-2.63937	-2.63937
Nett income after tax		2.17166	2.17166	2.17166	4.901693	4.901693	4.901693	4.901693	4.901693	4.901693	4.901693
Cash flow	-12.80946104	2.17166	2.17166	2.17166	4.901693	4.901693	4.901693	4.901693	4.901693	4.901693	4.901693
IRR	24%										
Discount Factor % p.a.	23.64652757										
Discount Factor	1	0.990099	0.980296	0.97059	0.96098	0.951466	0.942045	0.932718	0.923483	0.91434	0.905287
Present Value	-12.80946104	2.150158	2.128869	2.107791	4.71043	4.663793	4.617616	4.571897	4.526631	4.481813	4.437439
Nett Present Value	-12.80946104	-10.6593	-8.53043	-6.42264	-1.71221	2.951581	7.569197	12.14109	16.66773	21.14954	25.58698

Sales Decreases by 20%



Cash flow	-12.80946104	0.090494	0.090494	0.090494	2.820527	2.820527	2.820527	2.820527	2.820527	2.820527	2.820527
IRR	7%										
Discount Factor % p.a.	6.793052704										
Discount Factor	1	0.990099	0.980296	0.97059	0.96098	0.951466	0.942045	0.932718	0.923483	0.91434	0.905287
Present Value	-12.80946104	0.089598	0.088711	0.087833	2.710471	2.683635	2.657064	2.630757	2.604709	2.57892	2.553386
Nett Present Value	-12.80946104	-12.7199	-12.6312	-12.5433	-9.83285	-7.14921	-4.49215	-1.86139	0.743317	3.322237	5.875623

0 0 0 0 0 0 0 0 0 8.192915 0

8.192915

DCF Calculation for Breathable Membrane Film Blowing Plant
Amounts are expressed in South African R mil

Years	0	1	2	3	4	5	6	7	8	9	10
Capital Investment	-12.7274272										
Working Capital	-0.08203381										
		1000000	1100000	1210000	1331000	1464100	1610510	1771561	1948717	2143589	2357948
		16.008967	17.60986	19.37085	21.30793	23.43873	25.7826	28.36086	31.19695	34.31664	37.74831
Sales		16.008967	19.37085	23.43873	28.36086	34.31664	41.52314	50.243	60.79402	73.56077	89.00853
Operating Costs		-5.266107	-5.792718	-6.37199	-7.009189	-7.710108	-8.481119	-9.329231	-10.26215	-11.28837	-12.41721
Net Income Before Tax		10.742859	13.57813	17.06674	21.35167	26.60653	33.04202	40.91376	50.53187	62.2724	76.59132
Tax Allowance of 33% on investment		-4.200051	-4.200051	-4.200051							
Taxable Income		6.5428082	9.37808	12.86669	21.35167	26.60653	33.04202	40.91376	50.53187	62.2724	76.59132
Tax at 35% p.a.		-2.289983	-3.282328	-4.50334	-7.473085	-9.312287	-11.56471	-14.31982	-17.68615	-21.79534	-26.80696
Nett income after tax		4.2528253	6.095752	8.363347	13.87859	17.29425	21.47731	26.59395	32.84572	40.47706	49.78436
Cash flow	-12.809461	4.2528253	6.095752	8.363347	13.87859	17.29425	21.47731	26.59395	32.84572	40.47706	49.78436
IRR	66%										
Discount Factor % p.a.	66.30490775										
Discount Factor	1	0.990099	0.980296	0.97059	0.96098	0.951466	0.942045	0.932718	0.923483	0.91434	0.905287
Present Value	-12.809461	4.2107181	5.975642	8.117382	13.33705	16.45488	20.2326	24.80465	30.33247	37.00979	45.06913
Nett Present Value	-12.809461	-8.598743	-2.623101	5.494281	18.83133	35.28621	55.51881	80.32347	110.6559	147.6657	192.7349

Payback Period

3.05 years



	IRR	OC	SP	P	IRR	OC	SP	P	IRR	OC	SP	P	IRR	OC	SP	P	IRR	OC	SP	P		
	39.1%	0.0%	0.0%	0.0%	37.6%	2.5%	0.0%	0.0%	35.9%	5.0%	0.0%	0.0%	33.9%	7.5%	0.0%	0.0%	31.4%	10.0%	0.0%	0.0%		
	43.1%	0.0%	0.0%	2.5%	41.9%	2.5%	0.0%	2.5%	40.4%	5.0%	0.0%	2.5%	38.7%	7.5%	0.0%	2.5%	36.8%	10.0%	0.0%	2.5%		
Annual increase in operating costs	0.1				0.1				0.1				0.1				0.1				0.1	
Annual increase in selling price	0.1				0.1				0.1				0.1				0.1				0.1	
Annual increase in volume	0.1				0.1				0.1				0.1				0.1				0.1	
IRR																					66%	
Payback Period																						3.04661
Selling Price																						16.00897
	47.0%	0.0%	0.0%	5.0%	45.9%	2.5%	0.0%	5.0%	44.6%	5.0%	0.0%	5.0%	43.2%	7.5%	0.0%	5.0%	41.5%	10.0%	0.0%	5.0%		
	50.7%	0.0%	0.0%	7.5%	49.7%	2.5%	0.0%	7.5%	48.6%	5.0%	0.0%	7.5%	47.4%	7.5%	0.0%	7.5%	45.9%	10.0%	0.0%	7.5%		
	54.3%	0.0%	0.0%	10.0%	53.4%	2.5%	0.0%	10.0%	52.4%	5.0%	0.0%	10.0%	51.3%	7.5%	0.0%	10.0%	50.1%	10.0%	0.0%	10.0%		
	43.1%	0.0%	2.5%	0.0%	41.9%	2.5%	2.5%	0.0%	40.4%	5.0%	2.5%	0.0%	38.7%	7.5%	2.5%	0.0%	36.8%	10.0%	2.5%	0.0%		
	47.1%	0.0%	2.5%	2.5%	46.0%	2.5%	2.5%	2.5%	44.7%	5.0%	2.5%	2.5%	43.3%	7.5%	2.5%	2.5%	41.6%	10.0%	2.5%	2.5%		
	50.9%	0.0%	2.5%	5.0%	49.9%	2.5%	2.5%	5.0%	48.8%	5.0%	2.5%	5.0%	47.6%	7.5%	2.5%	5.0%	46.1%	10.0%	2.5%	5.0%		
	54.6%	0.0%	2.5%	7.5%	53.7%	2.5%	2.5%	7.5%	52.7%	5.0%	2.5%	7.5%	51.6%	7.5%	2.5%	7.5%	50.4%	10.0%	2.5%	7.5%		
	58.1%	0.0%	2.5%	10.0%	57.3%	2.5%	2.5%	10.0%	56.4%	5.0%	2.5%	10.0%	55.5%	7.5%	2.5%	10.0%	54.4%	10.0%	2.5%	10.0%		
	47.0%	0.0%	5.0%	0.0%	45.9%	2.5%	5.0%	0.0%	44.6%	5.0%	5.0%	0.0%	43.2%	7.5%	5.0%	0.0%	41.5%	10.0%	5.0%	0.0%		
	50.9%	0.0%	5.0%	2.5%	49.9%	2.5%	5.0%	2.5%	48.8%	5.0%	5.0%	2.5%	47.6%	7.5%	5.0%	2.5%	46.1%	10.0%	5.0%	2.5%		
	54.7%	0.0%	5.0%	5.0%	53.8%	2.5%	5.0%	5.0%	52.8%	5.0%	5.0%	5.0%	51.7%	7.5%	5.0%	5.0%	50.5%	10.0%	5.0%	5.0%		
	58.3%	0.0%	5.0%	7.5%	57.5%	2.5%	5.0%	7.5%	56.6%	5.0%	5.0%	7.5%	55.7%	7.5%	5.0%	7.5%	54.6%	10.0%	5.0%	7.5%		
	61.9%	0.0%	5.0%	10.0%	61.1%	2.5%	5.0%	10.0%	60.3%	5.0%	5.0%	10.0%	59.5%	7.5%	5.0%	10.0%	58.5%	10.0%	5.0%	10.0%		
	50.7%	0.0%	7.5%	0.0%	49.7%	2.5%	7.5%	0.0%	48.6%	5.0%	7.5%	0.0%	47.4%	7.5%	7.5%	0.0%	45.9%	10.0%	7.5%	0.0%		
	54.6%	0.0%	7.5%	2.5%	53.7%	2.5%	7.5%	2.5%	52.7%	5.0%	7.5%	2.5%	51.6%	7.5%	7.5%	2.5%	50.4%	10.0%	7.5%	2.5%		
	58.3%	0.0%	7.5%	5.0%	57.5%	2.5%	7.5%	5.0%	56.6%	5.0%	7.5%	5.0%	55.7%	7.5%	7.5%	5.0%	54.6%	10.0%	7.5%	5.0%		
	62.0%	0.0%	7.5%	7.5%	61.2%	2.5%	7.5%	7.5%	60.4%	5.0%	7.5%	7.5%	59.6%	7.5%	7.5%	7.5%	58.6%	10.0%	7.5%	7.5%		
	65.5%	0.0%	7.5%	10.0%	64.9%	2.5%	7.5%	10.0%	64.1%	5.0%	7.5%	10.0%	63.3%	7.5%	7.5%	10.0%	62.5%	10.0%	7.5%	10.0%		
	54.3%	0.0%	10.0%	0.0%	53.4%	2.5%	10.0%	0.0%	52.4%	5.0%	10.0%	0.0%	51.3%	7.5%	10.0%	0.0%	50.1%	10.0%	10.0%	0.0%		
	58.1%	0.0%	10.0%	2.5%	57.3%	2.5%	10.0%	2.5%	56.4%	5.0%	10.0%	2.5%	55.5%	7.5%	10.0%	2.5%	54.4%	10.0%	10.0%	2.5%		
	61.9%	0.0%	10.0%	5.0%	61.1%	2.5%	10.0%	5.0%	60.3%	5.0%	10.0%	5.0%	59.5%	7.5%	10.0%	5.0%	58.5%	10.0%	10.0%	5.0%		
	65.5%	0.0%	10.0%	7.5%	64.9%	2.5%	10.0%	7.5%	64.1%	5.0%	10.0%	7.5%	63.3%	7.5%	10.0%	7.5%	62.5%	10.0%	10.0%	7.5%		
	69.1%	0.0%	10.0%	10.0%	68.5%	2.5%	10.0%	10.0%	67.8%	5.0%	10.0%	10.0%	67.1%	7.5%	10.0%	10.0%	66.3%	10.0%	10.0%	10.0%		

Appendix E: Manufacturing Equipment Details

Single Screw Extruder

Manufacturer:	Rapha Extruders
Screw diameter:	25mm
Screw L/D:	30
Screw speed range:	0-300rpm

Twin Screw Extruder

Manufacturer:	Berstorff
Model:	EV 40
Screw configuration:	Counter rotating
Screw diameter:	30mm
Screw L/D:	25
Screw speed range:	0-230Hz

Film Blower

Manufacturer:	LabTech Engineering Company LTD
Model:	LF-400 COEX
Die Type:	3-Layer Pancake Type
Screw speed range:	0-300rpm

Film Blower Single Screw Extruders

Manufacturer:	LabTech Engineering Company LTD
Model:	LE 25-30/CV
Screw diameter:	25mm
Screw L/D:	30
Screw speed range:	0-300rpm

Strand Cutter

Manufacturer:	Scheer
Model:	SGS 100-E
Rotor speed:	175-1000rpm
Rotor diameter:	200mm
Rotor width:	100mm
Number of teeth:	32

Side Cut Pelletizer

Manufacturer:	LabTech Engineering Company LTD
Model:	LSC 108
Output:	100kg.hr ⁻¹ (max)
Pellet length:	300µm - 50mm



Appendix F: Cup Design for WVTR Testing

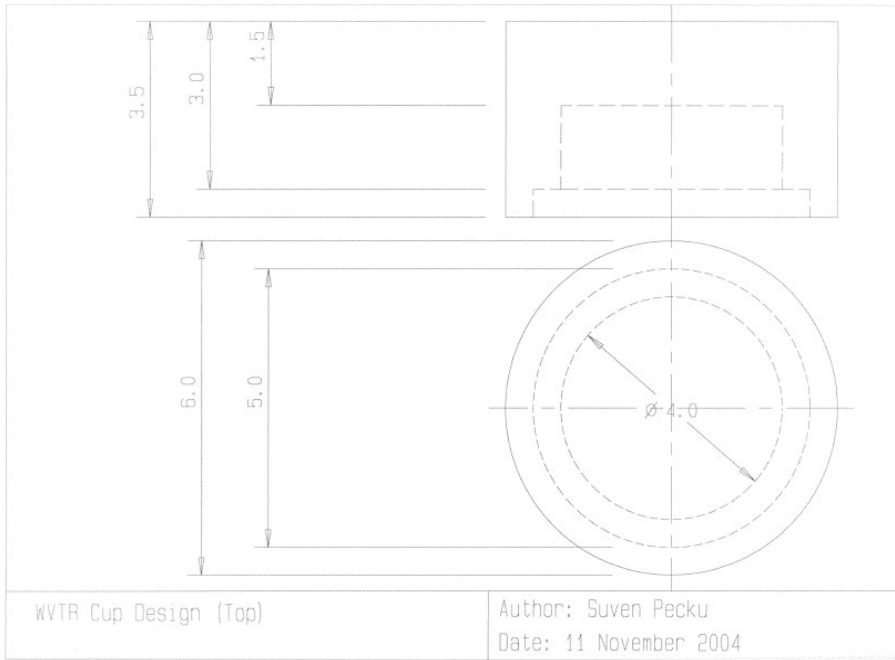


Figure F.1. Drawing of the top section of the WVTR cup

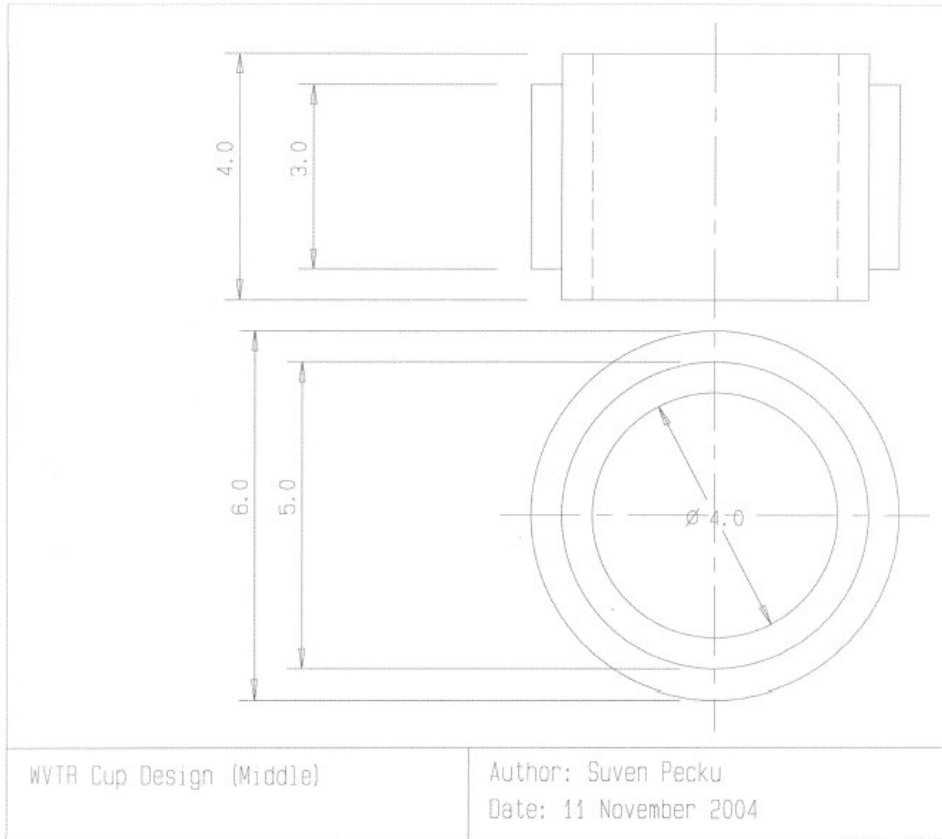


Figure F.2. Drawing of the middle section of the WVTR cup

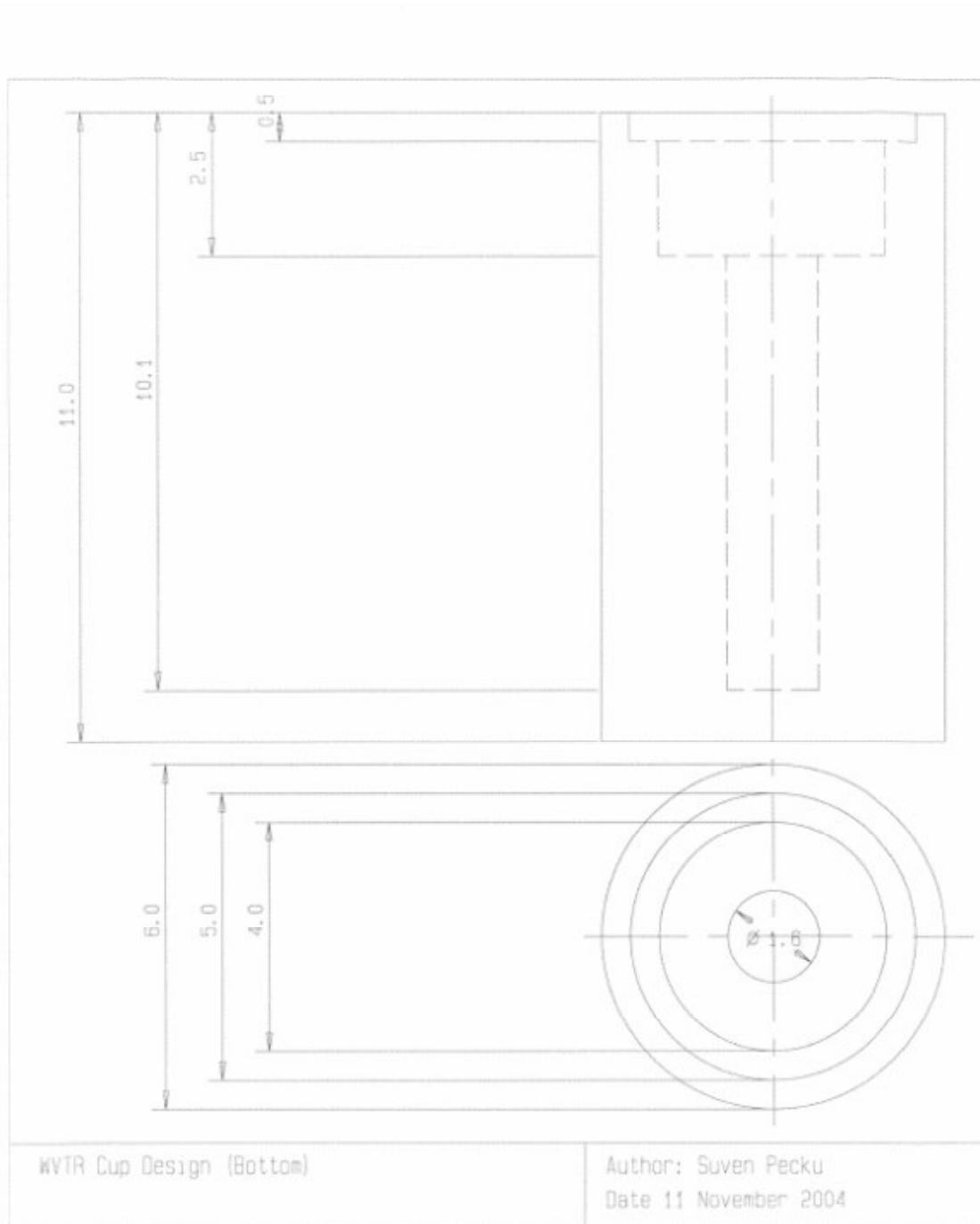


Figure F.3. Drawing of the bottom section of the WVTR cup

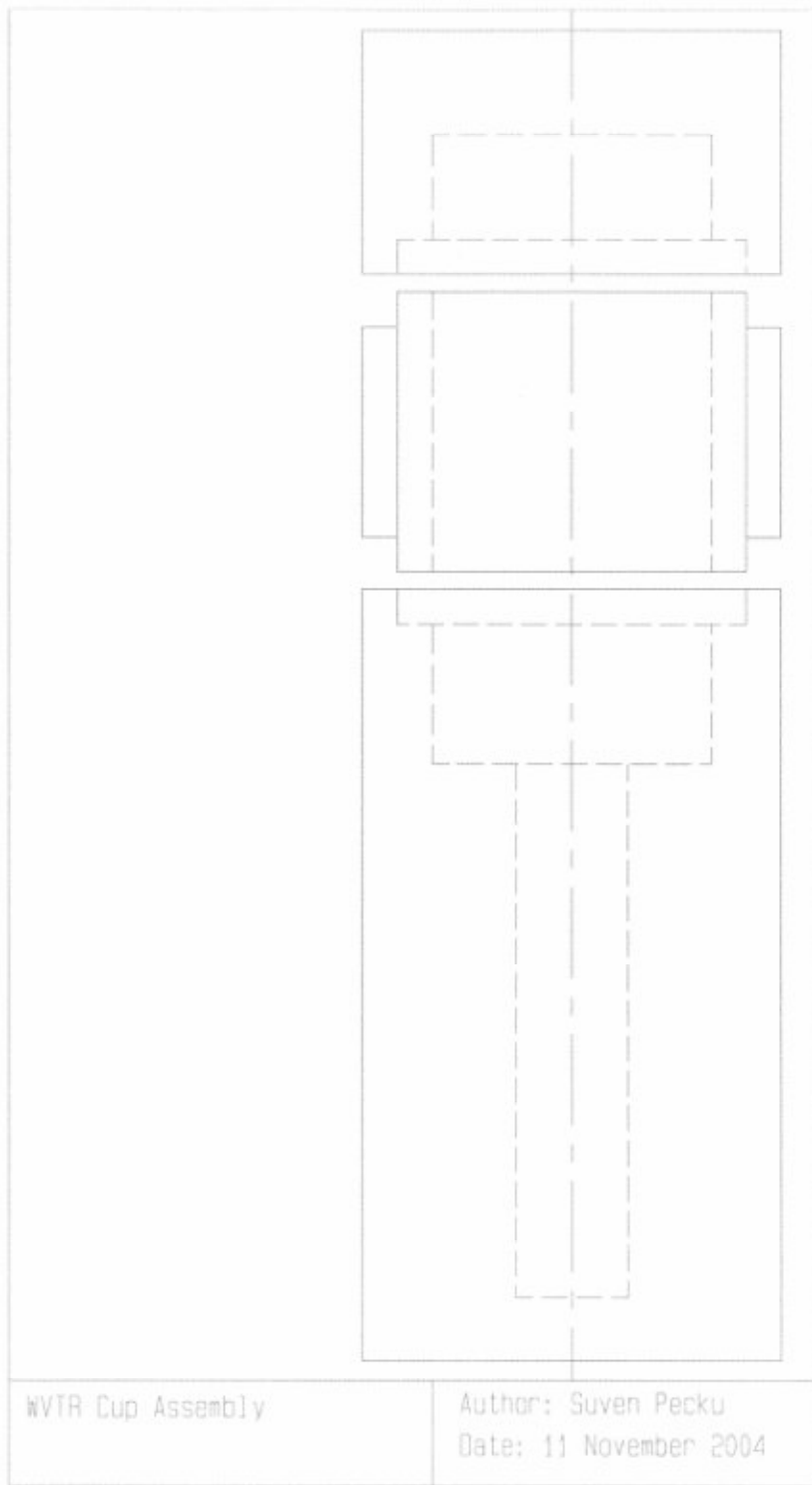


Figure F.4. Drawing of the assembled WVTR cup

Appendix G: Pellethane Data Sheet

Product Information



PELLETHANE* 2103-70A

Thermoplastic Polyurethane Elastomer

- High MVTR

Properties	Test Method	Values ⁽¹⁾
Physical		
Specific Gravity	ASTM D 792	1.06
Mould Shrinkage (1.6 mm [1/16"] thick plaques), %		
MD		0.4-0.5
TD		-0.3-0.8
Mechanical		
Durometer Hardness, Shore A (+/-4)	ASTM D 2240	72A
Tensile Modulus at	ASTM D 412	
50% elongation, MPa (psi)		2.1 (300)
100% elongation, MPa (psi)		3.0 (440)
300% elongation, MPa (psi)		5.2 (750)
Ultimate Tensile Strength, MPa (psi)	ASTM D 412	24.7 (3580)
Ultimate Elongation, %	ASTM D 412	730
Elongation Set After Break, %	ASTM D 412	50
Tear Strength, Die "C", KN/m (pli)	ASTM D 624	66.5 (380)
Compression Set	ASTM D 395	
22 hours at 25 °C (77 °F), %	Method B	25
22 hours at 70 °C (158 °F), %		75
Taber Abrasion Resistance	ASTM D 1044	
1000 g, 1,000 cycles; H-22 wheel (coarser), mg		3
Flexural Modulus, MPa (psi)	ASTM D 790	-
Thermal		
Vicat Softening Temperature, °C (°F)	ASTM D 1525	75.6 (168)
Coefficient of Linear Thermal Expansion, 10 ⁻⁶ mm/mm/°C	ASTM D 696	175 (97 10 ⁻⁶ in/in/°F)
Glass Transition Temperature, °C (°F)	DSC	-69 (-92)
Rheological		
Melt Index, 190 °C, 8700 g, g/10 min	ASTM D 1238	11
Processing Information		
Recommended Drying Temperature, °C (°F)		80-95 (180-200)
Recommended Melt Temperature (Moulding), °C (°F)		195-210 (380-410)
Recommended Melt Temperature (Extrusion), °C (°F)		190-205 (370-400)
Recommended Mould Temperature, °C (°F)		15-60 (60-140)

(1) Typical values, not to be construed as specifications. Users should confirm results by their own tests.